Force-Unconstrained Poses of Redundantly Actuated Planar Parallel Manipulators

by

Flavio Firmani
B. Eng., National Autonomous University of Mexico, 1999

A Dissertation Submitted in Partial Fulfillment of the
Requirements for the Degree of

DOCTOR OF PHILOSOPHY

in the Department of Mechanical Engineering.

Force-Unconstrained Poses of Redundantly Actuated Planar Parallel Manipulators

by

Flavio Firmani
B. Eng., National Autonomous University of Mexico, 1999

Supervisory Committee

Dr. R. P. Podhorodeski, Supervisor (Department of Mechanical Engineering)

Dr. Z. Dong, Departmental Member (Department of Mechanical Engineering)

Dr. P. Wild, Departmental Member (Department of Mechanical Engineering)

Dr. P. Agathoklis, Outside Member (Department of Electrical Engineering)

Dr. C. M. Gosselin, External Examiner (Dép. Génie Mécanique, Université Laval)

Supervisory Committee

Supervisor: Dr. Ron P. Podhorodeski (Department of Mechanical Engineering)

Departamental Member: Dr. Zuomin Dong (Department of Mechanical Engineering)

Departamental Member: Dr. Peter Wild (Department of Mechanical Engineering)

Outside Member: Dr. Pan Agathoklis (Department of Electrical Engineering)

External Member: Dr. Clément M. Gosselin (Dép. de Génie Mécanique, Université Laval)

Abstract

Parallel manipulators are prone to have force-unconstrained configurations. If the resultant forces together do not span the system of forces to be applied or sustained, the manipulator is degenerate and is force unconstrained. Physically, the mobile platform can have motion even if all the actuated joints are locked, i.e., the manipulator can instantaneously gain one or more degrees of freedom that are unconstrained by the actuators. Since force-unconstrained configurations are uncontrollable, the identification and elimination of such configurations become critical.

Two methodologies for identifying the force-unconstrained poses are analyzed. The first method involves the differentiation of the nonlinear kinematic constraints of the input and output variables with respect to time. The second method makes use of the reciprocal screws associated with the actuated joints. Force-unconstrained poses of planar manipulators are analyzed depending on their actuation:

Non Redundant Planar Parallel Manipulators.- Force-unconstrained poses of non-redundantly actuated planar parallel manipulators can be mathematically expressed as a function of the three variables that define the dimensional space of the manipulator, i.e., the location and orientation of the mobile platform. As a conse-

quence, these poses can be plotted as surfaces in the mentioned three dimensional space, i.e., there are two orders of infinity of force-unconstrained poses. Examples of force-unconstrained poses of parallel manipulators are presented: 3-R$\underline{P}$R, 3-$\underline{P}$RR, and 3-$\underline{R}$RR, where the underscore indicates the actuated joint. For the 3-R$\underline{P}$R manipulator, a comparison and discussion between both methodologies is carried out. For the 3-$\underline{P}$RR and 3-$\underline{R}$RR manipulators, an efficient technique for identifying their force-unconstrained poses, based upon having joint displacements as known values, is presented.

Planar Parallel Manipulators with In-Branch Redundancy.- Force-unconstrained poses of planar parallel manipulators with actuated joints replacing passive joints lead to conditions of the joint displacements that have to be satisfied. In particular, the $\underline{RR}$R - 2R$\underline{R}$R, $\underline{PR}$R - 2$\underline{P}$RR, and $\underline{RR}$R - 2$\underline{R}$RR layouts are analyzed. In addition, equivalent mechanisms, whose motions describe the path of continuous force-unconstrained poses, are presented. The force-unconstrained poses of the analyzed layouts with in-branch redundancy represent curves in the three dimensional space, i.e., there is one order of infinity of force-unconstrained poses.

Planar Parallel Manipulators with Additional Actuated Branches.- Force-unconstrained poses of planar parallel manipulators with the inclusion of actuated branches, beyond three, lead to a system of multivariable polynomials. Elimination methods are used to reduce the multivariable polynomials to a single polynomial in terms of one variable. In particular, Gröbner Bases and dialytic elimination methods are employed. The actuation layouts 4-R$\underline{P}$R, 4-$\underline{P}$RR, and 4-$\underline{R}$RR are analyzed. The force-unconstrained poses of the analyzed planar parallel manipulators with additional actuated branches also represent curves in the mentioned three dimensional space, i.e., there is one order of infinity of force-unconstrained poses.

Table of Contents

List of Tables

List of Figures

List of Nomenclature

The following list provides the nomenclature used in the dissertation. Some symbols might have been used to denote different quantities in the text. These cases are noted. Some symbols that are defined in the text have been omitted from this list.

General

Notation used for manipulator layouts.

R	Revolute joint.
P	Prismatic joint.
H	Helical joint.
C	Cylindrical joint.
U	Universal joint.
E	Planar joint.
S	Spherical joint.
_	An underscore indicates an actuated joint, e.g., $\underline{\text{R}}$.
m-	Indication of the number of branches of a manipulator, e.g., 3-UPS, where 3 is the number of branches and UPS the sequence of joints.
b-m	Connection points of the branches between a base b platform and a mobile m platform.

Scalars are expressed in *italics.*

a_i, b_i, c_i, etc	These elements are often used as coefficients unless indicated.
b_{x_i} and b_{y_i}	Location of the base of the i^{th} branch.
$c\alpha$	Abbreviation for cosine of α, $\cos(\alpha)$, or any other angle.
d	Displacement of a prismatic joint.
l_i	Edge of the mobile platform.
n	Total number of actuated joints in a manipulator.
m	Total number of degrees of freedom of a manipulator.
n_k	Number of actuated joints in branch k.
n_b	Total number of branches.
p_L	Pitch of a screw.
r	Coupler length.
q_i	Variable associated with the joint displacements after applying half-angle substitution.
$s\alpha$	Abbreviation for sine of α, $\sin(\alpha)$, or any other angle.
t	Variable associated with the orientation of the mobile platform after applying half-angle substitution.
w	Wrench intensity.
α, β, γ, and ψ	Angles related to the design of the manipulator, unless indicated.
$\alpha_{_T}$	Twist amplitude.
θ_{j_i}	Joint angles, where j denotes the joint and i the branch.
λ	Eigenvalue.
ρ_i	Link lengths.
σ	Singular value.
ϕ	Orientation of the mobile platform.

Vector and screw quantities are denoted in **bold**.

$\mathbf{b}_i$	Position vector describing the i^{th} base branch.
$\mathbf{f}$	Vector of exerted forces on the end-effector, $\mathbf{f} = \{f_x, f_y, f_z\}^{\mathrm{T}}$.
$\mathbf{F}$	Screw quantity, referred to as wrench.
$\mathbf{F}_g$	Generalized vector of forces, $\mathbf{F}_g = \{\mathbf{f}^{\mathrm{T}}, \mathbf{m}^{\mathrm{T}}\}^{\mathrm{T}}$.
$\boldsymbol{l}$	Unit vector defining the direction of a line, $\boldsymbol{l} = \{l_x, l_y, l_z\}^{\mathrm{T}}$.
$\boldsymbol{l}_o$	Moment of a line about the origin of a reference frame.
$\mathbf{m}$	Vector of exerted moments on the end-effector, $\mathbf{m} = \{m_x, m_y, m_z\}^{\mathrm{T}}$.
$\mathbf{P}_a$	Position vector of point a.
$\mathbf{q}$	Vector of joint displacements.
$\dot{\mathbf{q}}$	Vector of joint rates.
$\mathbf{q}_2$ and $\mathbf{q}_2'$	Vectors containing power products of q_2.
$\mathbf{Q}_2$	Associated eigenvector with λ, $\mathbf{Q}_2 = \{\mathbf{q}_2^{\mathrm{T}}, \mathbf{q}_2^{\mathrm{T}}\lambda, \ldots, \mathbf{q}_2^{\mathrm{T}}\lambda^n\}^{\mathrm{T}}$.
$\bar{\mathbf{r}}$	Position vector with respect to a reference frame.
$\mathbf{s}$ and $\mathbf{s}_o$	Unit screw coordinates.
$\mathbf{t}$, $\mathbf{t}'$, and $\hat{\mathbf{t}}$	Vectors containing power products of t.
$\mathbf{T}$	Associated eigenvector with λ, $\mathbf{T} = \{\mathbf{t}^{\mathrm{T}}, \mathbf{t}^{\mathrm{T}}\lambda, \ldots, \mathbf{t}^{\mathrm{T}}\lambda^n\}^{\mathrm{T}}$.
$\mathbf{v}$	Vector of linear velocities, $\mathbf{v} = \{v_x, v_y, v_z\}^{\mathrm{T}}$.
$\mathbf{V}$	Screw quantity, referred to as twist.
$\mathbf{W}$	Associated reciprocal screw.
$\mathbf{w}$	Vector of wrench intensities.
$\mathbf{x}$	Vector describing the pose (position and orientation) of the end-effector.
$\dot{\mathbf{x}}$	Vector describing the angular and linear velocities of the end-efector, $\dot{\mathbf{x}} = \{\boldsymbol{\omega}^{\mathrm{T}}, \mathbf{v}^{\mathrm{T}}\}^{\mathrm{T}}$.

$\hat{\mathbf{z}}$	Joint direction.
\$	Screw coordinates.
$\$_{rev}$ and $\$_{pris}$	Screw coordinates of a revolute and a prismatic joint, respectively.
$\bar{\mathbf{0}}$	Null vector.
$\boldsymbol{\alpha}_{\mathbf{T}}$	Vector of twist amplitudes.
$\dot{\Omega}$	Vector of active $\dot{\Omega}_a$ and passive $\dot{\Omega}_p$ joint velocities, $\dot{\Omega} = \{\dot{\Omega}_a^{\mathrm{T}}, \dot{\Omega}_p^{\mathrm{T}}\}^{\mathrm{T}}$.
$\boldsymbol{\tau}$	Vector of applied torques and forces.
$\boldsymbol{\omega}$	Vector of angular velocities, $\boldsymbol{\omega} = \{\omega_x, \omega_y, \omega_z\}^{\mathrm{T}}$.

Matrices are denoted in **bold** and are contained in square brackets.

$[\mathbf{A}]$ and $[\mathbf{B}]$	Jacobian matrices.
$[\mathbf{D}]$	Diagonal matrix.
$[\mathbf{H}]$	Force transformation matrix.
$\mathbf{I}$ and $\mathbf{0}$	Identity and null matrices.
$[\mathbf{J}]$	Jacobian matrix where $[\mathbf{J}] = [\mathbf{B}]^{-1}[\mathbf{A}]$.
$[\mathbf{K}]$	Equivalent matrix used for the standard eigenvalue problem.
$[\mathbf{K}_1]$ and $[\mathbf{K}_2]$	Equivalent matrices used for the generalized eigenvalue problem.
${}^{i}_{j}[\mathbf{R}]$	Rotation matrix describing the orientation of frame j with respect to frame i.
${}^{i}_{j}[\mathbf{T}]$	Homogeneous transformation matrix of frame j with respect to frame i.
${}^{\mathrm{ref}}[\mathbf{W}]$	Associated reciprocal screw matrix with respect to {ref}.
${}^{\mathrm{ref}}[\mathbf{W}_i]$	The i^{th} sub-matrix of ${}^{\mathrm{ref}}[\mathbf{W}]$.

${}^{\text{ref}}[\$]$	Screw matrix with respect to reference frame {ref}.
$[\Psi]$	Square matrix whose entries are polynomials in t.
$[\Psi']$	Non-square matrix whose entries are polynomials in t.
$[\Psi_i]$	The i^{th} coefficient matrix of a polynomial matrix.
$[\Delta(\cdot)]$	Jacobian matrix.

Superscripts and Subscripts

$[(\cdot)]^{\text{T}}$	Transpose of a matrix.
$[(\cdot)]^{-1}$	Inverse of a matrix.
$\times \quad \tilde{} \quad \circ$	Markers.
${}^{\text{ref}}(\cdot)$	Describing a quantity (vector, screw, or matrix) with respect to a reference frame.
${}^{(\text{i})}(\cdot)$	This left superscript is used to distinguish coefficients.
$(\cdot)_{j_i}$	Refering to the j^{th} joint of the i^{th} branch of an element (angle, displacement, or magnitude).
$(\cdot)_{k_i}$	Refering to the k^{th} actuated joint of the i^{th} branch.
$r_{i\to j}$	A position vector that describes the location of a frame j with respect to a frame i.

Operators

$\{\cdot\}$	Reference frame, such as $\{ref\}$ or $\{cen\}$.
$\langle\cdot\rangle$	Ideal.
$p([\mathbf{T}])$	Operator that extracts the last column from matrix $[\mathbf{T}]$.

$f(\cdot)$, $g(\cdot)$, and $h(\cdot)$	Function of $(\cdot)$.
$F(\mathbf{x}) = 0$ and $G(\mathbf{x}) = 0$	Set of polynomials in $\mathbf{x}$.
$H(\mathbf{x}, t) = 0$	Homotopy function.
$\frac{\partial f(\cdot)}{\partial \mathbf{x}}$	Partial derivative of $f(\cdot)$ with respect to $\mathbf{x}$.
$\dot{(\cdot)}$	Time derivative of $(\cdot)$.
$\|[(\cdot)]\|$ or $det([(\cdot)])$	Determinant of a matrix.
$\cdot$	Inner product of vector quantities.
$\times$	Cross product of vector quantities.
$\circledast$	Reciprocal product of screw quantities.
$\sum$	Summation.
$\prod$	Product.
$\subseteq (\cdot)$ and $\subset (\cdot)$	Subset of $(\cdot)$.
$\in (\cdot)$	Member of $(\cdot)$.
$f \xrightarrow{g} h$	Reduction of f by g, with h being the remainder in a polynomial division.
$l_t(\cdot)$	Leading term of a polynomial.
$l_c(\cdot)$	Leading coefficient, coefficent of the leading term $l_t(\cdot)$.
$l_p(\cdot)$	Leading power product of a polynomial.
$lcm(\cdot)$	Least common multiple of monomials.

Acknowledgements

I would like to thank my supervisor, Dr. Ron P. Podhorodeski, for his support and guidance throughout this dissertation. Furthermore, I would deeply express my gratitude to Ron for introducing me to the fascinating world of kinematics but mostly for tutoring me through diverse aspects of the academic life.

I want to extend my gratitude to my committee members, Dr. Pan Agathoklis, Dr. Peter Wild, and Dr. Zuomin Dong, for their comments and suggestions.

I would like to thank my external examiner, Dr. Clément Gosselin, whose exceptional expertise in kinematics of manipulators and numerous publications in this area happen to be the main references of my dissertation. I am truly honored to have him as my external examiner.

I would like to thank my fellow students, in particular the former and current members of the Robotics and Mechanisms Laboratory, for the numerous discussions that we have had regarding topics related to my dissertation and especially for embracing me in such a delighting working environment.

I would like to acknowledge the Natural Sciences and Engineering Research Council (NSERC) of Canada whose financial support has made my research possible.

Finally, I would like to thank my wife Carmen and her parents for their unconditional love and support that allow me to reach goals beyond my expectations and my parents for their enormous encouragement and their absolute confidence in me throughout my life.

To my Wife Carmen, my Parents, and in Memory of Nonna Memma

Chapter 1

Introduction

1.1 Overview

In this chapter, definitions of the terminology used throughout the dissertation are presented, as well as a brief introduction of parallel manipulators, force-unconstrained poses, and redundant actuation. This is followed by a literature review regarding these topics. Then, the motivation and contributions of this work are presented. Finally, this chapter ends with a brief summary of the remaining chapters.

1.2 Definitions

Manipulators are mechanical devices composed of links that are connected with joints. The mobility of a manipulator depends on the degrees of freedom (dof) that it possesses. That is, the number of independent variables required to specify the posture of the mechanism. The task space coordinates are referred to as the degrees of freedom of the space in which the manipulator is intended to function. For instance,

a planar manipulator requires three variables, namely two translations along axes defining a plane and one orientation about the axis normal to the plane. Links can be either rigid or flexible bodies. In this dissertation however, only rigid links are considered. Joints are classified accordingly to their type of motion. Joints with one degree of freedom include: revolute (R), rotation of a link about the axis defined by the joint; prismatic (P), translation of a link along the joint axis; and helical (H), translation and rotation of a link along and about the joint axis, similar to a nut moving on a bolt. Joints with multiple degrees of freedom include: cylindrical (C), independent translation and rotation of a link along and about the joint axis; universal (U), two rotations about two different intersecting joint axes; planar (E), two translations along two different joint axes; and spherical (S), three rotations about three different intersecting joint axes.

1.3 Parallel Manipulators

1.3.1 Manipulator Classes

According to their topology, manipulators are divided into three classes, serial, parallel, and hybrid. Resembling a human arm, serial manipulators are comprised of a concatenation of links connected by joints. The last link of this serial chain is named the end-effector. Parallel manipulators are closed-loop chains, where a moving platform is connected to a base platform by several independent serial chains. The mobile platform represents the end-effector of the manipulator, also known as the payload. Each independent serial chain will be called a branch. Hybrid manipulators are a combination of serial and parallel manipulators.

Parallel manipulators compared to serial manipulators have higher structural stiffness, greater payload accuracy, and higher end-effector accelerations but also have smaller and less dexterous workspaces and the existence of force-degenerate configurations. An extensive comparison between these manipulators can be found in (Merlet, 2000).

1.3.2 Origins of Parallel Manipulators

The concept of distributing the load on the links by connecting the end-effector to the ground led to the origin of closed-loop kinematic chains. This was discussed as early as 1645 by Christopher Wren (Merlet, 2000). The first designs of parallel manipulators were made in the 1930's[1]. However, the manipulator that transformed the course of mechanisms was introduced by Gough (1956). This mechanism was conceived for testing tires. Later, Stewart (1965) suggested flight simulators could be controlled using a parallel manipulator. The proposed mechanism was similar to the one previously presented by Gough. In this dissertation, this architecture will be identified as the Stewart-Gough platform.

1.3.3 Applications of Parallel Manipulators

Parallel manipulators have been used in several applications. Merlet (2000) classified different applications of parallel manipulators as:

- Space and Telescopes.- Projects regarding space research and telescopes require extreme accuracy. In space, parallel manipulators can be instrumented for

[1]For further information about the evolution of parallel manipulators please refer to http://www.parallemic.org

testing docking and vibration systems (Merlet, 2000). Another application in space is for assembling purposes (Smith III and Nguyen, 1991). Modern telescopes based on the Cassegrain optic system require correction of the image due to aberrations of the atmosphere, structural vibrations, or wind-induced motions (Carretero et al., 1997). Parallel manipulators are used to correct such distortions by either moving the secondary mirror (Firmani, 1999) or each one of the segments of the primary mirror (Smith, 1997).

- Medical.- Due to their accuracy, parallel manipulators have been considered for delicate applications. Grace et al. (1993) considered the Stewart-Gough platform with a hypodermic needle attached to the mobile platform for ophthalmic surgery. Wendlandt and Sastry (1994) designed a 3-dof parallel manipulator that controls endoscopic tools. Lazarevic (1997) proposed a version of the Stewart-Gough platform for coronary-artery bypass graft surgery. Di Gregorio and Parenti-Castelli (2001) proposed a 6-dof mechanism that works as an external fixation device to reduce long-bone fracture. Li and Payandeh (2002) optimized the workspace of a spherical parallel manipulator meant to be used for laparoscopic surgery.

- Industrial.- Recent machine tools have been designed based on parallel manipulators. In particular, modern milling machines are based on parallel architectures. Giddings & Lewis company presented the first milling machine (Variax) of this type, which was based on the Stewart-Gough platform in 1994 (Merlet, 2000). Afterward, other companies such as Ingersoll, Geodetics, Toyoda, Honda, Okuma and Sena, among others, have built milling machines based on closed-loop kinematic chain architectures. Other applications of parallel ma-

nipulators in the machining field are painting (Pollard patented in 1942 the first industrial parallel manipulator design for car painting, as reported by Miller, 2004), parts handling (Clavel, 1991, developed the Delta robot, a well known and largely exploited manipulator, and it is commonly used for pick and place of lightweight objects and assemblies), cutting (Bruzzone et al., 2002, used a Delta-type architecture for laser-cutting), and welding (Wu et al., 2003, designed a parallel manipulator for welding inside the International Thermonuclear Experimental Reactor). More specific applications of parallel manipulators in industry can be found in (Destefani, 2003).

- Joysticks.- Parallel manipulators can be implemented as joysticks, see for instance the RSI Joystick (Sobejko, 2002). Although their architecture is compact and handy, the disadvantage of having a small workspace constrains an application that requires a large range of motion. Joysticks based on a parallel architecture can be used as remote controllers of robots in industrial, medical, space, and underwater applications.

- Simulators.- Stewart's picture of having parallel manipulators controlling flight simulators turned out to be accurate. Several companies currently produce flight simulators based on the Stewart-Gough platform. CAE, Frasca, NASA, Kawasaki, and Thales Training & Simulation, stand among the most important manufacturers. In addition, other simulators have been produced such as vehicle, ship, and even equestrian simulators (Merlet, 2000).

- Others.- Devices meant for other applications have been built based on parallel manipulator architectures. The European Synchrotron Radiation Facility (ESRF) designed a fine positioning device (Fajardo and Rey-Bakaikoa, 1995).

The Vibration, Isolation, Suppression, and Steering System (VISS), a structural vibrator control device was developed by the US Air Force (Cobb et al., 1999).

This dissertation addresses planar parallel manipulators, which can be used in applications related to part handling, metal cutting, deburring, and simulation devices for terrestrial vehicle simulators (Gosselin et al., 1996). Moreover, parallel manipulators can be conceived as the mobile base of a more complex device such as a hybrid manipulator. An example of a planar parallel manipulator is the Reconfigurable Planar Parallel Manipulator (RPPM) developed by Fisher et al. (2001 and 2004), and shown in Figure 1.1.

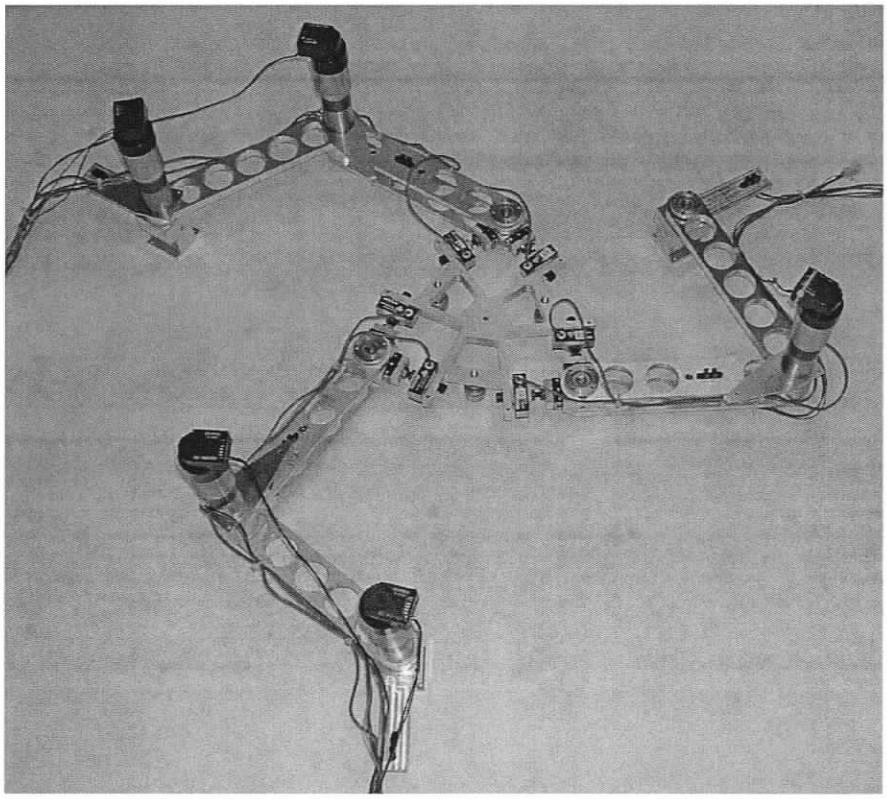

Figure 1.1: Reconfigurable Planar Parallel Manipulator.

1.3.4 Kinematic Problems in Parallel Manipulators

The kinematic problems that are faced using serial and parallel manipulators relate to displacement, velocity, and static force. Each of these problems is divided into forward and inverse solutions.

- Displacement.- The forward displacement solution is referred to as the problem of solving the pose (position and orientation, $\mathbf{x}$) of the mobile platform knowing the joint displacements ($\mathbf{q}$) of all sensed joints. For parallel manipulators, this problem is more difficult than for serial manipulators because of the existence of passive (unsensed) joints and multiple solutions. In general, the forward displacement solution of parallel manipulators is a non-linear problem based on the loop-closure equations that involve the design variables of the manipulator. In many cases, this problem is solved using elimination techniques. The inverse displacement solution deals with the problem of solving for the joint displacements knowing the pose of the mobile platform. For parallel manipulators, this problem is solved individually for each one of the branches.

- Velocity.- The forward velocity solution is defined as the problem that solves for the velocities (angular and translational) of the end-effector ($\dot{\mathbf{x}}$) knowing the joint rates ($\dot{\mathbf{q}}$). This is achieved by computing the operator that relates both $\dot{\mathbf{x}}$ and $\dot{\mathbf{q}}$, known as the Jacobian. The inverse velocity solution deals with the problem of solving for the joint rates by knowing a desired velocity of the end-effector. A velocity degeneracy occurs when the manipulator loses at least one degree of freedom of motion. In parallel manipulators, this problem occurs in each branch individually.

- Static Force.- The forward force solution is defined as the problem that solves for the forces and moments of the end-effector ($\mathbf{F}_g$) by knowing the applied torques or forces ($\boldsymbol{\tau}$), for revolute and prismatic joints respectively. The Jacobian is once again the operator that relates them. The inverse force solution deals with the problem of solving for $\boldsymbol{\tau}$ knowing a desired $\mathbf{F}_g$ of the end-effector. A force degeneracy occurs when a parallel manipulator is placed in a configuration where the mobile platform gains at least one degree of freedom of motion.

1.4 Force-Unconstrained Poses

The mechanical design of parallel manipulators deals with different properties such as the reachable and dexterous workspace, as well as, the rigidity of the manipulator. The workspace of a manipulator is related to the geometrical parameters of all the rigid elements, i.e., link lengths, shapes of the mobile and fixed platforms, and joint limits. Ideally, the manipulator should act as a rigid structure when the actuated joints are locked. However, parallel manipulators are susceptible of having unconstrained motion, i.e., the mobile platform can have motion even if all actuated joints are locked. This lack of rigidity is usually caused by two problems: singular configurations and joint clearances.

Merlet (1989) defined that a singular configuration of a parallel manipulator corresponds to a configuration where the manipulator is not rigid, i.e., a force-degenerate configuration. If the branch resultant forces together do not span the system of forces to be applied or sustained, the manipulator is degenerate and is force unconstrained. The manipulator may instantaneously gain one or more unconstrained motion degrees of freedom.

Voglewede and Ebert-Uphoff (2002) noticed that small unconstrained motion exists in all configurations due to the finite clearances of the joints. For actuated joints, the backlash originating in the actuators can be substantially reduced with the use of harmonic drives. Nevertheless, passive joints are prone to have such clearance due to the complexity of their manufacture and assembly within tolerances.

1.5 Redundant Actuation

In serial manipulators all joints are sensed and actuated. If the number of joints exceeds the number of task space variables the manipulator becomes redundant. In parallel manipulators each branch is composed of actuated and passive joints. The term fully-parallel manipulator is given to those manipulators whose number of branches is strictly equal to the number of degrees of freedom of the end-effector. Therefore, each branch of a fully-parallel manipulator contains only one actuator. Generally, the degrees of freedom of one branch correspond to the degrees of freedom of the end-effector. Redundancy in parallel manipulators can occur in three different forms: sensing redundancy, joint redundancy, and actuation redundancy (Nokleby, 2003). Sensing redundancy is defined as passive joints being measured. Joint redundancy refers to redundant joints within the branches, i.e., the number of joint degrees of freedom of one branch is higher than the motion degrees of freedom of the end-effector. Actuation redundancy occurs when the number of actuated joints is higher than the number of degrees of freedom of the end-effector. The latter can be classified in two groups: in-branch redundant actuation (inclusion of extra actuators within the branches) and additional branches (inclusion of extra actuated branches). For a fully-parallel manipulator with additional actuated branches, the number of branches

is greater than the total degrees of freedom of the manipulator.

Merlet (1996a) described that the inclusion of redundant actuators may lead to improvements in various analyses such as forward kinematics, singular configurations, and optimal force control and calibration. In order to reduce uncertainty configurations, Notash and Podhorodeski considered over-constrained parallel manipulators by including either redundant actuation within branch(es) (1994) or redundant branches (1996). Sobejko (2002) included sensing redundancy in the RSI Joystick allowing self-calibration and fault-tolerant operation. Nokleby et al. (2005) and Zibil et al. (2006) demonstrated that the use of redundant actuation within branches significantly improves the force capabilities of parallel manipulators.

1.6 Literature Review

1.6.1 Parallel Manipulators

Problems related to forward and inverse displacement solutions, singular configurations, dexterous workspace, and optimal design of parallel manipulators have been studied since the 1980's.

The Stewart-Gough platform is a 6-dof manipulator, where the two platforms are connected by six branches. The layout of each branch[2] is U-P-S. The forward displacement problem of the Stewart-Gough platform has been analyzed for different platform configurations, which depend on the unique locations of the connection points between the branches and the base and mobile (b-m) platforms. For instance, the forward displacement problem of the *3-3* layout was formulated by Griffis and

[2] where the underscore indicates the acuated joint

Duffy (1989) yielding 8 reflected solution pairs. For the *6-3* layout, Innocenti and Parenti-Castelli (1990) determined forward displacement solutions in terms of the roots to a single variable 16^{th} order polynomial based on the three loop-closure equations of an equivalent spatial mechanism. Similarly, Nanua et al. (1990) identified 16 solutions of this layout. However, these layouts lead to mechanical design problems, such as collision among the limbs that can reduce the performance of the manipulator. For the 6-6 layout, or the general Stewart-Gough manipulator, Raghavan (1993) demonstrated with numerical examples that the maximum number of solutions is 40. Husty (1996) determined a 40^{th} order univariable polynomial that describes all possible solutions of the general Stewart-Gough platform.

Several studies relate to both optimum design and dexterity of the workspace of parallel manipulators, such as Fichter (1986), Gosselin (1990a), Pittens and Podhorodeski (1993), and Masory and Wang (1995).

Planar Parallel Manipulators

According to the layout of a branch, there are seven possible combinations of planar parallel manipulators with homogeneous branch layouts: RRR, RPR, PRR, PPR, RRP, PRP, and RPP, as shown in Figure 1.2.

The inverse displacement problem of planar parallel manipulators is not very complicated, although it must be considered that for some layouts multiple solutions exist. For this problem, the location of the centre of the mobile platform as well as the orientation of the mobile platform with respect to a horizontal line are known. Thus, the location of the point of connection between each branch and the platform can be determined based on the geometry of the platform. The solution of the displacement of each joint is resolved independently for each branch.

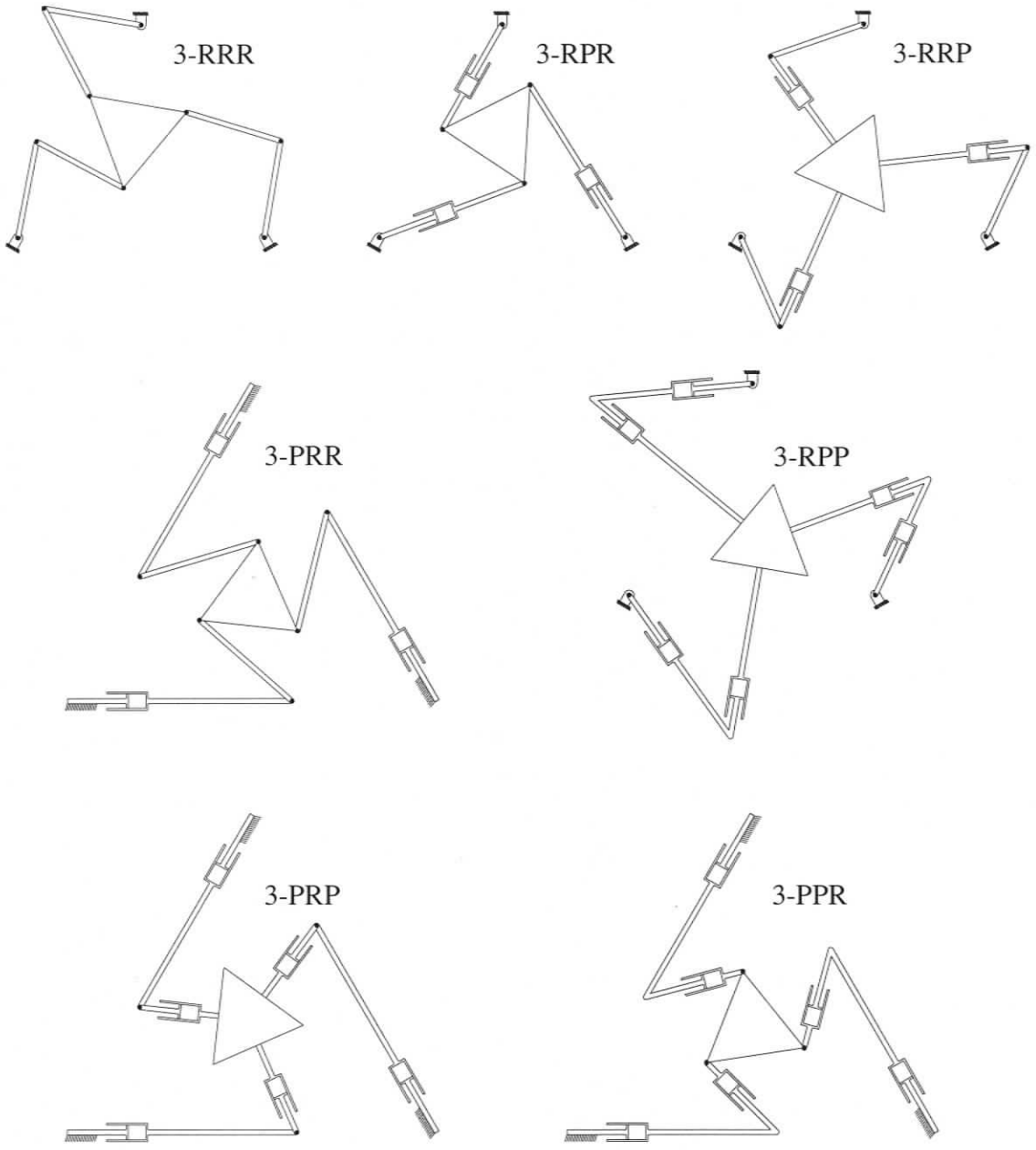

Figure 1.2: Planar Parallel Manipulators with Homogeneous Branch Layouts.

The forward displacement problem, on the other hand, is much more difficult. The joint displacement variables are known and the position and orientation of the mobile platform are yet to be found. For the forward displacement problem of the 3-R<u>P</u>R and 3-<u>R</u>RR, Gosselin et al. (1992) derived a sixth order polynomial, whose roots represent the possible postures that the manipulator can have for that specific set of joint displacements. Gosselin and Merlet (1994) made a more detailed analysis of the forward displacement solution based on the architecture of the manipulator. Depending on the position of the actuated joint, there are 21 actuation layouts; Merlet (1996b) identified that the solution of the forward displacement problem of all these combinations is based on three equivalent basic chains.

Merlet et al. (1998) developed algorithms that determine various workspaces, namely reachable, inclusive, total orientation, and dextrous, of planar parallel manipulators. These analyses featured the 3-RPR manipulator. Gosselin and Angeles (1988) presented an analysis of the optimum kinematic design of the 3-RRR. This work was based on the symmetry, workspace, and isotropy of the Jacobian matrix.

1.6.2 Force-Unconstrained Poses

Different approaches for analyzing force-unconstrained configurations have been proposed, such as, the identification of the conditions that cause the lines associated with the actuated joints to be linearly dependent, and the singularity analysis of the Jacobian matrices. Using the first analysis, Merlet (1989) identified the conditions of force-unconstrained configurations of the 6-3 Stewart-Gough platform. Collins and Long (1995) and Notash (1998) identified the conditions that cause two different 6-dof (joystick-type) manipulators to be force unconstrained. On the other hand, Gosselin

and Angeles (1990) analyzed singularities in Jacobian matrices resulting from differentiating the nonlinear kinematic constraints of the input and output variables with respect to time. This analysis is described in detail in Section 2.2.1.

The singularity analysis of the Jacobian matrix has been treated both analytically and numerically. Analytic methods, based on setting the determinant of the Jacobian matrix to zero, have been successfully implemented for planar parallel manipulators, but also for spherical 3-dof parallel manipulators (Sefrioui and Gosselin, 1994), special 6-dof manipulators (Tahmasebi and Tsai, 1994), and general 6-dof manipulators (Mayer St-Onge and Gosselin, 1996). Numerical techniques that predict how close a pose is from a singularity have been considered. These techniques are generally defined with indices, such as the condition number (Gosselin, 1990c), quality index, which involves the numerical value of the Jacobian matrix determinant (Zhang and Duffy, 1998), and the incorporation of several indices (Voglewede and Ebert-Uphoff, 2004).

Force-Unconstrained Poses of Planar Parallel Manipulators

For planar manipulators, three dimensions of task-space coordinates exist. These coordinates can be represented by the location (x and y) and orientation (ϕ) of the mobile platform.

Sefrioui and Gosselin (1995) identified the singular poses of the 3-RPR layout. For constant payload orientation, these singularities can be plotted as quadratic curves in the xy plane. Mohammadi-Daniali et al. (1995) illustrated all possible singularities that the 3-RRR can have. Gosselin and Wang (1997) reported the singularity loci of a 3-RRR manipulator with collinear base and mobile platform joints are expressed by a multivariable polynomial in x and y of degrees 48 and 64, respectively. Bonev and

Gosselin (2001) reported that, for constant orientation, the singularity loci of every branch arrangement of the 3-$\underline{R}$RR configuration can be represented by curves of degree 42. Chan and Ebert-Uphoff (2001) determined the manifold of singularities and showed how unconstrained motions are projected onto it. Bonev (2002) and Bonev et al. (2003) presented a detailed study of the singular configurations of all possible actuation configurations of 3-dof planar parallel manipulators using screw theory.

1.6.3 Redundancy

Collins (1997) proposed a method for choosing redundant actuator locations that provide singularity-free motions. Pseudoinverse techniques were applied for solving the inverse of the Jacobian. Zlatanov et al. (1998a) presented a comprehensive classification of the singularities of redundant mechanisms. Dasgupta and Mruthyunjaya (1998) showed that the use of redundant actuation can lead to a reduction or even an elimination of force singularities. Similarly, O'Brien and Wen (1999) showed that the use of redundancy improves the manipulability of the original mechanism by comparing the condition number of non-redundant and redundant manipulators. Chan (2001) stated that by using a single redundant actuator, the dimension of the manifold of singularities could be reduced by an order of one.

Redundancy of Planar Parallel Manipulators

Firmani and Podhorodeski (2002 and 2004a) eliminated families of force unconstrained configurations by including redundant actuation within one branch. Further, Firmani and Podhorodeski (2004b and 2005b) investigated the force-unconstrained

poses of the 4-R$\underline{P}$R manipulator by analyzing the force-unconstrained poses of two three-branch assemblies. This analysis leads to two polynomials in three variables and by means of Gröbner Bases a quartic polynomial in terms of two task-space variables is determined. Similarly, Firmani and Podhorodeski (2005a and 2005c) identified for the 4-$\underline{P}$RR manipulator, the force-unconstrained poses that represent curves of degree 64 in a three-dimensional space defined by the task-space variables.

Wang and Gosselin (2004) added an extra revolute joint to one branch of the 3-R$\underline{P}$R manipulator, i.e., joint redundancy with actuation yielding a $\underline{R}$R$\underline{P}$R-2R$\underline{P}$R layout. The conditions that make this manipulator force unconstrained were identified. As a consequence, the singularity loci are reduced to a closed-loop curve. Ebrahimi et al. (2006) proposed a planar parallel manipulator which contains joint redundancy in every branch (3-$\underline{PR}$RR). Manipulators with joint redundancy may be efficiently employed for singularity avoidance. That is, the two actuated joints of each branch can be manipulated in such a way that the condition number is minimized.

1.7 Motivation and Contributions

Closed-loop chains or parallel manipulators have shown interesting qualities over serial architectures, such as higher structural stiffness, greater payload accuracy, and higher end-effector accelerations. These advantages have allowed them to be considered for numerous applications, as described previously in Section 1.3.3. Nevertheless, parallel manipulators are prone to have force-unconstrained configurations and a smaller and less dextrous workspace. When a parallel manipulator is force unconstrained, the mobile platform gains one (or more) degree(s) of freedom of motion, even if all the actuators are locked. Thus, the manipulator becomes uncontrollable.

As an initial contribution, the force-unconstrained poses of non-redundant planar parallel manipulators are identified. In contrast to the results found in the literature, the formulation carried out in this study leads to much simpler results providing a better computation efficiency. The force-unconstrained poses of non-redundant planar parallel manipulators are described by surfaces in a three-dimensional space defined by the position and orientation of the mobile platform, i.e., there are two orders of infinity of force-unconstrained poses.

The focus of this dissertation is to improve the capabilities of parallel manipulators by eliminating families of force-unconstrained poses. Furthermore, the elimination of force-unconstrained poses increases the dexterity of the manipulator. Thus, the major contribution of this dissertation is the elimination of force-unconstrained poses by including redundancy within the device. Two types of redundancy are considered: redundancy within branches and the inclusion of additional actuated branches.

In the first case, force-unconstrained poses of planar parallel manipulators with actuated joints replacing passive joints lead to conditions of the joint displacements that have to be satisfied. Equivalent mechanisms, whose paths represent the force-unconstrained poses of the manipulators under study, are presented. For the case of including additional branches, the identification of force-unconstrained poses is, without any doubt, a difficult challenge based on systems of non-linear equations. Elimination methods are used to reduce the multivariable polynomials to a single polynomial in terms of one variable. In particular, Gröbner Bases and dialytic elimination methods are employed. The force-unconstrained poses of redundant planar parallel manipulators are described by curves in the three-dimensional space defined by the position and orientation of the mobile platform, i.e., there is one order of infinity of force-unconstrained poses.

The methodology employed in this work is based on screw quantities. The use of kinematic geometry allows a better understanding of the displacements, velocities, and forces of a manipulator. This is clearly evident in the study of force-unconstrained poses, where the use of screw quantities provides a clear insight as to how the forces are acting on the mechanism and why the manipulator becomes degenerate in some configurations. The traditional time-derivative methodology, on the other hand, does not provide a clear understanding of the interaction of forces acting on the mechanism.

1.8 Outline of Dissertation

The following is a brief summary of the remaining chapters of the dissertation.

Chapter 2: Analysis of Force-Unconstrained Poses

Chapter 2 presents methods for identifying force-unconstrained poses of parallel manipulators. The first method consists of differentiating the loop-closure equations that describe the kinematic chains of the manipulator. The second method involves the reciprocal screws associated with the actuated joints. Both methods are compared. Techniques for identifying force-unconstrained configurations are discussed.

Chapter 3: Force-Unconstrained Poses of Non-Redundant Planar Parallel Manipulators

Chapter 3 presents the force-unconstrained poses of non-redundant planar parallel manipulators. This chapter begins with a brief introduction of planar parallel manipulators and their actuation layouts. The force-unconstrained poses of the 3-R$\underline{P}$R,

3-PRR, and 3-RRR are solved. In particular, for the 3-RPR, a well-studied manipulator, a comparison is made between the two methodologies described in this dissertation, namely input and output speed relationship and screw theory. For the 3-PRR and 3-RRR manipulators, an efficient approach to identify force-unconstrained poses is proposed using screw theory.

Chapter 4: Force-Unconstrained Poses of Redundant Planar Parallel Manipulators with In-Branch Actuation

Chapter 4 discusses the effect of including a greater number of actuators within the branches than the total degrees of freedom of the manipulator. In particular, the force-unconstrained poses of the RRR-2RRR, PRR-2PRR, and RRR-2RRR actuation layouts are presented. In each case, there are two conditions that cause degenerate configurations. These conditions are identified and equivalent mechanisms, whose motions describe the paths of continuous singularities of the planar parallel manipulators, are presented. An analysis of manipulators with further actuation is also conducted.

Chapter 5: Force-Unconstrained Poses of Redundant Planar Parallel Manipulators with Additional Branches

Chapter 5 considers the inclusion of an additional actuated branch. The identification of force-unconstrained poses of the 4-RPR, 4-PRR, and 4-RRR are presented. Each problem leads to a non-linear system of equations. For the 4-RPR manipulator, the non-linear systems of equations is solved using Gröbner Bases. For the 4-PRR and 4-RRR manipulators, due to the complexity of their non-linear system of equations, an exhaustive elimination method based on the Sylvester's dialytic elimination technique

is carried out.

Chapter 6: Conclusions and Recommendations for Future Work

Chapter 6 presents the conclusions of the theory and the results obtained in this dissertation. In addition, this chapter makes recommendations for further research.

Chapter 2

Analysis of Force-Unconstrained Poses

2.1 Overview

In this chapter, methods for identifying force-unconstrained poses of parallel manipulators are presented. The first method is based on the input-output speed relationship, i.e., the differentiation of the nonlinear kinematic constraints of the input (joint displacements) and the output (task space coordinates) variables with respect to time. Further, a detailed classification of types of singular configurations is described. The second method makes use of the reciprocal screws associated with the actuated joints. This method is described at length due to its strong physical interpretation of robot kinematics. The analogy between both methods is proved. Techniques for identifying force-unconstrained configurations are presented. The chapter ends with a discussion of the described methods and techniques.

2.2 Time Derivative Method

2.2.1 Input-Output Speed Relationship

Parallel manipulators are based on closed-loop kinematic chains. These chains are characterized by a set of input variables $\mathbf{q}$, which correspond to the displacement of the n actuated joints, and by a set of m output coordinates $\mathbf{x}$, which define the position and orientation of the end-effector. According to the number of actuated joints n and the number of task space coordinates or degrees of freedom of the linkage m, the following classification can be made: if $n = m$, which is the general case, the manipulator is termed exactly constrained, if $n > m$, the manipulator is overconstrained due to the presence of redundant actuators, and if $n < m$, the manipulator is underconstrained in which case the manipulator cannot achieve an arbitrary pose. The relationship between the input and output variables is given by a non-linear $n-$dimensional vector equation

$$\boldsymbol{f}(\mathbf{q}, \mathbf{x}) = \bar{\mathbf{0}} \tag{2.1}$$

For an exactly constrained manipulator, Gosselin and Angeles (1990) analyzed singularities in Jacobian matrices resulting from differentiating the nonlinear kinematic constraints of Eq. (2.1), with respect to time. This leads to a relationship of input $\dot{\mathbf{q}}$ (joint rates) and output $\dot{\mathbf{x}}$ (end-effector velocity) speeds

$$[\mathbf{A}]\,\dot{\mathbf{x}} = [\mathbf{B}]\,\dot{\mathbf{q}} \tag{2.2}$$

where

$$[\mathbf{A}] = \frac{\partial f(\mathbf{q}, \mathbf{x})}{\partial \mathbf{x}} \qquad \text{and} \qquad [\mathbf{B}] = \frac{\partial f(\mathbf{q}, \mathbf{x})}{\partial \mathbf{q}}$$

are both $m \times m$ Jacobian matrices.

2.2.2 Classification of Singular Configurations

Gosselin and Angeles (1990) reported three different types of singularities for closed-loop kinematic chains: Type I (instantaneous motion singularity) occurs when [**B**] is singular, Type II (force singularity) occurs when [**A**] is singular, and Type III occurs when both are singular. If [**B**] is singular, the mobility of the end-effector is restricted by additional constraints, i.e., the manipulator loses one or more instantaneous-motion degrees of freedom. This type of singularity is analogous to the ones present in serial manipulators. If [**A**] is singular, the end-effector still has some mobility even when all actuators are locked, i.e., the manipulator will gain one or more instantaneous degrees of freedom.

Tsai (1999) redefined singularities of Type I and Type II as inverse and direct kinematic singularities, respectively. An inverse kinematic singularity occurs when infinitesimal motion of the mobile platform along certain directions cannot be accomplished and the manipulator can resist forces and moments in some directions even if the actuated joints are not locked. A direct kinematic singularity happens when the mobile platform possesses infinitesimal motion in some directions even if the actuators are completely locked and the manipulator cannot resist forces and moments in some directions.

Ma and Angeles (1991) defined parallel manipulators that cannot sustain an arbitrary force in a large number of configurations as having architectural singularities. Based on Eq. (2.2) a unique Jacobian can be formed

$$\dot{\mathbf{q}} = [\mathbf{J}]\,\dot{\mathbf{x}} \tag{2.3}$$

where $[\mathbf{J}] = [\mathbf{B}]^{-1}[\mathbf{A}]$. Ma and Angeles identified some conditions for when the Jacobian matrix [**J**] of special architectures of the Stewart-Gough platform is always

singular throughout the workspace.

Zlatanov et al. (1994a and 1994b) made a more extended classification of the singular configurations of parallel manipulators based on the relationship between output and input speeds

$$\dot{\mathbf{x}} = [\Delta(\mathbf{q})]\ \dot{\Omega} \tag{2.4}$$

where $\dot{\Omega} = \begin{bmatrix} \dot{\Omega}_a^{\mathrm{T}} & \dot{\Omega}_p^{\mathrm{T}} \end{bmatrix}^{\mathrm{T}}$, with $\dot{\Omega}_a$, $\dot{\Omega}_p$, and $\dot{\mathbf{x}}$ being the vectors of active joint velocities, passive joint velocities, and the end-effector's velocities, respectively. This relationship leads to two groups of singularities: type R (redundant) and type I (impossible).

The singularities of type R are redundant input (RI), redundant output (RO), and redundant passive motion (RPM). The RI singularities occur when the motion of the platform along certain directions cannot be achieved while the actuators have motion, i.e., $\dot{\mathbf{x}} = 0$, $\dot{\Omega}_a \neq 0$ and $\dot{\Omega}_p \neq 0$; this singularity is equivalent to the instantaneous motion singularity, i.e., $[\mathbf{B}]$ is singular in Eq. (2.2). The RO singularities occur when the mobile platform has instantaneous motion along some directions while the actuators are locked, i.e., $\dot{\mathbf{x}} \neq 0$, $\dot{\Omega}_a = 0$ and $\dot{\Omega}_p \neq 0$; this singularity is equivalent to the force singularity, i.e., $[\mathbf{A}]$ is singular in Eq. (2.2). The RPM singularities happen when the passive joints allow motion even if the actuated joints and the mobile platform are locked, i.e., $\dot{\mathbf{x}} = 0$, $\dot{\Omega}_a = 0$ and $\dot{\Omega}_p \neq 0$.

The singularities of type I are impossible input (II), impossible output (IO), and increased instantaneous mobility (IIM). The II singularities occur when an arbitrary velocity of the joints $\dot{\Omega}_a$ cannot satisfy the velocity equation Eq. (2.4) for any combination of $\dot{\mathbf{x}}$ and $\dot{\Omega}_p$. The IO singularities occur when there is a $\dot{\mathbf{x}}$ for which Eq. (2.4) cannot be satisfied for any combination of $\dot{\Omega}$. The IIM singularities happen

when the instantaneous motion is greater than the full-cycle mobility of the kinematic chain, also referred to as an uncertainty configuration by Hunt (1978); this singularity is equivalent to the combined singularity, i.e., both [**A**] and [**B**] are singular. Thus, the mobile platform can move instantaneously even if all the actuators are locked; but also the mobile platform cannot move along certain directions even if all the actuated joints undergo instantaneous motion.

Zlatanov et al. (1998b) also presented a more detailed classification by considering the combinations among the types of singularities.

Zlatanov et al. (2002) identified a special type of singularity known as constraint singularity. This singularity occurs in manipulators with n-dof with $n < 6$ and the mobile platform gains instantaneously one degree of freedom motion. This singularity, however, cannot be identified using the velocity relationship, i.e., [**A**] is not singular.

2.3 Screw Theory Method

2.3.1 Line Coordinates

A line can be specified by two points, e.g., $\mathbf{P}_a$ and $\mathbf{P}_b$. Mathematically, these points define position vectors, whose elements are projections on the axes of a reference frame. Given that the points can be located anywhere on the line, one of the projections can be chosen freely, yielding only four independent quantities. Similarly, a line can be defined by a point $\mathbf{P}_a$ and a direction $\boldsymbol{l} = \mathbf{P}_b - \mathbf{P}_a$. The point can be placed anywhere on the line and the direction is constrained to be a unit vector, again yielding four independent parameters.

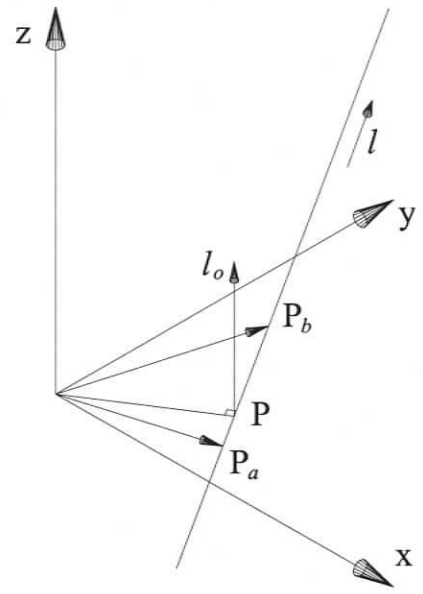

Figure 2.1: Definition of Plücker Coordinates for a Line in Space.

Plücker (1868-9) or line coordinates is another way to represent a line in space (Woo and Freudenstein, 1970). Let $\boldsymbol{l}$ be the unit vector defining the direction of the line and $\boldsymbol{l}_o$ be the moment of the line about the origin of the reference frame, which is defined as

$$\boldsymbol{l}_o = \mathbf{P} \times \boldsymbol{l} \tag{2.5}$$

and shown in Figure 2.1. Since $\boldsymbol{l}$ is a unit vector and the moment $\boldsymbol{l}_o$ is orthogonal to the direction, the following conditions have to be satisfied:

$$l_x^2 + l_y^2 + l_z^2 = 1 \tag{2.6a}$$

$$\boldsymbol{l}_o \cdot \boldsymbol{l} = 0 \tag{2.6b}$$

Line coordinates, therefore, only represent four independent quantities.

2.3.2 Screw Coordinates

Background

The concept of a screw axis was mentioned as early as 1763 by Giulio Mozzi. On helicoidal motion, there are two movements, one that is a rotation about an axis that crosses the centre of gravity, and the other is linear and common to all the points of the body and is parallel to the axis of rotation. Mozzi referred to this axis as a spontaneous axis of rotation. A more detailed historical overview about Mozzi's work is presented in Ceccarelli (2000).

The pioneer on Screw Theory was Robert S. Ball (1900), who created the terminology that is used today. A screw ($) is a line in space having an associated pitch and is represented as:

$$\$ = \left\{ \begin{array}{c} \mathbf{s} \\ \mathbf{s}_o \end{array} \right\} = \left\{ \begin{array}{c} \boldsymbol{l} \\ \boldsymbol{l}_o + p_L \ \boldsymbol{l} \end{array} \right\} \tag{2.7}$$

where $\mathbf{s}$ and $\mathbf{s}_o$ are the unit screw coordinates, $\boldsymbol{l}$ and $\boldsymbol{l}_o$ are the Plücker coordinates of the line, and p_L is the pitch of the screw. The pitch of the screw is a scalar of linear magnitude defined as "the rectilinear distance through which the nut is translated parallel to the axis of the screw, while the nut is rotated through the angular unit of circular measure" (Ball, 1900). Therefore, the pitch is the ratio of the linear translation to the angular rotation. The pitch of a screw is zero if there is a pure rotation about the screw axis, while the pitch of the screw is infinite if there is pure translation along the screw axis.

Screw Coordinates of the Joints of Spatial Parallel Manipulators

Joints of manipulators can be modelled with screw coordinates as follows:

$$\$ = \left\{ \begin{array}{c} \hat{\mathbf{z}} \\ \vec{\mathbf{r}} \times \hat{\mathbf{z}} + p_L \, \hat{\mathbf{z}} \end{array} \right\} \tag{2.8}$$

where $\hat{\mathbf{z}}$ and $\vec{\mathbf{r}}$ are the direction and position vector of a joint with respect to a reference frame, respectively.

For revolute joints the associated pitch is equal to zero (pure rotation). Therefore, the above expression can be reduced to

$$\$_{rev} = \left\{ \begin{array}{c} \hat{\mathbf{z}} \\ \vec{\mathbf{r}} \times \hat{\mathbf{z}} \end{array} \right\} \tag{2.9}$$

For prismatic joints the associated pitch is equal to infinity (pure translation), and by normalizing Eq. (2.8) the following screw coordinates result

$$\$_{pris} = \left\{ \begin{array}{c} \bar{\mathbf{0}} \\ \hat{\mathbf{z}} \end{array} \right\} \tag{2.10}$$

Screw Coordinates of the Joints of Planar Parallel Manipulators

Since parallel manipulators are composed of multiple branches, screw coordinates are labeled ${}^{\text{ref}}\$_{j_i}$, where j and i represent the joint and branch respectively and {ref} is a reference frame, which in further chapters will be referred to as an inertial frame instantaneously attached to the mobile platform. Thus, the joints of parallel manipulators modelled with screw coordinates with respect to {ref} are

$${}^{\text{ref}}\$_{j_i} = \left\{ \begin{array}{c} {}^{\text{ref}}\hat{\mathbf{z}}_{j_i} \\ ({}^{\text{ref}}\vec{\mathbf{r}}_{\text{ref}\rightarrow j_i} \times {}^{\text{ref}}\hat{\mathbf{z}}_{j_i} + p_L \, {}^{\text{ref}}\hat{\mathbf{z}}_{j_i}) \end{array} \right\} \tag{2.11}$$

where ${}^{\text{ref}}\hat{\mathbf{z}}_{j_i}$ and $({}^{\text{ref}}\vec{\mathbf{r}}_{\text{ref}\to j_i} \times {}^{\text{ref}}\hat{\mathbf{z}}_{j_i})$ are the direction and moment of the j^{th} joint of the i^{th} branch with respect to $\{\text{ref}\}$, respectively. Thus, the coordinates of revolute and prismatic joints can be found from:

$$\text{Revolute} \quad {}^{\text{ref}}\$_{j_i} = \begin{Bmatrix} {}^{\text{ref}}\hat{\mathbf{z}}_{j_i} \\ ({}^{\text{ref}}\vec{\mathbf{r}}_{\text{ref}\to j_i} \times {}^{\text{ref}}\hat{\mathbf{z}}_{j_i}) \end{Bmatrix} \tag{2.12}$$

$$\text{Prismatic} \quad {}^{\text{ref}}\$_{j_i} = \begin{Bmatrix} \hat{0} \\ {}^{\text{ref}}\hat{\mathbf{z}}_{j_i} \end{Bmatrix} \tag{2.13}$$

2.3.3 Twists and Wrenches

Background

Mozzi's work was rigorously proved by Michel Chasles (1830), who published the theorem for the general motion of rigid bodies: "Any displacement of a rigid body can be effected by a single rotation about a unique axis combined with a unique translation parallel to that axis" (Roth, 1984). Louis Poinsot (1806) presented the theorem regarding forces and moments applied on a rigid body: "Any system of forces (and moments) applied to a rigid body can be uniquely replaced by a single force and a couple, in such a way that the single force is parallel to the axis of the couple" (Roth, 1984).

Modelling Twists and Wrenches with Screw Coordinates

Chasles' and Poinsot's Theorems can be modelled with screw quantities. The angular velocity $\boldsymbol{\omega}$ and the translational velocity $\mathbf{v}$ of a point of a moving body may be represented by three-dimensional vectors that can be assembled into a screw quantity

V called a twist,

$$\mathbf{V} = \alpha_{\mathrm{T}} \$ = \left\{ \begin{array}{c} \boldsymbol{\omega} \\ \mathbf{v} \end{array} \right\} \tag{2.14}$$

where α_{T} is known as the twist amplitude (Ball, 1900) and its magnitude, for a finite-pitch twist, corresponds to the magnitude of the angular velocity $\boldsymbol{\omega}$, so the direction of the screw **s** is a unit vector as shown in Eq. (2.7). For an infinite-pitch twist (a pure translational velocity), α_{T} corresponds to the magnitude of **v**. The pitch of the twist is the ratio of the translational velocity to the angular velocity. The pitch of a twist is zero if there is pure rotational velocity about the screw axis, while the pitch of the twist is infinite if there is pure translational velocity along the screw axis.

On the other hand, the resultant force **f** and the moment **m** acting at a point on the body can be assembled into a similar screw quantity **F** called a wrench,

$$\mathbf{F} = w\$' = \left\{ \begin{array}{c} \mathbf{f} \\ \mathbf{m} \end{array} \right\} \tag{2.15}$$

where w is known as the wrench intensity (Ball, 1900) and its magnitude, for a finite-pitch wrench, corresponds to the magnitude of the force vector **f**. For an infinite-pitch wrench (a pure moment), w corresponds to the magnitude of **m**. The pitch of a wrench is the ratio of the moment to the force. A pure force is a wrench of zero pitch and a pure moment is a wrench of infinite pitch.

In general, the twist and wrench are composed of six elements, i.e., for a twist, there are three rotations about and three translations along a reference frame; while for a wrench there are three pure forces along and three moments about a reference frame. For a manipulator with $n - dof$, where $n < 6$, such as planar manipulators, the same $6 - n$ coordinates of the joint twists and the output twist will be zero at

any configuration (Zlatanov et al., 1994c). For planar manipulators, \$ is the screw system of planar motion, which can be spanned by a rotation and two translations. Therefore, the twist and wrench will have only three non-zero coordinates. The twist is based on one angular velocity ω_z and two linear velocities v_x and v_y, while the wrench is comprised of two forces f_x and f_y and one moment m_z, i.e., $\mathbf{V} = \{\boldsymbol{\omega}^{\mathrm{T}}; \mathbf{v}^{\mathrm{T}}\}^{\mathrm{T}} = \{\omega_z; v_x, v_y\}^{\mathrm{T}}$ and $\mathbf{F} = \{\mathbf{f}^{\mathrm{T}}; \mathbf{m}^{\mathrm{T}}\}^{\mathrm{T}} = \{f_x, f_y; m_z\}^{\mathrm{T}}$, respectively.

Reciprocity

To define the concept of reciprocity for revolute and prismatic joints, assume a wrench acting on a twist. If the line of action of a force crosses the axis of a revolute joint, the force does not affect the rotation of the joint; i.e., the force cannot exert any moment about the joint. Therefore, the force is reciprocal to the joint. Also, if the moment of the wrench is perpendicular to the revolute joint axis, the moment is reciprocal to the joint. If the line of action of a force is perpendicular to the direction of a prismatic joint, the force does not affect the translation of the joint. Also a moment, regardless of its direction, is reciprocal to a prismatic joint. Two screws are said to be reciprocal if the power developed by the wrench on a twist is zero (Hunt, 1978). The wrench and twist are reciprocal if their reciprocal product is zero, i.e.,

$$\mathbf{V} \circledast \mathbf{F} = \boldsymbol{\omega} \cdot \mathbf{m} + \mathbf{v} \cdot \mathbf{f} = 0 \tag{2.16}$$

where $\circledast$ denotes the reciprocal product[1] between two screws.

[1]For planar manipulators, the reciprocal product of Eq. (2.16) is defined as:

$$\{\omega_z; v_x, v_y\} \circledast \{f_x, f_y; m_z\} = \omega_z \cdot m_z + v_x \cdot f_x + v_y \cdot f_y = 0$$

The velocity and static force problems of serial and parallel manipulators using screw theory are described in Appendix A.

2.3.4 Force-Unconstrained Poses

In this section, the methodology used to identify the force-unconstrained poses of parallel manipulators is described. The forces that can be applied (sustained) by a branch can be modelled with associated reciprocal screws. The force exerted by the k^{th} actuated joint of the i^{th} branch is characterized by a screw, $\mathbf{W}_{k_i}$, reciprocal to all joints of the i^{th} branch except for the actuated joint k, i.e.,

$$\$_{j_i} \circledast \mathbf{W}_{k_i} = 0, \text{ for } j \neq k \tag{2.17}$$

where $\$_{j_i}$ denotes the screw coordinates of all joints $j \neq k$ of the i^{th} branch. In general, reciprocal screws are composed of six elements; however, for a planar case, ${}^{\text{ref}}\mathbf{W}_{k_i}$ will have only three non-zero coordinates.

The force that can be applied by the i^{th} branch is

$$\mathbf{F}_i = \sum_{k=1}^{n_k} \mathbf{W}_{k_i} w_{k_i} \tag{2.18}$$

where w_{k_i} is the wrench intensity of the k^{th} actuated joint of the i^{th} branch and n_k is the number of actuated joints in the i^{th} branch. Notice that $n_k = 1$ for a fully-parallel manipulator. Assembling the associated reciprocal screws of the actuated joints of the device in a matrix yields

$$[\mathbf{W}] = [...\mathbf{W}_{k_i}...] \tag{2.19}$$

for $k = 1, \ldots, n_k$, and $i = 1, \ldots, n_b$, where n_b is the number of branches. The matrix $[\mathbf{W}]$ will be referred to as the associated reciprocal screw matrix and allows

the wrench acting on the mobile platform of the manipulator to be determined by

$$\mathbf{F} = \left\{ \begin{array}{c} \mathbf{f} \\ \\ \mathbf{m} \end{array} \right\} = \sum_{i=1}^{n_b} \mathbf{F}_i = [\mathbf{W}] \ \mathbf{w} \tag{2.20}$$

where $\mathbf{w}$ is the vector of wrench intensities. If the applied force is given and the vector of intensities is unknown, inversion of $[\mathbf{W}]$ allows $\mathbf{w}$ to be found as:

$$\mathbf{w} = [\mathbf{W}]^{-1} \ \mathbf{F} \tag{2.21}$$

If $[\mathbf{W}]$ is singular, an arbitrary force $\mathbf{F}$ cannot be sustained, i.e., the device is force unconstrained.

2.4 Analogy Between Methods

Under static conditions, the relationship between the torques (revolute joints) or forces (prismatic joints) applied by the actuated joints and the forces and moments exerted at the end-effector that describes the equilibrium of the system (Gosselin, 1990b) is given by

$$\mathbf{F}_g = [\mathbf{J}]^T \ \boldsymbol{\tau} \tag{2.22}$$

where $\mathbf{F}_g$ is the generalized vector of forces and moments acting at the end-effector (wrench), $\boldsymbol{\tau}$ is the vector of actuated torques or forces, and $[\mathbf{J}] = [\mathbf{B}]^{-1} [\mathbf{A}]$.

On the other hand, the relationship between the exerted wrench $\mathbf{F}$ and the vector of wrench intensities $\mathbf{w}$, previously defined in Eq. (2.20), can be expressed in terms of the torques or forces applied by the actuated joints, as shown in Appendix A.3.2,

$$\mathbf{w} = [\mathbf{D}] \, \boldsymbol{\tau} \tag{2.23}$$

where [**D**] involves the inverse of the reciprocal products of the actuated joints, i.e.,

$$[\mathbf{D}] = \begin{bmatrix} \ddots & & 0 \\ & \frac{1}{\$_{k_i} \circledast \mathbf{W}_{k_i}} & \\ 0 & & \ddots \end{bmatrix} \tag{2.24}$$

Substituting Eq. (2.23) in Eq.(2.20) yields

$$\mathbf{F} = [\mathbf{W}]\,[\mathbf{D}]\,\boldsymbol{\tau} \tag{2.25}$$

Since $\mathbf{F}_g \equiv \mathbf{F}$, Eq. (2.22) and Eq. (2.25) are equivalent, and the following analogy of the methods prevails

$$[\mathbf{W}]\,[\mathbf{D}] \equiv [\mathbf{J}]^{\mathrm{T}} \tag{2.26}$$

2.5 Mathematical Techniques for Identifying Force-Unconstrained Poses

2.5.1 Basic Approaches

Mathematically, the manipulator is force unconstrained when matrix [**W**] (or the Jacobian matrix [**A**] using the time derivative method) is singular. This is the reason why these special configurations are commonly referred to as singularities. There are three basic approaches to identify force-unconstrained configurations: numerical, analytical, and geometrical.

2.5.2 Numerical Technique

Numerical techniques predict how close a pose is from a singularity and are generally defined with indices. In general, the numerical technique if computationally efficient

can be implemented in real-time applications. For serial manipulators, Yoshikawa (1990) proposed indices to measure the capability of a manipulator to execute a desired task based on the determinant and the singular values of the Jacobian matrix. Gosselin (1990c) proposed dexterity indices that are frame invariant using the Jacobian condition number, addressing the problem that the entries of the Jacobian matrix are components of a different nature (linear and angular velocities), i.e., scaling the dimensions of the manipulator affects the value of the condition number.

Gosselin (1990b) related the stiffness and the singularities of parallel manipulators by means of the condition number. Park and Kim (1998) considered adding weighting matrices resulting in a condition number that is frame invariant; nevertheless, the weighting matrices have to be chosen in an arbitrary manner (Merlet, 2000). Lee et al. (1999) introduced the so-called quality index, which is the quotient of the absolute value of the Jacobian determinant over the maximum value of the Jacobian determinant for a particular manipulator,

$$\lambda = \frac{|\det([\mathbf{J}])|}{\det([\mathbf{J}]_m)} \tag{2.27}$$

where $0 \leq \lambda \leq 1$. This method was also considered for redundant manipulators based on derivations of the Stewart-Gough platform, namely for the 4-4 manipulator (Zhang and Duffy, 1998), the 8-4 manipulator (Zhang et al., 2000a), and the 8-8 manipulator (Zhang et al., 2000b), where the numbers represent the attachment layout between the fixed and mobile platforms. For redundant manipulators the quality index is given by

$$\lambda = \sqrt{\frac{\left|\det([\mathbf{J}]\,[\mathbf{J}]^{\mathrm{T}})\right|}{\det([\mathbf{J}]_m\,[\mathbf{J}]_m^{\mathrm{T}})}} \tag{2.28}$$

Voglewede and Ebert-Uphoff (2004) incorporated several measures into a constrained optimization problem, resulting in a general eigenvalue problem. The op-

timization framework involves four measures, namely, minimal eigenvalue, power, stiffness, and natural frequency. However, the incorporation of all these measures may not be suitable for real time application.

2.5.3 Analytical Technique

Analytical techniques are based on setting the symbolical solution of the Jacobian matrix determinant to zero, i.e., forcing $[\mathbf{A}]$ or $[\mathbf{W}]$ to be singular. Solving for the determinant is generally a very complicated algebraic process even using symbolic computation software (Merlet, 2000). Also, another inconvenience may arise with this technique, finding the roots of the determinant, which can be expressed as a polynomial. Nevertheless, the resulting polynomial corresponds to all possible force-unconstrained poses.

This technique has been implemented in parallel manipulators with simple architectures, such as planar manipulators, spherical manipulators, and special 6-dof manipulators. Among works related to planar manipulators, Sefrioui and Gosselin (1995) and Mohammadi-Daniali et al. (1995) applied the time derivative technique; Collins and McCarthy (1998) and Husty et al. (1999) projected the kinematic constraints into the planar quaternion space to simplify the non-linear terms; and Bonev et al. (2003) and Firmani and Podhorodeski (2004b) used screw quantities. Sefrioui and Gosselin (1994) determined the singularity loci of spherical 3-dof parallel manipulators. Tahmasebi and Tsai (1994) showed the conditions that lead to singular configurations of a special 6-dof manipulator. Mayer St-Onge and Gosselin (1996) showed that the singularity loci of the general 6-6 Stewart-Gough platform can be determined by expanding the determinant by the cofactors of the first row. This

process is repeated until the cofactors are 3×3 matrices and analytical expressions of their determinants can be obtained.

The analytical technique is definitely computationally expensive but it can be performed during the design process prior to the construction of the manipulator. The main advantage of this technique over the numerical approach stands in understanding the nature of these singularities: how these singularities may change with different design specifications, and how these singularities may be affected with the inclusion of redundancy.

2.5.4 Geometrical Technique

Based on screw theory, an approach to identify singular configurations of parallel manipulators involving line geometry has been considered. Dandurand (1984) addressed the problem of rigidity conditions of compound spatial grids by means of line geometry. This approach is implemented in parallel manipulators by determining if the associated reciprocal screw matrix is rank deficient. Since the columns of the associated reciprocal screw matrix consist of Plücker or line coordinates, the singularity analysis of parallel manipulators is based on finding geometrical conditions for linear dependency among these lines. The identification of force-unconstrained configurations is carried out synthetically. A detailed classification of the dependency between lines was developed by Merlet (1989), and then augmented by Hao and McCarthy (1998) who included additional subcases. Basically, this classification consists of five types of linearly dependent lines based on the resulting rank of the Jacobian. A singularity of type n occurs when one associated reciprocal screw is a linear combination of at least n other associated reciprocal screws.

Some of the relevant articles related to the identification of force-unconstrained configurations in parallel manipulators using Grassmann line geometry follow. Merlet (1989) identified the conditions of force-unconstrained configurations of the 6-3 Stewart-Gough platform. Collins and Long (1995) determined all possible line dependencies of a 6-dof joystick formed with three pantograph linkages. Notash (1998) identified uncertainty configurations of the RSI joystick and, in addition, presented a detailed analysis of how the different types of singularities can be eliminated by including redundant actuation. Ebert-Uphoff et al. (2002) introduced, for manipulators with three branches and two actuators in each branch, a characteristic tetrahedron, whose singularity corresponds to the singularity of the manipulator.

For planar parallel manipulators, the conditions that cause the associated reciprocal screw matrix to be rank deficient are:

- Type 1 (rank($[\mathbf{W}]$) = 1).- *All associated reciprocal screws being collinear.* This type of singularity will occur if and only if the architecture of the manipulator is such that all associated reciprocal screws can be collinear.

- Type 2 (rank($[\mathbf{W}]$) = 2).- *All associated reciprocal screws intersecting at a common point (planar pencil).* This is the general type of singularity for planar parallel manipulators, which includes the case when all associated reciprocal screws are parallel, i.e., intersection at infinity.

Mohammadi-Daniali et al. (1995) described the unconstrained motion, gained by the manipulator, based on the existence of a planar pencil. If the associated reciprocal screws intersect at infinity, the mobile platform can move along the direction normal to the direction of the associated reciprocal screws, this occurs even if all the actuators are locked; likewise, a force in the normal direction cannot be sustained

by the actuators. Whereas, if the reciprocal screws intersect at a common point other than infinity, the mobile platform can rotate about that point, even if all the actuators are locked, likewise, a moment applied to the mobile platform cannot be balanced by the actuators.

2.6 Discussion

In this Chapter, force-unconstrained configurations of parallel manipulators were analyzed with two methods: time derivative and screw theory. Also, different techniques that can be adopted to identify these configurations were described. A discussion of these methods and techniques follows.

With the time derivative method, the differentiation of the non-linear kinematic constraints may lead to large expressions. However, this method has the advantage that the Jacobian matrix $[\mathbf{A}]$ is a function of the position and orientation of the mobile platform, which represents the pose of the manipulator. Whereas, with the screw theory method the entries of the associated reciprocal screw matrix, $[\mathbf{W}]$, which are a function of joint displacements, tend to be compact and sometimes the associated reciprocal screws can be geometrically identified. However, the problem arises when the joint displacements are transformed into the task space variables.

The mathematical techniques described in this Chapter can be implemented depending on the singularity analysis approach. Numerical techniques provide the information of how close a pose of the manipulator is from a singular configuration making these techniques suitable for real-time applications. Another use for these techniques could be to identify force-unconstrained poses by setting one of the described indices as the objective function of an optimization problem. Whenever the

index function is minimized, the manipulator is force unconstrained; however, such analysis would only identify a single pose. These techniques are not appropriate for the identification of all force-unconstrained poses because they would require a large number of starting points in the optimization algorithm.

Analytical methods yield a multivariable expression that represents all possible force-unconstrained poses. The graphical representation of these poses is defined by a manifold or a set of manifolds in the same dimensional space. These manifolds can be plotted by assuming all variables but one, so the expression is reduced to a single-variable polynomial. For instance, the singularity-locus expression of non-redundant planar parallel manipulators results in a three-variable equation, thus two variables may be assumed yielding a two-dimensional manifold[2]. The roots of the single-variable polynomial will determine the force-unconstrained poses of the manipulator. If an analytical technique is feasible for a specific manipulator, it can be used as an important parameter for the design of the manipulator as well as for the design of the trajectory that the manipulator may follow.

The screw theory method has the advantage of incorporating the geometrical technique, which provides a geometrical insight allowing a visualization of specific kinematic conditions that cause the manipulator to be force unconstrained. In this dissertation, planar parallel manipulators are considered, thus analytical solutions are feasible.

In the following chapters a study of force-unconstrained configurations for non-redundant and redundant planar parallel manipulators is presented.

[2]This analysis is presented in detail in Chapter 3.

Chapter 3

Force-Unconstrained Poses of Non-Redundant Planar Parallel Manipulators

3.1 Overview

In this chapter, the force-unconstrained poses of non-redundant planar parallel manipulators are presented. First, an introduction of planar parallel manipulators and possible actuation layouts is described. Then, detailed examples, namely the 3-RPR, 3-PRR, and 3-RRR manipulators, are presented. Each manipulator problem contains a literature review, description of the mechanism, Denavit and Hartenberg parameters, solution of their screws and reciprocal screws, kinematic analysis, and force-unconstrained poses. The chapter ends with a discussion of the obtained results.

3.2 Introduction

As mentioned in Section 1.6.1 and illustrated in Figure 1.2, there are seven planar parallel manipulators with homogeneous layouts of branches. With the same criteria, the actuation of these manipulators will be considered homogeneous, i.e., the same joint in all branches will be actuated. This leads to twenty-one possible actuation layouts. Bonev (2002) and Bonev et al. (2003) analyzed all possible actuation layouts, which are described in Table 3.1. There are some manipulators that have invalid actuation schemes as described by Williams II and Shelley (1997). The Jacobian matrix of these manipulators is rank deficient at any configuration. The invalid actuation schemes are branches composed of two prismatic joints and one revolute joint, with the latter being actuated (Merlet, 1996b). Physically, if all the actuators are locked, the points of connection between the mobile platform and the branches can be located at any position on the plane. Since this is true for all three branches, the platform can translate on the plane yielding uncontrollable degrees of freedom. Such mechanisms are marked with $^{\times}$. There are also mechanisms that are kinematically equivalent, i.e., the inversion of the mechanism yields another one (e.g., $\underline{\mathrm{P}}\mathrm{RR} \equiv \mathrm{RR}\underline{\mathrm{P}}$). These mechanisms are marked with $\bar{}$. The R$\underline{\mathrm{R}}$R mechanism is kinematically equivalent to the R$\underline{\mathrm{P}}$R mechanism and is marked with $^{\circ}$. Thus, the nine mechanisms in bold are the unique possible actuation layouts.

Table 3.1: Actuation Layouts of Each Branch.

R$\underline{\mathrm{R}}$R	**R$\underline{\mathrm{P}}$R**	R$\underline{\mathrm{P}}\mathrm{P}^{\times}$	**P$\underline{\mathrm{R}}$R**	**P$\underline{\mathrm{P}}$R**	**PP$\underline{\mathrm{R}}$**	**RR$\underline{\mathrm{P}}$**
R$\underline{\mathrm{R}}\mathrm{R}^{\circ}$	**R$\underline{\mathrm{P}}$R**	**R$\underline{\mathrm{P}}$P**	**P$\underline{\mathrm{R}}$R**	P$\underline{\mathrm{R}}\mathrm{P}^{\times}$	PP$\underline{\mathrm{R}}^{\bar{}}$	RR$\underline{\mathrm{P}}^{\bar{}}$
RR$\underline{\mathrm{R}}^{\bar{}}$	RP$\underline{\mathrm{R}}^{\bar{}}$	RP$\underline{\mathrm{P}}^{\bar{}}$	PR$\underline{\mathrm{R}}^{\bar{}}$	PR$\underline{\mathrm{P}}^{\bar{}}$	PP$\underline{\mathrm{R}}^{\times}$	RR$\underline{\mathrm{P}}^{\bar{}}$

The forces applied by each actuated joint of the layouts described in Table 3.1 are modelled with associated reciprocal screws. Based on the definition of reciprocity given in Section 2.3.1, the associated reciprocal screws of the actuated joints (joint 1 actuated W_{1_i} and joint 2 actuated W_{2_i}) are illustrated in Figure 3.1.

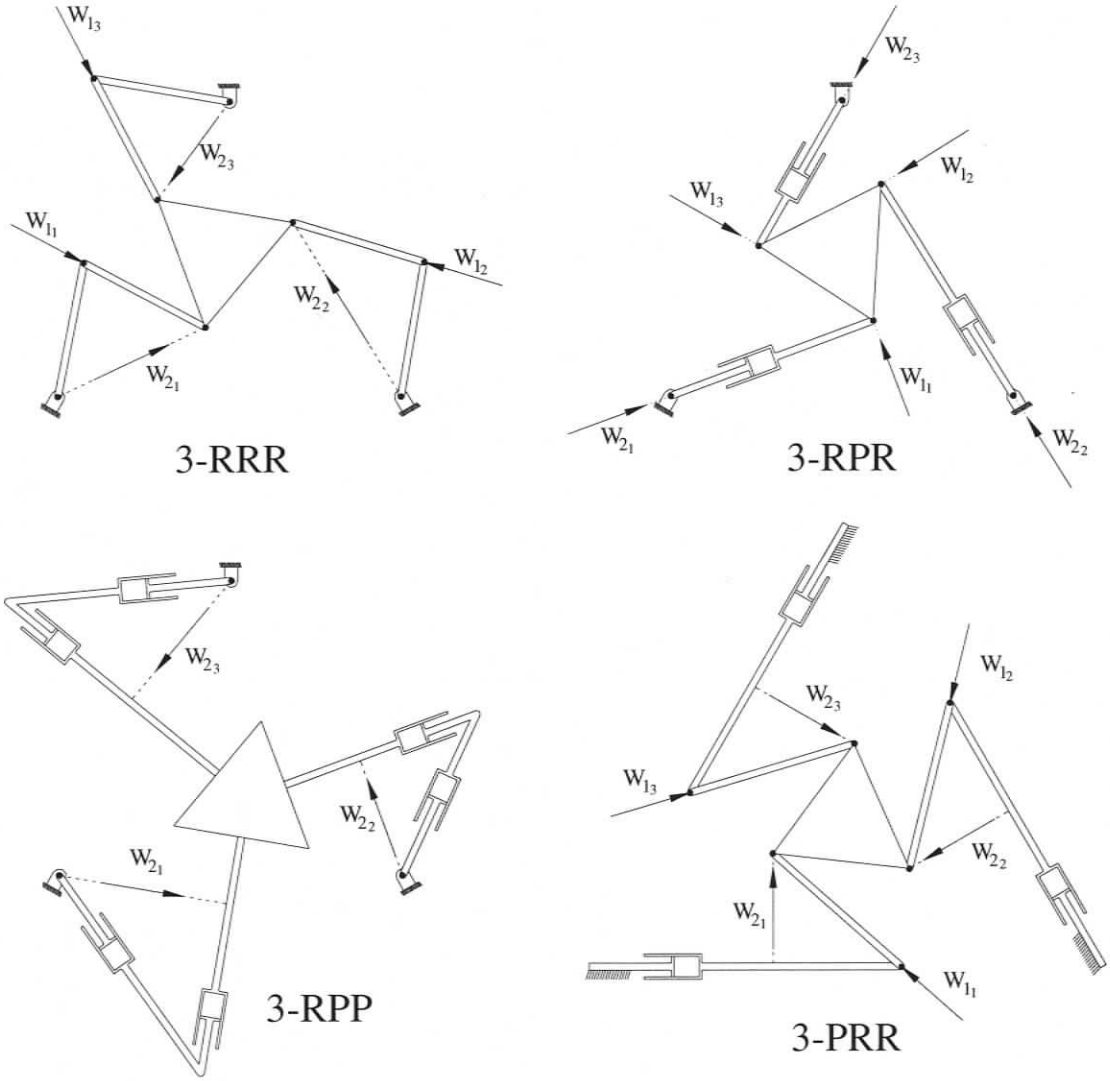

Figure 3.1: Representation of the Associated Reciprocal Screws on PPMs.

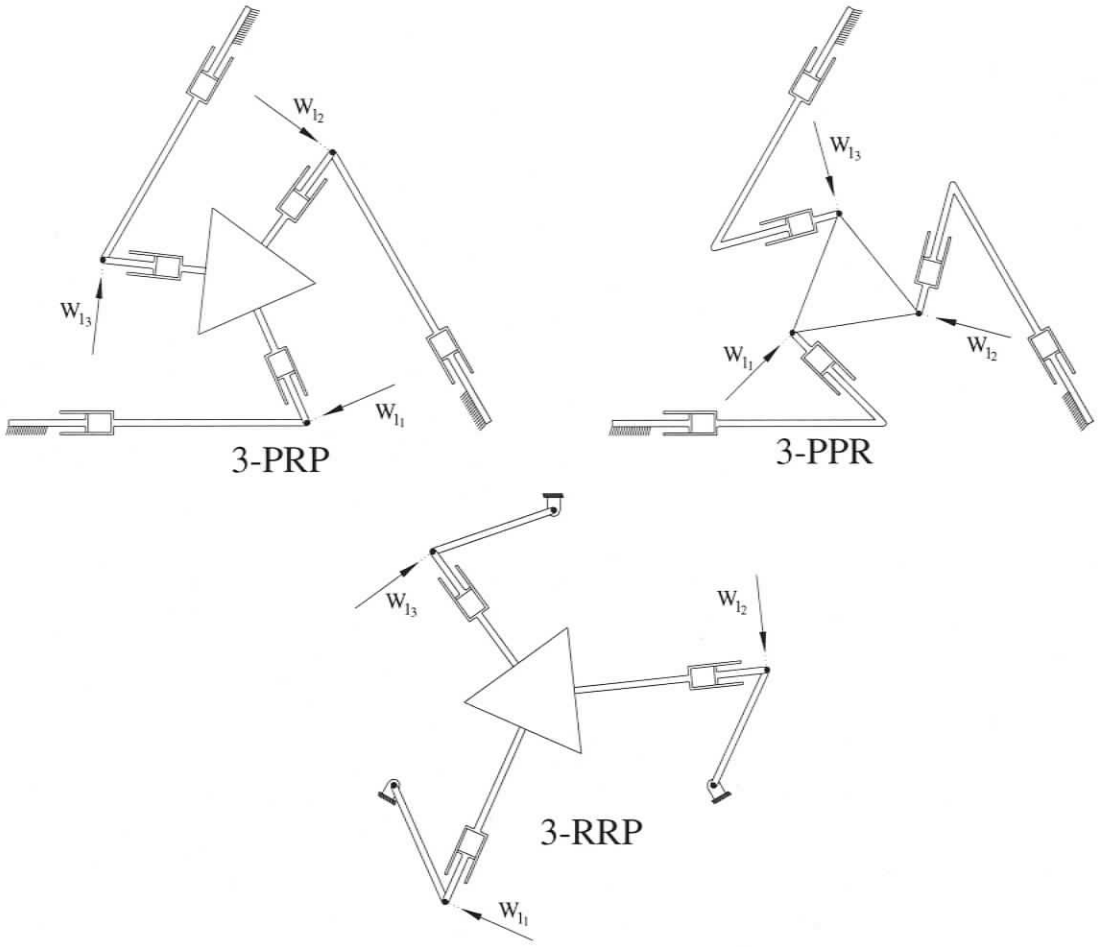

Figure 3.1 (cont'd): Representation of the Associated Reciprocal Screws on PPMs.

The associated reciprocal screw matrix [**W**] for each possible actuation layout are assembled as follows:

$$\text{First joint being actuated} \qquad [\mathbf{W}] = \begin{bmatrix} \mathbf{W}_{1_1} & \mathbf{W}_{1_2} & \mathbf{W}_{1_3} \end{bmatrix}$$

$$\text{Second joint being actuated} \qquad [\mathbf{W}] = \begin{bmatrix} \mathbf{W}_{2_1} & \mathbf{W}_{2_2} & \mathbf{W}_{2_3} \end{bmatrix}$$

A force-unconstrained pose occurs when all associated reciprocal screws intersect at a common point, also known as planar pencil singularity (Hunt, 1978), i.e., matrix

[**W**] is singular. Thus, force-unconstrained poses can be identified by setting to zero the determinant of [**W**], i.e., $|[\mathbf{W}]| = 0$.

Among the remaining mechanisms, the ones containing a passive prismatic joint will not be considered in this dissertation because it would not be reasonable to include a prismatic joint, which is usually a fairly expensive device, as a passive joint. This leads to only three mechanisms to be examined: 3-R<u>P</u>R, 3-<u>P</u>RR, and 3-<u>R</u>RR.

3.3 Force-Unconstrained Poses of the 3-R<u>P</u>R PPM

3.3.1 Background

The 3-R<u>P</u>R manipulator may be considered as the planar version of the Stewart-Gough platform (Dasgupta and Mruthyunjaya, 2000). This device is not very suitable for industrial applications that required high speeds because of the high inertia due to the weighty actuators within the mobile linkage (Bonev, 2002). In spite of this, the 3-R<u>P</u>R manipulator is a good reference as an introductory mechanism for the other manipulators studied in this dissertation, which present a greater challenge.

The forward displacement problem of this manipulator was solved by Gosselin et al. (1992), who derived a sixth order polynomial whose roots represent all possible postures of the manipulator for a specific set of joint displacements. Analytical expressions of the singularity loci of this manipulator were identified by Sefrioui and Gosselin (1995), yielding two quadratic surfaces in a three-dimensional space defined by the position (x and y) and orientation (ϕ) of the mobile platform. For constant payload orientation, these singularities can be plotted as quadratic curves in the xy plane as either hyperbolas, parabolas, or ellipses. The derivation of the analyti-

cal expressions was obtained using the input-output speed relationship of Eq. (2.2). Collins (1997) and Collins and McCarthy (1998) applied Clifford algebra of the projective plane yielding a quartic polynomial in the homogeneous coordinates represented by quaternions. Similarly, Husty et al. (1999) projected the kinematic constraints into the planar quaternion space and carried out a parametrization of the singularity surface. Kong and Gosselin (2000) analyzed the singularity loci of this manipulator with similar platforms resulting in two conditions. The first condition shows that if the mobile platform is either oriented as or rotated 180° with respect to the fixed platform, the manipulator will be force unconstrained. The second condition shows that in any other orientation there will be circles of singularities. Bonev (2002) and Bonev et al. (2003) identified, besides the force-unconstrained poses, redundant passive motion (RPM) singularities. These singularities occur when the displacement of one of the prismatic joints is zero. Thus, the passive revolute joints are collinear allowing motion even if the actuated joints and the mobile platform are locked. Li et al. (2006) presented the singularity loci of this manipulator and analyzed, for a given position, the maximal singularity-free zones, which are represented by cylinders.

In this section, the Denavit and Hartenberg (DH) parameters (Denavit and Hartenberg, 1955) of each branch are determined using Craig's convention (Craig, 1987). Then the time derivative and screw theory methods are applied and subsequently compared. Finally, an example of force-unconstrained poses is presented.

3.3.2 Denavit and Hartenberg Parameters

The notation of the geometric variables of the manipulator are shown in Figure 3.2. The DH parameters describing the 3-R$\underline{P}$R layout are given in Table 3.2, where j and

i represent the joint and branch numbers, respectively, and $\{\text{ref}\}\equiv\{3_1\}$. To keep the DH parameters in a general form $l_1 = 0$, $\beta_1 = 0$, $\beta_2 = \pi$, and $\beta_3 = \pi - \alpha_3$.

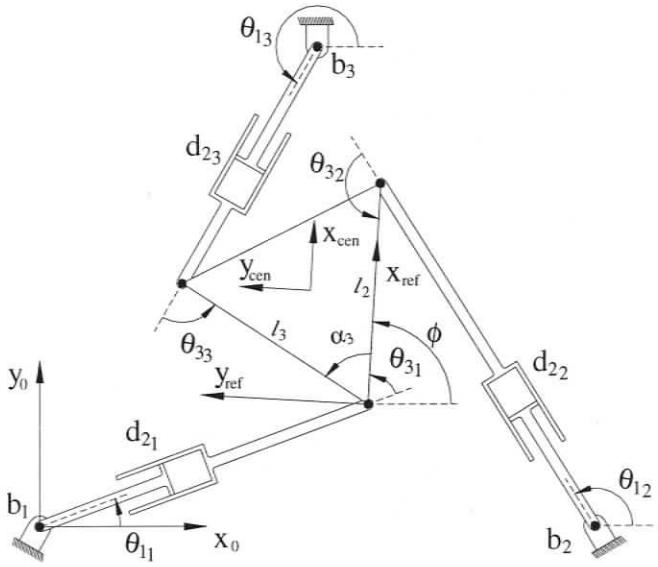

Figure 3.2: Layout of the 3-RPR Planar Parallel Manipulator.

Table 3.2: DH Parameters of the 3-RPR Manipulator.

$j-1$	α_{j-1}	a_{j-1}	d_j	θ_{j_i}	j
b_i	0	0	0	$\theta_{1_i} - \frac{\pi}{2}$	1_i
1_i	$-\frac{\pi}{2}$	0	d_{2_i}	0	2_i
2_i	$\frac{\pi}{2}$	0	0	$\theta_{3_i} + \frac{\pi}{2}$	3_i
3_i	0	l_i	0	β_i	ref

The homogeneous transform, ${}^{0}_{b_i}[\mathbf{T}]$, of the i^{th} branch base $b_i = [bx_i, by_i]^{\mathrm{T}}$ for $i = 1, 2, 3$ with respect to $\{0\}$ is shown below.

$$ {}^{0}_{b_i}[\mathbf{T}] = \begin{bmatrix} 1 & 0 & 0 & bx_i \\ 0 & 1 & 0 & by_i \\ 0 & 0 & 1 & 0 \\ 0 & 0 & 0 & 1 \end{bmatrix} \tag{3.1} $$

3.3.3 Time Derivative Method

The following equations describing the forward displacement solution can be obtained

$$ x = bx_i + d_{2_i} \cos(\theta_{1_i}) + l_i \cos(\theta_{1_i} + \theta_{3_i} + \beta_i) \tag{3.2a} $$

$$ y = by_i + d_{2_i} \sin(\theta_{1_i}) + l_i \sin(\theta_{1_i} + \theta_{3_i} + \beta_i) \tag{3.2b} $$

$$ \phi = \theta_{1_i} + \theta_{3_i} + \beta_i \tag{3.2c} $$

where $l_1 = 0$, $\beta_1 = 0$, $\beta_2 = \pi$, and $\beta_3 = \pi - \alpha_3$.

In order to eliminate θ_{1_i} Eq. (3.2c) is substituted in Eqs. (3.2a and 3.2b). Then, θ_{3_i} is eliminated by squaring and adding Eqs. (3.2a and 3.2b) together, yielding

$$ d_{2_1}^2 = x^2 + y^2 \tag{3.3a} $$

$$ d_{2_2}^2 = (x + l_2 \cos\phi - bx_2)^2 + (y + l_2 \sin\phi)^2 \tag{3.3b} $$

$$ d_{2_3}^2 = (x + l_3 \cos(\phi + \alpha_3) - bx_3)^2 + (y + l_3 \sin(\phi + \alpha_3) - by_3)^2 \tag{3.3c} $$

The time derivative of these equations lead to the relationship between the input

and output speeds $[\mathbf{A}]\,\dot{\mathbf{x}} = [\mathbf{B}]\,\dot{\mathbf{q}}$, where matrix $[\mathbf{A}]$ is described as

$$[\mathbf{A}] = \frac{\partial f(\mathbf{q},\mathbf{x})}{\partial \mathbf{x}} = 2\begin{bmatrix} x & y & 0 \\ x - bx_2 + l_2 c\phi & y + l_2 s\phi & l_2\,(yc\phi - (x - bx_2)\,s\phi) \\ x - bx_3 + l_3 c\,(\phi + \alpha_3) & y - by_3 + l_3 s\,(\phi + \alpha_3) & l_3\,((y - by_3)\,c\,(\phi + \alpha_3) - (x - bx_3)\,s\,(\phi + \alpha_3)) \end{bmatrix} \tag{3.4}$$

where s and c are the sine and cosine of the angles, while matrix $[\mathbf{B}]$ is described as

$$[\mathbf{B}] = \frac{\partial f(\mathbf{q},\mathbf{x})}{\partial \mathbf{q}} = 2\begin{bmatrix} d_{2_1} & 0 & 0 \\ 0 & d_{2_2} & 0 \\ 0 & 0 & d_{2_3} \end{bmatrix} \tag{3.5}$$

Finally, the combined Jacobian $[\mathbf{J}]$ that allows solving $\dot{\mathbf{q}} = [\mathbf{J}]\,\dot{\mathbf{x}}$ (inverse velocity problem) is

$$[\mathbf{J}] = [\mathbf{B}]^{-1}\,[\mathbf{A}] \tag{3.6}$$
$$= \begin{bmatrix} \frac{x}{d_{2_1}} & \frac{y}{d_{2_1}} & 0 \\ \frac{x - bx_2 + l_2 c\phi}{d_{2_2}} & \frac{y + l_2 s\phi}{d_{2_2}} & \frac{l_2(yc\phi - (x - bx_2)s\phi)}{d_{2_2}} \\ \frac{x - bx_3 + l_3 c(\phi + \alpha_3)}{d_{2_3}} & \frac{y - by_3 + l_3 s(\phi + \alpha_3)}{d_{2_3}} & \frac{l_3((y - by_3)c(\phi + \alpha_3) - (x - bx_3)s(\phi + \alpha_3))}{d_{2_3}} \end{bmatrix}$$

3.3.4 Screw Theory Method

Screw Quantities

For the 3-RPR, the following joint screws written in matrix form per branch result:

$${}^{\text{ref}}[\$_1] = \begin{bmatrix} {}^{\text{ref}}\$_{1_1} & {}^{\text{ref}}\$_{2_1} & {}^{\text{ref}}\$_{3_1} \end{bmatrix}$$
$$= \begin{bmatrix} 1 & 0 & 1 \\ d_{2_1} \sin(\theta_{3_1}) & \cos(\theta_{3_1}) & 0 \\ d_{2_1} \cos(\theta_{3_1}) & -\sin(\theta_{3_1}) & 0 \end{bmatrix} \tag{3.7a}$$

$$
\begin{aligned}
{}^{\text{ref}}[\$_2] &= [\ {}^{\text{ref}}\$_{1_2}\quad {}^{\text{ref}}\$_{2_2}\quad {}^{\text{ref}}\$_{3_2}\ ] \\
&= \begin{bmatrix} 1 & 0 & 1 \\ -d_{2_2}\sin(\theta_{3_2}) & -\cos(\theta_{3_2}) & 0 \\ -d_{2_2}\cos(\theta_{3_2}) - l_2 & \sin(\theta_{3_2}) & -l_2 \end{bmatrix} \qquad (3.7b) \\
{}^{\text{ref}}[\$_3] &= [\ {}^{\text{ref}}\$_{1_3}\quad {}^{\text{ref}}\$_{2_3}\quad {}^{\text{ref}}\$_{3_3}\ ] \\
&= \begin{bmatrix} 1 & 0 & 1 \\ -d_{2_3}\sin(\theta_{3_3}-\alpha_3) + l_3\sin\alpha_3 & -\cos(\theta_{3_3}-\alpha_3) & l_3\sin\alpha_3 \\ -d_{2_3}\cos(\theta_{3_3}-\alpha_3) - l_3\cos\alpha_3 & \sin(\theta_{3_3}-\alpha_3) & -l_3\cos\alpha_3 \end{bmatrix} \qquad (3.7c)
\end{aligned}
$$

The associated reciprocal screws of the actuated joints are found using the reciprocal products of Eq. (2.17) as follows:

Branch 1 $\mathbf{W}_{2_1} \circledast \$_{j_1} = 0$, for j $\neq$2; yielding

$$ {}^{\text{ref}}\mathbf{W}_{2_1} = \{\cos\theta_{3_1},\ -\sin\theta_{3_1};\ 0\}^{\text{T}} \qquad (3.8a) $$

Branch 2 $\mathbf{W}_{2_2} \circledast \$_{j_2} = 0$, for j $\neq$2; yielding

$$ {}^{\text{ref}}\mathbf{W}_{2_2} = \{-\cos\theta_{3_2},\ \sin\theta_{3_2};\ l_2\sin\theta_{3_2}\}^{\text{T}} \qquad (3.8b) $$

Branch 3 $\mathbf{W}_{2_3} \circledast \$_{j_3} = 0$, for j $\neq$2; yielding

$$ {}^{\text{ref}}\mathbf{W}_{2_3} = \{-\cos(\theta_{3_3}-\alpha_3),\ \sin(\theta_{3_3}-\alpha_3);\ l_3\sin\theta_{3_3}\}^{\text{T}} \qquad (3.8c) $$

where the sign given to the first two elements of the associated reciprocal screws defines the direction of the applied forces, i.e., $\mathbf{F}_i = \mathbf{W}_{2_i} w_{2_i}$ for $i = 1, 2, 3$. Notice that if $w_{2_i} > 0$ the i^{th} branch will push the mobile platform and when $w_{2_i} < 0$ the i^{th} branch will pull the mobile platform.

Finally, the associated reciprocal screw matrix is assembled

$$ {}^{\text{ref}}[\mathbf{W}] = \begin{bmatrix} \cos\theta_{3_1} & -\cos\theta_{3_2} & -\cos(\theta_{3_3} - \alpha_3) \\ -\sin\theta_{3_1} & \sin\theta_{3_2} & \sin(\theta_{3_3} - \alpha_3) \\ 0 & l_2\sin\theta_{3_2} & l_3\sin\theta_{3_3} \end{bmatrix} \tag{3.9} $$

As mentioned before, if ${}^{\text{ref}}[\mathbf{W}]$ becomes singular, an arbitrary force $\mathbf{F}$ cannot be sustained. This occurs when its determinant is zero, i.e.,

$$ \begin{aligned} |{}^{\text{ref}}[\mathbf{W}]| &= l_2\sin(\theta_{3_2})\left(\sin(\theta_{3_1})\cos(\theta_{3_3} - \alpha_3) - \cos(\theta_{3_1})\sin(\theta_{3_3} - \alpha_3)\right) \\ &\quad + l_3\sin(\theta_{3_3})\left(\cos(\theta_{3_1})\sin(\theta_{3_2}) - \sin(\theta_{3_1})\cos(\theta_{3_2})\right) = 0 \end{aligned} \tag{3.10} $$

3.3.5 Comparison between Both Methods

The resulting matrix for the screw theory method is written in terms of the joint angles θ_{3_i}. In order to express these associated reciprocal screws in terms of the location and orientation of the platform, the following vector loop equations with respect to {ref} are employed:

Branch 1

$$ -d_{2_1}\cos(-\theta_{3_1}) = -x\cos\phi - y\sin\phi \tag{3.11a} $$

$$ -d_{2_1}\sin(-\theta_{3_1}) = x\sin\phi - y\cos\phi \tag{3.11b} $$

By isolating the terms $\cos\theta_{3_1}$ and $\sin\theta_{3_1}$ from the above equations and substituting them back in Eq. (3.8a), the following form of ${}^{\text{ref}}\mathrm{W}_{2_1}$ results,

$$ {}^{\text{ref}}\mathbf{W}_{2_1} = \frac{1}{d_{2_1}}\left\{ \begin{array}{ccc} x\cos\phi + y\sin\phi & -x\sin\phi + y\cos\phi & 0 \end{array} \right\}^{\mathrm{T}} \tag{3.12} $$

Transforming the associated reciprocal screw to a frame $\{\text{ref}_0\}$ located at 3_1 but oriented as $\{0\}$ yields

$$ {}^{\text{ref}_0}\mathbf{W}_{2_1} = {}^{\text{ref}_0}_{\text{ref}}[\mathbf{R}]\, {}^{\text{ref}}\mathbf{W}_{2_1} = \frac{1}{d_{2_1}} \left\{ \begin{array}{ccc} x & y & 0 \end{array} \right\}^{\text{T}} \tag{3.13} $$

where

$$ {}^{\text{ref}_0}_{\text{ref}}[\mathbf{R}] = \left[\begin{array}{ccc} \cos\phi & -\sin\phi & 0 \\ \sin\phi & \cos\phi & 0 \\ 0 & 0 & 1 \end{array} \right] \tag{3.14} $$

Branch 2

$$ l_2 + d_{2_2}\cos(-\theta_{3_2}) = (bx_2 - x)\cos\phi - y\sin\phi \tag{3.15a} $$

$$ d_{2_2}\sin(-\theta_{3_2}) = -(bx_2 - x)\sin\phi - y\cos\phi \tag{3.15b} $$

By substituting the trigonometric terms of θ_{3_2} in Eq. (3.8b) the following form of ${}^{\text{ref}}\mathbf{W}_{2_2}$ results

$$ {}^{\text{ref}}\mathbf{W}_{2_2} = \frac{1}{d_{2_2}} \left\{ \begin{array}{c} -(bx_2 - x)\cos\phi + y\sin\phi + l_2 \\ (bx_2 - x)\sin\phi + y\cos\phi \\ l_2\left((bx_2 - x)\sin\phi + y\cos\phi\right) \end{array} \right\} \tag{3.16} $$

Transforming to $\{\text{ref}_0\}$ yields

$$ {}^{\text{ref}_0}\mathbf{W}_{2_2} = {}^{\text{ref}_0}_{\text{ref}}[\mathbf{R}]\, {}^{\text{ref}}\mathbf{W}_{2_2} = \frac{1}{d_{2_2}} \left\{ \begin{array}{c} x - bx_2 + l_2\cos\phi \\ y + l_2\sin\phi \\ l_2\left(y\cos\phi - (x - bx_2)\sin\phi\right) \end{array} \right\} \tag{3.17} $$

Branch 3

$$ l_3 c\alpha_3 + d_{2_3} c(\alpha_3 - \theta_{3_3}) = (bx_3 - x)\,c\phi + (by_3 - y)\,s\phi \tag{3.18a} $$

$$ l_3 s\alpha_3 + d_{2_3} s(\alpha_3 - \theta_{3_3}) = -(bx_3 - x)\,s\phi + (by_3 - y)\,c\phi \tag{3.18b} $$

yielding

$$c\left(\theta_{3_3}-\alpha_3\right) = \frac{1}{d_{2_3}}\left(\left(bx_3-x\right)c\phi+\left(by_3-y\right)s\phi-l_3c\alpha_3\right) \tag{3.19a}$$

$$s\left(\theta_{3_3}-\alpha_3\right) = \frac{1}{d_{2_3}}\left(\left(bx_3-x\right)s\phi-\left(by_3-y\right)c\phi+l_3s\alpha_3\right) \tag{3.19b}$$

The third element of ${}^{\text{ref}}\mathrm{W}_{2_3}$ involves the term $\sin\theta_{3_3}$ which can be found by multiplying Eqs. (3.18a and 3.18b) by $s\alpha_3$ and $-c\alpha_3$, respectively, and adding them together, i.e.,

$$\sin\theta_{3_3} = \frac{1}{d_{2_3}}\left(\left(bx_3-x\right)s\left(\phi+\alpha_3\right)-\left(by_3-y\right)c\left(\phi+\alpha_3\right)\right) \tag{3.20}$$

substituting Eqs. (3.19a, 3.19b, and 3.20) into Eq. (3.8c) yields

$${}^{\text{ref}}\mathbf{W}_{2_3} = \frac{1}{d_{2_3}}\begin{Bmatrix} -\left(bx_3-x\right)c\phi-\left(by_3-y\right)s\phi+l_3c\alpha_3 \\ \left(bx_3-x\right)s\phi-\left(by_3-y\right)c\phi+l_3s\alpha_3 \\ l_3\left(\left(bx_3-x\right)s\left(\phi+\alpha_3\right)-\left(by_3-y\right)c\left(\phi+\alpha_3\right)\right) \end{Bmatrix} \tag{3.21}$$

and transforming yields

$${}^{\text{ref}_0}\mathbf{W}_{2_3} = {}^{\text{ref}_0}_{\text{ref}}[\mathbf{R}]\,{}^{\text{ref}}\mathbf{W}_{2_3} = \frac{1}{d_{2_3}}\begin{Bmatrix} x-bx_3+l_3c\left(\phi+\alpha_3\right) \\ y-by_3+l_3s\left(\phi+\alpha_3\right) \\ l_3\left(\left(y-by_3\right)c\left(\phi+\alpha_3\right)-\left(x-bx_3\right)s\left(\phi+\alpha_3\right)\right) \end{Bmatrix} \tag{3.22}$$

Finally, the associated reciprocal screw matrix of this manipulator is assembled as follows:

$$\begin{aligned} {}^{\text{ref}_0}[\mathbf{W}] &= \begin{bmatrix} {}^{\text{ref}_0}\mathbf{W}_{2_1} & {}^{\text{ref}_0}\mathbf{W}_{2_2} & {}^{\text{ref}_0}\mathbf{W}_{2_3} \end{bmatrix} \\ &= \begin{bmatrix} \frac{x}{d_{2_1}} & \frac{x-bx_2+l_2c\phi}{d_{2_2}} & \frac{x-bx_3+l_3c(\phi+\alpha_3)}{d_{2_3}} \\ \frac{y}{d_{2_1}} & \frac{y+l_2s\phi}{d_{2_2}} & \frac{y-by_3+l_3s(\phi+\alpha_3)}{d_{2_3}} \\ 0 & \frac{l_2(yc\phi-(x-bx_2)s\phi)}{d_{2_2}} & \frac{l_3((y-by_3)c(\phi+\alpha_3)-(x-bx_3)s(\phi+\alpha_3))}{d_{2_3}} \end{bmatrix} \end{aligned} \tag{3.23}$$

Thus, the analogy between the time derivative method and the screw theory method is satisfied, i.e.,

$$^{\text{ref}_0}[\mathbf{W}][\mathbf{D}] \equiv [\mathbf{J}]^{\mathrm{T}} = \left([\mathbf{B}]^{-1}[\mathbf{A}]\right)^{\mathrm{T}} \tag{3.24}$$

where $[\mathbf{D}]$ turns out to be a 3×3 identity matrix.

$$[\mathbf{D}] = \begin{bmatrix} \frac{1}{\mathbf{W}_{2_1} \circledast \$_{2_1}} & 0 & 0 \\ 0 & \frac{1}{\mathbf{W}_{2_2} \circledast \$_{2_2}} & 0 \\ 0 & 0 & \frac{1}{\mathbf{W}_{2_3} \circledast \$_{2_3}} \end{bmatrix} = \begin{bmatrix} 1 & 0 & 0 \\ 0 & 1 & 0 \\ 0 & 0 & 1 \end{bmatrix}$$

3.3.6 Force-Unconstrained Poses

The determinant of the Jacobian (or associated reciprocal screw matrix) leads to an equation in terms of x, y, and ϕ. Assuming values of x and y within the workspace of the manipulator, and applying half-angle substitution to ϕ, i.e.,

$$\sin(\phi) = \frac{2t}{1+t^2} \quad \text{and} \quad \cos(\phi) = \frac{1-t^2}{1+t^2} \tag{3.25a}$$

where

$$t = \tan\left(\frac{\phi}{2}\right) \tag{3.25b}$$

a quartic polynomial in t results,

$$a_0 t^4 + a_1 t^3 + a_2 t^2 + a_3 t + a_4 = 0 \tag{3.26}$$

where the coefficients a_i (for $i = 0, ..., 4$) are shown in Appendix D.2.

The obtained position of the mobile platform is referred to the origin of *{ref}*. However, it can be transformed to the origin of frame *{cen}*, which is located at the centre of the platform and oriented as *{ref}*, as explained in Appendix B.3.

Example.-

A numerical example of the force-unconstrained poses of the centre of the platform of the 3-RPR manipulator is presented. Both platforms are equilateral triangles, their sides are 2.5 m for the fixed platform and 1 m for the mobile platform. The stroke of the prismatic joints are $0 \leqslant d_{2_i} \leqslant 3\ m$, for $i = 1, 2, 3$. The force-unconstrained poses of the 3-RPR manipulator are plotted in the three-dimensional space defined by x, y, and ϕ; and are shown in Figure 3.3. The greyscale gradient visually aids the magnitude of the orientation.

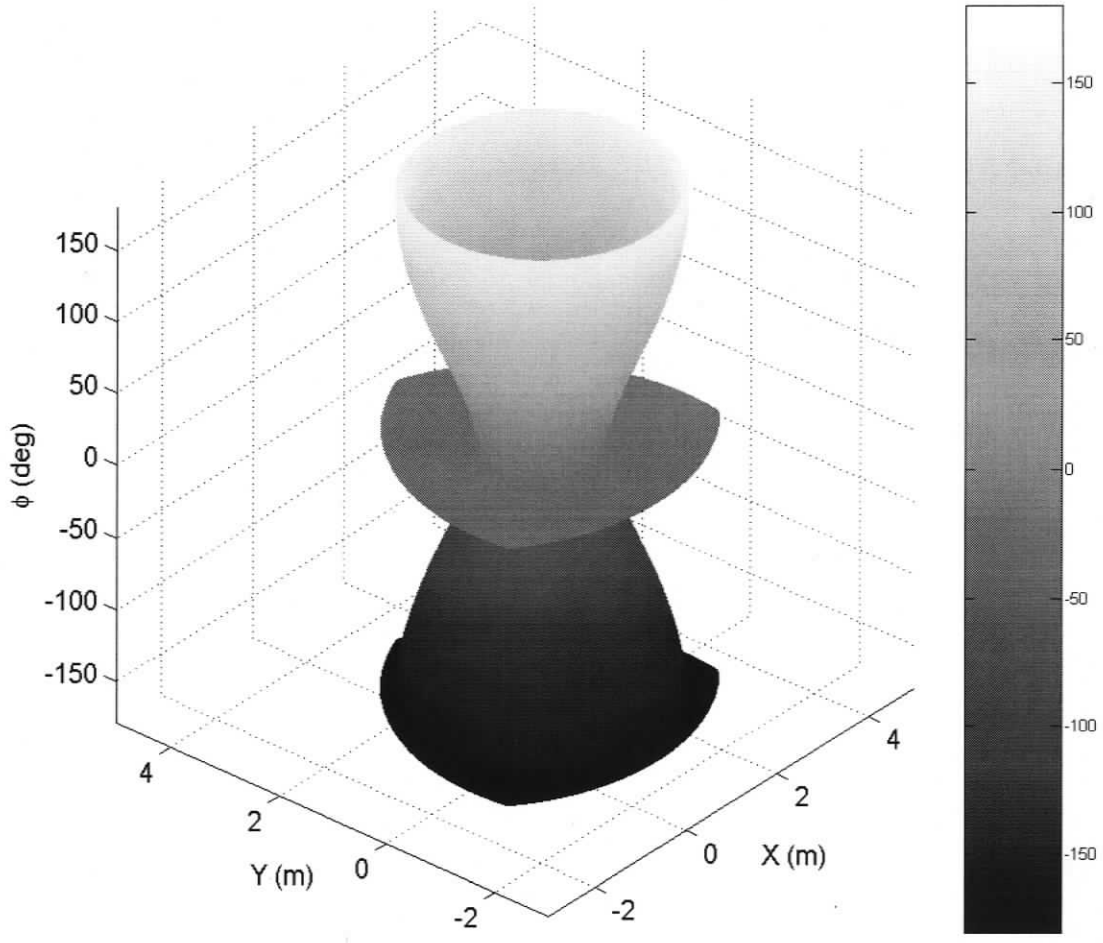

Figure 3.3: Force-Unconstrained Poses of the 3-RPR Manipulator.

Notice that in the above figure two planes of force-unconstrained poses (at $\phi = 0°$ and $\phi = -180°$) resulted. This is due to the similarity of the two platforms, i.e., the fixed and the mobile platform are similar triangles. Thus, if the mobile platform is either parallel or rotated 180° with respect to the fixed platform, the associated reciprocal screws will always intersect at a common point. Also, for any other orientation, the locus of singularities show a circular shape. These results corroborate the previous study made by Kong and Gosselin (2000), and shown in Li et al. (2006).

The RPM singularities were not shown in Figure 3.3. These singularities occur when the displacement of a prismatic joint is zero. This redundant motion yields a full-cycle as described by Bonev et al. (2003). Regardless of the orientation of the mobile platform, the row of the Jacobian matrix involving the branch with the zero-displacement prismatic joint is a zero row, i.e., the Jacobian matrix is, therefore, rank deficient. Physically, the mobile platform can rotate freely about the base of the prismatic joint whose displacement is zero. The RPM singularities represent spirals in the three-dimensional space. The projection of these spirals leads to circles in the xy plane. The centre of each circle is located at the branch base of the prismatic joint with zero displacement and the radius is defined by the distance between this base and the centre of the mobile platform.

3.4 Force-Unconstrained Poses of the 3-PRR PPM

3.4.1 Background

The 3-PRR manipulator was first introduced by Gosselin et al. (1996). Each branch is composed of a prismatic joint fixed to the base, followed by two revolute joints separated by a link. In order to reduce the inertia of the mechanism, the prismatic joints are actuated allowing high speed applications. In (Gosselin et al., 1996), the kinematic analysis of the inverse and forward problems, the input and output speed Jacobian matrices, and a workspace description were presented.

For a constant payload orientation, Bonev (2002) and Bonev et al. (2003) identified the singular configurations of this manipulator. The singularity loci are represented by a 20^{th}-order multivariable polynomial in terms of x and y. However, an exhaustive process of simplification is required because the resulting equation is expressed in terms of square roots. The geometric identification of all singular poses requires ϕ to be varied, i.e., $0 \leqslant \phi < 2\pi$, making this method computationally expensive.

To the best of the author's knowledge, no mathematical software can determine a single symbolic expression for force-unconstrained poses of the 3-PRR in terms of the variables x, y, and ϕ. Nevertheless, if a symbolic expression were to be found, the force-unconstrained poses could be plotted by assuming two of these variables, i.e., there is an order of two infinities ($O(\infty^2)$) of choices. In this dissertation, to make the solution more efficient, the two 'free' variables are chosen to be joint displacements.

In this section, the force-unconstrained poses of the 3-PRR are identified. First, the Denavit and Hartenberg parameters of each branch are determined. Second, screws and associated reciprocal screws are found. Third, the loop-closure equa-

tions that define the geometry of the manipulator are derived. Fourth, the elimination process is carried out by properly selecting the 'free' variables, and the force-unconstrained poses are identified.

3.4.2 Denavit and Hartenberg Parameters

The notation of the geometric variables of the manipulator are shown in Figure 3.4. DH parameters describing the 3-PRR layout are given in Table 3.3, where j and i represent the joint and branch numbers, respectively, and $\{\text{ref}\}$ is a reference frame located at $\{3_1\}$. To keep the DH parameters in a general form $l_1 = 0$, $\beta_1 = 0$, $\beta_2 = \pi$, and $\beta_3 = \pi - \alpha_3$.

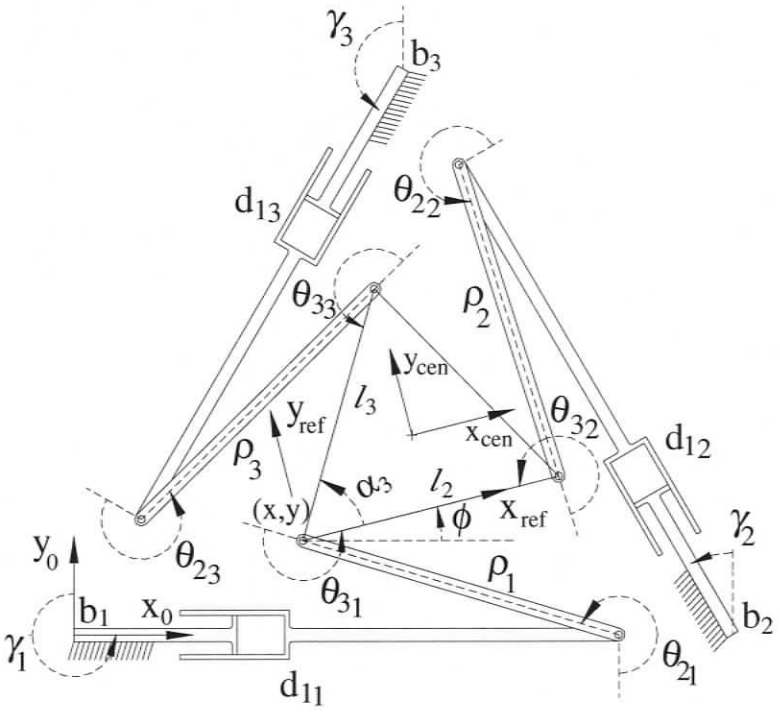

Figure 3.4: Layout of the 3-PRR Planar Parallel Manipulator.

Table 3.3: DH Parameters of the 3-PRR Manipulator.

$j-1$	α_{j-1}	a_{j-1}	d_j	θ_{j_i}	j
b_i	$-\frac{1}{2}\pi$	0	d_{1_i}	0	1_i
1_i	$\frac{1}{2}\pi$	0	0	θ_{2_i}	2_i
2_i	0	ρ_i	0	θ_{3_i}	3_i
3_i	0	l_i	0	β_i	ref

The homogeneous transform, ${}^{0}_{b_i}[\mathbf{T}]$, of each branch base b_i with respect to $\{0\}$ is shown below, with bx_i and by_i being the position of the i^{th} base, and γ_i the orientation of the i^{th} prismatic joint.

$$ {}^{0}_{b_i}[\mathbf{T}] = \begin{bmatrix} \cos(\gamma_i) & -\sin(\gamma_i) & 0 & bx_i \\ \sin(\gamma_i) & \cos(\gamma_i) & 0 & by_i \\ 0 & 0 & 1 & 0 \\ 0 & 0 & 0 & 1 \end{bmatrix} \tag{3.27} $$

3.4.3 Screw Quantities

The following joint screws written in a matrix form per branch result:

$$ {}^{ref}[\$_1] = [\ {}^{ref}\$_{1_1} \quad {}^{ref}\$_{2_1} \quad {}^{ref}\$_{3_1}\ ] = \begin{bmatrix} 0 & 1 & 1 \\ \sin(\theta_{2_1}+\theta_{3_1}) & \rho_1 \sin(\theta_{3_1}) & 0 \\ \cos(\theta_{2_1}+\theta_{3_1}) & \rho_1 \cos(\theta_{3_1}) & 0 \end{bmatrix} \tag{3.28a} $$

$$ {}^{ref}[\$_2] = [\ {}^{ref}\$_{1_2} \quad {}^{ref}\$_{2_2} \quad {}^{ref}\$_{3_2}\ ] = \begin{bmatrix} 0 & 1 & 1 \\ -\sin(\theta_{2_2}+\theta_{3_2}) & -\rho_2 \sin\theta_{3_2} & 0 \\ -\cos(\theta_{2_2}+\theta_{3_2}) & -\rho_2 \cos\theta_{3_2} - l_2 & -l_2 \end{bmatrix} \tag{3.28b} $$

$$
\begin{aligned}
{}^{\text{ref}}[\$_3] &= [\ {}^{\text{ref}}\$_{1_3}\ \ {}^{\text{ref}}\$_{2_3}\ \ {}^{\text{ref}}\$_{3_3}\ ] \\
&= \begin{bmatrix} 0 & 1 & 1 \\ -\sin(\theta_{2_3}+\theta_{3_3}-\alpha_3) & -\rho_3\sin(\theta_{3_3}-\alpha_3)+l_3\sin\alpha_3 & l_3\sin\alpha_3 \\ -\cos(\theta_{2_3}+\theta_{3_3}-\alpha_3) & -\rho_3\cos(\theta_{3_3}-\alpha_3)-l_3\cos\alpha_3 & -l_3\cos\alpha_3 \end{bmatrix}
\end{aligned} \tag{3.28c}
$$

The associated reciprocal screws of the prismatic actuated joints are found using reciprocal products of Eq. (2.17) as follows:

Branch 1 $\mathbf{W}_{1_1} \circledast \$_{j_1} = 0$, for j $\neq$1; yielding

$$
{}^{\text{ref}}\mathbf{W}_{1_1} = \{\cos\theta_{3_1},\ -\sin\theta_{3_1};\ 0\}^{\text{T}} \tag{3.29a}
$$

Branch 2 $\mathbf{W}_{1_2} \circledast \$_{j_2} = 0$, for j $\neq$1; yielding

$$
{}^{\text{ref}}\mathbf{W}_{1_2} = \{-\cos\theta_{3_2},\ \sin\theta_{3_2};\ l_2\sin\theta_{3_2}\}^{\text{T}} \tag{3.29b}
$$

Branch 3 $\mathbf{W}_{1_3} \circledast \$_{j_3} = 0$, for j $\neq$1; yielding

$$
{}^{\text{ref}}\mathbf{W}_{1_3} = \{-\cos(\theta_{3_3}-\alpha_3),\ \sin(\theta_{3_3}-\alpha_3);\ l_3\sin\theta_{3_3}\}^{\text{T}} \tag{3.29c}
$$

Finally, the associated reciprocal screw matrix is assembled

$$
{}^{\text{ref}}[\mathbf{W}] = \begin{bmatrix} \cos\theta_{3_1} & -\cos\theta_{3_2} & -\cos(\theta_{3_3}-\alpha_3) \\ -\sin\theta_{3_1} & \sin\theta_{3_2} & \sin(\theta_{3_3}-\alpha_3) \\ 0 & l_2\sin\theta_{3_2} & l_3\sin\theta_{3_3} \end{bmatrix} \tag{3.30}
$$

The manipulator is force-unconstrained when the determinant of ${}^{\text{ref}}[\mathbf{W}]$ equals zero, i.e.,

$$
\begin{aligned}
|{}^{\text{ref}}[\mathbf{W}]| &= l_2\sin(\theta_{3_2})\left(\sin(\theta_{3_1})\cos(\theta_{3_3}-\alpha_3)-\cos(\theta_{3_1})\sin(\theta_{3_3}-\alpha_3)\right) \\
&\quad + l_3\sin(\theta_{3_3})\left(\cos(\theta_{3_1})\sin(\theta_{3_2})-\sin(\theta_{3_1})\cos(\theta_{3_2})\right) = 0
\end{aligned} \tag{3.31}
$$

3.4.4 Loop-Closure Equations

The relationship between the joint angles of each branch and the pose (x, y and ϕ) of the mobile platform is defined by the loop-closure equation that describe *{ref}* with respect to *{0}*, i.e.,

$$x = bx_i - d_{1_i}\sin(\gamma_i) + \rho_i\cos(\gamma_i + \theta_{2_i}) + l_i\cos(\gamma_i + \theta_{2_i} + \theta_{3_i}) \quad (3.32a)$$

$$y = by_i + d_{1_i}\cos(\gamma_i) + \rho_i\sin(\gamma_i + \theta_{2_i}) + l_i\sin(\gamma_i + \theta_{2_i} + \theta_{3_i}) \quad (3.32b)$$

$$\phi = \gamma_i + \theta_{2_i} + \theta_{3_i} + \beta_i \quad (3.32c)$$

where $i = 1, 2, 3$, with bx_i and by_i representing the position of the bases and γ_i the orientations of the prismatic joints with respect to *{0}*.

In order to eliminate θ_{2_i} Eq. (3.32c) is substituted in Eqs. (3.32a and 3.32b). Then, d_{1_i} is eliminated by multiplying Eqs. (3.32a and 3.32b) by $c(\gamma_i)$ and $s(\gamma_i)$, respectively, and adding them together, yielding

$$\begin{aligned} f_i(x,\ y,\ \phi,\ \theta_{3_i}) = &\left(y - by_i - \rho_i s(\phi - \theta_{3_i} - \beta_i) - l_i s(\phi - \beta_i)\right) s(\gamma_i) \\ &+ \left(x - bx_i - \rho_i c(\phi - \theta_{3_i} - \beta_i) - l_i c(\phi - \beta_i)\right) c(\gamma_i) = 0 \end{aligned} \quad (3.33)$$

where $\beta_1 = 0$, $\beta_2 = \pi$, and $\beta_3 = \pi - \alpha_3$.

3.4.5 Force-Unconstrained Poses

There are four equations (Eq.(3.31) and Eqs. (3.33), $i = 1, 2, 3$) and six variables (x, y, ϕ, and θ_{3_i}, for $i = 1, 2, 3$). It would be desirable to eliminate all θ_{3_i} and remain with an expression in terms of the task space variables; however, this elimination cannot be performed symbolically in a symbolic computation software, such as Maple or Mathematica, because the simplification process will eventually lead to square roots whose elimination requires squaring already large equations.

A more efficient way to solve this problem is to choose the 'free' variables to be two of the third joint angles, for example θ_{3_1} and θ_{3_2}, allowing θ_{3_3} to be computed with Eq. (3.31). This yields two possible solutions θ_{3_3} and $\theta_{3_3} - \pi$. Both θ_{3_3} solutions make the third associated reciprocal screw intersect the common point of the other two associated reciprocal screws. The θ_{3_i} values define the orientation of links ρ_i with respect to the mobile platform.

Now the problem is reduced to assembling the mobile platform and links with the arrangement of the prismatic joints, fixed to the base, using the loop-closure equations. The numerical values of θ_{3_i} are substituted in Eq. (3.33). Half-angle substitution, as shown in Eq. (3.25a), is applied to ϕ, and the loop-closure equations, Eq. (3.33), become a function of x, y, and t, with t being a quadratic variable. These equations are written in matrix form as

$$[\Psi]\,\mathbf{x} = \begin{bmatrix} \psi_{11} & \psi_{12} & \psi_{13} \\ \psi_{21} & \psi_{22} & \psi_{23} \\ \psi_{31} & \psi_{32} & \psi_{33} \end{bmatrix} \begin{bmatrix} x \\ y \\ 1 \end{bmatrix} = \bar{0} \tag{3.34}$$

where the elements of $[\Psi]$ are quadratic polynomials in t and constants (as shown in Appendix D.2), and $\bar{0}$ is a 3 by 1 null vector.

In order to satisfy Eq. (3.34), matrix $[\Psi]$ has to be singular, i.e., $|[\Psi]| = 0$. Since each element of $[\Psi]$ is a quadratic polynomial in t, the determinant of $[\Psi]$ leads to a 6^{th}-order polynomial. The roots of this polynomial represent the force-unconstrained poses of the manipulator, where ϕ is obtained from t, and values for x and y are found from the first two rows of Eq. (3.34), i.e.,

$$\begin{bmatrix} x \\ y \end{bmatrix} = - \begin{bmatrix} \psi_{11} & \psi_{12} \\ \psi_{21} & \psi_{22} \end{bmatrix}^{-1} \begin{bmatrix} \psi_{13} \\ \psi_{23} \end{bmatrix} \tag{3.35}$$

thus,

$$x = \frac{\psi_{12}\psi_{23} - \psi_{22}\psi_{13}}{\psi_{11}\psi_{22} - \psi_{12}\psi_{21}} \quad \text{and} \quad y = \frac{\psi_{21}\psi_{13} - \psi_{11}\psi_{23}}{\psi_{11}\psi_{22} - \psi_{12}\psi_{21}} \tag{3.36}$$

The resulting position is transformed to the centre of the platform as explained in Appendix B.3.

Given that there are eight possible solutions of the inverse kinematics (Gosselin et al., 1996), an identification of the solutions that lead to singular configurations is carried out. Chablat and Wenger (1998) referred to each arrangement given by the solutions of the inverse kinematics as *working modes*. One pose may make two or more working modes singular. That is, the force-unconstrained configurations of each working mode is described by a surface or surfaces in the $x - y - \phi$ space and whenever these surfaces intersect, two or more solutions of the inverse kinematics are singular.

Example.-

A numerical example of the force-unconstrained poses of the centre of the platform of the 3-PRR manipulator is presented. Both platforms are equilateral triangles, their sides are 2.5 m for the fixed platform and 1 m for the mobile platform. The angle of the bases are $\gamma_1 = -90°$, $\gamma_2 = 30°$, and $\gamma_3 = 150°$, and the link lengths are $\rho_i = 1$ m, for i = 1,2,3. Figure 3.5 illustrates, for each working mode[1], surfaces of force-unconstrained poses in the $x - y - \phi$ space. Figure 3.6 shows the combination of all eight configurations. Each plot shows the projections on the xy plane.

[1]There are up to two solutions for each branch. Each configuration is labeled depending on the length of the prismatic joint + for longer and - for shorter.

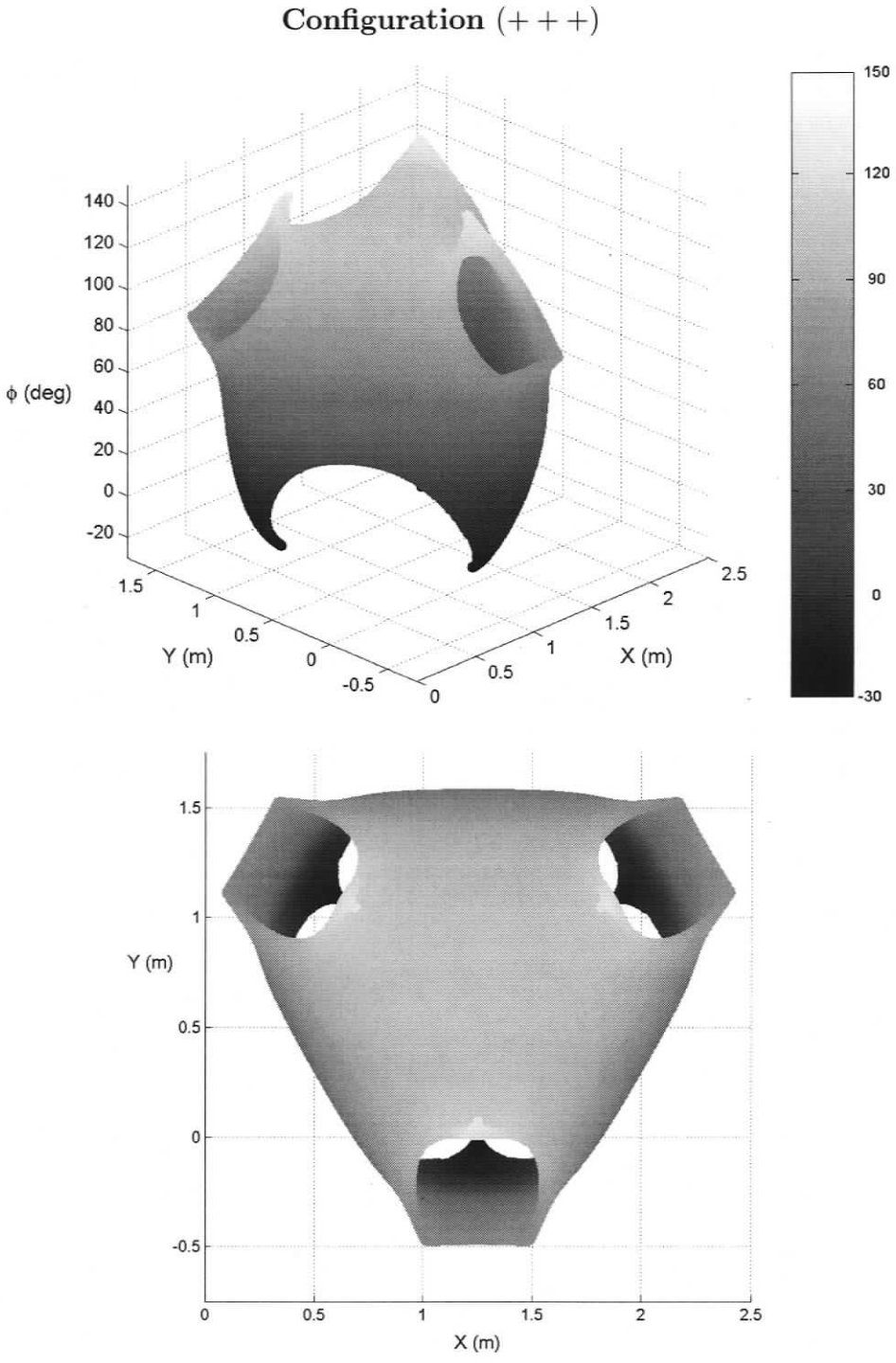

Figure 3.5: Force-Unconstrained Poses of the 3-PRR Manipulator.

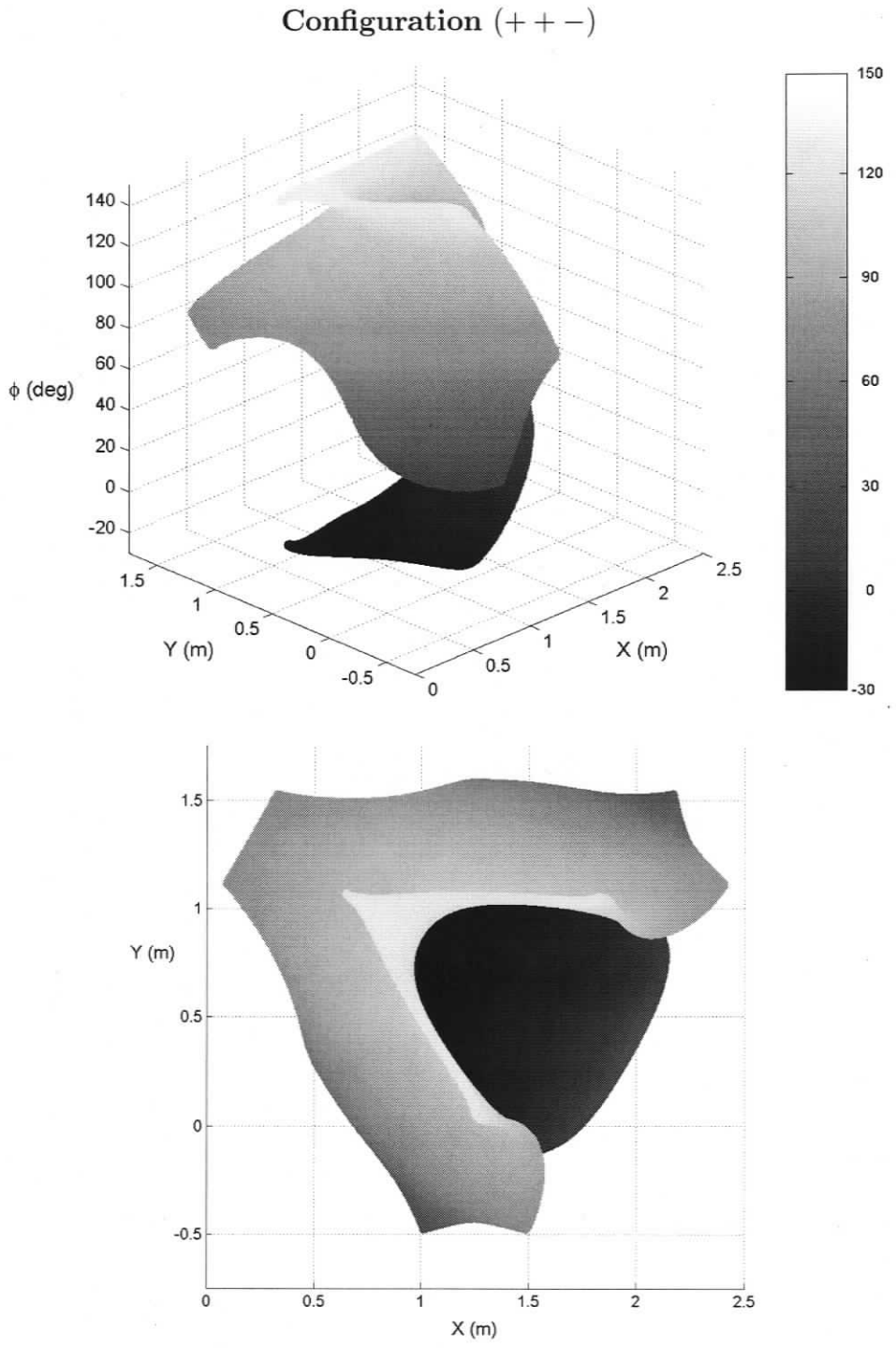

Figure 3.5 (cont'd): Force-Unconstrained Poses of the 3-PRR Manipulator.

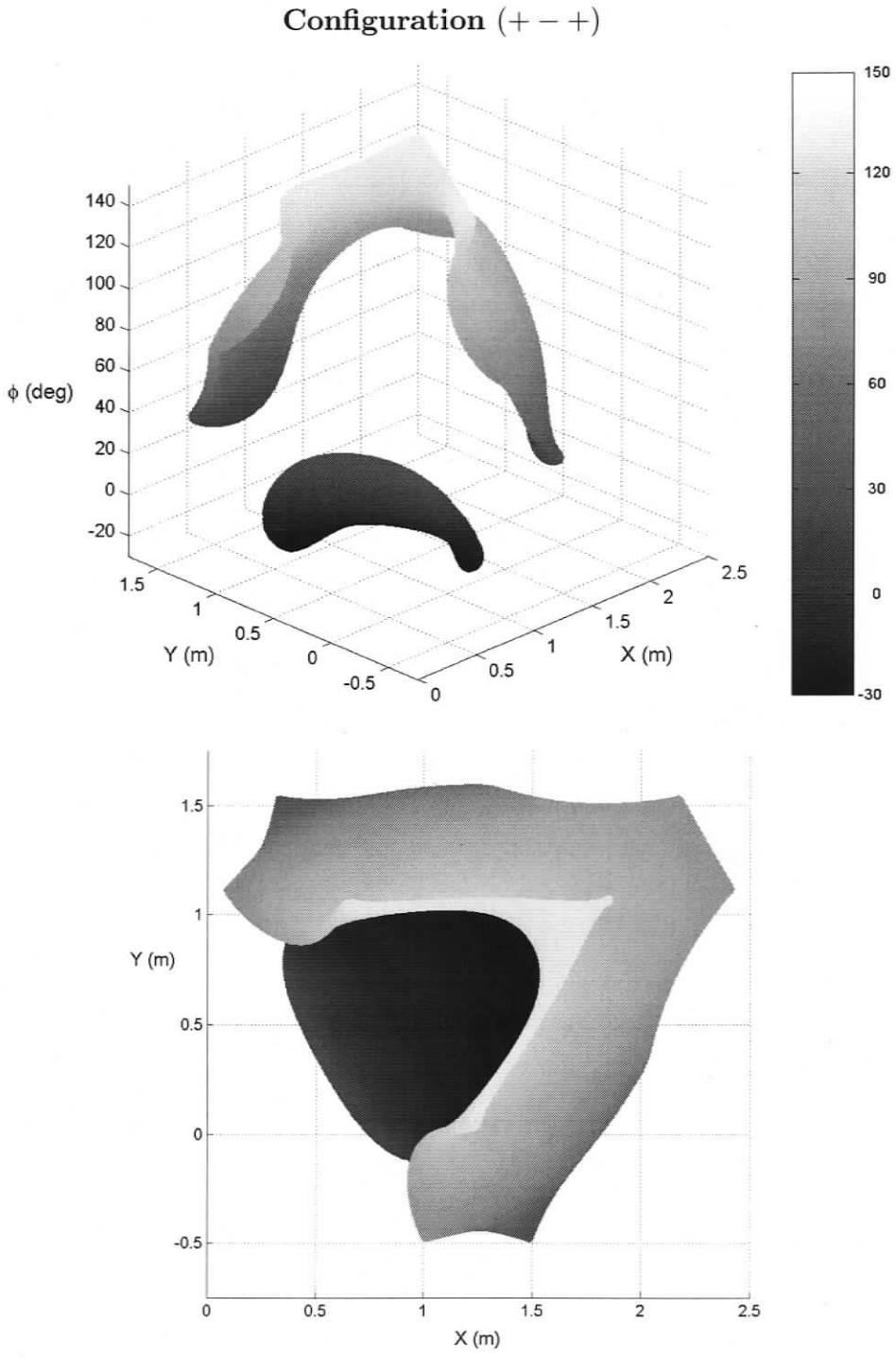

Figure 3.5 (cont'd): Force-Unconstrained Poses of the 3-PRR Manipulator.

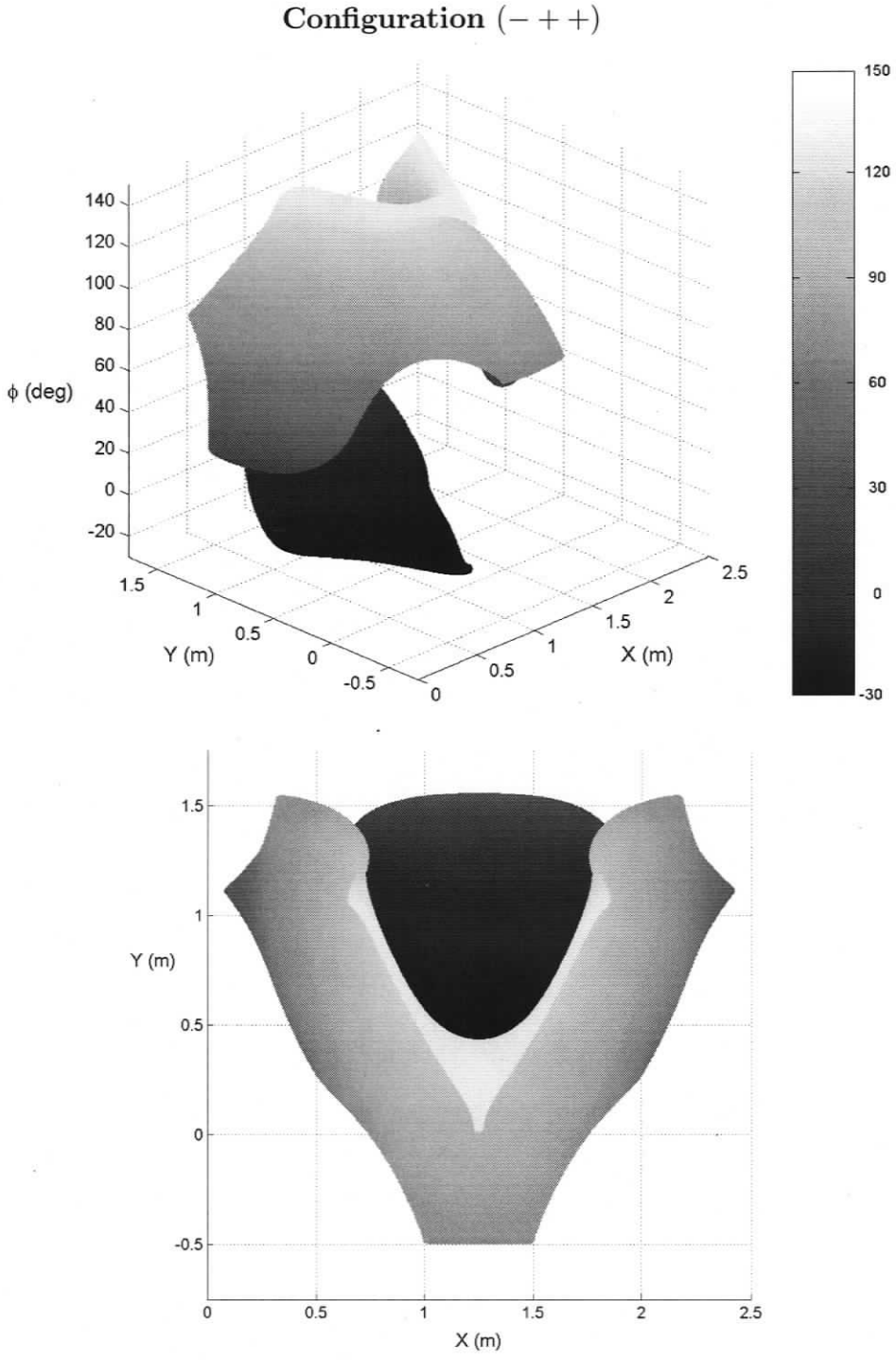

Figure 3.5 (cont'd): Force-Unconstrained Poses of the 3-PRR Manipulator.

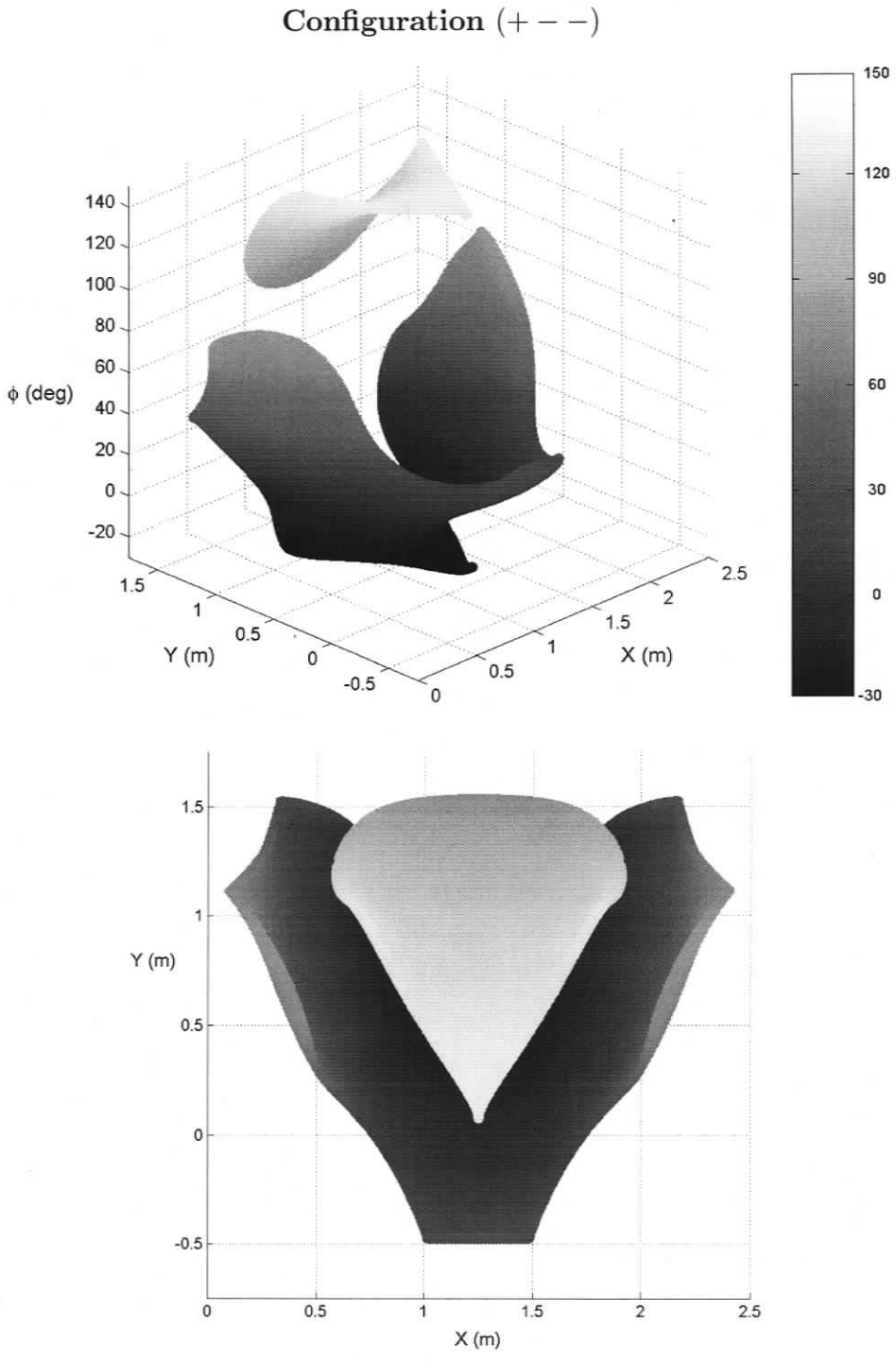

Figure 3.5 (cont'd): Force-Unconstrained Poses of the 3-PRR Manipulator.

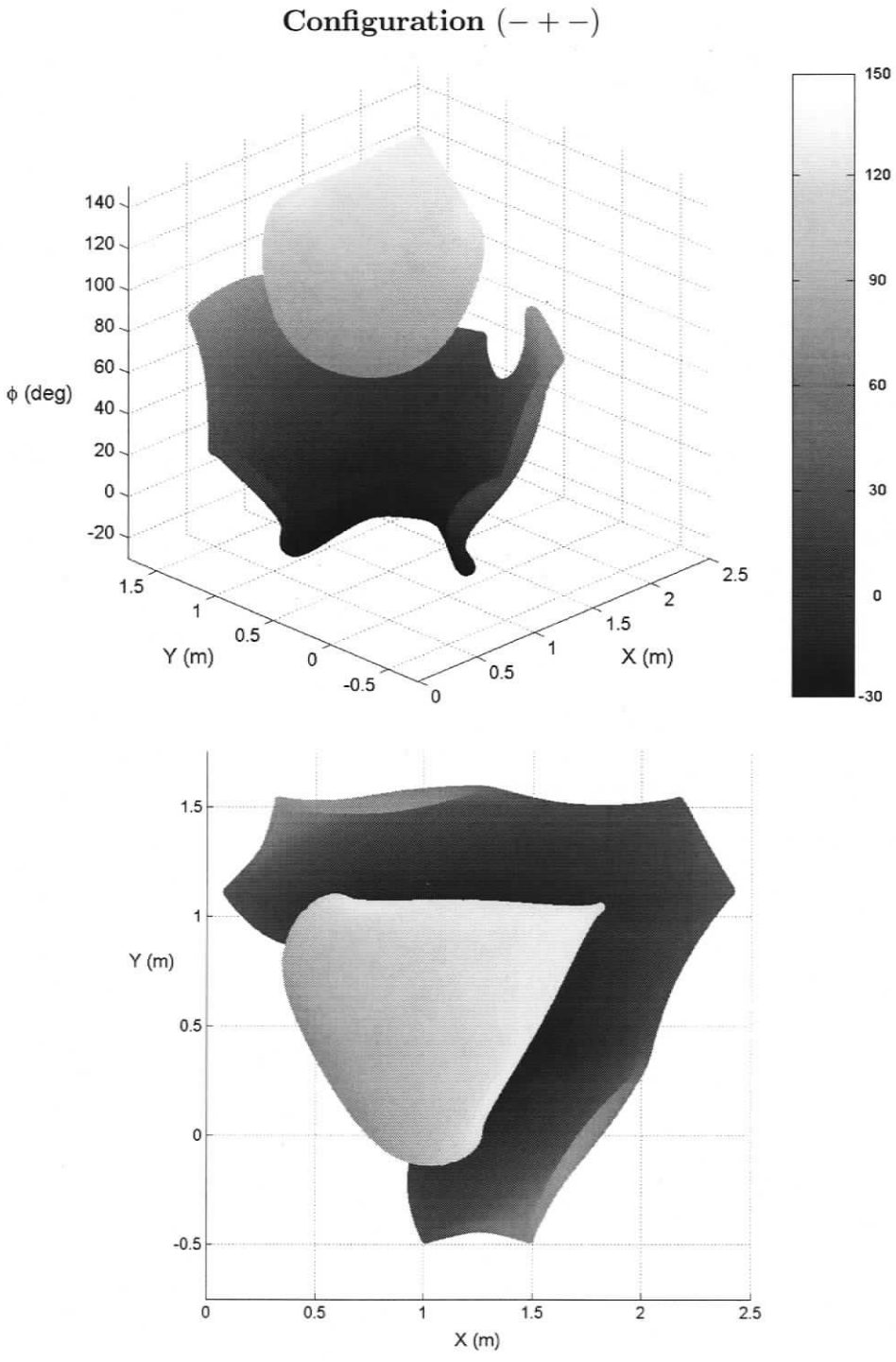

Figure 3.5 (cont'd): Force-Unconstrained Poses of the 3-PRR Manipulator.

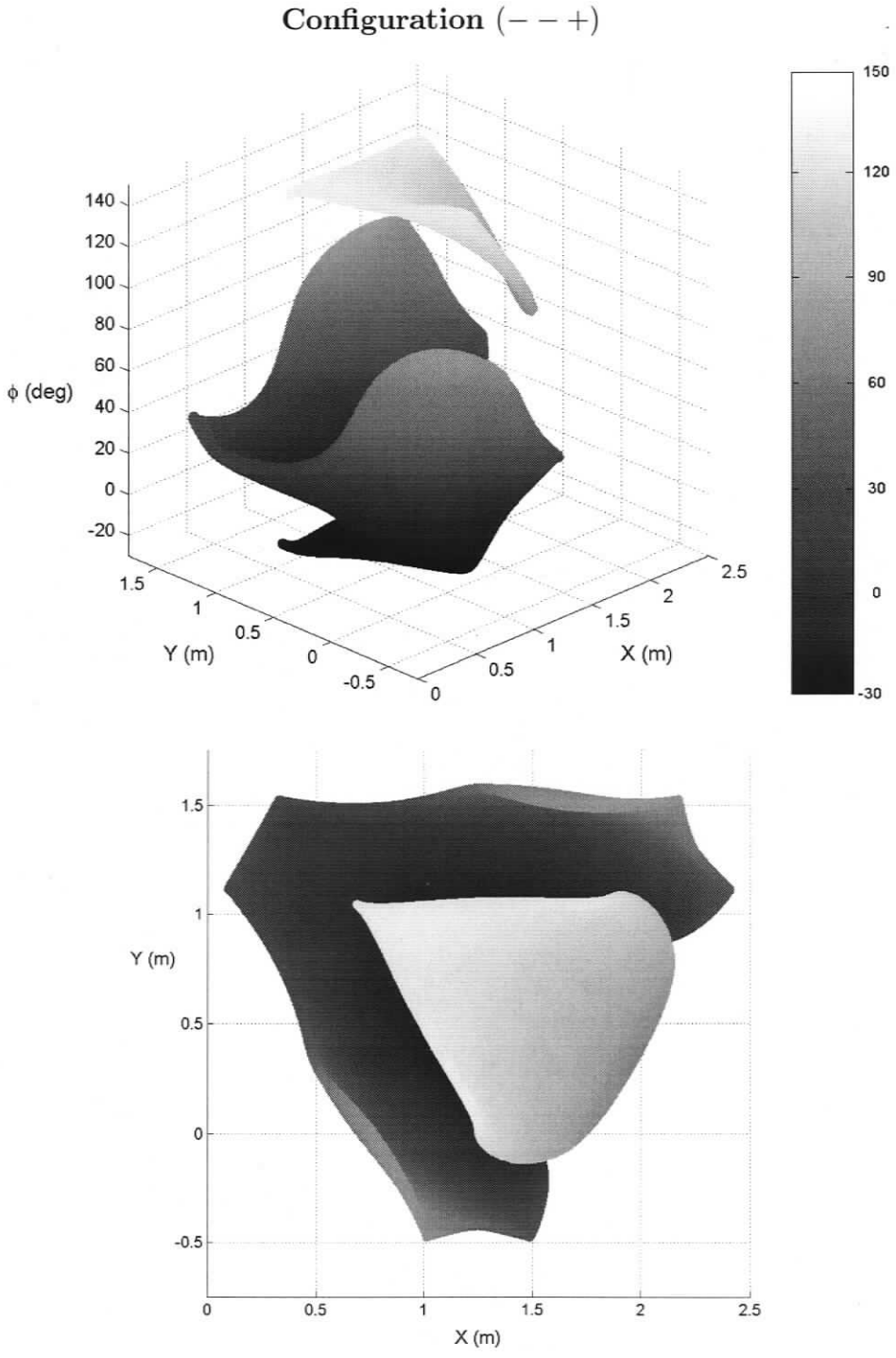

Figure 3.5 (cont'd): Force-Unconstrained Poses of the 3-PRR Manipulator.

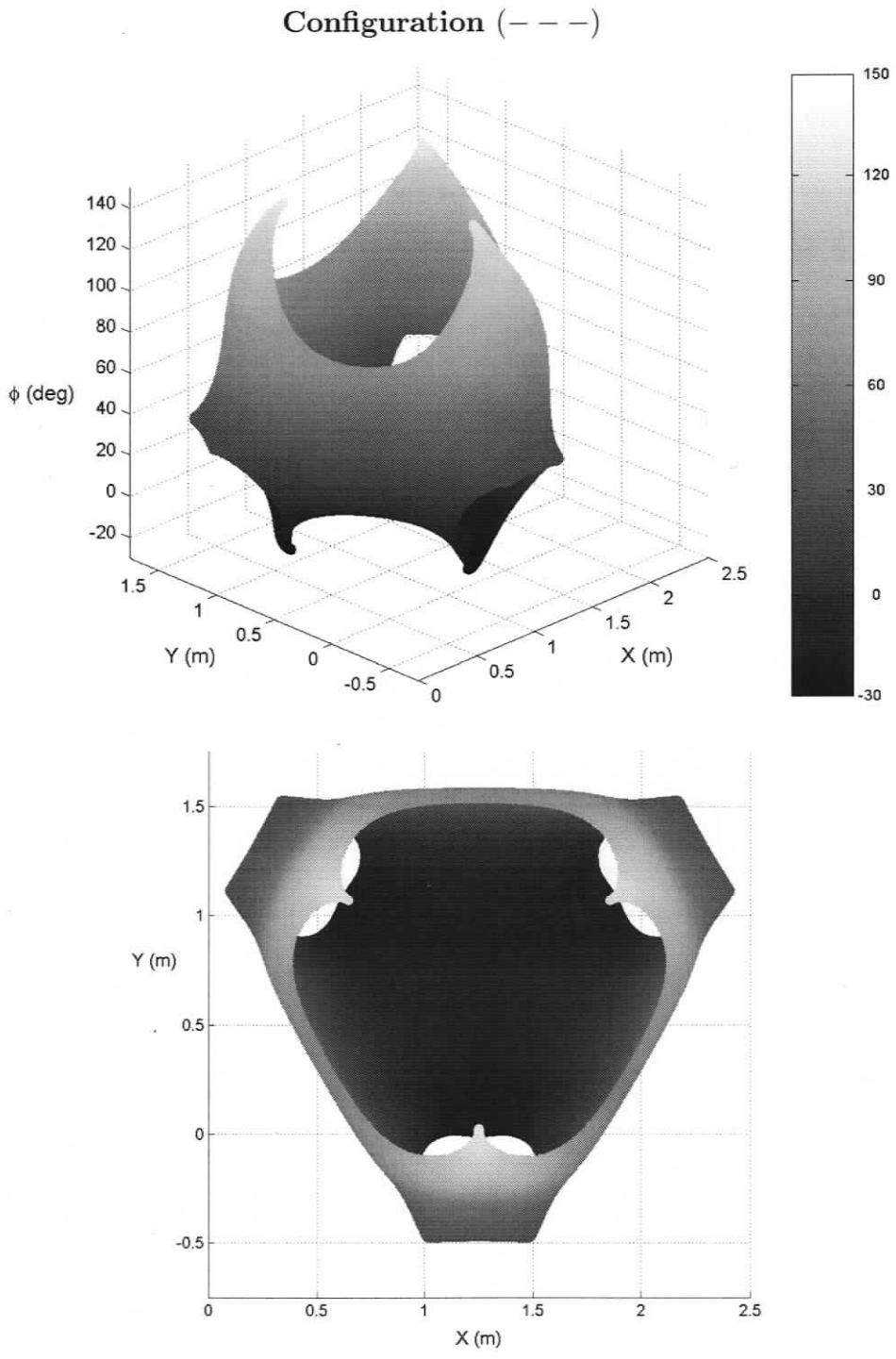

Figure 3.5 (cont'd): Force-Unconstrained Poses of the 3-PRR Manipulator.

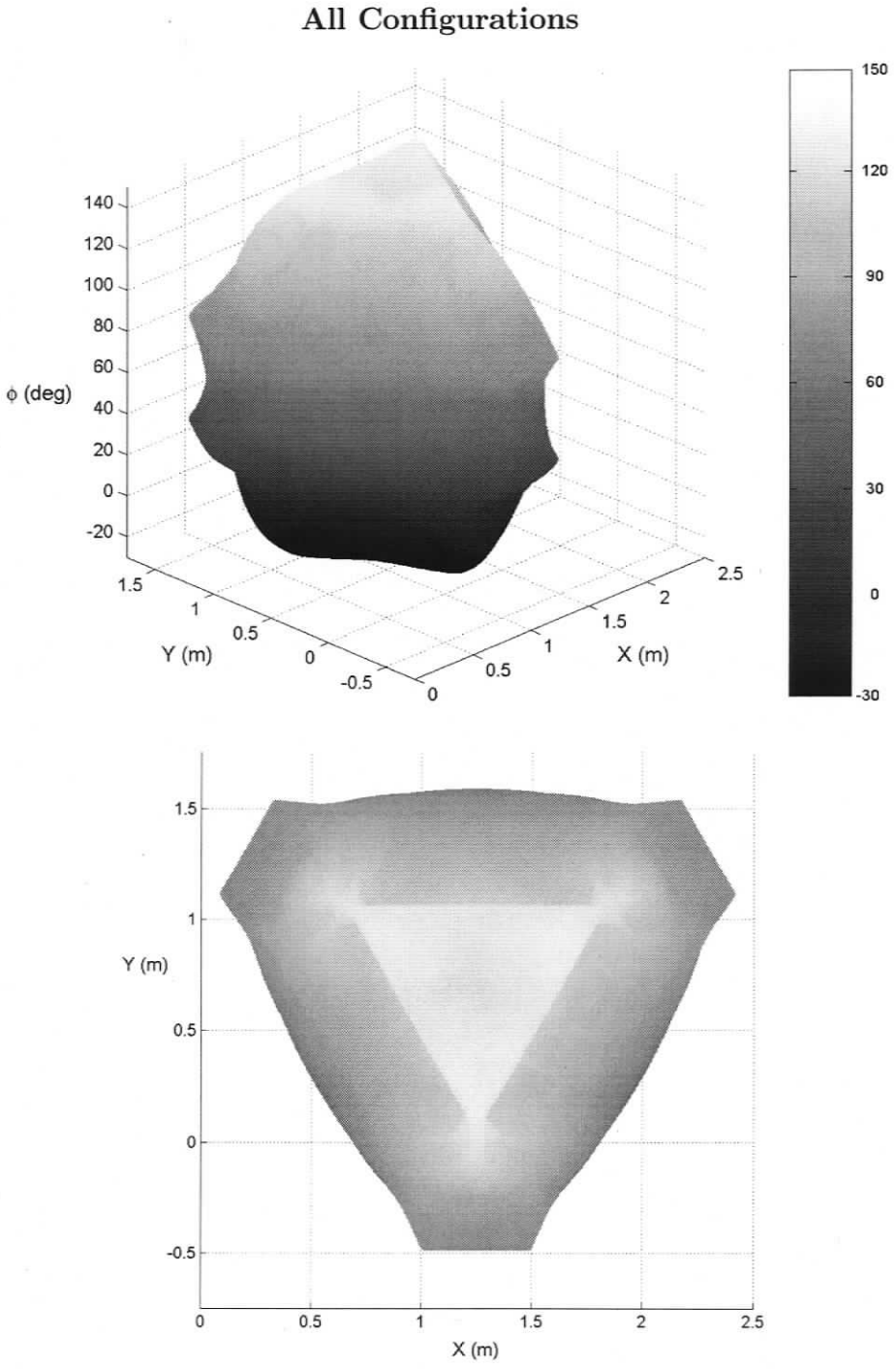

Figure 3.6: All Force-Unconstrained Poses of the 3-PRR Manipulator.

3.5 Force-Unconstrained Poses of the 3-RRR PPM

3.5.1 Background

The 3-RRR manipulator was studied in detail by Gosselin and Angeles (1988). Each branch is composed of three revolute joints separated by links. To reduce the inertia of the mechanism, the revolute joints fixed to the bases are considered to be actuated. Gosselin and Angeles noted that the link lengths should be equal to achieve symmetry and to maximize the workspace and that there are eight solutions for the inverse kinematics.

The first attempt to determine the singularity loci of a 3-dof planar manipulator with revolute joints is attributed to Gosselin and Wang (1997). In the work of Gosselin and Wang, the singularity loci are represented by a multivariable polynomial in x and y, whose highest degrees are 48 in x and 64 in y. Nevertheless, this study was performed to a manipulator with collinear base and mobile platform joints. Later, Bonev and Gosselin (2001) reported loci of locations that result in the 3-RRR manipulator being force unconstrained. As a result, the singularity loci of every branch arrangement or working mode can be represented by curves of degree 42 in terms of x and y.

The force-unconstrained poses would yield an expression in terms of x, y, and ϕ. However, this expression cannot be found symbolically. The identification of force-unconstrained poses can be accomplished by assuming two joint displacement variables, i.e., two 'free' variables.

In this section, the force-unconstrained poses of the 3-RRR manipulator are identified as with the process used for the 3-PRR manipulator. First, the DH parameters

of each branch are determined. Second, screws and associated reciprocal screws are found. Third, the loop-closure equations that define the geometry of the manipulator are derived. Fourth, the elimination process yielding the identification of the force-unconstrained poses is carried out for the assumed 'free' variables.

3.5.2 Denavit and Hartenberg Parameters

The notation of the geometric variables of the manipulator are shown in Figure 3.7. DH parameters describing the 3-RRR layout are given in Table 3.4, where j and i represent the joint and branch numbers, respectively, and $\{\text{ref}\}\equiv\{3_1\}$. To keep the DH parameters in a general form $l_1 = 0$, $\beta_1 = 0$, $\beta_2 = \pi$, and $\beta_3 = \pi - \alpha_3$.

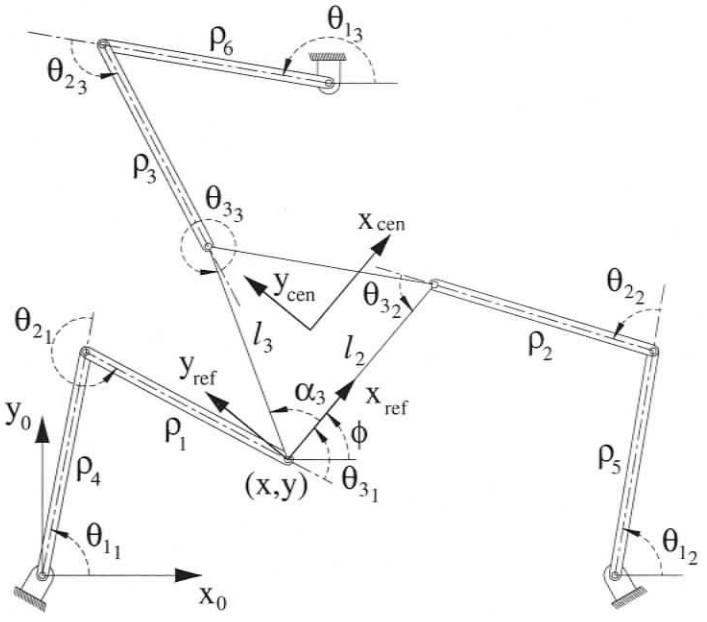

Figure 3.7: Layout of the 3-RRR Planar Parallel Manipulator.

Table 3.4: DH Parameters of the 3-RRR Manipulator.

$j-1$	α_{j-1}	a_{j-1}	d_j	θ_{j_i}	j
b_i	0	0	0	θ_{1_i}	1_i
1_i	0	ρ_{i+3}	0	θ_{2_i}	2_i
2_i	0	ρ_i	0	θ_{3_i}	3_i
3_i	0	l_i	0	β_i	ref

The homogeneous transform, ${}^{0}_{b_i}[\mathbf{T}]$, of each branch base, $b_i = [bx_i,\, by_i]^{\mathrm{T}}$, with respect to $\{0\}$ is shown below.

$$ {}^{0}_{b_i}[\mathbf{T}] = \begin{bmatrix} 1 & 0 & 0 & bx_i \\ 0 & 1 & 0 & by_i \\ 0 & 0 & 1 & 0 \\ 0 & 0 & 0 & 1 \end{bmatrix} \tag{3.37} $$

3.5.3 Screw Quantities

For the 3-RRR , the following joint screws written in a matrix form per branch result:

$$ \begin{aligned} {}^{\mathrm{ref}}[\$_1] &= \begin{bmatrix} {}^{\mathrm{ref}}\$_{1_1} & {}^{\mathrm{ref}}\$_{2_1} & {}^{\mathrm{ref}}\$_{3_1} \end{bmatrix} \\ &= \begin{bmatrix} 1 & 1 & 1 \\ \rho_4 \sin(\theta_{2_1} + \theta_{3_1}) + \rho_1 \sin(\theta_{3_1}) & \rho_1 \sin(\theta_{3_1}) & 0 \\ \rho_4 \cos(\theta_{2_1} + \theta_{3_1}) + \rho_1 \cos(\theta_{3_1}) & \rho_1 \cos(\theta_{3_1}) & 0 \end{bmatrix} \end{aligned} \tag{3.38a} $$

$$ \begin{aligned} {}^{\mathrm{ref}}[\$_2] &= \begin{bmatrix} {}^{\mathrm{ref}}\$_{1_2} & {}^{\mathrm{ref}}\$_{2_2} & {}^{\mathrm{ref}}\$_{3_2} \end{bmatrix} \\ &= \begin{bmatrix} 1 & 1 & 1 \\ -\rho_5 \sin(\theta_{2_2} + \theta_{3_2}) - \rho_2 \sin\theta_{3_2} & -\rho_2 \sin\theta_{3_2} & 0 \\ -\rho_5 \cos(\theta_{2_2} + \theta_{3_2}) - \rho_2 \cos\theta_{3_2} - l_2 & -\rho_2 \cos\theta_{3_2} - l_2 & -l_2 \end{bmatrix} \end{aligned} \tag{3.38b} $$

$$
\begin{aligned}
{}^{\text{ref}}[\$_3] &= \left[\, {}^{\text{ref}}\$_{1_3} \quad {}^{\text{ref}}\$_{2_3} \quad {}^{\text{ref}}\$_{3_3} \,\right] \\
&= \begin{bmatrix} 1 & 1 & 1 \\ P & -\rho_3 \sin(\theta_{3_3} - \alpha_3) + l_3 \sin\alpha_3 & l_3 \sin\alpha_3 \\ Q & -\rho_3 \cos(\theta_{3_3} - \alpha_3) - l_3 \cos\alpha_3 & -l_3 \cos\alpha_3 \end{bmatrix}
\end{aligned} \tag{3.38c}
$$

$$
\begin{aligned}
\text{where } P &= -\rho_6 \sin(\theta_{2_3} + \theta_{3_3} - \alpha_3) - \rho_3 \sin(\theta_{3_3} - \alpha_3) + l_3 \sin\alpha_3 \\
Q &= -\rho_6 \cos(\theta_{2_3} + \theta_{3_3} - \alpha_3) - \rho_3 \cos(\theta_{3_3} - \alpha_3) - l_3 \cos\alpha_3
\end{aligned}
$$

The associated reciprocal screws of the actuated joints are found using the reciprocal products of Eq. (2.17):

Branch 1 $\mathbf{W}_{1_1} \circledast \$_{j_1} = 0$, for j $\neq$1; yielding

$$
{}^{\text{ref}}\mathbf{W}_{1_1} = \{\cos\theta_{3_1}, \ -\sin\theta_{3_1}; \ 0\}^{\text{T}} \tag{3.39a}
$$

Branch 2 $\mathbf{W}_{1_2} \circledast \$_{j_2} = 0$, for j $\neq$1; yielding

$$
{}^{\text{ref}}\mathbf{W}_{1_2} = \{-\cos\theta_{3_2}, \ \sin\theta_{3_2}; l_2 \sin\theta_{3_2}\}^{\text{T}} \tag{3.39b}
$$

Branch 3 $\mathbf{W}_{1_3} \circledast \$_{j_3} = 0$, for j $\neq$1; yielding

$$
{}^{\text{ref}}\mathbf{W}_{1_3} = \{-\cos(\theta_{3_3} - \alpha_3), \ \sin(\theta_{3_3} - \alpha_3); l_3 \sin\theta_{3_3}\}^{\text{T}} \tag{3.39c}
$$

Finally, the associated reciprocal screw matrix is assembled

$$
{}^{\text{ref}}[\mathbf{W}] = \begin{bmatrix} \cos\theta_{3_1} & -\cos\theta_{3_2} & -\cos(\theta_{3_3} - \alpha_3) \\ -\sin\theta_{3_1} & \sin\theta_{3_2} & \sin(\theta_{3_3} - \alpha_3) \\ 0 & l_2 \sin\theta_{3_2} & l_3 \sin\theta_{3_3} \end{bmatrix} \tag{3.40}
$$

Matrix ${}^{\text{ref}}[\mathbf{W}]$ becomes singular if its determinant is zero, i.e.,

$$
\begin{aligned}
|{}^{\text{ref}}[\mathbf{W}]| &= l_2 \sin(\theta_{3_2}) \left(\sin(\theta_{3_1}) \cos(\theta_{3_3} - \alpha_3) - \cos(\theta_{3_1}) \sin(\theta_{3_3} - \alpha_3)\right) \\
&\quad + l_3 \sin(\theta_{3_3}) \left(\cos(\theta_{3_1}) \sin(\theta_{3_2}) - \sin(\theta_{3_1}) \cos(\theta_{3_2})\right) = 0
\end{aligned} \tag{3.41}
$$

3.5.4 Loop-Closure Equations

The relationship between the joint angles of each branch and the pose (x, y and ϕ) of the mobile platform is defined by the forward kinematics of each branch, which describes $\{ref\}$ with respect to $\{0\}$, i.e.,

$$x = bx_i + \rho_{i+3}\cos(\theta_{1_i}) + \rho_i\cos(\theta_{1_i} + \theta_{2_i}) + l_i\cos(\theta_{1_i} + \theta_{2_i} + \theta_{3_i}) \quad (3.42a)$$

$$y = by_i + \rho_{i+3}\sin(\theta_{1_i}) + \rho_i\sin(\theta_{1_i} + \theta_{2_i}) + l_i\sin(\theta_{1_i} + \theta_{2_i} + \theta_{3_i}) \quad (3.42b)$$

$$\phi = \theta_{1_i} + \theta_{2_i} + \theta_{3_i} + \beta_i \quad (3.42c)$$

where $i = 1, 2, 3$.

In order to eliminate θ_{1_i} and θ_{2_i}, Eqs. (3.42a, 3.42b, and 3.42c) are sequentially substituted and squared, yielding

$$\begin{aligned} f_i(x,\ y,\ \phi,\ \theta_{3_i}) = {} & x^2 + (-2l_i\cos(\phi - \beta_i) - 2\rho_{i+3}\cos(\phi - \theta_{3_i} - \beta_i) - 2bx_i)x \\ & + y^2 + (-2l_i\sin(\phi - \beta_i) - 2\rho_{i+3}\sin(\phi - \theta_{3_i} - \beta_i) - 2by_i)y \\ & + 2l_i\rho_{i+3}\cos(\phi - \beta_i)\cos(\phi - \theta_{3_i} - \beta_i) + 2l_ibx_i\cos(\phi - \beta_i) \\ & + 2l_i\rho_{i+3}\sin(\phi - \beta_i)\sin(\phi - \theta_{3_i} - \beta_i) + 2l_iby_i\sin(\phi - \beta_i) \\ & + 2\rho_{i+3}bx_i\cos(\phi - \theta_{3_i} - \beta_i) + 2\rho_{i+3}by_i\sin(\phi - \theta_{3_i} - \beta_i) \\ & + bx_i^2 + by_i^2 + l_i^2 + \rho_{i+3}^2 - \rho_i^2 \end{aligned} \quad (3.43)$$

for $i = 1, 2, 3$.

3.5.5 Force-Unconstrained Poses

There are four equations, i.e., Eq.(3.41) and Eqs. (3.43), and six variables (x, y, ϕ, and θ_{3_i}, for $i = 1, 2, 3$). Following the same process carried out for the 3-PRR, the 'free' variables are considered to be joint displacements, in particular θ_{3_1} and

θ_{3_2}. Two solutions for θ_{3_3} are obtained with Eq. (3.41). The resulting values of θ_{3_i} constrain the manipulator to be force unconstrained. The pose of the manipulator is obtained by substituting the values of θ_{3_i} in Eq. (3.43).

Let Eq.(3.43) be written as

$$f_i(x,\ y,\ \phi) = x^2 + k_{1,i}x + y^2 + k_{2,i}y + k_{3,i} = 0 \tag{3.44}$$

where the coefficients $k_{j,i}$ are shown in Appendix D.2.

Notice that the coefficients of the squared terms of x and y in Eq. (3.44) are ones. To reduce these quadratic terms, equation $f_1(x,\ y,\ \phi) = 0$ is subtracted from equations $f_2(x,\ y,\ \phi) = 0$ and $f_3(x,\ y,\ \phi) = 0$ as follows:

$$\begin{aligned} h_1(x,\ y,\ \phi) &= f_2(x,y,\phi) - f_1(x,\ y,\ \phi) \\ &= (k_{1,2} - k_{1,1})\,x + (k_{2,2} - k_{2,1})\,y + (k_{3,2} - k_{3,1}) \\ &= a_{1,1}x + a_{1,2}y - b_1 = 0 \end{aligned} \tag{3.45}$$

and

$$\begin{aligned} h_2(x,\ y,\ \phi) &= f_3(x,y,\phi) - f_1(x,\ y,\ \phi) \\ &= (k_{1,3} - k_{1,1})\,x + (k_{2,3} - k_{2,1})\,y + (k_{3,3} - k_{3,1}) \\ &= a_{2,1}x + a_{2,2}y - b_2 = 0 \end{aligned} \tag{3.46}$$

where $a_{i,1} = (k_{1,i+1} - k_{1,1})$, $a_{i,2} = (k_{2,i+1} - k_{2,1})$, and $b_i = -(k_{3,i+1} - k_{3,1})$ are functions of ϕ, for $i = 1, 2$.

The system of linear equations Eqs. (3.45 and 3.46) can be written in matrix form.

$$\begin{bmatrix} a_{1,1} & a_{1,2} \\ a_{2,1} & a_{2,2} \end{bmatrix} \begin{bmatrix} x \\ y \end{bmatrix} = \begin{bmatrix} b_1 \\ b_2 \end{bmatrix} \tag{3.47}$$

The solution of x and y is determined by inverting the above matrix yielding

$$x = \frac{a_{2,2}b_1 - a_{1,2}b_2}{a_{1,1}a_{2,2} - a_{1,2}a_{2,1}} \qquad y = \frac{a_{1,1}b_2 - a_{2,1}b_1}{a_{1,1}a_{2,2} - a_{1,2}a_{2,1}} \tag{3.48}$$

The expressions obtained for x and y are then substituted in $f_1(x, y, \phi) = 0$. It is important to mention that Gosselin and Merlet (1994) used this elimination technique to solve the forward kinematics of the 3-RPR manipulator. Half-angle substitution is applied to ϕ (with t being the corresponding value of ϕ) and the denominator is cleared yielding a polynomial of degree 10 in t.

$$\sum_{i=0}^{10} c_i t^i = 0 \tag{3.49}$$

Numerical solutions of x and y are obtained from substituting the corresponding value of ϕ in Eqs. (3.48). The obtained pose is then transformed to frame $\{cen\}$, as described in Appendix B.3.

Example.-

A numerical example of the force-unconstrained poses of the centre of the platform of the 3-RRR manipulator is presented. Both platforms are equilateral triangles, their sides are 2.5 m for the fixed platform and 1 m for the mobile platform. The link lengths are $\rho_i = 1\ m$, for $i = 1, \ldots, 6$. Figure 3.8 illustrates, for each solution of the inverse kinematics[2], surfaces of force-unconstrained poses in the $x - y - \phi$ space. Figure 3.9 shows the combination of all surfaces. Each plot shows the projections on the xy plane.

[2]There are up to two solutions for each branch. Each configuration is labeled depending on the configuration of the elbow, + for elbow-down and - for elbow-up.

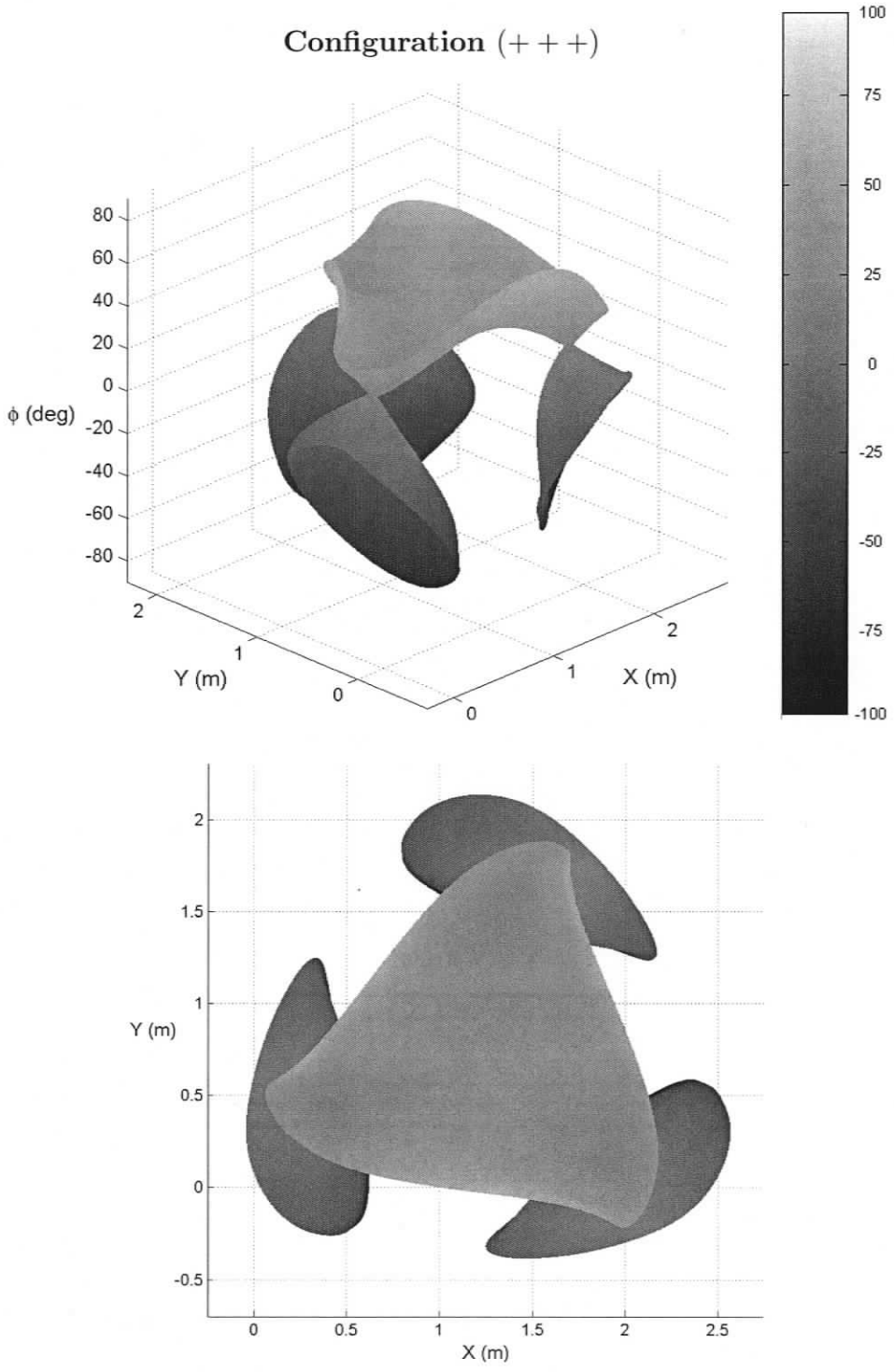

Figure 3.8: Force-Unconstrained Poses of the 3-RRR Manipulator.

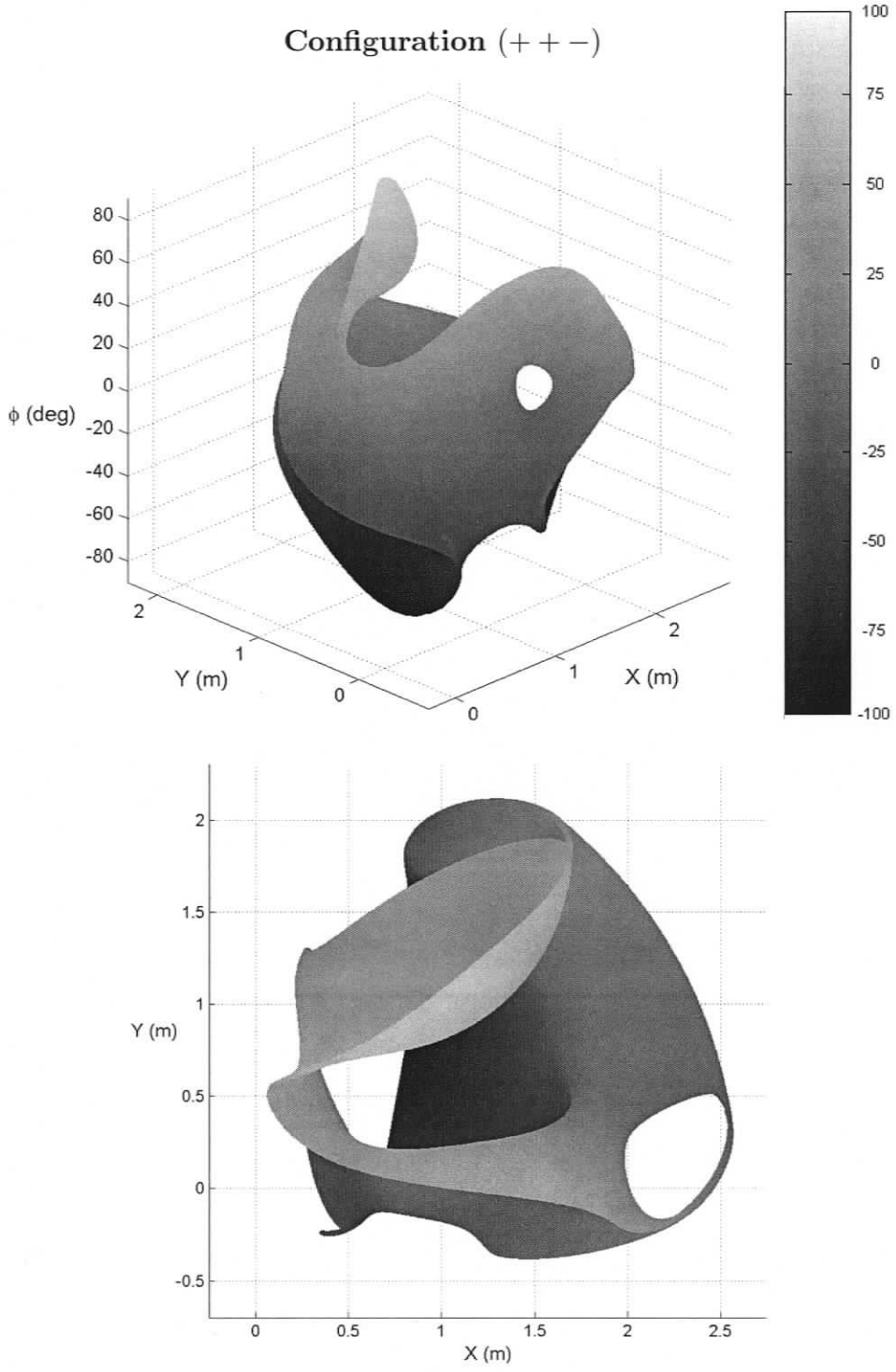

Figure 3.8 (cont'd): Force-Unconstrained Poses of the 3-RRR Manipulator.

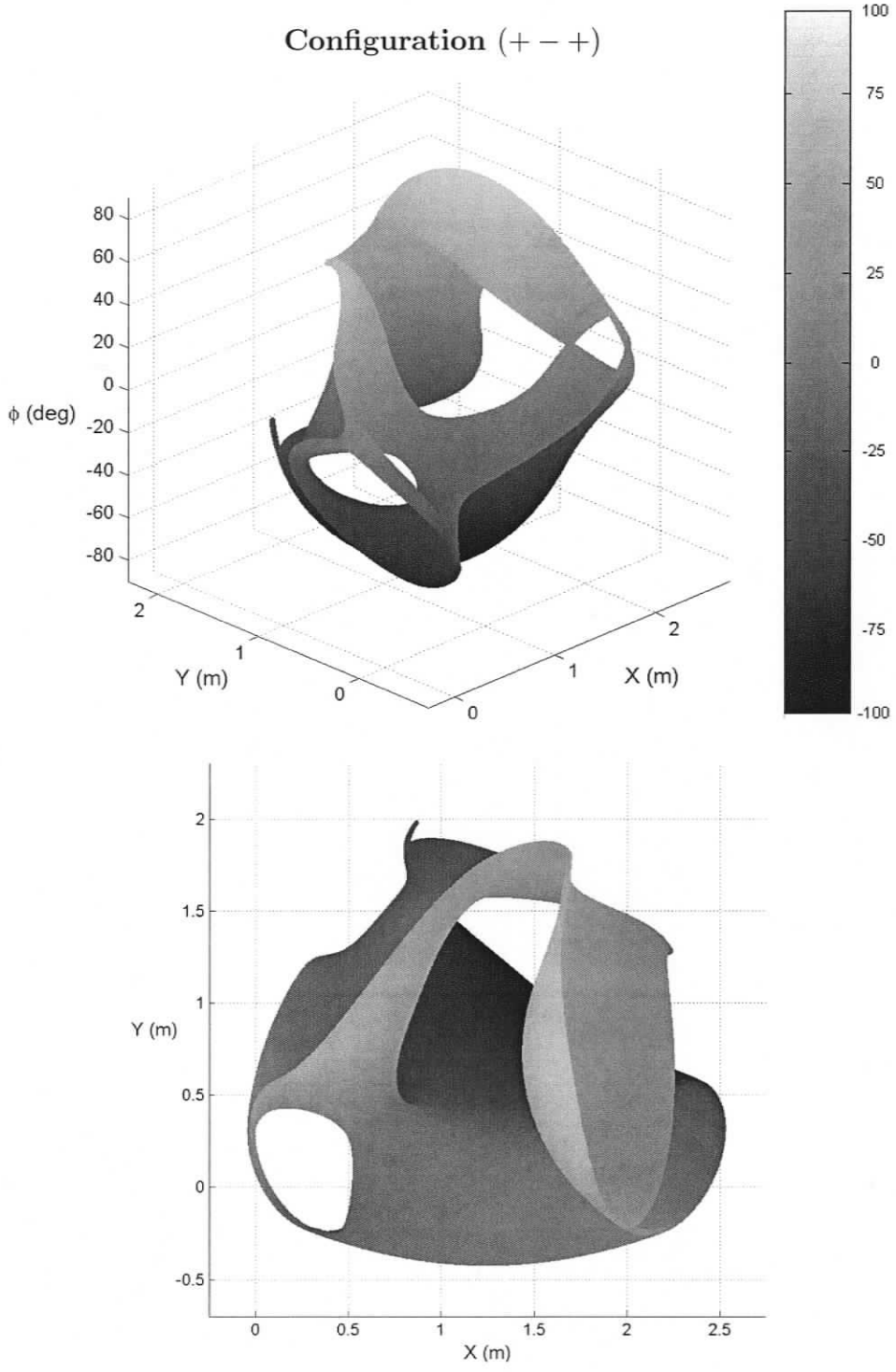

Figure 3.8 (cont'd): Force-Unconstrained Poses of the 3-RRR Manipulator.

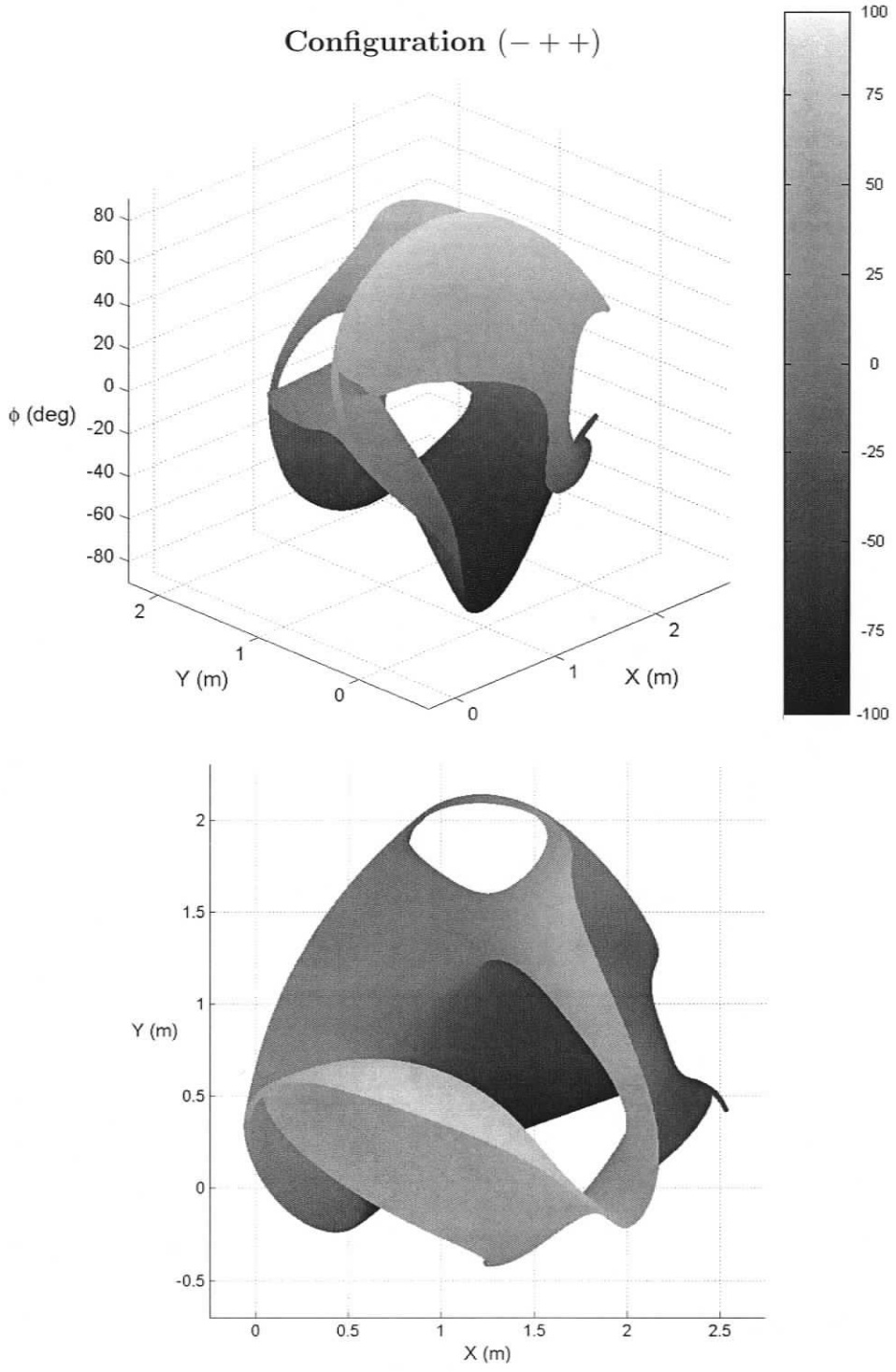

Figure 3.8 (cont'd): Force-Unconstrained Poses of the 3-RRR Manipulator.

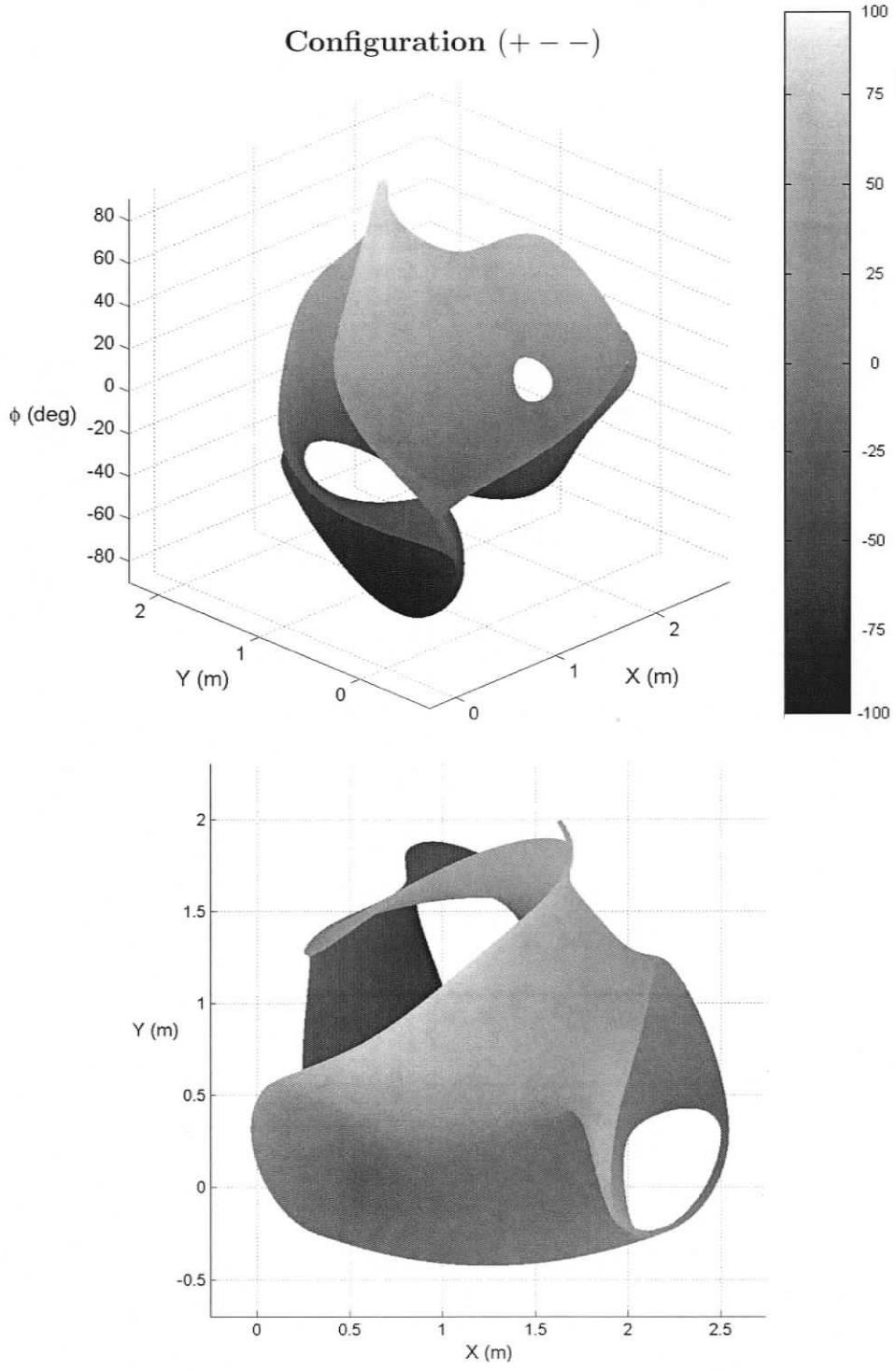

Figure 3.8 (cont'd): Force-Unconstrained Poses of the 3-RRR Manipulator.

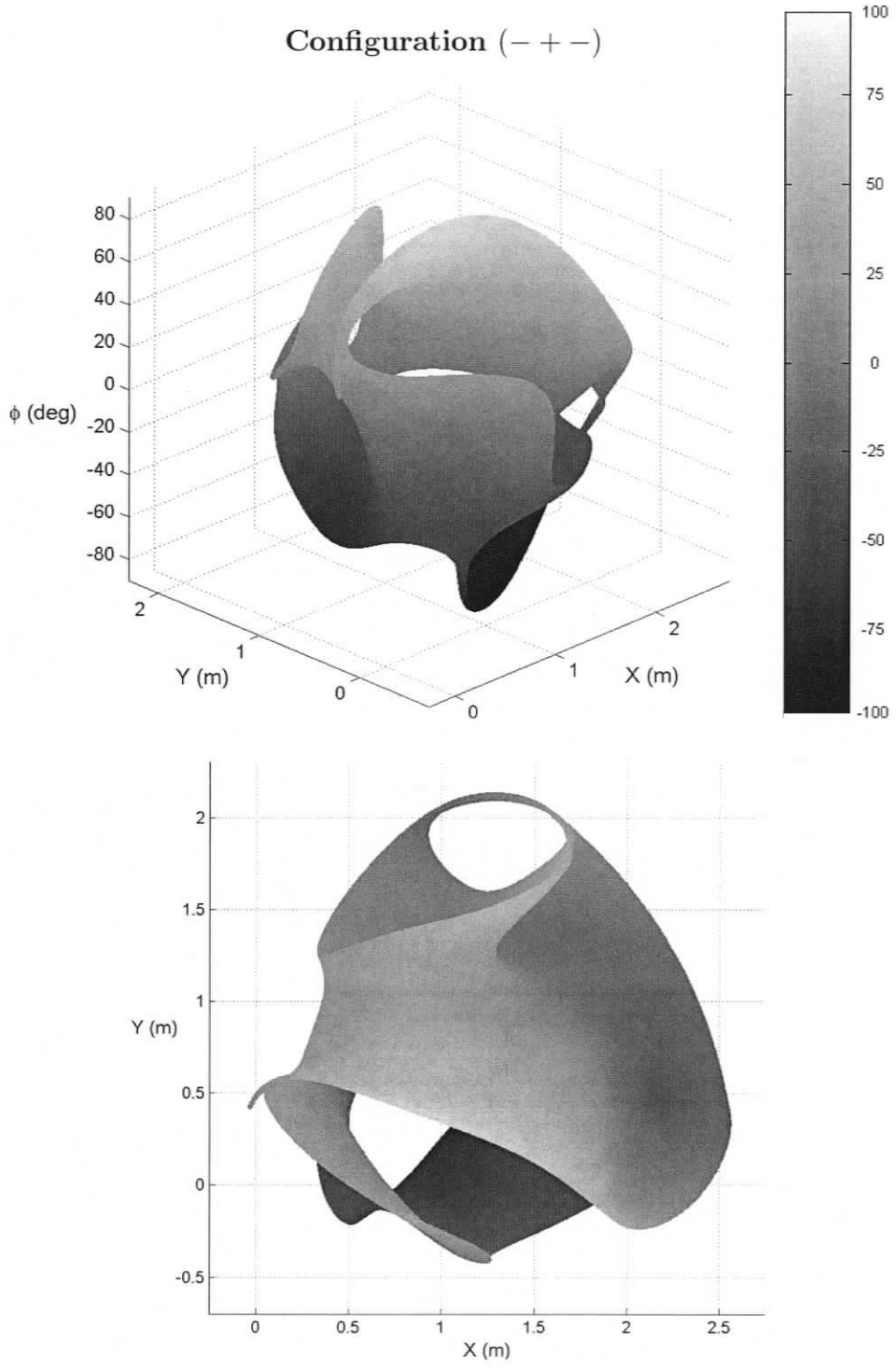

Figure 3.8 (cont'd): Force-Unconstrained Poses of the 3-RRR Manipulator.

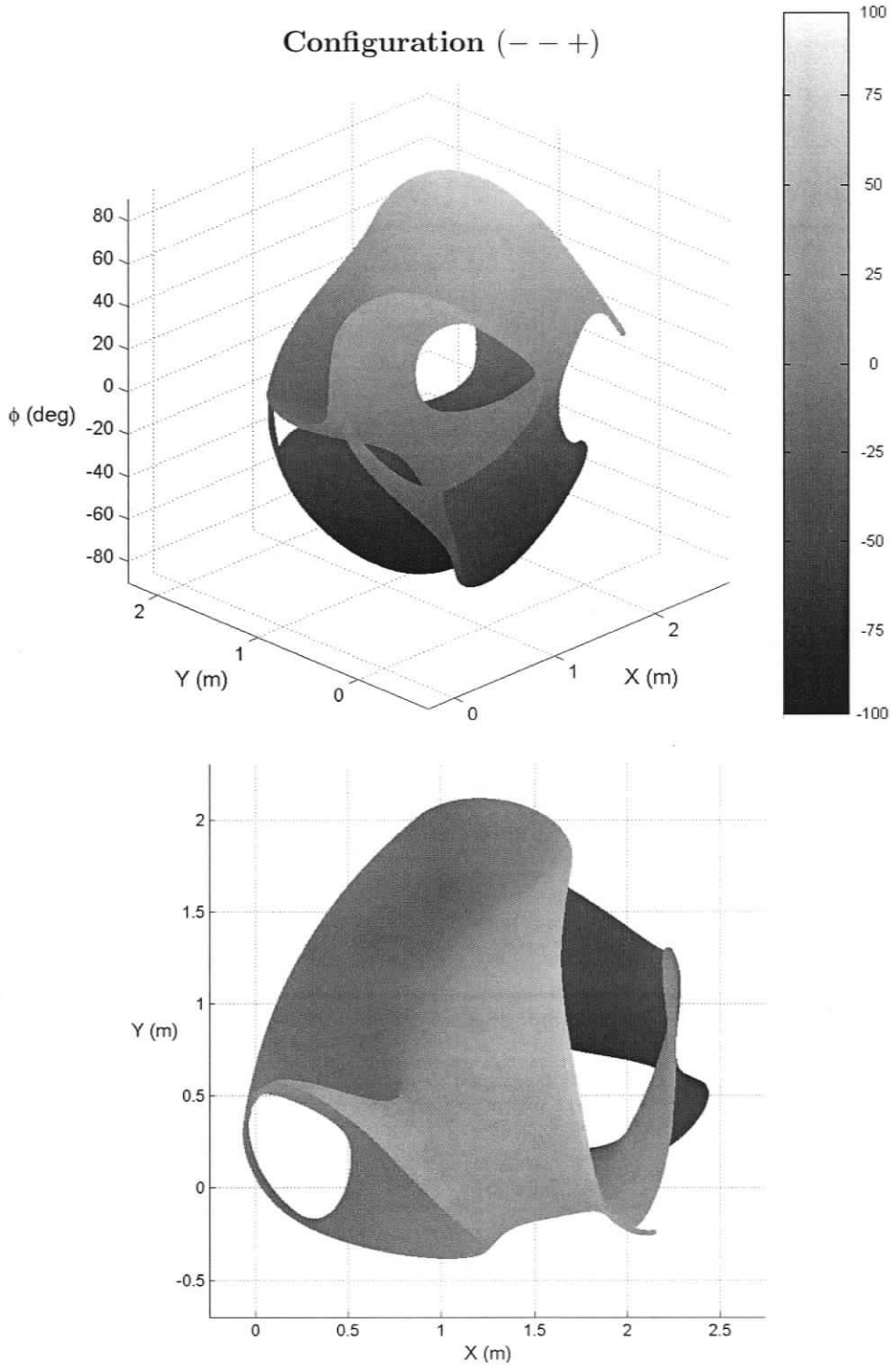

Figure 3.8 (cont'd): Force-Unconstrained Poses of the 3-RRR Manipulator.

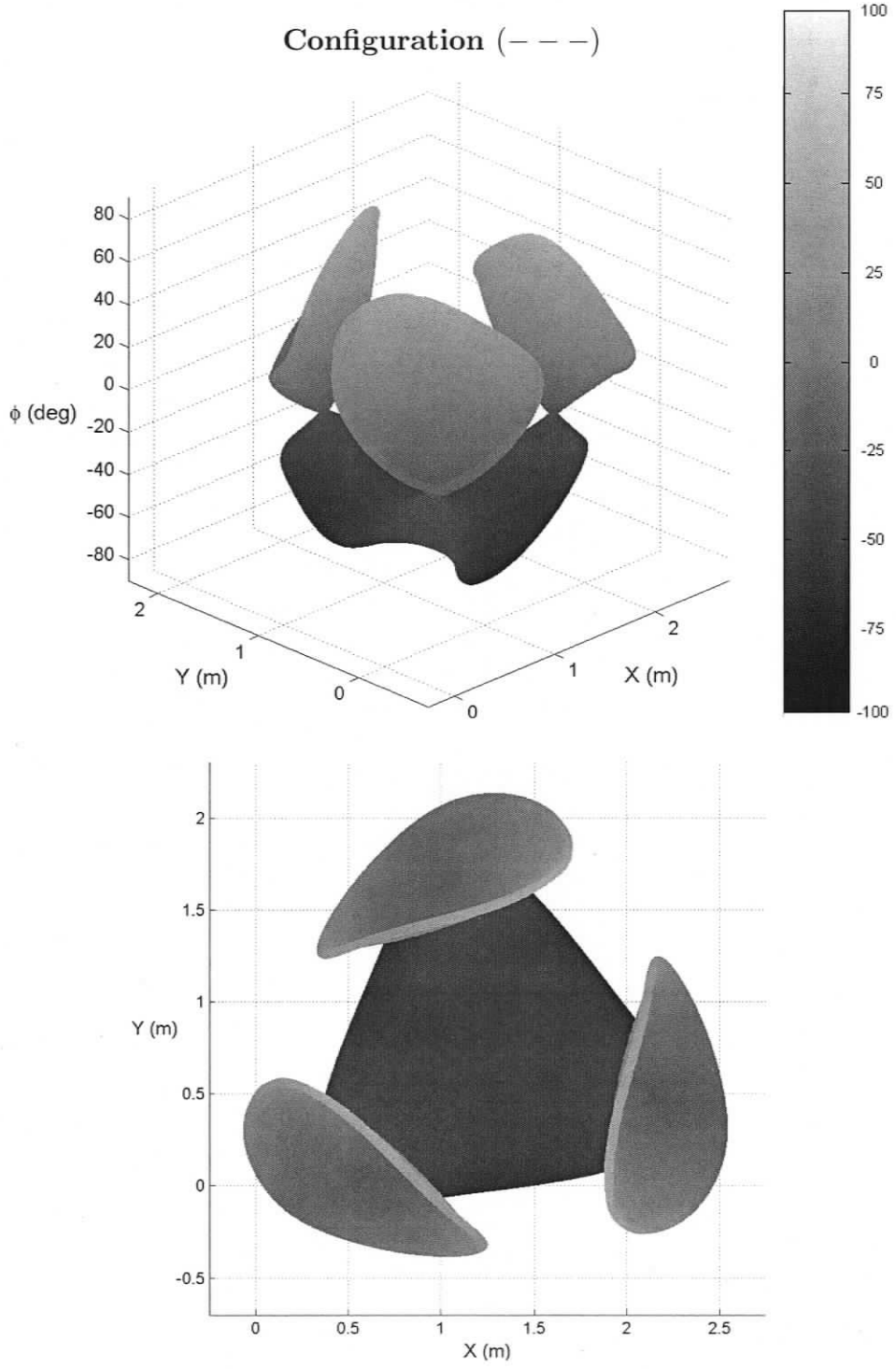

Figure 3.8 (cont'd): Force-Unconstrained Poses of the 3-RRR Manipulator.

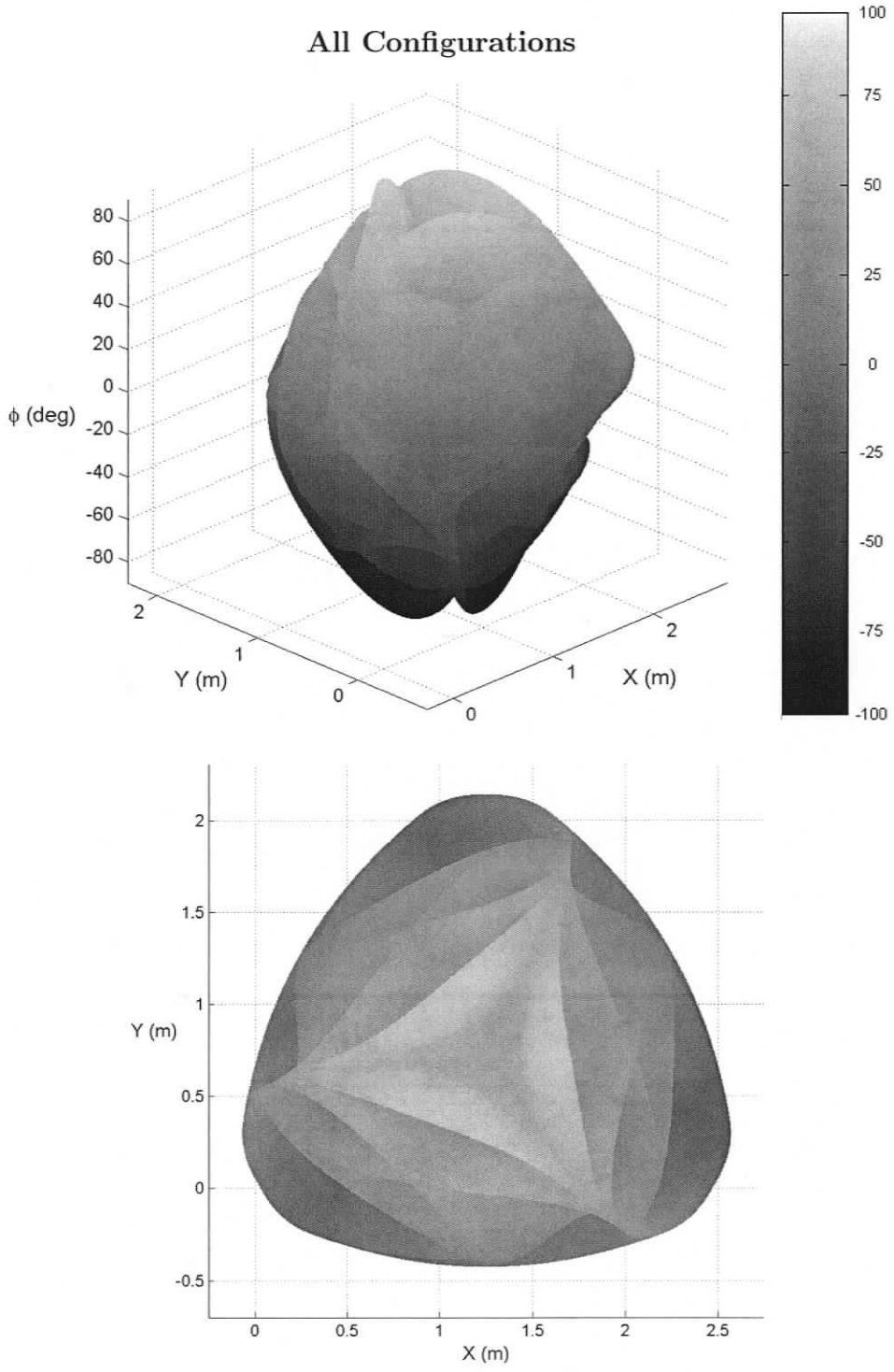

Figure 3.9: All Force-Unconstrained Poses of the 3-RRR Manipulator.

3.6 Discussion

In this chapter, force-unconstrained poses of the planar parallel manipulators that are the most feasible for industrial applications were presented. That is, manipulators that contain passive prismatic joints were excluded, yielding only three mechanisms to be examined: 3-R$\underline{P}$R, 3-$\underline{P}$RR, and 3-$\underline{R}$RR. The force-unconstrained poses of these mechanisms were plotted in a three-dimensional space defined by the position and orientation of the mobile platform, yielding surfaces, or an order of two infinities ($O(\infty^2)$), of force-unconstrained poses.

For the 3-R$\underline{P}$R manipulator, the time derivative method turned out to be more appropriate because of the simplicity of the problem. The Jacobian matrix is a function of the variables that define the pose of the end-effector, i.e., x, y, and ϕ. With the screw theory method, the associated reciprocal screw matrix is a function of the third joint displacements of each branch and through loop closure equations the joint displacements were converted into the pose variables. It is important to mention that the transformations that followed (transformation of the reference frame) had the single purpose of comparing both methodologies. Nonetheless, the screw theory method allows a strong perception of the physical representation of force-unconstrained configurations. Furthermore, if the third joint of each branch was to be sensed, an efficient formulation for real-time applications would result.

For the 3-$\underline{P}$RR and 3-$\underline{R}$RR manipulators, the screw theory method was considered. Primarily, for the physical meaning of the associated reciprocal screws. Secondly, for the effective and compact method used to identify the force-unconstrained configurations. The proposed methodology allows the identification of force-unconstrained poses for all working modes, rather than single working modes as in Bonev et al.

(2003); this aspect may be important if the third joints were sensed, no need to change parameters in equations. This methodology also allows the implementation to any design of the manipulators, as opposed to specific architectures as in Gosselin and Wang (1997). Given that there is $O(\infty^2)$ of force-unconstrained poses, it was considered to assign numerical values to two of the joint displacement variables. This consideration allowed the problem to be solved in a more efficient form. For the 3-PRR manipulator, the problem of identifying force-unconstrained configurations was reduced from a 20^{th} order polynomial, as described in the literature Bonev (2002) and Bonev et al. (2003), to a 6^{th} order polynomial. Similarly for the 3-RRR manipulator, the problem was reduced from a 42^{nd} order polynomial, as referred in Bonev and Gosselin (2001), to a 10^{th} order polynomial.

It is important to mention that the degree of the surfaces of force-unconstrained poses, for these two manipulators, has not been reduced, i.e., the degree of the surfaces are still represented by a 20^{th} and a 42^{nd} order polynomials in the position variables (x and y). With the proposed formulation, the real roots of the 6^{th} and 10^{th} order polynomials represent the number of assemblies that the mobile platform along with the second links (ρ_i, for $i = 1, 2, 3$), whose orientation are defined by θ_{3_i}, can have in the workspace of the manipulators. Nevertheless, the problem of identifying force-unconstrained configurations was indeed reduced.

As shown in the results, the surfaces of force-unconstrained poses are not convex. Thus, each graph was plotted using a large number of points, over a million points per working mode. To the contrary, the use of a mesh grid would have distorted the shape of the surfaces.

Chapter 4

Force-Unconstrained Poses of Planar Parallel Manipulators with In-Branch Redundancy

4.1 Overview

This chapter discusses the effect of including a greater number of actuators than the total degrees of freedom. In particular, the replacement of passive joints for active joints is considered. Depending on the actuation layout of the manipulator, there are two conditions that cause degenerate configurations. These conditions are identified for the following actuation layouts: RRR-2RRR, PRR-2PRR, and RRR-2RRR, with the first branch of each layout involving in-branch actuation redundancy. Equivalent mechanisms, whose motions describe the paths of continuous singularities of the mentioned actuation layouts, are presented. An analysis of manipulators with further actuation is also conducted.

4.2 Introduction

The inclusion of redundancy may lead to the elimination of families of force-unconstrained poses. For instance, to reduce uncertainty configurations, Notash and Podhorodeski considered over-constrained parallel manipulators by including either in-branch redundant actuation (1994) or redundant branches (1996). Lee and Kim (1993) discussed the use of in-branch redundancy to overcome singular configurations. Dasgupta and Mruthyunjaya (1998) defined the static relationship between the actuator forces $\mathbf{F}$ and the desired force $\mathbf{T}$ at the end-effector as $\mathbf{T} = [\mathbf{H}]\,\mathbf{F}$, where $[\mathbf{H}] \in \mathbf{R}^{m \times n}$ represents the force transformation matrix of a redundant actuation system. They demonstrated that the dimension of the singularity manifold (DOSM) of the device is given by:

$$DOSM = (m - 1) - (n - m) \tag{4.1}$$

with $m < n$, where m and n are referred to as the number of degrees of freedom and the number of actuated joints, respectively. Therefore, it is expected that with the inclusion of one extra actuator, the dimension of the singularity manifold will be reduced by an order of one.

For manipulators with redundant actuation, the associated reciprocal screw matrix is an $m \times n$ non-square matrix and thus taking its determinant is not possible.

In order to determine under which conditions the associated reciprocal screw matrix $[\mathbf{W}]$ is rank deficient, Singular Value Decomposition (SVD, Golub and Van Loan, 1983) can be applied. Assume that the rank of $[\mathbf{W}]$ is r, i.e., $r = rank([\mathbf{W}])$, where

$r \leqslant m$. Based on SVD, matrix $[\mathbf{W}]$ can be decomposed as

$$[\mathbf{W}] = [\mathbf{U}] \begin{bmatrix} \mathbf{S}_r & \mathbf{0} \\ \mathbf{0} & \mathbf{0} \end{bmatrix} [\mathbf{V}] \tag{4.2}$$

where $[\mathbf{U}]$ and $[\mathbf{V}]$ are $m \times m$ and $n \times n$ orthogonal matrices, respectively; and $[\mathbf{S}_r] = diag(\sigma_1, \sigma_2, \ldots, \sigma_r)$ is a diagonal matrix whose elements are the singular values of matrix $[\mathbf{W}]$. The rank of $[\mathbf{W}]$ can be also determined as follows:

$$r = rank([\mathbf{W}]) = rank([\mathbf{W}]\,[\mathbf{W}]^{\mathrm{T}}) \tag{4.3}$$

where $[\mathbf{W}]\,[\mathbf{W}]^{\mathrm{T}}$ is an $m \times m$ matrix.

A force-unconstrained pose will occur when $r < m$, i.e., $det([\mathbf{W}]\,[\mathbf{W}]^{\mathrm{T}}) = 0$. This approach was mentioned in (Merlet, 1996a).

Liao et al. (2004) developed a more thorough analysis of this approach using the Jacobian matrix, described in Eq. (2.3), where $[\mathbf{J}] = [\mathbf{B}]^{-1}\,[\mathbf{A}]$. They presented the following classification:

1. If $det([\mathbf{J}]^{\mathrm{T}}\,[\mathbf{J}]) = 0$, referred to as actuator singularity, where the end-effector can move even if all the actuators are locked. Thus, the manipulator is force unconstrained, i.e. matrix $[\mathbf{A}]$ is singular (Type II of singularities).

2. If $det([\mathbf{J}]^{\mathrm{T}}\,[\mathbf{J}]) = \infty$, referred to as end-effector singularity, where the end-effector loses one or more instantaneous degrees of freedom, i.e., matrix $[\mathbf{B}]$ is singular (Type I of singularities).

3. If $trace([\mathbf{J}]^{\mathrm{T}}\,[\mathbf{J}]) = \infty$, referred to as complex singularity, i.e., both matrices $[\mathbf{A}]$ and $[\mathbf{B}]$ are singular (Type III of singularities).

This approach can be easily implemented numerically (see for instance Voglewede and Ebert-Uphoff, 2004); however, if this approach was implemented for an analytical solution, the determinant would lead to a very long expression, which must be factorized in order to find the conditions that cause the associated reciprocal screw matrix to be rank deficient.

An alternative solution is obtained by setting the determinant of all unique $m \times m$ (3×3 for planar parallel manipulators) sub-matrices to zero. Merlet (1996a) referred to these minor matrices as the Jacobian matrices of the non-redundant manipulators that can be extracted from the redundant manipulator. The redundant manipulator is in a singular configuration if all the extracted manipulators are in a singular configuration, i.e., all the associated reciprocal screws must form a planar pencil. Dasgupta and Mruthyunjaya (1998) described this approach as the intersection of the hypersurfaces in the $m-$dimensional task space forming a lower dimensional manifold. This approach allows finding analytical expressions, or conditions, under which matrix $[\mathbf{W}]$ is rank deficient.

The actuation layouts analyzed in this chapter are RRR-2RRR, PRR-2PRR, and RRR-2RRR, whose notation implies that the first branch of each layout has two actuated joints.

4.3 Force-Unconstrained Poses of the RRR-2RRR

4.3.1 Degeneracy Conditions

The RRR-2RRR manipulator presents an actuation layout where all second joints are actuated, as well as the first joint of branch 1. Thus, the associated reciprocal screws of the actuated joints are determined using the reciprocal product equation, i.e., Eq. (2.17).

Branch 1

For joint 1_1 actuated: $\mathbf{W}_{1_1} \circledast \$_{j_1} = 0$, for j $\neq$1; yielding

$$^{\text{ref}}\mathbf{W}_{1_1} = \{c\theta_{3_1}, \ -s\theta_{3_1}; \ 0\}^{\text{T}} \tag{4.4a}$$

For joint 2_1 actuated: $\mathbf{W}_{2_1} \circledast \$_{j_1} = 0$, for j $\neq$2; yielding

$$^{\text{ref}}\mathbf{W}_{2_1} = \left\{ \begin{array}{c} \rho_4 c\left(\theta_{3_1} + \theta_{2_1}\right) + \rho_1 c\theta_{3_1} \\ -\rho_4 s\left(\theta_{3_1} + \theta_{2_1}\right) - \rho_1 s\theta_{3_1} \\ 0 \end{array} \right\} \tag{4.4b}$$

Branch 2

For joint 2_2 actuated: $\mathbf{W}_{2_2} \circledast \$_{j_2} = 0$, for j $\neq$2; yielding

$$^{\text{ref}}\mathbf{W}_{2_2} = \left\{ \begin{array}{c} -\rho_5 c\left(\theta_{3_2} + \theta_{2_2}\right) - \rho_2 c\theta_{3_2} \\ \rho_5 s\left(\theta_{3_2} + \theta_{2_2}\right) + \rho_2 s\theta_{3_2} \\ l_2\left(\rho_5 s\left(\theta_{3_2} + \theta_{2_2}\right) + \rho_2 s\theta_{3_2}\right) \end{array} \right\} \tag{4.4c}$$

Branch 3

For joint 2_3 actuated: $\mathbf{W}_{2_3} \circledast \$_{j_3} = 0$, for j $\neq$2; yielding

$$^{\text{ref}}\mathbf{W}_{2_3} = \left\{ \begin{array}{c} -\rho_6 c\left(\theta_{3_3} + \theta_{2_3} - \alpha_3\right) - \rho_3 c\left(\theta_{3_3} - \alpha_3\right) \\ \rho_6 s\left(\theta_{3_3} + \theta_{2_3} - \alpha_3\right) + \rho_3 s\left(\theta_{3_3} - \alpha_3\right) \\ l_3\left(\rho_6 s\left(\theta_{3_3} + \theta_{2_3}\right) + \rho_3 s\theta_{3_3}\right) \end{array} \right\} \tag{4.4d}$$

The associated reciprocal screw matrix of this actuation layout yields

$$^{\text{ref}}[\mathbf{W}] = \begin{bmatrix} ^{\text{ref}}\mathbf{W}_{1_1} & ^{\text{ref}}\mathbf{W}_{2_1} & ^{\text{ref}}\mathbf{W}_{2_2} & ^{\text{ref}}\mathbf{W}_{2_3} \end{bmatrix} \tag{4.5}$$

The sub-matrices of $^{\text{ref}}[\mathbf{W}]$ are as follows:

$$^{\text{ref}}[\mathbf{W}_A] = \begin{bmatrix} ^{\text{ref}}\mathbf{W}_{1_1} & ^{\text{ref}}\mathbf{W}_{2_1} & ^{\text{ref}}\mathbf{W}_{2_2} \end{bmatrix} \tag{4.6a}$$

$$^{\text{ref}}[\mathbf{W}_B] = \begin{bmatrix} ^{\text{ref}}\mathbf{W}_{1_1} & ^{\text{ref}}\mathbf{W}_{2_1} & ^{\text{ref}}\mathbf{W}_{2_3} \end{bmatrix} \tag{4.6b}$$

$$^{\text{ref}}[\mathbf{W}_C] = \begin{bmatrix} ^{\text{ref}}\mathbf{W}_{1_1} & ^{\text{ref}}\mathbf{W}_{2_2} & ^{\text{ref}}\mathbf{W}_{2_3} \end{bmatrix} \tag{4.6c}$$

$$^{\text{ref}}[\mathbf{W}_D] = \begin{bmatrix} ^{\text{ref}}\mathbf{W}_{2_1} & ^{\text{ref}}\mathbf{W}_{2_2} & ^{\text{ref}}\mathbf{W}_{2_3} \end{bmatrix} \tag{4.6d}$$

yielding the determinants:

$$|^{\text{ref}}[\mathbf{W}_A]| = -l_2\rho_4 s\theta_{2_1}\left(\rho_5 s\left(\theta_{3_2}+\theta_{2_2}\right)+\rho_2 s\theta_{3_2}\right) \tag{4.7a}$$

$$|^{\text{ref}}[\mathbf{W}_B]| = -l_3\rho_4 s\theta_{2_1}\left(\rho_6 s\left(\theta_{3_3}+\theta_{2_3}\right)+\rho_3 s\theta_{3_3}\right) \tag{4.7b}$$

Due to space limitations, the determinants of $^{\text{ref}}[\mathbf{W}_C]$ and $^{\text{ref}}[\mathbf{W}_D]$ have been omitted. Nevertheless, based on the conditions that make $|^{\text{ref}}[\mathbf{W}_A]| = |^{\text{ref}}[\mathbf{W}_B]| = 0$, the determinants of $^{\text{ref}}[\mathbf{W}_C]$ and $^{\text{ref}}[\mathbf{W}_D]$ will be checked. That is, if $|^{\text{ref}}[\mathbf{W}_C]| = |^{\text{ref}}[\mathbf{W}_D]| = 0$, the manipulator is force unconstrained.

To have $|^{\text{ref}}[\mathbf{W}_A]| = |^{\text{ref}}[\mathbf{W}_B]| = 0$ one of the following conditions must be true:

$$\begin{aligned} &\text{Condition 1} \quad \rho_5 s\left(\theta_{3_2}+\theta_{2_2}\right)+\rho_2 s\theta_{3_2} = 0 \\ &\qquad\qquad \text{and} \quad \rho_6 s\left(\theta_{3_3}+\theta_{2_3}\right)+\rho_3 s\theta_{3_3} = 0 \\ \text{or} \quad &\text{Condition 2} \quad s\theta_{2_1} = 0 \end{aligned}$$

An example of singular poses under these conditions are illustrated in Figure 4.1.

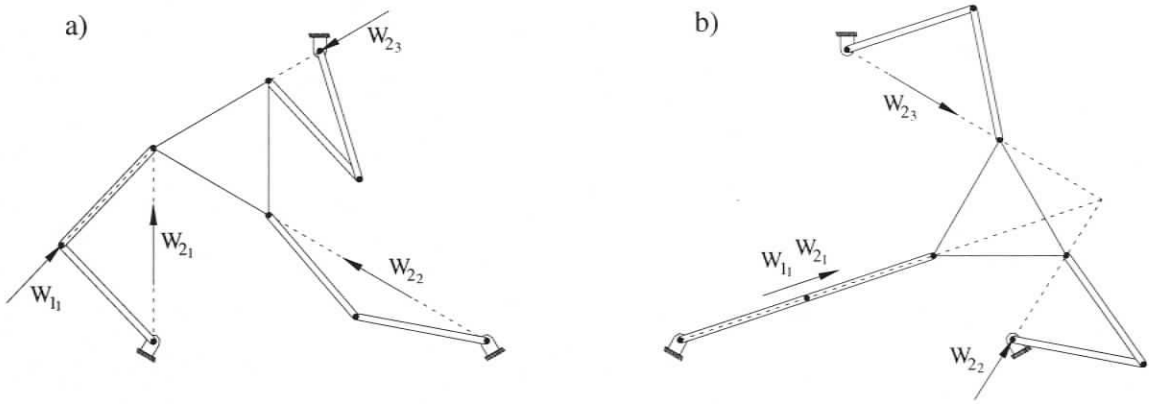

Figure 4.1: Force-Unconstrained Configurations of the RRR-2RRR Manipulator with a) Condition 1 and b) Condition 2.

4.3.2 Condition 1

Condition 1 makes the determinants of all the sub-matrices equal to zero. Expressions in terms of x, y, and ϕ that satisfy $|^{\text{ref}}[\mathbf{W}_A]| = |^{\text{ref}}[\mathbf{W}_B]| = |^{\text{ref}}[\mathbf{W}_C]| = |^{\text{ref}}[\mathbf{W}_D]| = 0$ can be found. The following loop-closure equations for branches 2 and 3 are considered.

Branch 2

$$p\left({}^{0}_{3_1}[\mathbf{T}]\ {}^{3_1}_{3_2}[\mathbf{T}]\ {}^{3_2}_{2_2}[\mathbf{T}]\ {}^{2_2}_{1_2}[\mathbf{T}]\right) = p\left({}^{0}_{1_2}[\mathbf{T}]\right) = \{bx_2, 0, 0\}^{\mathrm{T}}$$

$$= \begin{Bmatrix} x + c\phi\left(\rho_5 c\left(\theta_{3_2} + \theta_{2_2}\right) + \rho_2 c\theta_{3_2} + l_2\right) + s\phi\left(\rho_5 s\left(\theta_{3_2} + \theta_{2_2}\right) + \rho_2 s\theta_{3_2}\right) \\ y + s\phi\left(\rho_5 c\left(\theta_{3_2} + \theta_{2_2}\right) + \rho_2 c\theta_{3_2} + l_2\right) - c\phi\left(\rho_5 s\left(\theta_{3_2} + \theta_{2_2}\right) + \rho_2 s\theta_{3_2}\right) \\ 0 \end{Bmatrix} \tag{4.8}$$

where the operator $p(*)$ refers to the extraction of the $\mathbf{p}$ vector from the homogeneous transform

$$[\mathbf{T}] = \begin{bmatrix} \mathbf{n} & \mathbf{o} & \mathbf{a} & \mathbf{p} \\ 0 & 0 & 0 & 1 \end{bmatrix}$$

With Condition 1 satisfied, Eqs. (4.8) are reduced to

$$x + c\phi\left(\rho_5 c\left(\theta_{3_2} + \theta_{2_2}\right) + \rho_2 c\theta_{3_2} + l_2\right) = bx_2 \tag{4.9a}$$

$$y + s\phi\left(\rho_5 c\left(\theta_{3_2} + \theta_{2_2}\right) + \rho_2 c\theta_{3_2} + l_2\right) = 0 \tag{4.9b}$$

The loop-closure equation of branch 2 is reduced to its minimal expression by dividing Eq. (4.9b) by Eq. (4.9a)

$$\tan\phi = \frac{-y}{bx_2 - x} \tag{4.10}$$

Branch 3

$$p\left({}^{0}_{3_1}[\mathbf{T}]\ {}^{3_1}_{3_3}[\mathbf{T}]\ {}^{3_3}_{2_3}[\mathbf{T}]\ {}^{2_3}_{1_3}[\mathbf{T}]\right) = p\left({}^{0}_{1_3}[\mathbf{T}]\right) = \{bx_3, by_3, 0\}^{\mathrm{T}}$$

$$= \begin{Bmatrix} x + c\left(\phi + \alpha_3\right)\left(\rho_6 c\left(\theta_{3_3} + \theta_{2_3}\right) + \rho_3 c\theta_{3_3} + l_3\right) + s\left(\phi + \alpha_3\right)\left(\rho_6 s\left(\theta_{3_3} + \theta_{2_3}\right) + \rho_3 s\theta_{3_3}\right) \\ y + s\left(\phi + \alpha_3\right)\left(\rho_6 c\left(\theta_{3_3} + \theta_{2_3}\right) + \rho_3 c\theta_{3_3} + l_3\right) - c\left(\phi + \alpha_3\right)\left(\rho_6 s\left(\theta_{3_3} + \theta_{2_3}\right) + \rho_3 s\theta_{3_3}\right) \\ 0 \end{Bmatrix} \tag{4.11}$$

For Condition 1 to be true, i.e., $\rho_6 s\left(\theta_{3_3} + \theta_{2_3}\right) + \rho_3 s\theta_{3_3} = 0$, Eqs. (4.11) simplify to

$$x + c\left(\phi + \alpha_3\right)\left(\rho_6 c\left(\theta_{3_3} + \theta_{2_3}\right) + \rho_3 c\theta_{3_3} + l_3\right) = bx_3 \tag{4.12a}$$

$$y + s\left(\phi + \alpha_3\right)\left(\rho_6 c\left(\theta_{3_3} + \theta_{2_3}\right) + \rho_3 c\theta_{3_3} + l_3\right) = by_3 \tag{4.12b}$$

Dividing Eq. (4.12b) by Eq. (4.12a) yields

$$\tan\left(\phi + \alpha_3\right) = \frac{by_3 - y}{bx_3 - x} \tag{4.13}$$

The force-unconstrained poses of this manipulator occur when Eq. (4.10) and Eq. (4.13) are both satisfied. By solving for y in both equations and setting them equal, an expression of two unknowns x and ϕ results. Solving for x in terms of ϕ yields

$$x = \frac{bx_2\tan\left(\phi\right) - bx_3\tan\left(\phi + \alpha_3\right) + by_3}{\tan\left(\phi\right) - \tan\left(\phi + \alpha_3\right)} \tag{4.14}$$

Assume ϕ from 0 to 360° and find the corresponding values of x and y. The obtained pose is then transformed to frame $\{cen\}$, as described in Appendix B.3.

Example.-

An example of the force-unconstrained poses of the RRR - 2RRR manipulator, with Condition 1, is presented. Both platforms are equilateral triangles, their sides are 2.5 m for the fixed platform and 1 m for the mobile platform. The link lengths are $\rho_i = 1\ m$, for $i = 1, \ldots, 6$. The force-unconstrained poses are curves in the three-dimensional space defined by $x - y - \phi$ and are shown in Figure 4.2. The grey curve at the bottom of Figure 4.2 represents the projection of the force-unconstrained poses onto the horizontal plane.

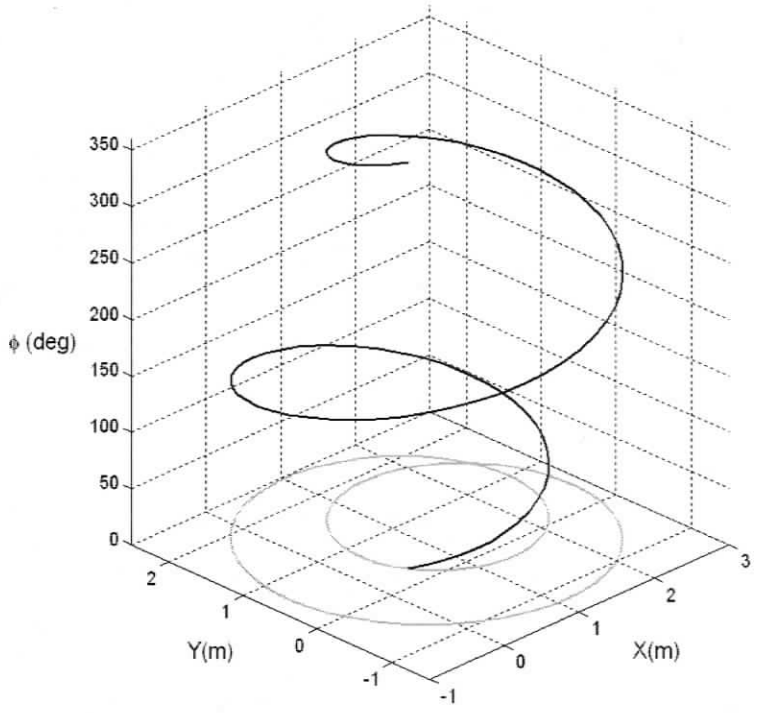

Figure 4.2: Loci of the Force-Unconstrained Poses of the RRR-2RRR Configuration with Condition 1.

The geometric meaning of Condition 1 implies that for the single-actuated branches the edges of the platform, l_2 and l_3, have to be collinear with the lines generated by the points w_i and b_i, for $i = 2, 3$, i.e., the associated reciprocal screws. An equivalent mechanism may be considered as an alternative for analyzing the singularity loci of Condition 1. This equivalent mechanism is composed of two prismatic joints connected at w_1 as shown in Figure 4.3. Thus, the equivalent device is reduced to a six-bar mechanism and the path followed by the centre of the mobile platform of this mechanism represents the force-unconstrained poses of the RRR-2RRR manipulator.

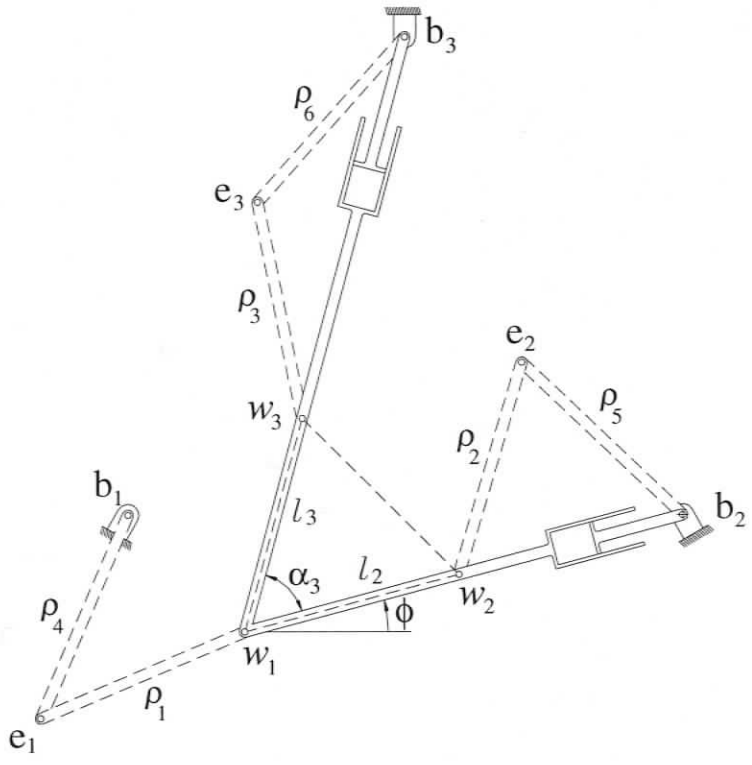

Figure 4.3: Equivalent Mechanism of Condition 1 for the RRR-2RRR Layout.

4.3.3 Condition 2

Condition 2 ($s\theta_{2_1} = 0$) does not satisfy $|^{\text{ref}}[\mathbf{W}_C]| = 0$ nor $|^{\text{ref}}[\mathbf{W}_D]| = 0$. With $s\theta_{2_1} = 0$, $|^{\text{ref}}[\mathbf{W}_D]|$ can be reduced, after simplification, to the same expression as $|^{\text{ref}}[\mathbf{W}_C]|$, i.e.,

$$|^{\text{ref}}[\mathbf{W}_C]| = \left\| \begin{bmatrix} {}^{\text{ref}}\mathbf{W}_{1_1} & {}^{\text{ref}}\mathbf{W}_{2_2} & {}^{\text{ref}}\mathbf{W}_{2_3} \end{bmatrix} \right\| \tag{4.15}$$

$$= \left\| \begin{bmatrix} (\rho_4 + \rho_1)c\theta_{3_1} & -\rho_5 c(\theta_{3_2} + \theta_{2_2}) - \rho_2 c\theta_{3_2} & -\rho_6 c(\theta_{3_3} + \theta_{2_3} - \alpha_3) - \rho_3 c(\theta_{3_3} - \alpha_3) \\ -(\rho_4 + \rho_1)s\theta_{3_1} & \rho_5 s(\theta_{3_2} + \theta_{2_2}) + \rho_2 s\theta_{3_2} & \rho_6 s(\theta_{3_3} + \theta_{2_3} - \alpha_3) + \rho_3 s(\theta_{3_3} - \alpha_3) \\ 0 & l_2(\rho_5 s(\theta_{3_2} + \theta_{2_2}) + \rho_2 s\theta_{3_2}) & l_3(\rho_6 s(\theta_{3_3} + \theta_{2_3}) + \rho_3 s\theta_{3_3}) \end{bmatrix} \right\|$$

Given that θ_{2_1} can be either 0° or 180°, an alignment of ρ_4 and ρ_1 yields two cases: a fully extended arm ($\theta_{2_1} = 0°$) or a folded back arm ($\theta_{2_1} = 180°$), the earlier being shown in Figure 4.1b. With either of these cases, a 2-dof, seven-bar mechanism results. However, the path followed by the resulting mechanism does not necessary represent singular configurations. Next, the two cases are analyzed.

Case 1: $\theta_{2_1} = 0°$

Let θ_{1_1} be an assumed variable from 0 to 360°. With θ_{1_1} and θ_{2_1} known, an expression that relates θ_{3_1} as a function of ϕ is obtained

$$\theta_{3_1} = \phi - \theta_{1_1} \tag{4.16}$$

Also, the position of the platform can be determined as follows:

$$w_1 = \begin{Bmatrix} x \\ y \end{Bmatrix} = \begin{Bmatrix} (\rho_4 + \rho_1)\cos(\theta_{1_1}) \\ (\rho_4 + \rho_1)\sin(\theta_{1_1}) \end{Bmatrix} \tag{4.17}$$

The orientation of the platform can be obtained through a substitution process. That is, the elements of the associated reciprocal screws shown in Eq. (4.15) can be written in terms of ϕ by means of the loop-closure equations of each branch.

Branch 1

By substituting Eqs. (4.16) and (4.17) in ${}^{\text{ref}}\mathbf{W}_{1_1}$, i.e., the first column of Eq.(4.15), the following relationship results:

$$ {}^{\text{ref}}\mathbf{W}_{1_1} = \begin{Bmatrix} (\rho_4+\rho_1)c\theta_{3_1} \\ -(\rho_4+\rho_1)s\theta_{3_1} \\ 0 \end{Bmatrix} = \begin{Bmatrix} (\rho_4+\rho_1)c(\phi-\theta_{1_1}) \\ -(\rho_4+\rho_1)s(\phi-\theta_{1_1}) \\ 0 \end{Bmatrix} = \begin{Bmatrix} xc\phi+ys\phi \\ -xs\phi+yc\phi \\ 0 \end{Bmatrix} \tag{4.18} $$

Branch 2

The elements of ${}^{\text{ref}}\mathbf{W}_{2_2}$ can be obtained using Eqs. (4.8). Writing Eqs. (4.8) in matrix form yields

$$ \begin{bmatrix} c\phi & s\phi \\ s\phi & -c\phi \end{bmatrix} \begin{bmatrix} \rho_5 c\left(\theta_{3_2}+\theta_{2_2}\right)+\rho_2 c\theta_{3_2} \\ \rho_5 s\left(\theta_{3_2}+\theta_{2_2}\right)+\rho_2 s\theta_{3_2} \end{bmatrix} = \begin{bmatrix} bx_2-x-l_2c\phi \\ -y-l_2s\phi \end{bmatrix} \tag{4.19} $$

hence,

$$ \begin{bmatrix} \rho_5 c\left(\theta_{3_2}+\theta_{2_2}\right)+\rho_2 c\theta_{3_2} \\ \rho_5 s\left(\theta_{3_2}+\theta_{2_2}\right)+\rho_2 s\theta_{3_2} \end{bmatrix} = \begin{bmatrix} -\left(x-bx_2\right)c\phi-ys\phi-l_2 \\ -\left(x-bx_2\right)s\phi+yc\phi \end{bmatrix} \tag{4.20} $$

Therefore, the associated reciprocal screw ${}^{\text{ref}}\mathbf{W}_{2_2}$ can be expressed in equivalent forms, i.e.,

$$ {}^{\text{ref}}\mathbf{W}_{2_2} = \begin{Bmatrix} -\rho_5 c\left(\theta_{3_2}+\theta_{2_2}\right)-\rho_2 c\theta_{3_2} \\ \rho_5 s\left(\theta_{3_2}+\theta_{2_2}\right)+\rho_2 s\theta_{3_2} \\ l_2\left(\rho_5 s\left(\theta_{3_2}+\theta_{2_2}\right)+\rho_2 s\theta_{3_2}\right) \end{Bmatrix} = \begin{Bmatrix} \left(x-bx_2\right)c\phi+ys\phi+l_2 \\ -\left(x-bx_2\right)s\phi+yc\phi \\ l_2\left(-\left(x-bx_2\right)s\phi+yc\phi\right) \end{Bmatrix} \tag{4.21} $$

Branch 3

The elements of ${}^{\text{ref}}\mathbf{W}_{2_3}$ are obtained using Eqs. (4.11). Writing Eqs. (4.11) in matrix form yields

$$\begin{bmatrix} c(\phi+\alpha_3) & s(\phi+\alpha_3) \\ s(\phi+\alpha_3) & -c(\phi+\alpha_3) \end{bmatrix} \begin{bmatrix} \rho_6 c(\theta_{3_3}+\theta_{2_3})+\rho_3 c(\theta_{3_3}) \\ \rho_6 s(\theta_{3_3}+\theta_{2_3})+\rho_3 s(\theta_{3_3}) \end{bmatrix} = \begin{bmatrix} bx_3 - x - l_3 c(\phi+\alpha_3) \\ by_3 - y - l_3 s(\phi+\alpha_3) \end{bmatrix} \tag{4.22}$$

Thus,

$$\begin{bmatrix} \rho_6 c(\theta_{3_3}+\theta_{2_3})+\rho_3 c(\theta_{3_3}) \\ \rho_6 s(\theta_{3_3}+\theta_{2_3})+\rho_3 s(\theta_{3_3}) \end{bmatrix} = \begin{bmatrix} \mu \\ \eta \end{bmatrix} \tag{4.23}$$

where

$$\mu = -(x - bx_3)\, c(\phi+\alpha_3) - (y - by_3)\, s(\phi+\alpha_3) - l_3$$
$$\eta = -(x - bx_3)\, s(\phi+\alpha_3) + (y - by_3)\, c(\phi+\alpha_3)$$

yielding the following associated reciprocal screw ${}^{\text{ref}}\mathbf{W}_{2_3}$

$${}^{\text{ref}}\mathbf{W}_{2_3} = \begin{Bmatrix} -\rho_6 c(\theta_{3_3}+\theta_{2_3}-\alpha_3) - \rho_3 c(\theta_{3_3}-\alpha_3) \\ \rho_6 s(\theta_{3_3}+\theta_{2_3}-\alpha_3) + \rho_3 s(\theta_{3_3}-\alpha_3) \\ l_3(\rho_6 s(\theta_{3_3}+\theta_{2_3}) + \rho_3 s\theta_{3_3}) \end{Bmatrix} = \begin{Bmatrix} -\mu c(\alpha_3) - \eta s(\alpha_3) \\ \eta c(\alpha_3) - \mu s(\alpha_3) \\ l_3\eta \end{Bmatrix} \tag{4.24}$$

The new expressions of the associated reciprocal screws are assembled in matrix form (${}^{\text{ref}}[\mathbf{W}_C]$). The determinant of this matrix is computed and half-angle substitution is applied to ϕ, yielding a 4^{th}-order polynomial in t, i.e.,

$$a_0 t^4 + a_1 t^3 + a_2 t^2 + a_3 t + a_4 = 0 \tag{4.25}$$

where the coefficients a_i are shown in Appendix D.3.1.

Example.-

An example of the force-unconstrained poses of the RRR - 2RRR manipulator with Condition 2 is shown in Figure 4.4. Both platforms are equilateral triangles, their sides are 2.5 m for the fixed platform and 1 m for the mobile platform. The link lengths of branch 1 are $\rho_4 = 1.5\ m$ and $\rho_1 = 1\ m$. The links of branches 2 and 3 are considered infinite. This assumption is made to show the closed-loop force-unconstrained poses. In the case that the link lengths of branches 2 and 3 were similar to the ones of branch 1, i.e., $\rho_5 = \rho_6 = 1.5\ m$ and $\rho_2 = \rho_3 = 1\ m$, the force-unconstrained poses would be small segments of the shown curves. The grey curve at the bottom of Figure 4.4 represents the projection of the force-unconstrained poses onto the horizontal plane.

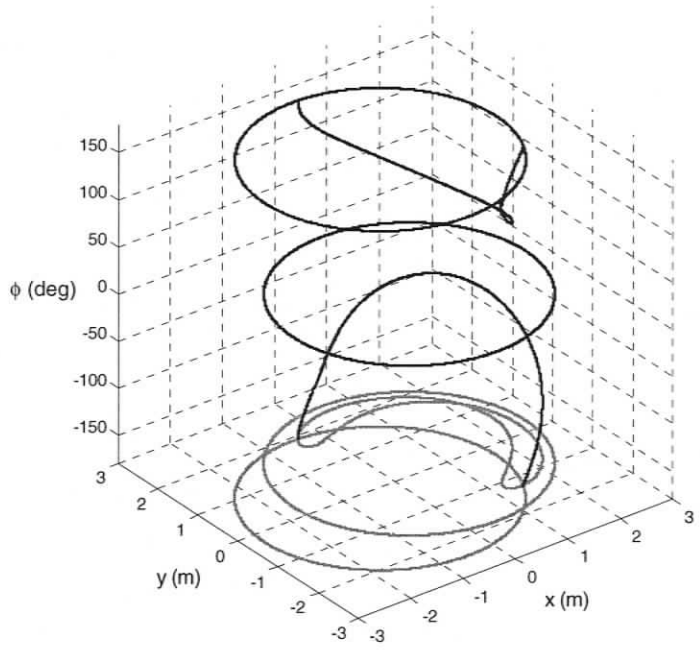

Figure 4.4: Force-Unconstrained Configurations of the RRR-2RRR Manipulator with Condition 2 (Case 1).

Case 2: $\theta_{2_1} = 180°$

With $\theta_{2_1} = 180°$, the position of the platform is defined as:

$$w_1 = \left\{ \begin{array}{c} x \\ y \end{array} \right\} = \left\{ \begin{array}{c} (\rho_4 - \rho_1)\cos(\theta_{1_1}) \\ (\rho_4 - \rho_1)\sin(\theta_{1_1}) \end{array} \right\} \tag{4.26}$$

Example.-

The force-unconstrained configurations of the manipulator described in the previous example are shown in Figure 4.5.

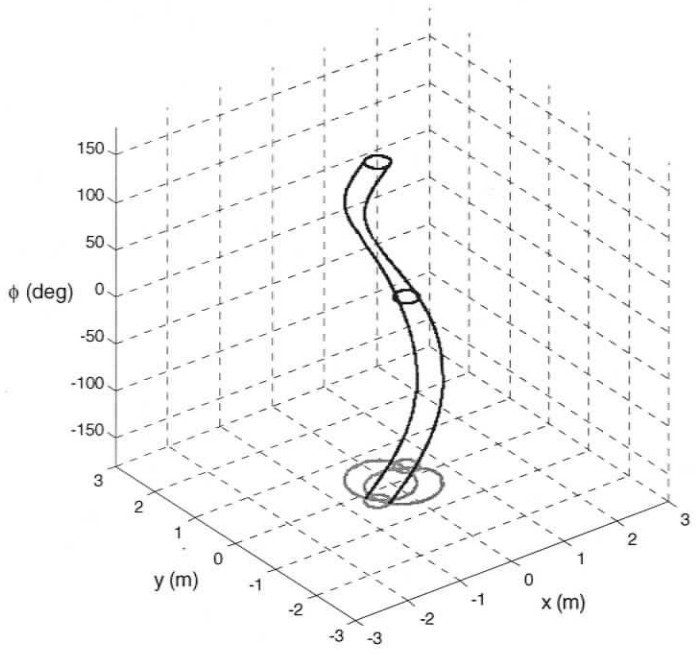

Figure 4.5: Force-Unconstrained Configurations of the RRR-2RRR Manipulator with Condition 2 (Case 2).

The circles that appear at $\phi = 0, 180°$ in Figures 4.4 and 4.5 are due to the fact that both platforms are similar. This situation has been already addressed for the 3-RPR manipulator, which could be considered as a kinematically equivalent manipulator when the length of the prismatic joint of branch 1 is kept constant.

4.4 Force-Unconstrained Poses of the PRR-2PRR

4.4.1 Degeneracy Conditions

Assume the 3-PRR manipulator with all the prismatic joints actuated, as well as the second joint of branch 1. The associated reciprocal screws of the second joint of the first branch is determined using the reciprocal product equation, i.e., Eq. (2.17).

For joint 2_1 actuated: $\mathbf{W}_{2_1} \circledast \$_{j_1} = 0$, for j $\neq$2; yielding

$$^{\text{ref}}\mathbf{W}_{2_1} = \left\{ \begin{array}{ccc} \cos\left(\theta_{3_1} + \theta_{2_1}\right) & -\sin\left(\theta_{3_1} + \theta_{2_1}\right) & 0 \end{array} \right\}^{\text{T}} \tag{4.27}$$

The associated reciprocal screw matrix of the PRR-2PRR is then assembled with the associated reciprocal screws of the actuated joints. For this configuration,

$$^{\text{ref}}\left[\mathbf{W}\right] = \left[\begin{array}{cccc} ^{\text{ref}}\mathbf{W}_{1_1} & ^{\text{ref}}\mathbf{W}_{2_1} & ^{\text{ref}}\mathbf{W}_{1_2} & ^{\text{ref}}\mathbf{W}_{1_3} \end{array} \right] \tag{4.28}$$

Thus, $^{\text{ref}}\left[\mathbf{W}\right]$ is divided in four sub-matrices, i.e.:

$$^{\text{ref}}\left[\mathbf{W}_A\right] = \left[\begin{array}{ccc} ^{\text{ref}}\mathbf{W}_{1_1} & ^{\text{ref}}\mathbf{W}_{2_1} & ^{\text{ref}}\mathbf{W}_{1_2} \end{array} \right] \tag{4.29a}$$

$$^{\text{ref}}\left[\mathbf{W}_B\right] = \left[\begin{array}{ccc} ^{\text{ref}}\mathbf{W}_{1_1} & ^{\text{ref}}\mathbf{W}_{2_1} & ^{\text{ref}}\mathbf{W}_{1_3} \end{array} \right] \tag{4.29b}$$

$$^{\text{ref}}\left[\mathbf{W}_C\right] = \left[\begin{array}{ccc} ^{\text{ref}}\mathbf{W}_{1_1} & ^{\text{ref}}\mathbf{W}_{1_2} & ^{\text{ref}}\mathbf{W}_{1_3} \end{array} \right] \tag{4.29c}$$

$$^{\text{ref}}\left[\mathbf{W}_D\right] = \left[\begin{array}{ccc} ^{\text{ref}}\mathbf{W}_{2_1} & ^{\text{ref}}\mathbf{W}_{1_2} & ^{\text{ref}}\mathbf{W}_{1_3} \end{array} \right] \tag{4.29d}$$

yielding the following determinants:

$$\left|^{\text{ref}}\left[\mathbf{W}_A\right]\right| = -l_2 \sin\theta_{3_2} \sin\theta_{2_1} \tag{4.30a}$$

$$\left|^{\text{ref}}\left[\mathbf{W}_B\right]\right| = -l_3 \sin\theta_{3_3} \sin\theta_{2_1} \tag{4.30b}$$

$$\begin{aligned} \left|^{\text{ref}}\left[\mathbf{W}_C\right]\right| = {} & l_2 \sin(\theta_{3_2}) \left(\sin(\theta_{3_1}) \cos(\theta_{3_3} - \alpha_3) - \cos(\theta_{3_1}) \sin(\theta_{3_3} - \alpha_3)\right) \\ & + l_3 \sin(\theta_{3_3}) \left(\cos(\theta_{3_1}) \sin(\theta_{3_2}) - \sin(\theta_{3_1}) \cos(\theta_{3_2})\right) \end{aligned} \tag{4.30c}$$

and

$$|^{\text{ref}}[\mathbf{W}_D]| = l_2 \sin(\theta_{3_2}) \left(\sin(\theta_{3_1} + \theta_{2_1}) \cos(\theta_{3_3} - \alpha_3) - \cos(\theta_{3_1} + \theta_{2_1}) \sin(\theta_{3_3} - \alpha_3)\right) + l_3 \sin(\theta_{3_3}) \left(\cos(\theta_{3_1} + \theta_{2_1}) \sin(\theta_{3_2}) - \sin(\theta_{3_1} + \theta_{2_1}) \cos(\theta_{3_2})\right) \tag{4.30d}$$

To have $|^{\text{ref}}[\mathbf{W}_A]| = |^{\text{ref}}[\mathbf{W}_B]| = 0$ either $s\theta_{3_2}$ and $s\theta_{3_3}$ or $s\theta_{2_1}$ must equal zero. That is, one of the two following conditions has to be satisfied for a force-unconstrained pose to exist:

$$\text{Condition 1} \quad s\theta_{3_2} = 0 \text{ and } s\theta_{3_3} = 0$$

$$\text{or} \quad \text{Condition 2} \quad s\theta_{2_1} = 0$$

An example of force-unconstrained configurations under these conditions are illustrated in Figure 4.6.

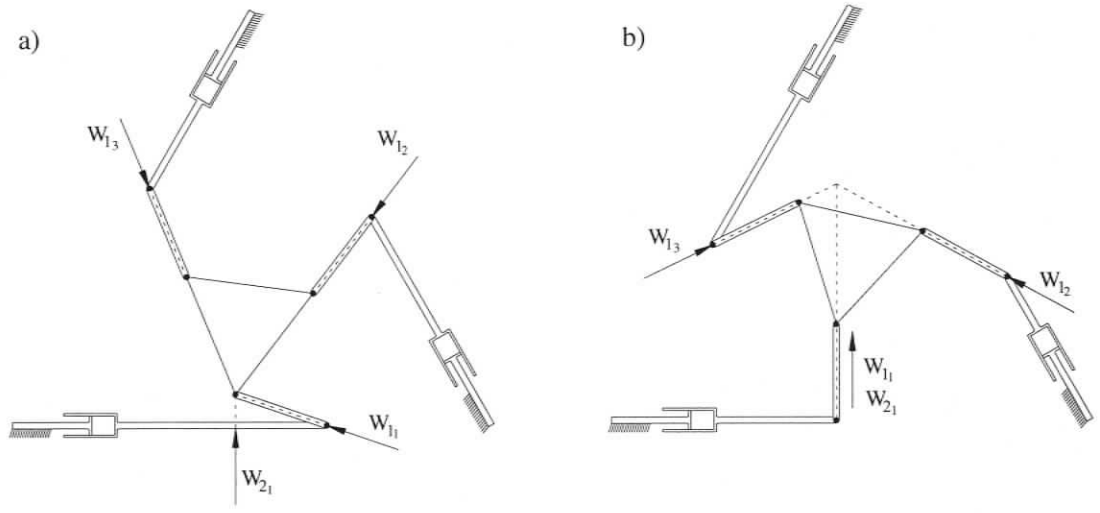

Figure 4.6: Force-Unconstrained Configurations of the PRR-2PRR Manipulator with a) Condition 1 and b) Condition 2.

Whether $|^{\text{ref}}[\mathbf{W}_C]| = |^{\text{ref}}[\mathbf{W}_D]| = 0$, for the above conditions, must be now checked.

4.4.2 Condition 1

For Condition 1 satisfied, the determinants of all sub-matrices are equal to zero. Therefore, expressions in terms of x, y, and ϕ that satisfy $|^{\text{ref}}[\mathbf{W}_A]| = |^{\text{ref}}[\mathbf{W}_B]| = |^{\text{ref}}[\mathbf{W}_C]| = |^{\text{ref}}[\mathbf{W}_D]| = 0$, can be found. These expressions are obtained with the loop-closure equations of branches 2 and 3.

Branch 2:

$$\begin{aligned} & p\left({}^{0}_{1_2}[\mathbf{T}] \;\; {}^{1_2}_{2_2}[\mathbf{T}] \;\; {}^{2_2}_{3_2}[\mathbf{T}] \;\; {}^{3_2}_{3_1}[\mathbf{T}]\right) = p\left({}^{0}_{3_1}[\mathbf{T}]\right) = \{x, y, 0\}^T \\ & = \left\{ \begin{array}{c} bx_2 - d_{1_2} s\gamma_2 + \rho_2 c\left(\gamma_2 + \theta_{2_2}\right) + l_2 c\left(\gamma_2 + \theta_{2_2} + \theta_{3_2}\right) \\ d_{1_2} c\gamma_2 + \rho_2 s\left(\gamma_2 + \theta_{2_2}\right) + l_2 s\left(\gamma_2 + \theta_{2_2} + \theta_{3_2}\right) \\ 0 \end{array} \right\} \end{aligned} \tag{4.31}$$

Since $\phi = \gamma_2 + \theta_{2_2} + \theta_{3_2} + \beta_2$, where $\beta_2 = \pi$, Eqs. (4.31) can be rewritten as:

$$bx_2 - d_{1_2} s\gamma_2 + \rho_2 c\left(\phi - \theta_{3_2} - \beta_2\right) + l_2 c\left(\phi - \beta_2\right) = x \tag{4.32a}$$

$$d_{1_2} c\gamma_2 + \rho_2 s\left(\phi - \theta_{3_2} - \beta_2\right) + l_2 s\left(\phi - \beta_2\right) = y \tag{4.32b}$$

In order to eliminate d_{1_2}, Eq. (4.32a) is multiplied by $c\gamma_2$ and Eq. (4.32b) is multiplied by $s\gamma_2$; then the resulting equations are subtracted, yielding

$$\left(x - bx_2\right) c\gamma_2 + ys\gamma_2 - l_2 c\left(\phi - \beta_2 - \gamma_2\right) - \rho_2 c\left(\phi - \theta_{3_2} - \beta_2 - \gamma_2\right) = 0 \tag{4.33}$$

where $s\theta_{3_2} = 0$ and $c\theta_{3_2} = \pm 1$.

Branch 3:

$$\begin{aligned} & p\left({}^{0}_{1_3}[\mathbf{T}] \;\; {}^{1_3}_{2_3}[\mathbf{T}] \;\; {}^{2_3}_{3_3}[\mathbf{T}] \;\; {}^{3_3}_{3_1}[\mathbf{T}]\right) = p\left({}^{0}_{3_1}[\mathbf{T}]\right) = \{x, y, 0\}^T \\ & = \left\{ \begin{array}{c} bx_3 - d_{1_3} s\gamma_3 + \rho_3 c\left(\gamma_3 + \theta_{2_3}\right) + l_3 c\left(\gamma_3 + \theta_{2_3} + \theta_{3_3}\right) \\ by_3 + d_{1_3} c\gamma_3 + \rho_3 s\left(\gamma_3 + \theta_{2_3}\right) + l_3 s\left(\gamma_3 + \theta_{2_3} + \theta_{3_3}\right) \\ 0 \end{array} \right\} \end{aligned} \tag{4.34}$$

Since $\phi = \theta_{1_2} + \theta_{2_2} + \theta_{3_2} + \beta_3$, where $\beta_3 = \pi - \alpha_3$, Eqs. (4.34) can be simplified similarly yielding

$$(x - bx_3)\, c\gamma_3 + (y - by_3)\, s\gamma_3 - l_3 c\,(\phi - \beta_3 - \gamma_3) - \rho_3 c\,(\phi - \theta_{3_3} - \beta_3 - \gamma_3) = 0 \tag{4.35}$$

where $s\theta_{3_3} = 0$ and $c\theta_{3_3} = \pm 1$.

There are four possible combinations of Eqs. (4.33 and 4.35) due to $c\theta_{3_2} = \pm 1$ and $c\theta_{3_3} = \pm 1$. Thus, for each combination, Eqs. (4.33 and 4.35) lead to a system of equations in three variables. Geometrically, these equations represent two sets of surfaces and their intersections would yield curves in the three-dimensional space defined by x, y, and ϕ, i.e., there is one order of infinity $O(\infty)$ of force-unconstrained poses. Assume angle ϕ from 0° to 360°. Since x and y are linear terms in Eqs. (4.33 and 4.35), the following problem results:

$$\begin{bmatrix} s\gamma_2 & -c\gamma_2 \\ s\gamma_3 & -c\gamma_3 \end{bmatrix} \begin{bmatrix} x \\ y \end{bmatrix} = \begin{bmatrix} a_1 \\ a_2 \end{bmatrix} \tag{4.36}$$

where a_1 and a_2 are constants of the already known values, i.e.,

$$a_1 = bx_2 c\gamma_2 - l_2 c\,(\phi - \beta_2 - \gamma_2) - \rho_2 c\,(\phi - \theta_{3_2} - \beta_2 - \gamma_2)$$
$$a_2 = bx_3 c\gamma_3 + by_3 s\gamma_3 + l_3 c\,(\phi - \beta_3 - \gamma_3) + \rho_3 c\,(\phi - \theta_{3_3} - \beta_3 - \gamma_3)$$

Finally, x and y are solved using Gaussian elimination. This analysis is repeated for each combination of $c\theta_{3_2}$ and $c\theta_{3_3}$. Nevertheless, the configurations when either $c\theta_{3_2} = -1$ or $c\theta_{3_3} = -1$, and even more when $c\theta_{3_2} = c\theta_{3_3} = -1$, are not likely to occur. That is, an assembly of the manipulator when one or both of the links ρ_k are folded back, for $k = 2, 3$, cannot be achieved.

Example.-

A numerical example of the force-unconstrained poses of the PRR - 2PRR manipulator is presented. Both platforms are equilateral triangles, their sides are 2.5 m for the fixed platform and 0.5 m for the mobile platform. The link lengths are $\rho_i = 1$ m, for $i = 1, 2, 3$. For this manipulator, only the combination when $c\theta_{3_2} = c\theta_{3_3} = 1$ leads to force-unconstrained configurations, as illustrated in Figure 4.7. The grey curve at the bottom of Figure 4.7 is the projection of the force-unconstrained poses on the horizontal plane.

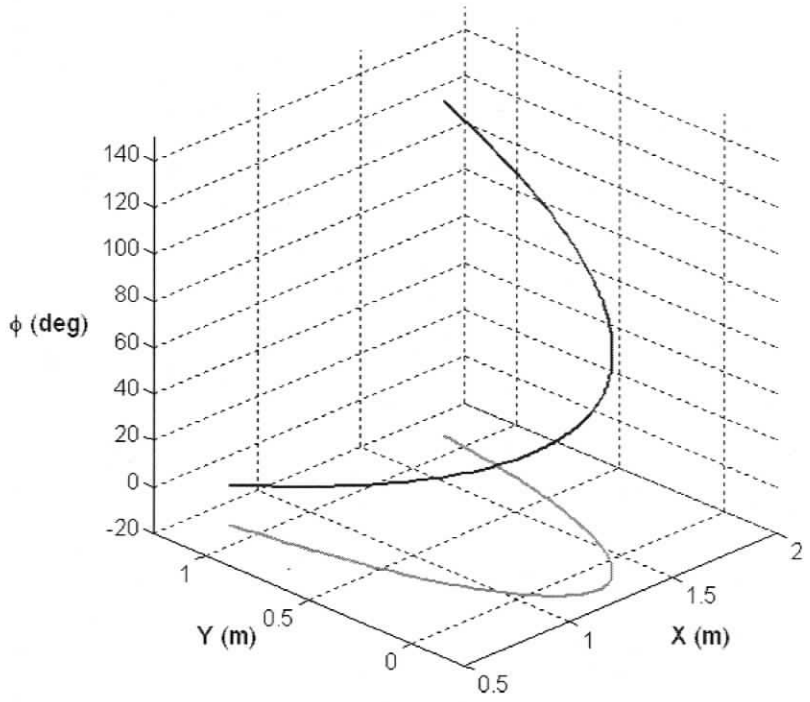

Figure 4.7: Force-Unconstrained Configurations of the PRR-2PRR Manipulator with Condition 1.

An equivalent-mechanism-based analysis can be made with Condition 1. For $s\theta_{3_2} = 0$ and $s\theta_{3_3} = 0$, branches 2 and 3 must have their second link collinear to

the platform edges. This implies that links ρ_2 and ρ_3 become part of the mobile platform yielding a six-bar mechanism. Therefore, the prismatic joints d_{1_2} and d_{1_3} are connected by a coupler r. There are four combinations of possible mechanisms depending on the orientation of ρ_2 and ρ_3. The six-bar mechanism depicted in Figure 4.8, which is the most likely to occur, shows ρ_2 and ρ_3 as extensions of the platform. In this case, the coupler r is determined using cosine law, i.e.,

$$\begin{aligned} r^2 &= (l_2+\rho_2)^2 + (l_3+\rho_3)^2 - 2\,(l_2+\rho_2)\,(l_3+\rho_3)\cos(\alpha_3) \\ &= a^2 + b^2 - 2ab\cos(\alpha_3) \end{aligned} \tag{4.37}$$

Two of the other mechanisms can be formed by folding back one of the links. The coupler, when ρ_2 is folded back, is found with $a = (l_2 - \rho_2)$, while the coupler when ρ_3 is folded back is determined with $b = (l_3 - \rho_3)$. The last mechanism requires both ρ_2 and ρ_3 folded back, i.e., $a = (l_2 - \rho_2)$ and $b = (l_3 - \rho_3)$.

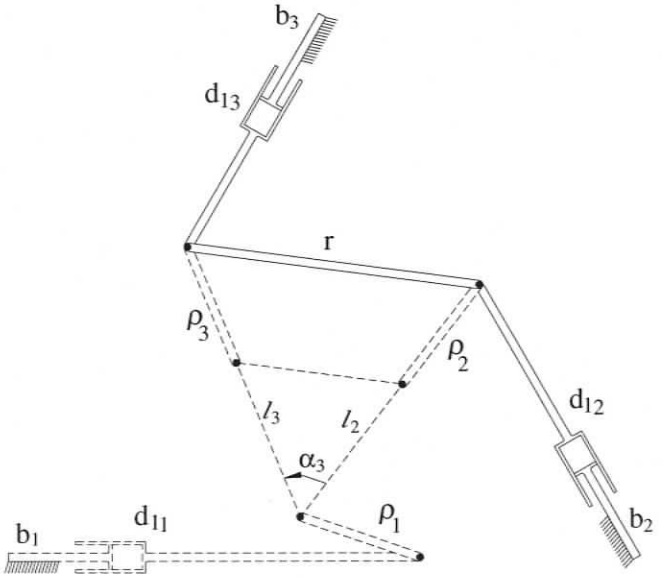

Figure 4.8: Equivalent Mechanism of Condition 1 for the PRR-2PRR Layout.

4.4.3 Condition 2

Condition 2 ($s\theta_{2_1} = 0$) does not satisfy $|^{\text{ref}}[\mathbf{W}_C]| = 0$ nor $|^{\text{ref}}[\mathbf{W}_D]| = 0$. Nevertheless with condition 2 true, $|^{\text{ref}}[\mathbf{W}_D]|$, which is a function of θ_{2_1}, is reduced to the same expression as $|^{\text{ref}}[\mathbf{W}_C]|$, which is the determinant of the non-redundant 3-PRR manipulator, i.e., Eq. (3.31). Since θ_{2_1} can be either 0° or 180°, the orientation of link ρ_1 is, therefore, perpendicular to the prismatic joint d_{1_1}.

Case 1 $\theta_{2_1} = 180°$

With $\theta_{2_1} = 180°$, link ρ_1 lies in the positive direction of axis y_0 (vertical), as shown in Figure 4.6, yielding a seven-bar mechanism. The position of $w_1 = \{x, y\}^{\mathrm{T}}$ yields

$$w_1 = \begin{Bmatrix} x \\ y \end{Bmatrix} = \begin{Bmatrix} d_{1_1} \\ \rho_1 \end{Bmatrix} \tag{4.38}$$

If the length of d_{1_1} is assumed, the problem is reduced to finding the orientation of the platform. With $\theta_{2_1} = 180°$, Eq. (3.32c) for $i = 1$, with $\beta_1 = 0$, is reduced to $\phi = \gamma_1 + \pi + \theta_{3_1}$. Thus, an expression of θ_{3_1} as a function of ϕ results:

$$\theta_{3_1} = \phi - \gamma_1 - \pi \tag{4.39}$$

Substituting Eq. (4.39) in Eq. (3.31) and applying half-angle substitution, with t, q_2, and q_3 being the corresponding variables of ϕ, θ_{3_2}, and θ_{3_3}, respectively, a polynomial of the following form results:

$$\begin{aligned} g(t, q_2, q_3) = (a_1t^2 + a_2t + a_3)q_2^2q_3 + (a_4t^2 + a_5t + a_6)q_2q_3^2 + (a_7t^2 + a_8t + a_9)q_2q_3 \\ +(a_{10}t^2 + a_{11}t + a_{12})q_2 + (a_{13}t^2 + a_{14}t + a_{15})q_3 = 0 \end{aligned} \tag{4.40}$$

where the coefficients a_i are shown in Appendix D.3.2.

On the other hand, the loop-closure equations of branches[1] 2 and 3, given in Eq. (3.33), are written using half-angle substitution, yielding the following polynomials:

$$f_1(t, q_2) = (b_1t^2 + b_2t + b_3)q_2^2 + (b_4t^2 + b_5t + b_6)q_2 + (b_7t^2 + b_8t + b_9) = 0 \quad (4.41)$$

$$f_2(t, q_3) = (c_1t^2 + c_2t + c_3)q_3^2 + (c_4t^2 + c_5t + c_6)q_3 + (c_7t^2 + c_8t + c_9) = 0 \quad (4.42)$$

where the coefficients b_i and c_i are shown in Appendix D.3.2.

Thus, a system of three polynomials ($g(t, q_2, q_3) = 0$, $f_1(t, q_2) = 0$, and $f_2(t, q_3) = 0$) in three variables (t, q_2, and q_3) results. As described in Eq. (C.4), applying Bezout's number to the polynomial system leads to up to 80 solutions, i.e.,

$$d_{\mathrm{T}} = \prod_{i=1}^{3} d_i = (5)(4)(4) = 80 \quad (4.43)$$

This can be reduced using m-homogenization by arranging the variables in three groups (t, q_2, q_3). The degrees of the three polynomials in the variables of each group is given in Table 4.1.

Table 4.1: Degrees of the 3-Homogeneous System.

Equation	Group $j = 1$ (t)	Group $j = 2$ (q_2)	Group $j = 3$ (q_3)
$g(t, q_2, q_3) = 0$	2	2	2
$f_1(t, q_2) = 0$	2	2	0
$f_2(t, q_3) = 0$	2	0	2

Therefore, the 3-homogeneous Bezout's number is determined with Eq. (C.5), i.e.,

$$\prod_{i=1}^{3}\left(\sum_{j=1}^{3} d_{ji}\beta_j\right) = (2\beta_1 + 2\beta_2 + 2\beta_3)\,(2\beta_1 + 2\beta_2)\,(2\beta_1 + 2\beta_3) \quad (4.44)$$

[1] With the imposed conditions, the loop-closure equation of branch 1 equals zero.

yielding $\prod_{j=1}^{3} \beta_j = 24\beta_1\beta_2\beta_3$. Thus, the 3-homogeneous Bezout's number is 24.

This system of polynomials can be solved using the Sylvester dialytic elimination method, which is based on a linearization of power products and is described in Appendix C.6. Let t be the suppressed variable. New linearly independent equations have to be generated, such that the number of power products matches the number of equations. In Table 4.2, new equations are generated by multiplying the original 3 equations by terms formed with the non-suppressed variables. The original and new power products are shown in bold.

Table 4.2: Generation of 13 Linearly Independent Polynomials.

$\text{eq}_1 = g(t, q_2, q_3) = 0$	$a'_1\mathbf{q}_2^2\mathbf{q}_3 + a'_2\mathbf{q}_2\mathbf{q}_3^2 + a'_3\mathbf{q}_2\mathbf{q}_3 + a'_4\mathbf{q}_2 + a'_5\mathbf{q}_3 = 0$
$\text{eq}_2 = f_1(t, q_2) = 0$	$b'_1\mathbf{q}_2^2 + b'_2q_2 + b'_3(\mathbf{1}) = 0$
$\text{eq}_3 = f_2(t, q_3) = 0$	$c'_1\mathbf{q}_3^2 + c'_2q_3 + c'_3 = 0$
$\text{eq}_4 = f_1(t, q_2)(q_3) = 0$	$b'_1q_2^2q_3 + b'_2q_2q_3 + b'_3q_3 = 0$
$\text{eq}_5 = f_2(t, q_3)(q_2) = 0$	$c'_1q_2q_3^2 + c'_2q_2q_3 + c'_3q_2 = 0$
$\text{eq}_6 = f_1(t, q_2)(q_3^2) = 0$	$b'_1\mathbf{q}_2^2\mathbf{q}_3^2 + b'_2q_2q_3^2 + b'_3q_3^2 = 0$
$\text{eq}_7 = f_1(t, q_2)(q_2q_3) = 0$	$b'_1\mathbf{q}_2^3\mathbf{q}_3 + b'_2q_2^2q_3 + b'_3q_2q_3 = 0$
$\text{eq}_8 = f_2(t, q_3)(q_2q_3) = 0$	$c'_1\mathbf{q}_2\mathbf{q}_3^3 + c'_2q_2q_3^2 + c'_3q_2q_3 = 0$
$\text{eq}_9 = g(t, q_2, q_3)(q_2) = 0$	$a'_1q_2^3q_3 + a'_2q_2^2q_3^2 + a'_3q_2^2q_3 + a'_4q_2^2 + a'_5q_2q_3 = 0$
$\text{eq}_{10} = g(t, q_2, q_3)(q_3) = 0$	$a'_1q_2^2q_3^2 + a'_2q_2q_3^3 + a'_3q_2q_3^2 + a'_4q_2q_3 + a'_5q_3^2 = 0$
$\text{eq}_{11} = f_1(t, q_2)(q_2q_3^2) = 0$	$b'_1\mathbf{q}_2^3\mathbf{q}_3^2 + b'_2q_2^2q_3^2 + b'_3q_2q_3^2 = 0$
$\text{eq}_{12} = f_2(t, q_3)(q_2^2q_3) = 0$	$c'_1\mathbf{q}_2^2\mathbf{q}_3^3 + c'_2q_2^2q_3^2 + c'_3q_2^2q_3 = 0$
$\text{eq}_{13} = g(t, q_2, q_3)(q_2q_3) = 0$	$a'_1q_2^3q_3^2 + a'_2q_2^2q_3^3 + a'_3q_2^2q_3^2 + a'_4q_2^2q_3 + a'_5q_2q_3^3 = 0$

where a'_i, b'_i, and c'_i, are quadratic polynomials in t.

There are 13 equations and 13 power products. It is important to mention that

equation $f_2(t, q_3)(q_2^2) = 0$ was not considered because it is linearly dependent on equations 2 through 6. Although, the above system of equations matched the number of power products, the final degree of the polynomial in t would be 26. The degree of the polynomial in t can be reduced to 24. This reduction is expected from the 3-homogeneous Bezout's number and is achieved by eliminating both eq_2 and eq_3 and by introducing equation $f_2(t, q_3)(q_2^2) = 0$. The equation $f_2(t, q_3)(q_2^2) = 0$ is no longer linearly dependent, allowing its introduction back into the polynomial system. Therefore, the system of 12 independent polynomials is shown in Table 4.3.

Table 4.3: Generation of 12 Linearly Independent Polynomials.

$\text{eq}_1 = g(t, q_2, q_3) = 0$	$a'_1\mathbf{q}_2^2\mathbf{q}_3 + a'_2\mathbf{q}_2\mathbf{q}_3^2 + a'_3\mathbf{q}_2\mathbf{q}_3 + a'_4\mathbf{q}_2 + a'_5\mathbf{q}_3 = 0$
$\text{eq}_2 = f_1(t, q_2)(q_3) = 0$	$b'_1q_2^2q_3 + b'_2q_2q_3 + b'_3q_3 = 0$
$\text{eq}_3 = f_2(t, q_3)(q_2) = 0$	$c'_1q_2q_3^2 + c'_2q_2q_3 + c'_3q_2 = 0$
$\text{eq}_4 = f_1(t, q_2)(q_3^2) = 0$	$b'_1\mathbf{q}_2^2\mathbf{q}_3^2 + b'_2q_2q_3^2 + b'_3\mathbf{q}_3^2 = 0$
$\text{eq}_5 = f_2(t, q_3)(q_2^2) = 0$	$c'_1q_2^2q_3^2 + c'_2q_2^2q_3 + c'_3\mathbf{q}_2^2 = 0$
$\text{eq}_6 = f_1(t, q_2)(q_2q_3) = 0$	$b'_1\mathbf{q}_2^3\mathbf{q}_3 + b'_2q_2^2q_3 + b'_3q_2q_3 = 0$
$\text{eq}_7 = f_2(t, q_3)(q_2q_3) = 0$	$c'_1\mathbf{q}_2\mathbf{q}_3^3 + c'_2q_2q_3^2 + c'_3q_2q_3 = 0$
$\text{eq}_8 = g(t, q_2, q_3)(q_2) = 0$	$a'_1q_2^3q_3 + a'_2q_2^2q_3^2 + a'_3q_2^2q_3 + a'_4q_2^2 + a'_5q_2q_3 = 0$
$\text{eq}_9 = g(t, q_2, q_3)(q_3) = 0$	$a'_1q_2^2q_3^2 + a'_2q_2q_3^3 + a'_3q_2q_3^2 + a'_4q_2q_3 + a'_5q_3^2 = 0$
$\text{eq}_{10} = f_1(t, q_2)(q_2q_3^2) = 0$	$b'_1\mathbf{q}_2^3\mathbf{q}_3^2 + b'_2q_2^2q_3^2 + b'_3q_2q_3^2 = 0$
$\text{eq}_{11} = f_2(t, q_3)(q_2^2q_3) = 0$	$c'_1\mathbf{q}_2^2\mathbf{q}_3^3 + c'_2q_2^2q_3^2 + c'_3q_2^2q_3 = 0$
$\text{eq}_{12} = g(t, q_2, q_3)(q_2q_3) = 0$	$a'_1q_2^3q_3^2 + a'_2q_2^2q_3^3 + a'_3q_2^2q_3^2 + a'_4q_2^2q_3 + a'_5q_2q_3^3 = 0$

Equations 1 through 12 can be written in matrix form. To reduce the number of arithmetic operations, equations are ordered in a heuristic manner $\{\text{eq}_{12}, \text{eq}_8, \text{eq}_9, \text{eq}_{10}, \text{eq}_{11}, \text{eq}_7, \text{eq}_6, \text{eq}_5, \text{eq}_4, \text{eq}_1, \text{eq}_3, \text{eq}_2\}$ so the bandwidth of the matrix is reduced.

Further minimization of the matrix bandwidth can be achieved using a permutation matrix (Watkins, 1991). Thus, the equations in matrix form are assembled as follows,

$$[\Psi]\mathbf{p} = \bar{\mathbf{0}} \tag{4.45}$$

where,

$$[\Psi] = \begin{bmatrix}
a'_1 & 0 & a'_2 & a'_3 & a'_4 & 0 & 0 & a'_5 & 0 & 0 & 0 & 0 \\
b'_1 & 0 & 0 & b'_2 & 0 & 0 & 0 & b'_3 & 0 & 0 & 0 & 0 \\
0 & a'_1 & 0 & a'_2 & a'_3 & a'_4 & 0 & 0 & a'_5 & 0 & 0 & 0 \\
0 & b'_1 & 0 & 0 & b'_2 & 0 & 0 & 0 & b'_3 & 0 & 0 & 0 \\
0 & 0 & c'_1 & c'_2 & c'_3 & 0 & 0 & 0 & 0 & 0 & 0 & 0 \\
0 & 0 & 0 & a'_1 & 0 & a'_2 & a'_3 & a'_4 & 0 & 0 & a'_5 & 0 \\
0 & 0 & 0 & c'_1 & c'_2 & c'_3 & 0 & 0 & 0 & 0 & 0 & 0 \\
0 & 0 & 0 & b'_1 & 0 & 0 & b'_2 & 0 & 0 & 0 & b'_3 & 0 \\
0 & 0 & 0 & 0 & a'_1 & 0 & a'_2 & a'_3 & a'_4 & 0 & 0 & a'_5 \\
0 & 0 & 0 & 0 & b'_1 & 0 & 0 & b'_2 & 0 & 0 & 0 & b'_3 \\
0 & 0 & 0 & 0 & 0 & 0 & c'_1 & c'_2 & c'_3 & 0 & 0 & 0 \\
0 & 0 & 0 & 0 & 0 & 0 & 0 & c'_1 & c'_2 & c'_3 & 0 & 0
\end{bmatrix} \quad \text{and} \quad \mathbf{p} = \begin{bmatrix}
q_2^3 q_3^2 \\ q_2^3 q_3 \\ q_2^2 q_3^3 \\ q_2^2 q_3^2 \\ q_2^2 q_3 \\ q_2^2 \\ q_2 q_3^3 \\ q_2 q_3^2 \\ q_2 q_3 \\ q_2 \\ q_3^2 \\ q_3
\end{bmatrix}$$

The elements of matrix $[\Psi]$ are quadratic polynomials in t. Although Eq. (4.45) could have a trivial solution, i.e., vector $\mathbf{p}$ containing zero elements, it would not be a solution to the polynomial system. As a matter of fact, such a trivial solution was originated as a consequence of eliminating the unit power product from the polynomial system with 13 equations. A solution of Eq. (4.45) can be attained by setting the determinant of matrix $[\Psi]$ equal to zero, yielding a 24^{th}-order polynomial in t. Nevertheless, a symbolic expression would be difficult to obtain. The coefficients of the determinant can be expressed numerically, but this would lead to floating point

arithmetic errors once the roots of the determinant are found. As an alternative, the roots of the polynomial can be obtained as an eigenvalue problem as shown in Appendix E. Matrix $[\Psi]$ can be expressed as a matrix polynomial, i.e.,

$$[\Psi] = [\Psi_2]t^2 + [\Psi_1]t + [\Psi_0] \tag{4.46}$$

where matrices $[\Psi_2]$, $[\Psi_1]$, and $[\Psi_0]$ are shown in Appendix D.3.2.

The roots of the determinant are equivalent to the eigenvalues of the following matrix,

$$[\mathbf{K}] = \begin{bmatrix} \mathbf{0} & \mathbf{I} \\ -[\Psi_2]^{-1}[\Psi_0] & -[\Psi_2]^{-1}[\Psi_1] \end{bmatrix} \tag{4.47}$$

where $\mathbf{0}$ and $\mathbf{I}$ are 12 by 12 null and identity matrices, respectively.

The eigenvalues represent the solutions of t, which are transformed into ϕ using half-angle substitution. The pose is then transformed from the position of w_1, found with Eq. (4.62), to the centre of the platform as shown in Eq. (B.17).

Case 2 $\theta_{2_1} = 0°$

With θ_{2_1} =0°, link ρ_1 lies on the negative direction of axis y_0. Thus, the position of $w_1 = \{x, y\}^{\mathrm{T}}$ is given by

$$w_1 = \begin{Bmatrix} x \\ y \end{Bmatrix} = \begin{Bmatrix} d_{1_1} \\ -\rho_1 \end{Bmatrix} \tag{4.48}$$

The analytical process to follow is the same as the one described for Case 1.

Example.-

The force unconstrained poses of a PRR-2PRR actuation layout of a manipulator based on the design considered in Section 3.4.2 are determined. The force-unconstrained poses of Condition 2, Case 1 (the larger curve) and Case 2 (the smaller curve) are plotted in the 3-dimensional space $\{x, y, \phi\}$ as shown in Figure 4.9. These curves include all four combinations of the prismatic joint inverse kinematics (shorter/longer) of branches 2 and 3. The grey loops at the bottom of the figure represent the projection of the force-unconstrained poses onto the xy plane.

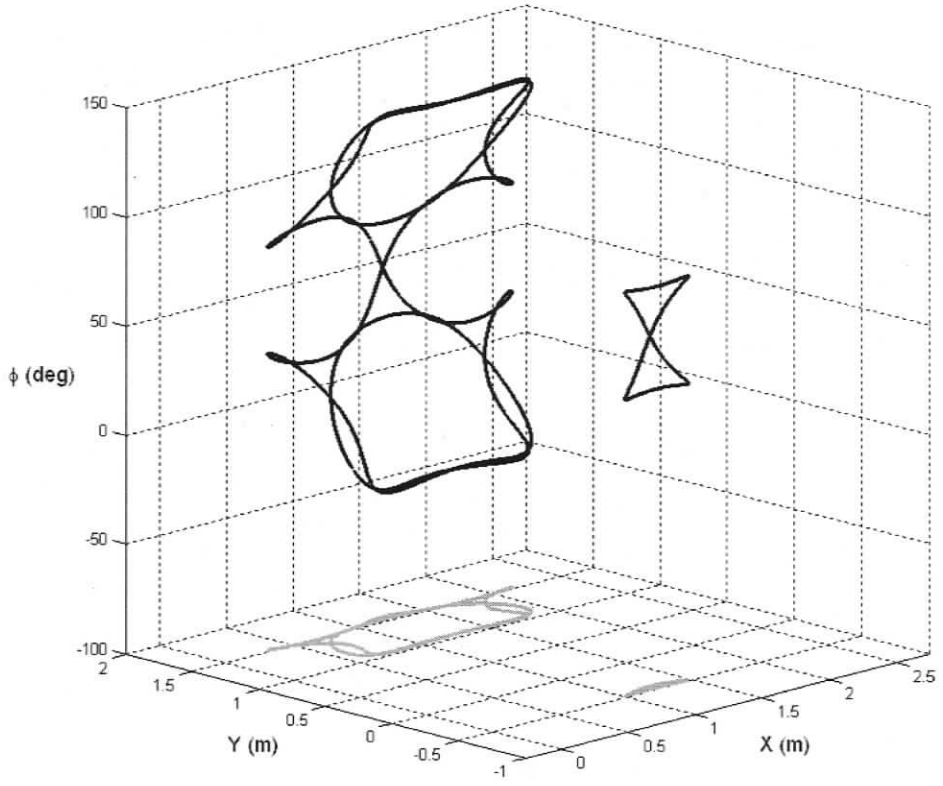

Figure 4.9: Loci of the Force-Unconstrained Poses of the PRR-2PRR Layout with Condition 2 (Cases 1 and 2).

4.5 Force-Unconstrained Poses of the RRR-2RRR

4.5.1 Degeneracy Conditions

This actuation of the 3-RRR manipulator is based on replacing the second joint (passive) of branch 1 with an actuated joint[2]. The associated reciprocal screw matrix of the RRR-2RRR is assembled with the associated reciprocal screws of the actuated joints. For this configuration:

$$^{\text{ref}}[\mathbf{W}] = \begin{bmatrix} ^{\text{ref}}\mathbf{W}_{1_1} & ^{\text{ref}}\mathbf{W}_{2_1} & ^{\text{ref}}\mathbf{W}_{1_2} & ^{\text{ref}}\mathbf{W}_{1_3} \end{bmatrix} \tag{4.49}$$

Thus, $^{\text{ref}}[\mathbf{W}]$ is divided into four sub-matrices, i.e.:

$$^{\text{ref}}[\mathbf{W}_A] = \begin{bmatrix} ^{\text{ref}}\mathbf{W}_{1_1} & ^{\text{ref}}\mathbf{W}_{2_1} & ^{\text{ref}}\mathbf{W}_{1_2} \end{bmatrix} \tag{4.50a}$$

$$^{\text{ref}}[\mathbf{W}_B] = \begin{bmatrix} ^{\text{ref}}\mathbf{W}_{1_1} & ^{\text{ref}}\mathbf{W}_{2_1} & ^{\text{ref}}\mathbf{W}_{1_3} \end{bmatrix} \tag{4.50b}$$

$$^{\text{ref}}[\mathbf{W}_C] = \begin{bmatrix} ^{\text{ref}}\mathbf{W}_{1_1} & ^{\text{ref}}\mathbf{W}_{1_2} & ^{\text{ref}}\mathbf{W}_{1_3} \end{bmatrix} \tag{4.50c}$$

$$^{\text{ref}}[\mathbf{W}_D] = \begin{bmatrix} ^{\text{ref}}\mathbf{W}_{2_1} & ^{\text{ref}}\mathbf{W}_{1_2} & ^{\text{ref}}\mathbf{W}_{1_3} \end{bmatrix} \tag{4.50d}$$

yielding the determinants:

$$\left|^{\text{ref}}[\mathbf{W}_A]\right| = -l_2\rho_4 s\theta_{3_2} s\theta_{2_1} \tag{4.51a}$$

$$\left|^{\text{ref}}[\mathbf{W}_B]\right| = -l_3\rho_4 s\theta_{3_3} s\theta_{2_1} \tag{4.51b}$$

$$\left|^{\text{ref}}[\mathbf{W}_C]\right| = l_2 s\theta_{3_3} s\left(\theta_{3_1} - \theta_{3_2}\right) - l_2 s\theta_{3_2} s\left(\theta_{3_1} - \theta_{3_3} + \alpha_3\right) \tag{4.51c}$$

$$\begin{aligned} \left|^{\text{ref}}[\mathbf{W}_D]\right| = {} & \left(\rho_4 c\left(\theta_{3_1} + \theta_{2_1}\right) + \rho_1 c\theta_{3_1}\right) s\theta_{3_2}\left(l_2 s\left(\theta_{3_3} - \alpha_3\right) - l_3 s\theta_{3_3}\right) \\ & + \left(\rho_4 s\left(\theta_{3_1} + \theta_{2_1}\right) + \rho_1 s\theta_{3_1}\right)\left(l_3 c\theta_{3_2} s\theta_{3_3} - l_2 s\theta_{3_2} c\left(\theta_{3_3} - \alpha_3\right)\right) \end{aligned} \tag{4.51d}$$

[2]This work was presented at the 2002 CSME Forum, Firmani and Podhorodeski (2002), and afterward published in Firmani and Podhorodeski (2004a).

To have $|^{\text{ref}}[\mathbf{W}_A]| = |^{\text{ref}}[\mathbf{W}_B]| = 0$ either $s\theta_{3_2}$ and $s\theta_{3_3}$ or $s\theta_{2_1}$ must equal zero, yielding the following conditions:

$$\text{Condition 1} \quad s\theta_{3_2} = 0 \text{ and } s\theta_{3_3} = 0$$

$$\text{or} \quad \text{Condition 2} \quad s\theta_{2_1} = 0$$

An example of force-unconstrained configurations under these conditions are illustrated in Figure 4.10.

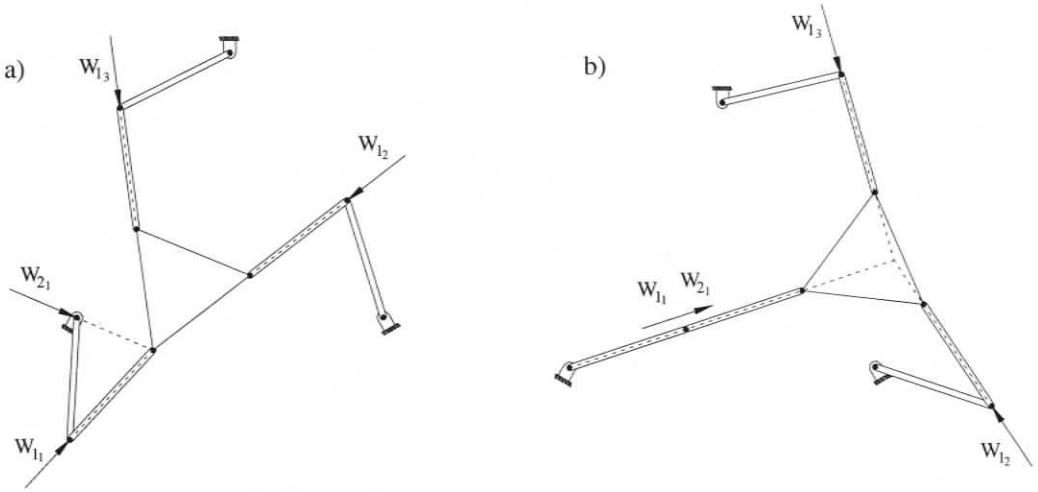

Figure 4.10: Force-Unconstrained Configurations of the RRR-2RRR Manipulator with a) Condition 1 and b) Condition 2.

Whether $|^{\text{ref}}[\mathbf{W}_C]| = |^{\text{ref}}[\mathbf{W}_D]| = 0$, for the above conditions, will be now checked.

4.5.2 Condition 1

For Condition 1 satisfied, the determinants of all of the sub-matrices are equal to zero. Therefore, expressions in terms of x, y, and ϕ that satisfy $|^{\text{ref}}[\mathbf{W}_A]| = |^{\text{ref}}[\mathbf{W}_B]| = |^{\text{ref}}[\mathbf{W}_C]| = |^{\text{ref}}[\mathbf{W}_D]| = 0$, can be found. These expressions are obtained with the loop-closure equations of branches 2 and 3.

Branch 2

$$p\left({}^{0}_{1_2}[\mathbf{T}]\ {}^{1_2}_{2_2}[\mathbf{T}]\ {}^{2_2}_{3_2}[\mathbf{T}]\ {}^{3_2}_{3_1}[\mathbf{T}]\right) = p\left({}^{0}_{3_1}[\mathbf{T}]\right) = \{x, y, 0\}^T$$
$$= \begin{Bmatrix} bx_2 + \rho_5 c\theta_{1_2} + \rho_2 c\left(\theta_{1_2} + \theta_{2_2}\right) + l_2 c\left(\theta_{1_2} + \theta_{2_2} + \theta_{3_2}\right) \\ \rho_5 s\theta_{1_2} + \rho_2 s\left(\theta_{1_2} + \theta_{2_2}\right) + l_2 s\left(\theta_{1_2} + \theta_{2_2} + \theta_{3_2}\right) \\ 0 \end{Bmatrix} \tag{4.52}$$

Since $\phi = \theta_{1_2} + \theta_{2_2} + \theta_{3_2} + \beta_2$, where $\beta_2 = \pi$, Eqs. (4.52) can be rewritten as:

$$\rho_5 c\theta_{1_2} = x - bx_2 + \rho_2 c\left(\phi - \theta_{3_2}\right) + l_2 c\phi \tag{4.53a}$$

$$\rho_5 s\theta_{1_2} = y + \rho_2 s\left(\phi - \theta_{3_2}\right) + l_2 s\phi \tag{4.53b}$$

In order to express an equation in terms of the platform's pose, Eqs. (4.53a and 4.53b) are squared and added. The resulting expression is simplified yielding

$$\begin{aligned} &\left(x - bx_2\right)^2 + y^2 + \rho_2^2 + l_2^2 - \rho_5^2 + 2\rho_2 l_2 c\theta_{3_2} + 2\left(x - bx_2\right)\left(l_2 + \rho_2 c\theta_{3_2}\right) c\phi + \\ &2y\left(l_2 + \rho_2 c\theta_{3_2}\right) s\phi = 0 \end{aligned} \tag{4.54}$$

where $s\theta_{3_2} = 0$ and $c\theta_{3_2} = \pm 1$.

Branch 3

$$p\left({}^{0}_{1_3}[\mathbf{T}]\ {}^{1_3}_{2_3}[\mathbf{T}]\ {}^{2_3}_{3_3}[\mathbf{T}]\ {}^{3_3}_{3_1}[\mathbf{T}]\right) = p\left({}^{0}_{3_1}[\mathbf{T}]\right) = \{x, y, 0\}^T$$
$$= \begin{Bmatrix} bx_3 + \rho_6 c\theta_{1_3} + \rho_3 c\left(\theta_{1_3} + \theta_{2_3}\right) + l_3 c\left(\theta_{1_3} + \theta_{2_3} + \theta_{3_3}\right) \\ by_3 + \rho_6 s\theta_{1_3} + \rho_3 s\left(\theta_{1_3} + \theta_{2_3}\right) + l_3 s\left(\theta_{1_3} + \theta_{2_3} + \theta_{3_3}\right) \\ 0 \end{Bmatrix} \tag{4.55}$$

Since $\phi = \theta_{1_2} + \theta_{2_2} + \theta_{3_2} + \beta_3$, where $\beta_3 = \pi - \alpha_3$, Eqs. (4.55) can be simplified similarly resulting in the following expression:

$$\begin{aligned} &\left(x - bx_3\right)^2 + \left(y - by_3\right)^2 + 2\rho_3 l_3 c\theta_{3_3} + 2\left(x - bx_3\right)\left(l_3 + \rho_3 c\theta_{3_3}\right) c\left(\phi + \alpha_3\right) + \\ &+2\left(y - by_3\right)\left(l_3 + \rho_3 c\theta_{3_3}\right) s\left(\phi + \alpha_3\right) + \rho_3^2 + l_3^2 - \rho_6^2 = 0 \end{aligned} \tag{4.56}$$

where $s\theta_{3_3} = 0$ and $c\theta_{3_3} = \pm 1$.

There are four possible combinations of Eqs. (4.54 and 4.56) due to $c\theta_{3_2} = \pm 1$ and $c\theta_{3_3} = \pm 1$. These equations geometrically represent two sets of surfaces. Their intersections yield four curves in the three-dimensional space defined by x, y, and ϕ. The four curves correspond to one order of infinity $O(\infty)$ of force-unconstrained poses of Condition 1 for the RRR - 2RRR actuation configuration.

Assume angle ϕ from 0° to 360°. Thus, Eqs. (4.54 and 4.56) can be written as:

$$x^2 + y^2 + a_1 x + a_2 y + a_3 = 0 \tag{4.57a}$$

$$x^2 + y^2 + b_1 x + b_2 y + b_3 = 0 \tag{4.57b}$$

where the coefficients a_i and b_i, which are a function of the assumed ϕ, are shown in Appendix D.3.3.

To solve this polynomial system, Eq. (4.57b) is subtracted from Eq. (4.57a), yielding a linear equation in x and y, i.e.,

$$(a_1 - b_1)\, x + (a_2 - b_2)\, y + (a_3 - b_3) = 0 \tag{4.58}$$

Hence, a solution for x is given as follows:

$$x = \frac{(b_2 - a_2)\, y + (b_3 - a_3)}{(a_1 - b_1)} = \frac{c_2 y + c_3}{c_1} \tag{4.59}$$

A second order polynomial in y results by substituting Eq. (4.59) in Eq. (4.57a), i.e.,

$$\left(c_2^2 + c_1^2\right) y^2 + \left(a_2 c_1^2 + 2 c_2 c_3 + a_1 c_1 c_2\right) y + c_3^2 + a_1 c_1 c_3 + a_3 c_1^2 = 0 \tag{4.60}$$

The roots of this polynomial are then substituted in Eq. (4.59). The obtained values of x and y are then transformed to the centre of the mobile platform with Eq. (B.17). This analysis is carried out for all four combinations, though the combination

when $c\theta_{3_2} = c\theta_{3_3} = -1$ is not likely to occur. For such combination, both links must be folded back.

Example.-

The force unconstrained poses of the RRR-2RRR actuation layout with Condition 1 is shown in Figure 4.11. Both platforms are equilateral triangles, their sides are 2.5 m for the fixed platform and 1 m for the mobile platform. The link lengths are $\rho_i = 1\ m$, for $i = 1, \ldots, 6$. The grey loops at the bottom of the figure represent the projection of the force-unconstrained poses onto the xy plane.

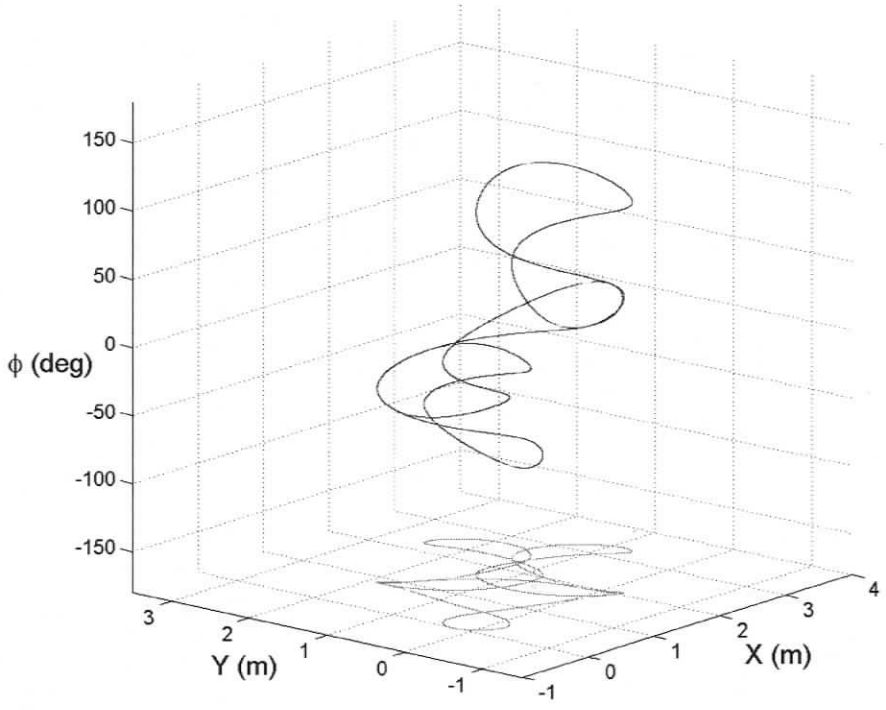

Figure 4.11: Loci of the Force-Unconstrained Poses of the RRR-2RRR Layout.

Physically, with Condition 1 true, an equivalent-mechanism-based analysis can be made. Since $s\theta_{3_2} = 0$ and $s\theta_{3_3} = 0$, branches 2 and 3 have their second link

collinear to the platform edges l_2 and l_3, respectively. Thus, for Condition 1 satisfied, ρ_2 and ρ_3 and the platform can be thought of as a rigid link. There are four possible assemblies depending upon the orientation of links ρ_2 and ρ_3, as previously discussed in Section 4.4. For each combination, a coupler of constant length r connects the joints e_2 and e_3. An example of an equivalent six-bar mechanism (1-dof), also known as the Stephenson III linkage described by Erdman et al. (2001), is shown in Figure 4.12.

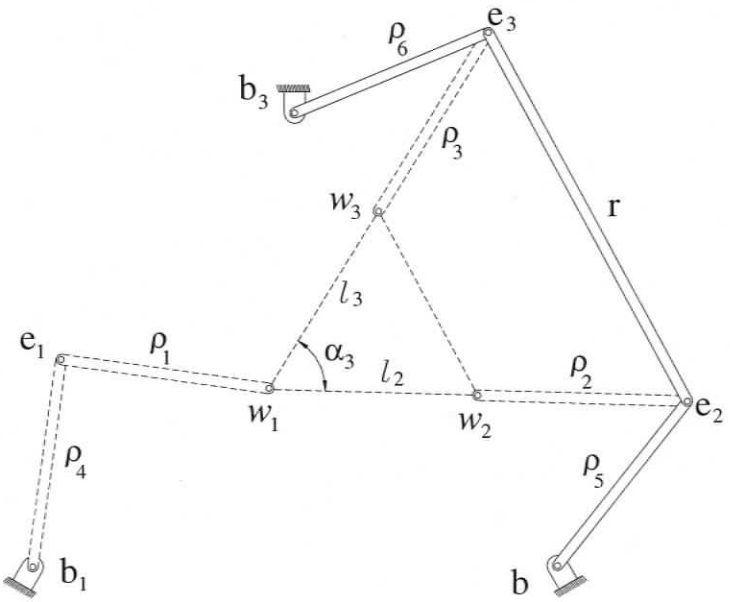

Figure 4.12: Equivalent Mechanism of Condition 1 for the RRR-2RRR Layout.

4.5.3 Condition 2

Condition 2 ($s\theta_{2_1} = 0$) does not satisfy $|^{\text{ref}}[\mathbf{W}_C]| = 0$ nor $|^{\text{ref}}[\mathbf{W}_D]| = 0$. However, $|^{\text{ref}}[\mathbf{W}_D]|$ is reduced to the same expression as $|^{\text{ref}}[\mathbf{W}_C]|$, i.e., the determinant of the non-redundant configuration 3-RRR, Eq. (3.41). Since θ_{2_1} can be either 0° or 180°,

an alignment of ρ_4 and ρ_1 occurs with Condition 2 true. Let ρ_{b_1} be the link formed with the alignment of links ρ_4 and ρ_1.

Case 1 $\theta_{2_1} = 0°$

With $\theta_{2_1} = 0°$, branch 1 is fully extended, i.e., $\rho_{b_1} = \rho_4 + \rho_1$. That leads to a seven-bar mechanism with 2-dof. If angle θ_{1_1} is assumed, the position of w_1 can be determined and the problem is reduced to finding the orientation of the mobile platform. Thus, the orientation of the mobile platform, shown in Eq. (3.42c) for $i = 1$, with $\beta_1 = 0$ and $\theta_{2_1} = 0$, is reduced to $\phi = \theta_{1_1} + \theta_{3_1}$. Therefore,

$$\theta_{3_1} = \phi - \theta_{1_1} \tag{4.61}$$

and the position of $w_1 = \{x, y\}^{\mathrm{T}}$ is given by

$$w_1 = \left\{ \begin{array}{c} x \\ y \end{array} \right\} = \left\{ \begin{array}{c} (\rho_4 + \rho_1)\cos(\theta_{1_1}) \\ (\rho_4 + \rho_1)\sin(\theta_{1_1}) \end{array} \right\} \tag{4.62}$$

Substituting Eq. (4.61) in Eq. (3.41) and applying half-angle substitution, as shown in Section 4.4.3, yields a polynomial of the form

$$\begin{aligned} g(t, q_2, q_3) = (a_1 t^2 + a_2 t + a_3) q_2^2 q_3 + (a_4 t^2 + a_5 t + a_6) q_2 q_3^2 + (a_7 t^2 + a_8 t + a_9) q_2 q_3 \\ + (a_{10} t^2 + a_{11} t + a_{12}) q_2 + (a_{13} t^2 + a_{14} t + a_{15}) q_3 = 0 \end{aligned} \tag{4.63}$$

where the coefficients a_i are shown in Appendix D.3.3.

The loop-closure equations of branches 2 and 3, given in Eq. (3.43) are expressed using the half-angle substitution variables as:

$$f_1(t, q_2) = (b_1 t^2 + b_2 t + b_3) q_2^2 + (b_4 t^2 + b_5 t + b_6) q_2 + (b_7 t^2 + b_8 t + b_9) = 0 \tag{4.64}$$

$$f_2(t, q_3) = (c_1 t^2 + c_2 t + c_3) q_3^2 + (c_4 t^2 + c_5 t + c_6) q_3 + (c_7 t^2 + c_8 t + c_9) = 0 \tag{4.65}$$

where the coefficients b_i and c_i are shown in Appendix D.3.3.

The resulting polynomial system is similar to the obtained system for the PRR-2PRR manipulator, the only difference being the coefficients of the polynomials. Therefore, the solution of the polynomial system, already presented in Section 4.4.3, leads to a 24×24 matrix $[\mathbf{K}]$, shown in Eq. (4.47). The eigenvalues of this matrix correspond to the solutions of t, which are then transformed into ϕ's using half-angle substitution. Finally, the pose is transformed from the position of w_1, found with Eq. (4.62), to the centre of the platform as shown in Eq. (B.17).

Example.-

The force unconstrained poses of a RRR-2RRR actuation layout of a manipulator, based on the design considered in Section 3.5.5, are determined. The force-unconstrained poses of Condition 2 are plotted in the 3-dimensional space $\{x, y, \phi\}$ as shown in Figure 4.13a. These curves include all four combinations of the elbow configurations (elbows up/down) of branches 2 and 3. The grey curve at the bottom of Figure 4.13a represents the projection of the force-unconstrained poses onto the xy plane. With the specified design parameters, there are two planes where the projected curves possess elements of symmetry. Let $u\phi$ and $v\phi$ be these planes (Figures 4.13b and 4.13c), where the axes u and v are perpendicular and parallel to the base joints b_2 and b_3, respectively.

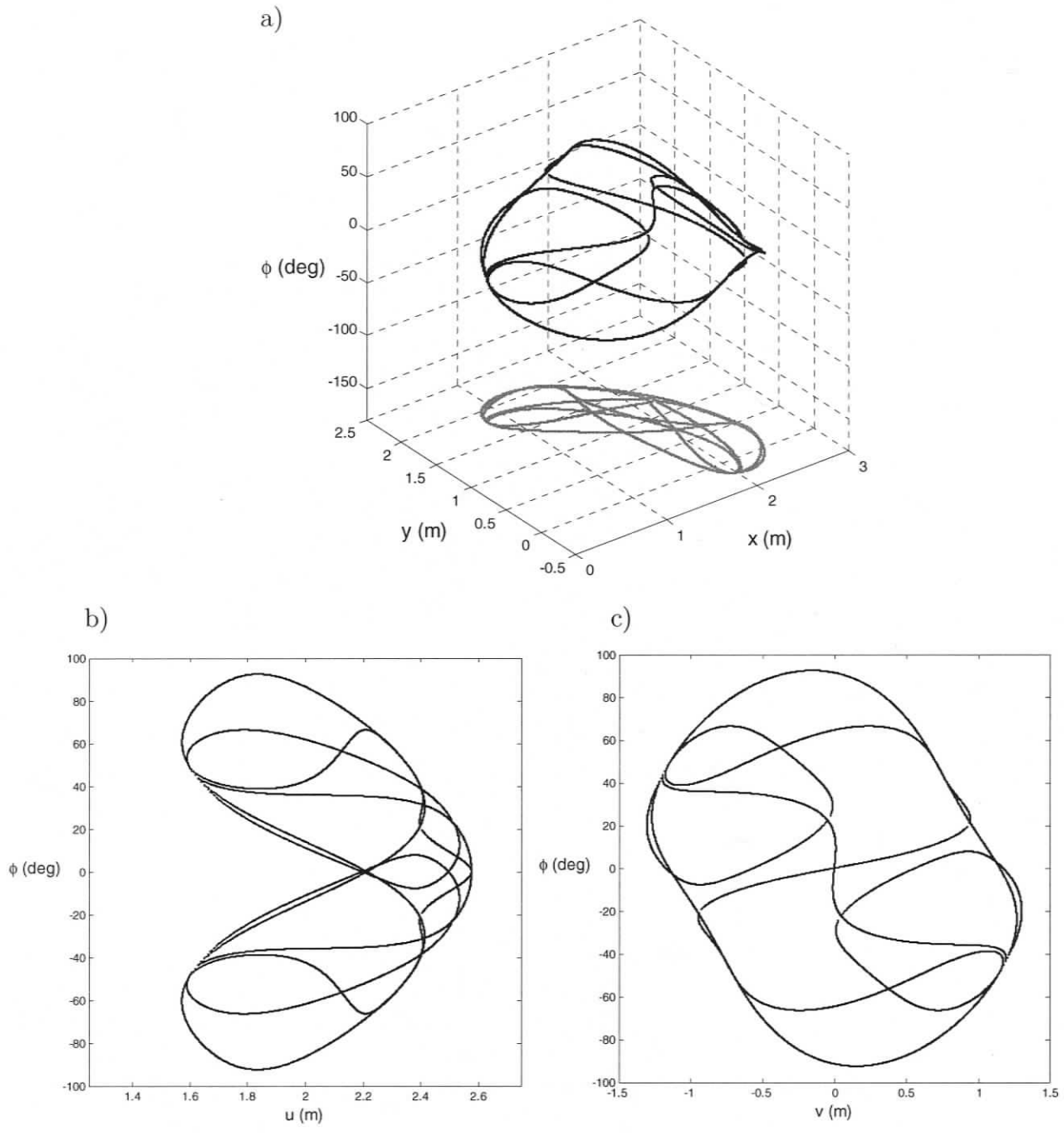

Figure 4.13: Loci of the Force-Unconstrained Poses of the RRR-2RRR Layout with Condition 2 (Case 1).

Case 2 θ_{2_1} **=180°**

With θ_{2_1} =180°, branch 1 is folded back, i.e., $\rho_{b_1} = \rho_4 - \rho_1$. If $\rho_4 \neq \rho_1$ the resulting mechanism will contain seven bars and 2-dof. The analysis of force-unconstrained configurations is carried out in a similar manner as the one presented for Case 1, with

$$w_1 = \left\{ \begin{array}{c} x \\ y \end{array} \right\} = \left\{ \begin{array}{c} (\rho_4 - \rho_1)\cos(\theta_{1_1}) \\ (\rho_4 - \rho_1)\sin(\theta_{1_1}) \end{array} \right\} \tag{4.66}$$

Nevertheless, if $\rho_4 = \rho_1$ ($\rho_{b_1} = 0$), point w_1 will be coincident with the base of branch 1, yielding a 6-bar mechanism and only 1-dof, i.e., the orientation of the platform. Since, branch 1 can rotate freely regardless to the orientation of the platform, the associated reciprocal screw of this branch can always intersect the common (intersection) point of the associated reciprocal screw of the other two branches. Therefore, for any pose of the manipulator and any configuration of branches 2 and 3, i.e., either elbow up or elbow down, there will be an orientation of the folded branch that will make the manipulator be force unconstrained.

Example.-

Assume the manipulator of the previous section with $\rho_1 = \rho_2 = \rho_3 = 1$ and $\rho_4 = \rho_5 = \rho_6 = 1.5$. The force-unconstrained configurations of this manipulator, when θ_{2_1} =180°, are shown in Figure 4.14a. The projected curves onto the xy-plane are depicted in grey at the bottom of Figure 4.14a. Also, the curves are projected onto the planes of symmetry $u\phi$ and $v\phi$, as shown in Figures 4.14b and 4.14c.

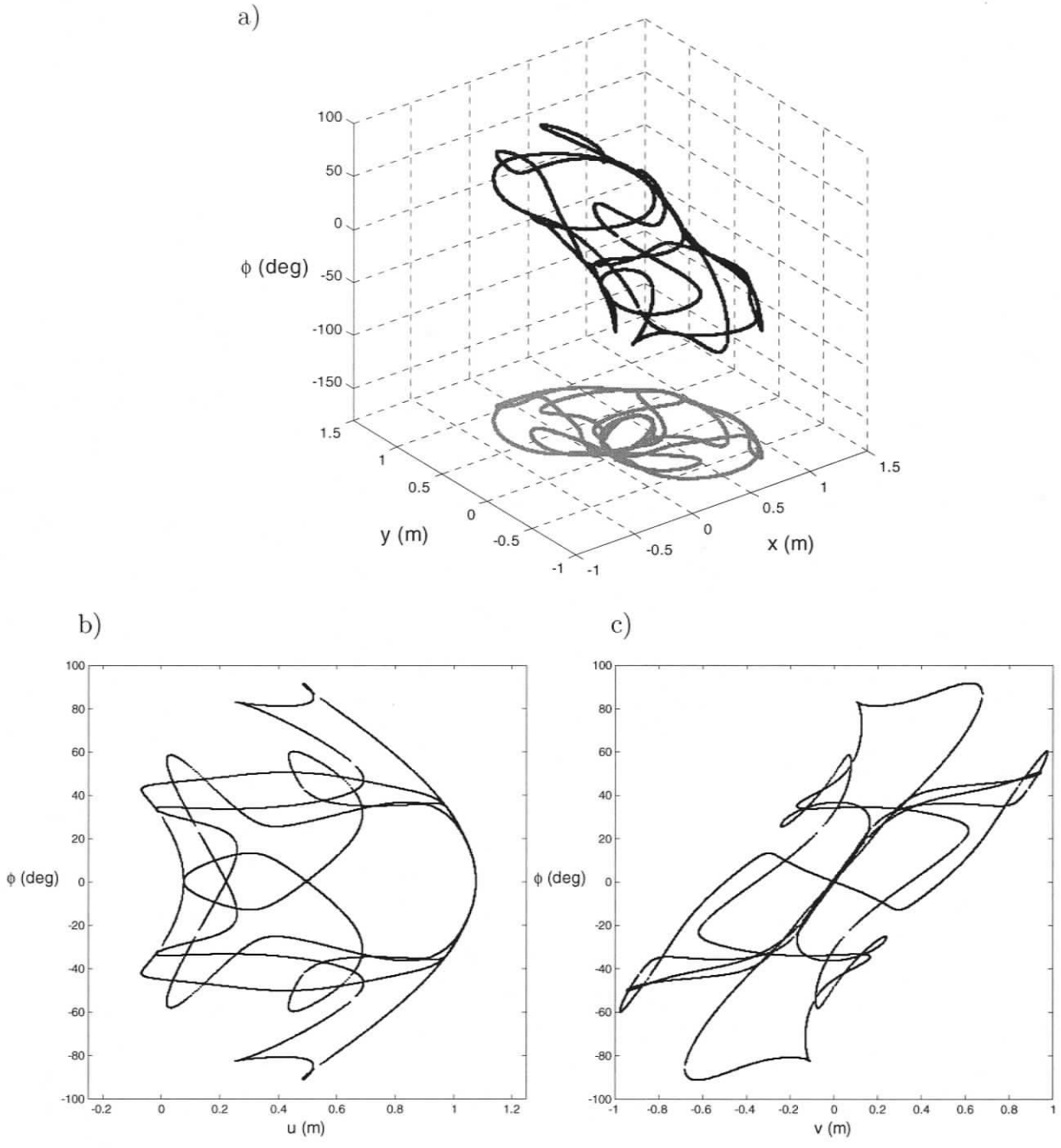

Figure 4.14: Loci of the Force-Unconstrained Poses of the RRR-2RRR Layout with Condition 2 (Case 2).

4.6 Further Actuation

For further actuation, the methodology to follow is exactly the same. The number of sub-matrices λ is found as the total number of possible combinations, i.e.,

$$\lambda = \frac{n!}{m!\,(n-m)!} \quad \text{for } m = 3 \tag{4.67}$$

where n represents the number of actuators.

In the case of five actuators, a 3 by 5 associated reciprocal screw matrix will be divided into 10 sub-matrices and all of their determinants must satisfy the condition of being equal to zero. Force-unconstrained poses are reduced by one order of infinity, i.e., for five actuators a finite number of force-unconstrained poses exist.

4.7 Discussion

In this chapter, the force-unconstrained poses of planar parallel manipulators with in-branch redundant actuation were studied. In particular, the RRR-2RRR, PRR-2PRR, and RRR-2RRR actuation layouts were presented. The force-unconstrained poses of these mechanisms were plotted in a three-dimensional space defined by the position and orientation of the mobile platform, yielding curves of force-unconstrained poses. That is, there was a reduction in the order of infinity of force-unconstrained poses from $O(\infty^2)$ for non-redundant planar parallel manipulators to $O(\infty)$ for planar parallel manipulators with one additional actuated joint. With further actuation, the force-unconstrained poses are reduced by one order of infinity for every additional actuated joint added into the system.

Besides the elimination of families of force-unconstrained poses, another advantage

of replacing passive joints with actuated joints is the improvement of the manipulator's accuracy. Passive joints play an important role in the accuracy of a parallel manipulator due to the complexity of their manufacture and assembly within tolerances. Furthermore, since passive joints may be subject to high internal forces, redundancy offers a better distribution of these forces. However, there are some disadvantages to including actuated joints within branches. For instance, the inertia of the manipulator increases causing a reduction in the characteristics of motion of the manipulator, such as the acceleration of the end-effector. Also, redundant parallel manipulators require a robust and reliable control system.

The methodology adopted in this chapter is based on reciprocal screws associated with the actuated joints. The assembly of the associated reciprocal screw matrix of any configuration of actuated joints is very simple. Every actuated joint is defined by an associated reciprocal screw that represents a column of the associated reciprocal screw matrix.

In all the actuation layouts presented, two of the four determinants turned out to be very simple allowing an easy identification and visualization of the conditions that make the manipulator force unconstrained. With Condition 1 true, all the determinants are equal to zero. Also, equivalent mechanisms, whose motion represents the force-unconstrained poses of the RRR-2RRR, PRR-2PRR, and RRR-2RRR manipulators, were conceived. These equivalent mechanisms are composed of six bars and have a mobility of one degree-of-freedom. With Condition 2 true, the remaining two determinants are not equal to zero and turned out to be the determinant of the non-redundant manipulator. Moreover, this condition constrains one kinematic variable in two different postures, referred to in the text as cases, yielding seven-bar mechanisms with a mobility of two degrees-of-freedom. By assuming one variable

from the kinematically-constrained branch, the position of the mobile platform can be identified, and by means of the determinant of the non-redundant manipulator and the loop closure equations of the other two branches, the orientation of the mobile platform is determined. For the RRR-2RRR manipulator, the orientation of the mobile platform is represented by a 4^{th}-order polynomial. Meanwhile, for the PRR-2PRR, and RRR-2RRR manipulators the orientation is described by 24^{th}-order polynomials.

In Chapter 3, the kinematic equivalence between the 3-RPR and the 3-RRR was discussed. Assume the first joint of branch 1 of the 3-RPR also actuated. Condition 1 also applies to the RPR-2RPR actuation layout. That is, the associated reciprocal screws of the first branch intersect at w_1, as shown in the representation of the associated reciprocal screws of the 3-RPR manipulator in Figure 3.1. Nevertheless, Condition 2 does not occur for this actuation layout because the associated reciprocal screws of branch 1 cannot be collinear.

Chapter 5

Force-Unconstrained Poses of Planar Parallel Manipulators with Additional Branches

5.1 Overview

The inclusion of an additional actuated branch, beyond the original three, is considered. The identification of force-unconstrained poses of the 4-R$\underline{P}$R, 4-$\underline{P}$RR, and 4-$\underline{R}$RR manipulators are presented. Each problem leads to a system of multivariable polynomials. Elimination methods are used to reduce the multivariable polynomials to a single polynomial in terms of one variable. For the 4-R$\underline{P}$R manipulator, the non-linear system of equations is solved using Gröbner Bases. For the 4-$\underline{P}$RR and 4-$\underline{R}$RR manipulators, due to the complexity of their non-linear systems of equations, an exhaustive elimination method based on the Sylvester's dialytic elimination is employed.

5.2 Introduction

5.2.1 Non-Redundant Mechanism Decoupling

The inclusion of an additional actuated branch is based on having every branch actuated by a single actuator. For manipulators with redundant actuation, the associated reciprocal screw matrix is an $m \times n$ non-square matrix, where m is the dimension of the task and n is the number of branches. Thus, taking its determinant is not possible. A solution, as proposed in Chapter 4, is to find conditions that make the determinant of all unique $m \times m$ sub-matrices equal to zero.

A physical representation of this technique is to decouple the manipulator into λ non-redundant mechanisms (where λ has been determined with Eq. (4.67)). Whenever a set of task space coordinates satisfies each $|[\mathbf{W}_i]| = 0$, for $i = 1, ..., \lambda$, the entire redundant manipulator is force unconstrained. With one degree of redundancy, four sub-matrices exist, yielding four determinants.

5.2.2 Dependency of Determinants

Nonetheless, there is a dependency among the determinants. For instance, a 3-dof planar parallel manipulator with one additional actuated branch leads to four sub-matrices; however, the manipulator is generally force unconstrained if the determinants of two sub-matrices are zero. This dependency can be explained by the geometric meaning of the associated reciprocal screws. Let us consider a force-unconstrained pose of the 4-PRR manipulator. Assume the sub-matrix formed with the first three branches of the manipulator, i.e., $[\mathbf{W}_1] = \begin{bmatrix} \mathbf{W}_{k_1} & \mathbf{W}_{k_2} & \mathbf{W}_{k_3} \end{bmatrix}$. If the manipulator is force unconstrained, its determinant must equal zero. This leads

to a so-called planar pencil singularity (all three associated reciprocal screws intersect at a common point), as shown in Figure 5.1a. Now, assume a second sub-matrix, say $[\mathbf{W}_2] = \begin{bmatrix} \mathbf{W}_{k_1} & \mathbf{W}_{k_2} & \mathbf{W}_{k_4} \end{bmatrix}$. If its determinant equals zero, the fourth associated reciprocal screw must intersect the common point of $\mathbf{W}_{k_1}$ and $\mathbf{W}_{k_2}$, as illustrated in Figure 5.1b. Thus, the redundant manipulator is force unconstrained if all associated reciprocal screws intersect at a common point, Figure 5.1c. That leads to the following syllogism, if $det([\mathbf{W}_1]) = det([\mathbf{W}_2]) = 0$, then $det([\mathbf{W}_3]) = det([\mathbf{W}_4]) = 0$, where $[\mathbf{W}_3] = \begin{bmatrix} \mathbf{W}_{k_1} & \mathbf{W}_{k_3} & \mathbf{W}_{k_4} \end{bmatrix}$ and $[\mathbf{W}_4] = \begin{bmatrix} \mathbf{W}_{k_2} & \mathbf{W}_{k_3} & \mathbf{W}_{k_4} \end{bmatrix}$. In general for every degree of redundancy, one equation, beyond the one from the original non-redundant manipulator, is not linearly dependent.

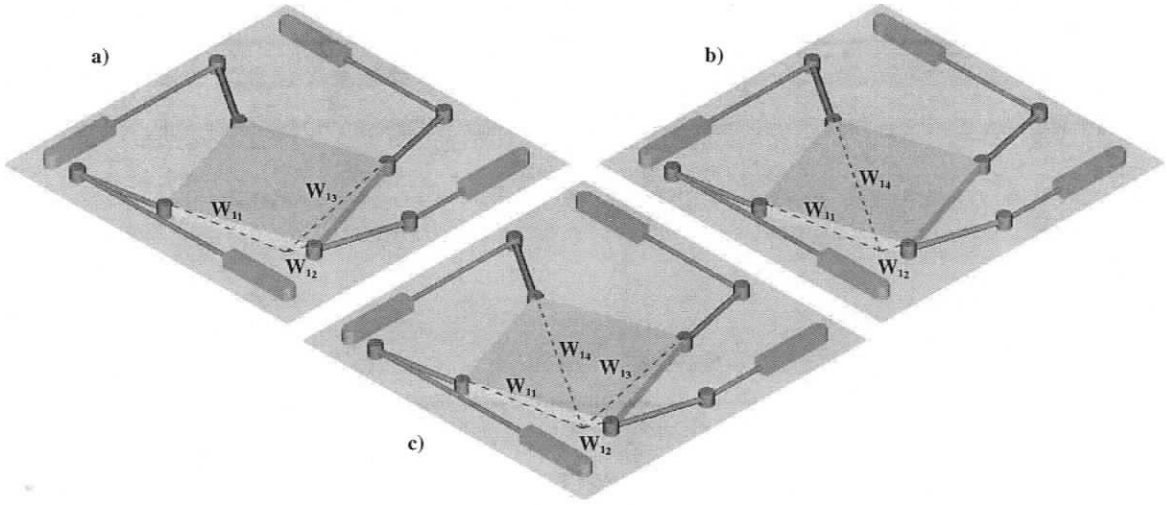

Figure 5.1: Dependency of the Submatrices Determinants Illustrated with Associated Reciprocal Screws.

In spite of the geometric interpretation of the associated reciprocal screws, this syllogism is just a necessary condition because there are some exceptions; that is,

there are some singular configurations that satisfy $det([\mathbf{W}_1]) = det([\mathbf{W}_2]) = 0$ but not the remaining determinants.

- Collinearity.- *When two associated reciprocal screws are collinear.* Assume the case when $\mathbf{W}_{k_1}$ and $\mathbf{W}_{k_2}$ are collinear ($\mathbf{W}_{k_1} = \mathbf{W}_{k_2}$). Let the point where $\mathbf{W}_{k_3}$ intersects the collinear reciprocal screws be c_1 and the point where $\mathbf{W}_{k_4}$ intersects the collinear reciprocal screws be c_2. Thus, the determinants of the sub-matrices satisfy the condition $det([\mathbf{W}_1]) = det([\mathbf{W}_2]) = 0$. Nevertheless, the points of intersection c_1 and c_2 will most likely be different points, as shown in Figure 5.2, implying $det([\mathbf{W}_3]) \neq 0$ and $det([\mathbf{W}_4]) \neq 0$. Therefore, if the chosen combinations involve both collinear associated reciprocal screws, the remaining determinants will not likely equal zero. To satisfy this exception, it is necessary to check if one of the remaining determinants equals zero.

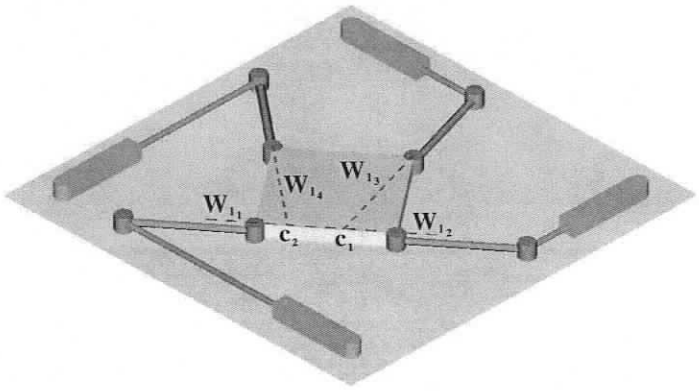

Figure 5.2: Exception when Associated Reciprocal Screws are Collinear.

- Coincidence.- *When two passive joints are coincident (or collinear in a spatial manipulator).* This special singularity occurs when two passive joints can have motion but the mobile platform remains fixed. This type of singularity

was defined as Redundant Passive Motion (*RPM*) by Zlatanov et al. (1994b). For instance, for the 3-R$\underline{\text{P}}$R manipulator, this type of singularity occurs when the displacement of the prismatic joint of the i^{th} branch equals zero, as shown by Bonev et al. (2003); i.e., the two passive revolute joints of the i^{th} branch will be coincident leading to an uncontrollable motion of the mobile platform. Mathematically, there are only two linearly independent reciprocal screws. For the 4-R$\underline{\text{P}}$R manipulator, the sub-matrices that contain the associated reciprocal screw of the i^{th} branch are rank deficient. For example, for the 4-RPR manipulator shown in Figure 5.3, the matrices that contain $\mathbf{W}_{k_1}$ are rank deficient; however, sub-matrix $[\mathbf{W}_4] = \begin{bmatrix} \mathbf{W}_{k_2} & \mathbf{W}_{k_3} & \mathbf{W}_{k_4} \end{bmatrix}$ is not singular, i.e., the associated reciprocal screws of this sub-matrix does not form a planar pencil. Therefore, it is necessary to check the sub-matrix that does not include the associated reciprocal screw of the i^{th} branch. In a real application, this special singularity would never happen (a prismatic joint provides a natural link offset). For the 3-$\underline{\text{P}}$RR and 3-$\underline{\text{R}}$RR manipulators, this singularity cannot happen as long as the links ρ_i are non-zero.

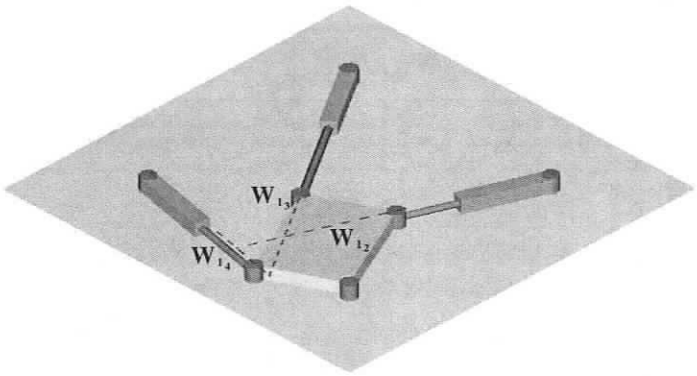

Figure 5.3: Exception when Two Passive Joints are Coincident.

These exceptions can be treated in a numerical manner. Once a force-unconstrained pose of the redundant manipulator is computed with two determinants, the obtained pose is then substituted into the remaining sub-matrices and their condition is verified.

If the time derivative method is used, an $n \times m$ non-square Jacobian matrix results. If the manipulator is in a force-unconstrained configuration, there is a dependency among the determinants of the sub-matrices formed with the rows of the Jacobian matrix. Although this row dependency does not have a clear physical meaning, the analogy between the Jacobian matrix and the associated reciprocal screw matrix corroborates such dependency. In conclusion, the number of nonlinearly dependent determinants is augmented by one, for each additional branch added.

With the time derivative method, the resulting two determinants form a system of two polynomial equations in three variables (x, y, and ϕ). With the screw theory method, the loop-closure equations, beyond the two determinants, are included in the polynomial system yielding six equations in seven variables (x, y, ϕ, and θ_{3_i}, for $i = 1, 2, 3, 4$). Thus, one variable is freely chosen. Methods used to solve systems of polynomial equations are described at length in Appendix C.

5.3 Force-Unconstrained Poses of the 4-RPR PPM

5.3.1 Analyzed Layout

The 4-RPR manipulator[1] is an overconstrained parallel manipulator as illustrated in Figure 5.4.

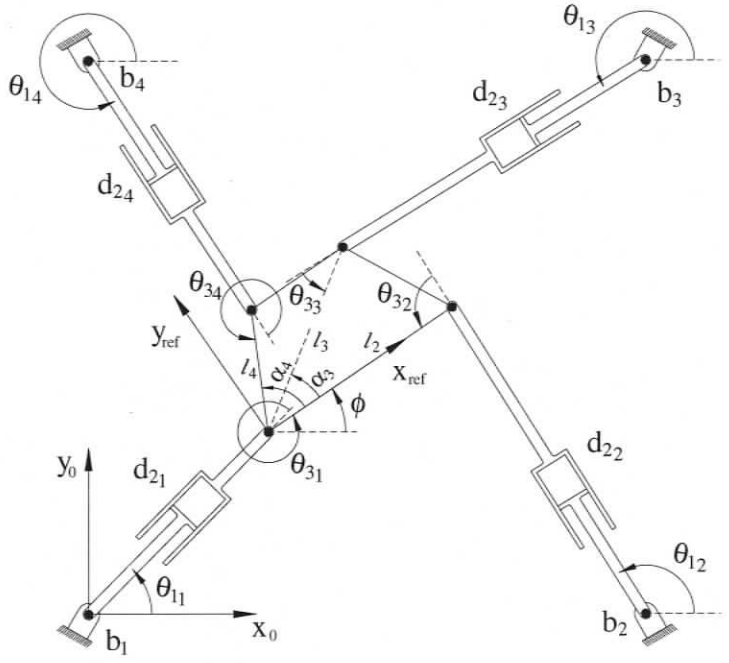

Figure 5.4: Layout of the 4-RPR Planar Parallel Manipulator.

Based on the 4-RPR manipulator, Husty et al. (2001) showed that a specific geometry of the manipulator platforms can lead to the same forward kinematic solutions as the original manipulator with just three branches.

[1]This work was presented at the 2004 CSME Forum, Firmani and Podhorodeski (2004b), and afterward published in Firmani and Podhorodeski (2005b).

For the 3-R$\underline{P}$R manipulator, besides the singularity of Type II, when [**A**] is singular, there is *RPM* singularity. With the time derivative method, the row of the Jacobian matrix [**A**] that describes the kinematic variables of the degenerate branch will be a zero row; i.e., the Jacobian matrix is rank deficient. However, for the 4-R$\underline{P}$R manipulator, *RPM* singularities will occur if and only if the sub-matrix that contains the non-degenerate branches is also singular. That is, forces exerted by the remaining prismatic joints can constrain the force that is being applied. Geometrically, if the prismatic joint displacement of the degenerate branch equals zero, the manipulator will be in a singular configuration if and only if the remaining associated reciprocal screws intersect at a common point (planar pencil). In this section, the force-unconstrained poses of the 4-R$\underline{P}$R manipulator are analyzed. In the following subsections, the Jacobian matrices are determined and through an elimination technique, namely Gröbner Bases, two determinants of the sub-matrices are employed to identify the force-unconstrained poses.

5.3.2 Derivation of Equations

The loop-closure equations of the first three branches of the 3-R$\underline{P}$R manipulator were derived in Section 3.3.3. The loop closure equation of the fourth branch is given by

$$d_{2_4}^2 = (x + l_4 c(\phi + \alpha_4) - bx_4)^2 + (y + l_4 s(\phi + \alpha_4) - by_4)^2 \tag{5.1}$$

The time derivative of all four equations leads to the relationship between the input and output speeds $[\mathbf{A}]\,\dot{\mathbf{x}} = [\mathbf{B}]\,\dot{\mathbf{q}}$, where [**A**], the force Jacobian, is a 4×3 matrix and [**B**], the velocity Jacobian, is a 4×4 matrix.

5.3.3 Force-Unconstrained Poses

Based on the dependency of the Jacobian rows, the determinants of two sub-matrices being equal to zero is a necessary condition. As Sefrioui and Gosselin (1995) described, the determinant of the 3-RPR leads to quadratic terms in x and y, with variable ϕ being suppressed. Let $\mathbf{P}_{\mathbf{J}_{123}}(x, y, \phi) = det([\mathbf{J}_{123}]) = 0$ be the resulting second order polynomial in x and y of the mechanism denoted by branches 1, 2, and 3; and $\mathbf{P}_{\mathbf{J}_{124}}(x, y, \phi) = det([\mathbf{J}_{124}]) = 0$ be the polynomial of the mechanism denoted by branches 1, 2, and 4. These polynomials have the following form:

$$\mathbf{P}_{\mathbf{J}_{123}} = g_1x^2 + g_2y^2 + g_3xy + g_4x + g_5y = 0 \tag{5.2a}$$

$$\mathbf{P}_{\mathbf{J}_{124}} = h_1x^2 + h_2y^2 + h_3xy + h_4x + h_5y = 0 \tag{5.2b}$$

where the coefficients g_i and h_i, for $i = 1, 2, 3, 4, 5$, are expressed in terms of ϕ, and shown in Appendix D.4.1.

The solution to the polynomial system leads to an n^{th}-order polynomial in terms of only two variables, i.e., $\mathbf{Q}_\mathbf{J}(x, \phi) = 0$, where y has already been eliminated. The degree of polynomial $\mathbf{Q}_\mathbf{J}(x, \phi)$ can be predicted with Bezout's number as shown in Appendix C.3.2. Since the degree of both polynomials. $\mathbf{P}_{\mathbf{J}_{123}}$ and $\mathbf{P}_{\mathbf{J}_{124}}$, is two, the upper bound degree of the polynomial system is $n = 4$.

A method for solving non-linear algebraic systems of equations is Gröbner Bases (Buchberger, 1965), which is based on ordering the power products of the initial equations and creating new equations without generating superfluous power products as shown in Appendix C.7. By means of Gröbner Bases, a 4^{th}-order polynomial $\mathbf{Q}_\mu$ in x and a first order polynomial $\mathbf{Q}_\eta$ in y result, where $\mathbf{Q}_\mu = \mathbf{Q}_\mathbf{J}(x, \phi)$. The symbolic computation of Gröbner Bases can be obtained using symbolic algebra software

packages such as Maple and Mathematica, yielding:

$$\mathbf{Q}_\mu = \mu_1 x^4 + \mu_2 x^3 + \mu_3 x^2 + \mu_4 x = 0 \tag{5.3a}$$

$$\mathbf{Q}_\eta = \eta_1 y + \eta_2 = 0 \tag{5.3b}$$

where the coefficients μ_i, for $i = 1, 2, 3, 4$, are expressed in terms of ϕ, and the coefficients η_i, for $i = 1, 2$, are expressed in terms of ϕ and x. These coefficients are shown in Appendix D.4.1.

The roots of $\mathbf{Q}_\mu$ correspond to potential x values of force-unconstrained poses, which are substituted back into $\mathbf{Q}_\eta$ to obtain the corresponding values of y. These values represent the force-unconstrained poses for the combination of the two chosen non-redundant mechanisms (1-2-3 and 1-2-4) or decoupled mechanisms. Each pose is then substituted numerically into the remaining sub-matrices to verify their condition. Finally, the pose is transformed from the position of w_1 to the centre of the mobile platform.

For one non-redundant mechanism, $O(\infty^2)$ of force-unconstrained poses exist (surfaces); while with inclusion of an additional branch, $O(\infty)$ of force-unconstrained poses exist (curves due to the intersection of surfaces). Given that $O(\infty)$ of force-unconstrained poses exists, the orientation of the platform ϕ is assumed for the range, 0° to 360°.

Example.-

The force-unconstrained poses of the 4-RPR are presented in Figure 5.5, where $l_2 = 1\ m$, $l_3 = 0.9\ m$, $l_4 = 0.28\ m$, $\alpha_3 = 33.7^\circ$, $\alpha_4 = 63.4^\circ$. The fixed platform is a square with 2.5 m per side. The figure shows two closed loops of force-unconstrained poses. Their projections are depicted in grey in the xy plane.

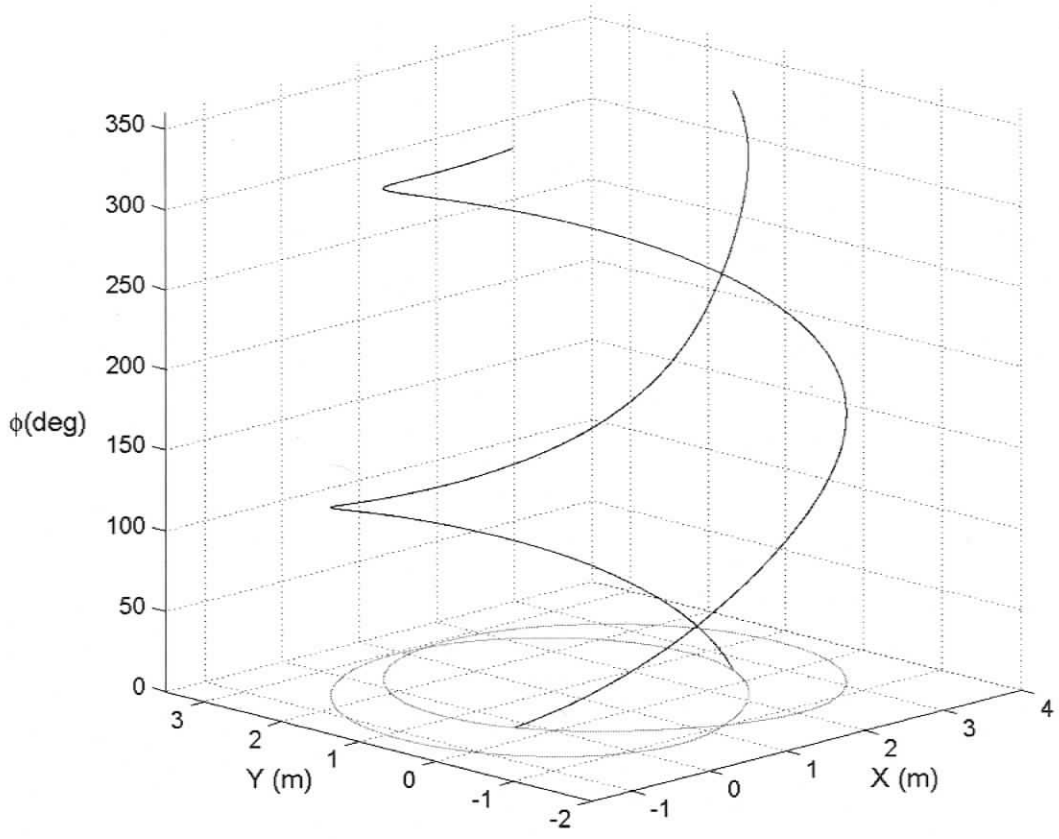

Figure 5.5: Force-Unconstrained Poses of the 4-RPR PPM with a Trapezoidal Payload Platform.

It is important to mention that for the two chosen sub-matrices, $[\mathbf{J}_{123}]$ and $[\mathbf{J}_{124}]$, *RPM* singularities appeared when the prismatic joint displacement of either branch 1 or branch 2 was zero. Nevertheless, the sub-matrix that did not involve the branch with the degenerate prismatic joint was not singular.

The shape of the platform and the arrangement of the bases play an important role in the nature of the force-unconstrained poses of the manipulator. Therefore, further investigation on different architectures is required.

5.4 Force-Unconstrained Poses of the 4-PRR PPM

5.4.1 Analyzed Layout

For the 4-PRR manipulator[2], shown in Figure 5.6, screw theory is employed yielding two non-linearly dependent determinants and four branches, i.e., six equations in seven variables. In the following subsections, the required equations are derived. Then through an elimination technique, the singular configurations of the 4-PRR planar parallel manipulator are identified.

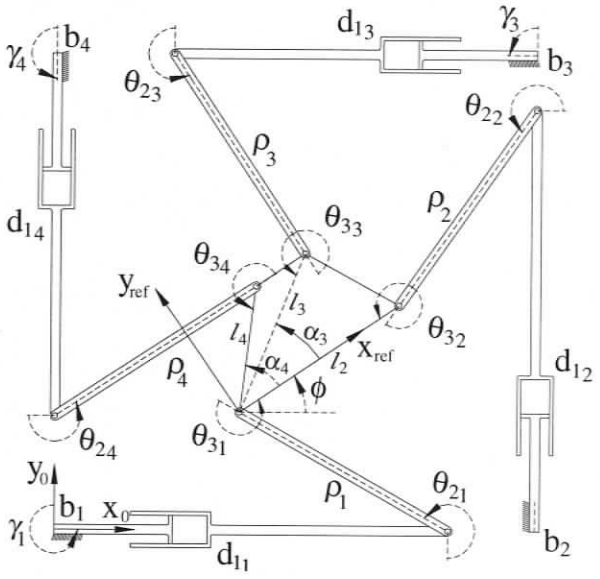

Figure 5.6: Layout of the 4-PRR Planar Parallel Manipulator.

Valasek et al. (2005) developed a prototype based on this layout named *Sliding Star*. The design consists of two parallel slides which form the base of this manipulator, two sliders (or prismatic joints) move along one slide and the other two move

[2]This work was presented at the 2005 CCToMM Forum, Firmani and Podhorodeski (2005a), and afterward published in Firmani and Podhorodeski (2005c).

along the second slide. This architecture was generated by means of maximizing both stiffness and dynamic values.

5.4.2 Derivation of Equations

The associated reciprocal screw of the actuated joint of the additional branch is

$$^{\text{ref}}\mathbf{W}_{1_4} = \{-\cos(\theta_{3_4} - \alpha_4),\ \sin(\theta_{3_4} - \alpha_4);\, l_4 \sin\theta_{3_4}\}^{\mathrm{T}} \tag{5.4}$$

yielding the following associated reciprocal screw matrix:

$$^{\text{ref}}[\mathbf{W}] = \begin{bmatrix} ^{\text{ref}}\mathbf{W}_{1_1} & ^{\text{ref}}\mathbf{W}_{1_2} & ^{\text{ref}}\mathbf{W}_{1_3} & ^{\text{ref}}\mathbf{W}_{1_4} \end{bmatrix} \tag{5.5}$$

Let the non-redundant mechanisms be composed of branches 1-2-3 and 1-2-4. The associated reciprocal screw matrices are assembled and their respective determinants are shown below.

For branches 1-2-3,

$$\begin{aligned} [^{\text{ref}}\mathbf{W}_1] &= \begin{bmatrix} ^{\text{ref}}\mathbf{W}_{1_1} & ^{\text{ref}}\mathbf{W}_{1_2} & ^{\text{ref}}\mathbf{W}_{1_3} \end{bmatrix} \\ &= \begin{bmatrix} \cos\theta_{3_1} & -\cos\theta_{3_2} & -\cos(\theta_{3_3} - \alpha_3) \\ -\sin\theta_{3_1} & \sin\theta_{3_2} & \sin(\theta_{3_3} - \alpha_3) \\ 0 & l_2 \sin\theta_{3_2} & l_3 \sin\theta_{3_3} \end{bmatrix} \end{aligned} \tag{5.6}$$

$$\begin{aligned} |^{\text{ref}}[\mathbf{W}_1]| &= l_2 \sin(\theta_{3_2})\left(\sin(\theta_{3_1})\cos(\theta_{3_3} - \alpha_3) - \cos(\theta_{3_1})\sin(\theta_{3_3} - \alpha_3)\right) \\ &\quad + l_3 \sin(\theta_{3_3})\left(\cos(\theta_{3_1})\sin(\theta_{3_2}) - \sin(\theta_{3_1})\cos(\theta_{3_2})\right) = 0 \end{aligned} \tag{5.7}$$

For branches 1-2-4,

$$
\begin{aligned}
[{}^{\text{ref}}\mathbf{W}_2] &= \begin{bmatrix} {}^{\text{ref}}\mathbf{W}_{1_1} & {}^{\text{ref}}\mathbf{W}_{1_2} & {}^{\text{ref}}\mathbf{W}_{1_4} \end{bmatrix} \\
&= \begin{bmatrix} \cos\theta_{3_1} & -\cos\theta_{3_2} & -\cos\left(\theta_{3_4}-\alpha_4\right) \\ -\sin\theta_{3_1} & \sin\theta_{3_2} & \sin\left(\theta_{3_4}-\alpha_4\right) \\ 0 & l_2\sin\theta_{3_2} & l_4\sin\theta_{3_4} \end{bmatrix}
\end{aligned} \tag{5.8}
$$

$$
\begin{aligned}
|{}^{\text{ref}}[\mathbf{W}_2]| &= l_2\sin(\theta_{3_2})\left(\sin(\theta_{3_1})\cos(\theta_{3_4}-\alpha_4)-\cos(\theta_{3_1})\sin(\theta_{3_4}-\alpha_4)\right) \\
&\quad +l_4\sin(\theta_{3_4})\left(\cos(\theta_{3_1})\sin(\theta_{3_2})-\sin(\theta_{3_1})\cos(\theta_{3_2})\right)=0
\end{aligned} \tag{5.9}
$$

The general loop-closure equation found in Eq. (3.33) is also applicable for the fourth branch; i.e.,

$$
\begin{aligned}
f_4(x,\ y,\ \phi,\ \theta_{3_4}) &= \left(y-by_4-\rho_4 s(\phi-\theta_{3_4}-\beta_4)-l_4 s(\phi-\beta_4)\right)s(\gamma_4)+ \\
&\quad \left(x-bx_4-\rho_4 c(\phi-\theta_{3_4}-\beta_4)-l_4 c(\phi-\beta_4)\right)c(\gamma_4)=0
\end{aligned} \tag{5.10}
$$

where $\beta_4=\pi-\alpha_4$.

5.4.3 Force-Unconstrained Poses

The force-unconstrained poses of the 4-PRR manipulator are defined as the intersection among the surfaces of two non-redundant 3-PRR planar parallel manipulators. There are six equations ($|{}^{\text{ref}}[\mathbf{W}_k]|=0$ and $f_i(x,\ y,\ \phi,\ \theta_{3_i})=0$, $k=1,2$ and $i=1,2,3,4$) and seven variables (x, y, ϕ, and θ_{3_i}, $i=1,2,3,4$); i.e., there is one 'free' variable. The choice of the 'free' variable is important because this will define the total degree of the final polynomial. For example, Bonev et al. (2003) demonstrated that for a constant payload orientation, i.e., ϕ the 'free' variable, the singular poses of the 3-PRR manipulator are represented by a 20^{th}-order polynomial.

By combining two non-redundant mechanisms and by applying Bezout's number, the force-unconstrained poses of the 4-PRR manipulator would be up to a 400^{th}-order polynomial. Although this number is an upper bound of the final degree of the polynomial, it is expected to be considerably large. As an alternative, either x or y can be chosen as the 'free' variable. Either choice would make the final degree even higher because both of them appear as linear terms in the loop-closure equations. This leads to the conclusion that one joint displacement, θ_{3_i}, should be considered. Since both θ_{3_3} and θ_{3_4} appear in only one determinant equation no significant gain is achieved. The correct choice would be between θ_{3_1} and θ_{3_2}. Let θ_{3_1} be the 'free' variable. Thus, a problem of six non-linear equations in six unknowns results:

$$
\begin{aligned}
f_1(x,\ y,\ \phi) &= 0 \quad \text{Loop-Closure Equation of branch 1} \\
f_2(x,\ y,\ \phi,\ \theta_{3_2}) &= 0 \quad \text{Loop-Closure Equation of branch 2} \\
f_3(x,\ y,\ \phi,\ \theta_{3_3}) &= 0 \quad \text{Loop-Closure Equation of branch 3} \\
f_4(x,\ y,\ \phi,\ \theta_{3_4}) &= 0 \quad \text{Loop-Closure Equation of branch 4} \\
g_1(\theta_{3_2},\ \theta_{3_3}) &= 0 \quad \text{Determinant of sub-matrix composed by branches 1-2-3} \\
g_2(\theta_{3_2},\ \theta_{3_4}) &= 0 \quad \text{Determinant of sub-matrix composed by branches 1-2-4}
\end{aligned}
$$

The solution of this system of non-linear equations requires an elimination technique. A summary of the elimination process is now described. First, half-angle substitution is applied to all joint angles θ_{3_i}. Second, variable x is eliminated using one loop-closure equation. Third, y is eliminated using another loop-closure equation. Fourth, variables θ_{3_3} and θ_{3_4} are eliminated separately using the determinant equations, leading to two equations in two unknowns (ϕ and θ_{3_2}). Fifth, half-angle substitution is applied to ϕ. Sixth, more equations are generated to match the num-

ber of power products. These equations are written in matrix form $[\Psi]\,\mathbf{t} = 0$. The elements of matrix $[\Psi]$ are a function of θ_{3_2}, while vector $\mathbf{t}$ contains power products of ϕ. Seventh, variable ϕ is eliminated by making matrix $[\Psi]$ singular, i.e., $|[\Psi]| = 0$. The determinant of $[\Psi]$ leads to a polynomial whose roots represent solutions of the force-unconstrained poses. The root finding problem is formulated as an eigenvalue problem. Eighth, the remaining variables are found through back substitution.

***Step 1*.- Applying Half-Angle Substitution to θ_{3_i}**

Apply half-angle substitution to the third joint angles, i.e.,

$$\sin(\theta_{3_i}) = \frac{2q_i}{1+q_i^2} \quad \text{and} \quad \cos(\theta_{3_i}) = \frac{1-q_i^2}{1+q_i^2}, \quad \text{where } q_i = \tan(\frac{\theta_{3_i}}{2}) \tag{5.11}$$

and where $i = 1, 2, 3$. The new variables are substituted back into their respective equations and the denominators are cleared. For further convenience, the coefficients of the five power products of equations $g_1(q_2,\, q_3) = 0$ and $g_2(q_2,\, q_4) = 0$ are collected ($a_{j,k}$ for $j = 1, 2$ and $k = 1, .., 5$) and are shown in Appendix D.4.2.

$$g_1(q_2,\, q_3) = a_{1,1}q_3q_2^2 + a_{1,2}q_3^2q_2 + a_{1,3}q_3q_2 + a_{1,4}q_3 + a_{1,5}q_2 = 0 \tag{5.12}$$

$$g_2(q_2,\, q_4) = a_{2,1}q_4q_2^2 + a_{2,2}q_4^2q_2 + a_{2,3}q_4q_2 + a_{2,4}q_4 + a_{2,5}q_2 = 0 \tag{5.13}$$

***Step 2*.- Eliminating x**

Eliminate variable x by isolating it from equation $f_1(x,\, y,\, \phi) = 0$, i.e.,

$$\begin{aligned} x = & -(y - by_1 - \rho_1 \sin(\phi - \theta_{3_1} - \beta_1) - l_1 \sin(\phi - \beta_1)) \tan(\gamma_1) \\ & + bx_1 + \rho_1 \cos(\phi - \theta_{3_1} - \beta_1) + l_1 \cos(\phi - \beta_1) \end{aligned} \tag{5.14}$$

Substitute x back in equations $f_2(x,\, y,\, \phi,\, q_2) = 0$, $f_3(x,\, y,\, \phi,\, q_3) = 0$, and $f_4(x,\, y,\, \phi,\, q_4) = 0$. The new equations, $f_i'(y,\, \phi,\, q_i) = 0$ for $i = 2, 3, 4$, are composed of 10 power

products. The coefficients of the power products are collected ($b_{i,k}$ for $i = 2, 3, 4$ and $k = 1, .., 10$) and are shown in Appendix D.4.2.

$$\begin{aligned} f_i'(y, \phi, q_i) &= b_{i,1}q_i^2 y + b_{i,2}q_i^2\cos(\phi) + b_{i,3}q_i^2\sin(\phi) + b_{i,4}q_i^2 + b_{i,5}q_i\cos(\phi) \\ &\quad + b_{i,6}q_i\sin(\phi) + b_{i,7}\cos(\phi) + b_{i,8}\sin(\phi) + b_{i,9}y + b_{i,10} \end{aligned} \tag{5.15}$$

***Step 3.*- Eliminating y**

Eliminate variable y by isolating it from equation $f_2'(y,\ \phi,\ q_2) = 0$, i.e.,

$$\begin{aligned} y &= (b_{2,2}q_2^2\cos(\phi) + b_{2,3}q_2^2\sin(\phi) + b_{2,4}q_2^2 + b_{2,5}q_i\cos(\phi) + b_{2,6}q_2\sin(\phi) \\ &\quad + b_{2,7}\cos(\phi) + b_{2,8}\sin(\phi) + b_{2,10})/(-b_{2,1}q_2^2 - b_{2,9}) \end{aligned} \tag{5.16}$$

Substitute y back into equations $f_3'(y,\ \phi,\ q_3) = 0$, and $f_4'(y,\ \phi,\ q_4) = 0$. The new equations, $f_i''(\phi,\ q_2,\ q_i) = 0$ for $i = 3, 4$, are composed of 20 power products. The coefficients of the power products are collected ($c_{i,k}$ for $i = 3, 4$ and $k = 1, .., 20$) and are shown in Appendix D.4.2.

$$\begin{aligned} f_i''(\phi,\ q_2,\ q_i) &= c_{i,1}q_2^2q_i^2\cos(\phi) + c_{i,2}q_2^2q_i^2\sin(\phi) + c_{i,3}q_2^2q_i\cos(\phi) + c_{i,4}q_2^2q_i\sin(\phi) \\ &\quad + c_{i,5}q_2^2\cos(\phi) + c_{i,6}q_2^2\sin(\phi) + c_{i,7}q_2^2q_i^2 + c_{i,8}q_2^2 + c_{i,9}q_2q_i^2\cos(\phi) \\ &\quad + c_{i,10}q_2q_i^2\sin(\phi) + c_{i,11}q_2\cos(\phi) + c_{i,12}q_2\sin(\phi) + c_{i,13}q_i^2\cos(\phi) \\ &\quad + c_{i,14}q_i^2\sin(\phi) + c_{i,15}q_i\cos(\phi) + c_{i,16}q_i\sin(\phi) + c_{i,17}\cos(\phi) \\ &\quad + c_{i,18}\sin(\phi) + c_{i,19}q_i^2 + c_{i,20} \end{aligned} \tag{5.17}$$

***Step 4.*- Eliminating q_3 and q_4**

Eliminate variable q_3 by isolating it from equation $g_1(q_2,\ q_3) = 0$ and substituting it back into equation $f_3''(\phi,\ q_2,\ q_3) = 0$. Similarly, eliminate variable q_4 by isolating it

from equation $g_2(q_2,\, q_4) = 0$ and substituting it back into equation $f_4''(\phi,\, q_2,\, q_4) = 0$. These two eliminations are not as simple as the previous ones because the variables being eliminated are non-linear. In order to eliminate the square roots that appear after the substitutions, the expressions must be squared. This leads to two new equations $h_j(\phi,\, q_2) = 0$, for $j = 1, 2$.

***Step 5*.- Applying Half-Angle Substitution to ϕ**

Apply half-angle substitution to ϕ, i.e.,

$$\sin(\phi) = \frac{2t}{1+t^2} \quad \text{and} \quad \cos(\phi) = \frac{1-t^2}{1+t^2}, \quad \text{where } t = \tan(\frac{\phi}{2}) \tag{5.18}$$

This yields two expressions of the form $h_j(t,\, q_2) = 0$, for $j = 1, 2$. These two expressions contain 45 power products because q_2 is a variable of degree 8 and t is a variable of degree 4. The power products are grouped and the coefficients d_{jr}, where $r = 5i + k + 1$, are collected. Due to space limitations in this dissertation, the coefficients $d_{j,r}$ are not shown.

$$h_j(t, q_2) = \sum_{i=0}^{8}\sum_{k=0}^{4} d_{j,r}\, q_2^i\, t^{\,k} = 0 \tag{5.19}$$

***Step 6*.- Generating more Equations**

Assemble a 2×5 matrix $[\Psi']$ by sorting the powers of t. This matrix is generated with equations $h_1(t,\, q_2) = 0$ and $h_2(t,\, q_2) = 0$ and its entries are 8^{th}-order polynomials in q_2.

$$[\Psi']\ \mathbf{t}' = \bar{\mathbf{0}} \tag{5.20}$$

where $[\Psi'] = \begin{bmatrix} \psi_{11} & \psi_{12} & \psi_{13} & \psi_{14} & \psi_{15} \\ \psi_{21} & \psi_{22} & \psi_{23} & \psi_{24} & \psi_{25} \end{bmatrix}$ and $\mathbf{t}' = \begin{bmatrix} t^4 & t^3 & t^2 & t & 1 \end{bmatrix}^{\mathrm{T}}$.

Generate additional equations such that the number of equations matches the number of power products. Equations $h_1(t,\, q_2) = 0$ and $h_2(t,\, q_2) = 0$ are multiplied by t, t^2, and t^3. This leads to an 8×8 matrix whose entries are still 8^{th}-order polynomials in q_2.

$$[\Psi]\ \mathbf{t} = \begin{bmatrix} \psi_{11} & \psi_{12} & \psi_{13} & \psi_{14} & \psi_{15} & 0 & 0 & 0 \\ \psi_{21} & \psi_{22} & \psi_{23} & \psi_{24} & \psi_{25} & 0 & 0 & 0 \\ 0 & \psi_{11} & \psi_{12} & \psi_{13} & \psi_{14} & \psi_{15} & 0 & 0 \\ 0 & \psi_{21} & \psi_{22} & \psi_{23} & \psi_{24} & \psi_{25} & 0 & 0 \\ 0 & 0 & \psi_{11} & \psi_{12} & \psi_{13} & \psi_{14} & \psi_{15} & 0 \\ 0 & 0 & \psi_{21} & \psi_{22} & \psi_{23} & \psi_{24} & \psi_{25} & 0 \\ 0 & 0 & 0 & \psi_{11} & \psi_{12} & \psi_{13} & \psi_{14} & \psi_{15} \\ 0 & 0 & 0 & \psi_{21} & \psi_{22} & \psi_{23} & \psi_{24} & \psi_{25} \end{bmatrix} \begin{bmatrix} t^7 \\ t^6 \\ t^5 \\ t^4 \\ t^3 \\ t^2 \\ t \\ 1 \end{bmatrix} = \bar{0} \qquad (5.21)$$

***Step 7.*- Solving for q_2**

Eliminate variable t by making matrix $[\Psi]$ singular; i.e., this condition makes Eq. (5.21) valid. Solving $|[\Psi]| = 0$ is extremely complicated because each entry of $[\Psi]$ is an 8^{th}-order polynomial. Moreover, the resulting determinant will be a 64^{th}-order polynomial and the computation of the roots of such a large polynomial may be susceptible to having floating point arithmetic problems. As an alternative, the roots of the determinant can be solved as a standard eigenvalue problem (Gohberg et al., 1982). This method is much more stable and is described in Appendix E.

Matrix $[\Psi]$ is written as a matrix polynomial,

$$[\Psi]\,(q_2) = \sum_{i=0}^{8} [\Psi_i]\, q_2^i \qquad (5.22)$$

where each entry of $[\Psi_i]$ corresponds to one of the coefficients d_{jr} found in Eq. (5.19).

The idea of this method is to assemble a 64×64 matrix $[\mathbf{K}]$ with each matrix of the matrix polynomial in the following form:

$$[\mathbf{K}] = \begin{bmatrix} \mathbf{0} & \mathbf{I} & \mathbf{0} & \cdots & \mathbf{0} \\ \mathbf{0} & \mathbf{0} & \mathbf{I} & \cdots & \mathbf{0} \\ \vdots & \vdots & \vdots & \ddots & \vdots \\ \mathbf{0} & \mathbf{0} & \mathbf{0} & \cdots & \mathbf{I} \\ -[\Psi_8]^{-1}[\Psi_0] & -[\Psi_8]^{-1}[\Psi_1] & -[\Psi_8]^{-1}[\Psi_2] & \cdots & -[\Psi_8]^{-1}[\Psi_7] \end{bmatrix} \tag{5.23}$$

where $\mathbf{0}$ and $\mathbf{I}$ are 8×8 null and identity matrices, respectively.

Matrix $[\mathbf{K}]$ is employed to formulate the standard eigenvalue problem as follows:

$$[\mathbf{K}]\,\mathbf{T} = \lambda \mathbf{T} \tag{5.24}$$

where λ is an eigenvalue which represents a solution of q_2, $\mathbf{T}$ is the associated eigenvector with λ of the form $\mathbf{T} = [\ \mathbf{t} \quad \mathbf{t}\lambda \quad \mathbf{t}\lambda^2 \quad \cdots \quad \mathbf{t}\lambda^7\ ]^{\mathrm{T}}$.

The eigenvalues of matrix $[\mathbf{K}]$ correspond precisely to the roots of the 64^{th}-order polynomial, i.e., all solutions of q_2 for a given value of θ_{3_1}.

Step 8.- **Back Substitution**

Compute the poses of the manipulator by substituting back the numerical values of q_2. That is, variable t can be determined using Gauss elimination of the problem

$$[\mathbf{A}]\,\hat{\mathbf{t}} = \mathbf{b} \tag{5.25}$$

where $[\mathbf{A}]$ is a 7×7 matrix formed with the first seven rows and columns of matrix $[\Psi]$, $\hat{\mathbf{t}}$ is a vector that contains the first seven elements of $\mathbf{t}$, and $\mathbf{b}$ is the negative of the first seven elements of the last column of matrix $[\Psi]$.

The already known variables can be transformed to their original angle expressions by using the half-angle substitution property, i.e., $t \Longrightarrow \phi$ and $q_2 \Longrightarrow \theta_{3_2}$. These values are substituted into Eq. (5.16) and y is solved. With ϕ and y known, x is evaluated with Eq. (5.14). Finally, the position is transformed to the centre of the mobile platform.

Example.-

The singular poses of a 4-$\underline{\text{P}}$RR with the following characteristics is presented: Both the fixed and mobile platforms are squares, whose sides are 2 m and 1 m, respectively. The angle of the bases are $\gamma_1 = 0°$, $\gamma_2 = 90°$, $\gamma_3 = 180°$, and $\gamma_4 = 270°$ (same configuration as in Figure 5.6). The link lengths are $\rho_i = 1\ m$, for $i = 1, \ldots, 4$. Figure 5.7 illustrates the loci of the single order of force-unconstrained poses of the platform centre in the $x - y - \phi$ space. The projection of the curves on the xy plane is shown onto the plot at the bottom of the figure.

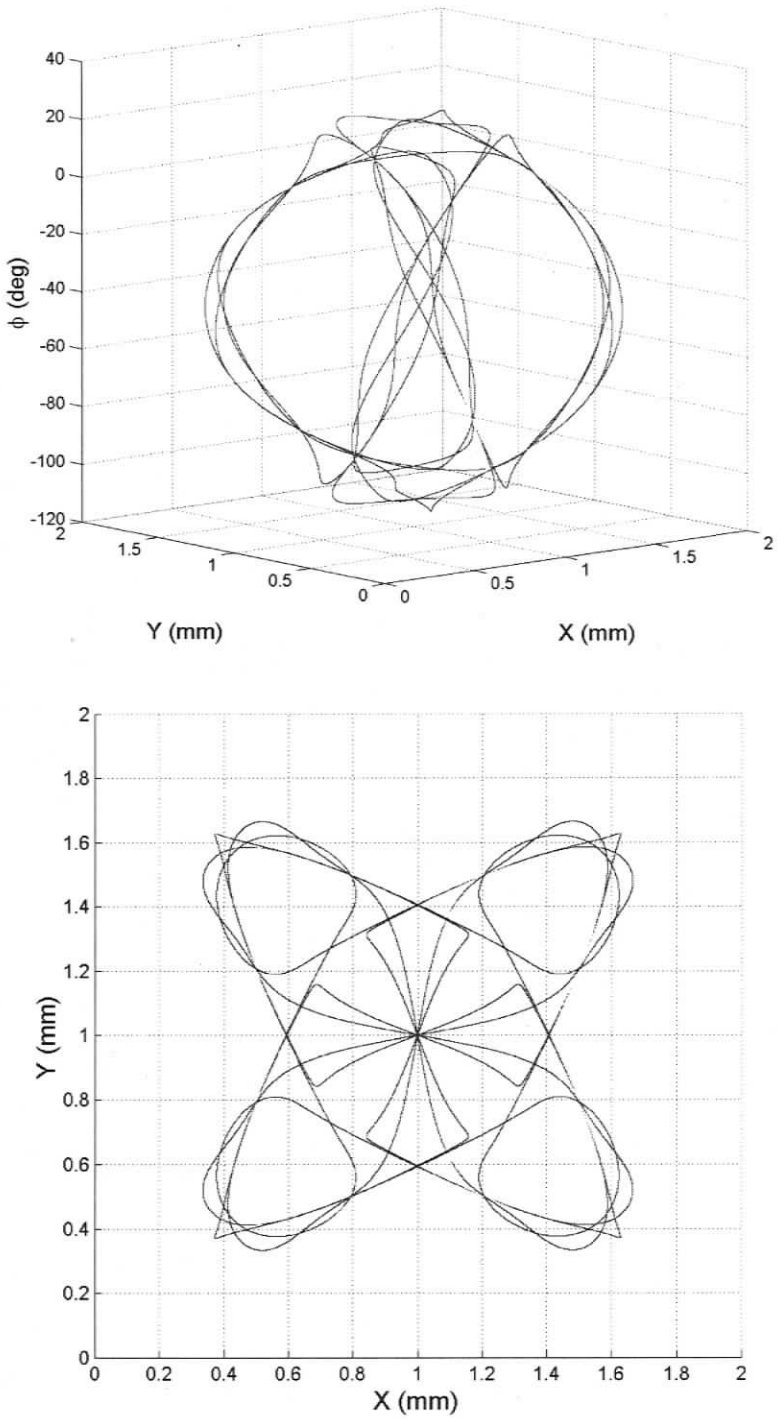

Figure 5.7: Force-Unconstrained Poses of the 4-PRR Manipulator.

5.5 Force-Unconstrained Poses of the 4-RRR PPM

5.5.1 Analyzed Layout

The 4-RRR manipulator, shown in Figure 5.8, has been widely analyzed from the control perspective, see for instance Liu et al. (2001) and Muller (2005).

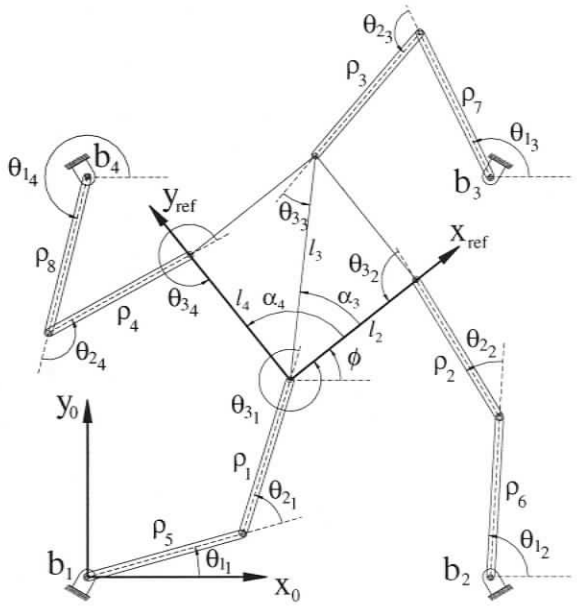

Figure 5.8: Layout of the 4-RRR Planar Parallel Manipulator.

Voglewede (2004) developed constrained optimization algorithms that numerically determines the "closeness" of singular configurations for both the 3-RRR and 4-RRR manipulators. For one working mode, Voglewede presented plots on the $x-y$ plane. For any location of the 3-RRR manipulator, there is one and only one platform orientation that makes the manipulator force unconstrained[3]. For the 4-RRR manip-

[3]This condition was found for a particular manipulator but it is not always the case as shown in the results of this dissertation in Figures 3.9.

ulator, the projection of the singular configurations on the $x-y$ plane leads to curves of force-unconstrained poses. The results were compared using different formulations (as presented in Voglewede and Ebert-Uphoff, 2004) and the plots showed some discrepancy on the quality of the curves. Nevertheless, the singularities of every plot occurred in the same region.

In this section, an analytical method for determining the force-unconstrained poses of the 4-RRR manipulator is presented. First the equations: two non-linearly dependent determinants and four loop closure equations regarding the branches' kinematics are derived. Then through exhaustive elimination techniques, the singularity loci of the 4-RRR planar parallel manipulator are identified.

5.5.2 Derivation of Equations

The associated reciprocal screw of the actuated joint of the additional branch is

$$^{\text{ref}}\mathbf{W}_{1_4} = \{-\cos(\theta_{3_4} - \alpha_4),\ \sin(\theta_{3_4} - \alpha_4);\, l_4 \sin\theta_{3_4}\}^{\mathrm{T}} \tag{5.26}$$

yielding the following associated reciprocal screw matrix:

$$^{\text{ref}}[\mathbf{W}] = \begin{bmatrix} ^{\text{ref}}\mathbf{W}_{1_1} & ^{\text{ref}}\mathbf{W}_{1_2} & ^{\text{ref}}\mathbf{W}_{1_3} & ^{\text{ref}}\mathbf{W}_{1_4} \end{bmatrix} \tag{5.27}$$

Notice that $^{\text{ref}}[\mathbf{W}]$ is exactly the same as the one found for the 4-PRR manipulator. Let the non-redundant mechanisms be composed of branches 1-2-3 and 1-2-4. The determinants of $[^{\text{ref}}\mathbf{W}_1] = \begin{bmatrix} ^{\text{ref}}\mathbf{W}_{1_1} & ^{\text{ref}}\mathbf{W}_{1_2} & ^{\text{ref}}\mathbf{W}_{1_3} \end{bmatrix}$ and $[^{\text{ref}}\mathbf{W}_2] = \begin{bmatrix} ^{\text{ref}}\mathbf{W}_{1_1} & ^{\text{ref}}\mathbf{W}_{1_2} & ^{\text{ref}}\mathbf{W}_{1_4} \end{bmatrix}$ are shown below:

$$\begin{aligned} |^{\text{ref}}[\mathbf{W}_1]| \;=\; & l_2 \sin(\theta_{3_2})\left(\sin(\theta_{3_1})\cos(\theta_{3_3} - \alpha_3) - \cos(\theta_{3_1})\sin(\theta_{3_3} - \alpha_3)\right) \\ & + l_3 \sin(\theta_{3_3})\left(\cos(\theta_{3_1})\sin(\theta_{3_2}) - \sin(\theta_{3_1})\cos(\theta_{3_2})\right) = 0 \end{aligned} \tag{5.28}$$

$$
\begin{aligned}
|^{\text{ref}}[\mathbf{W}_2]| \;=\; & l_2 \sin(\theta_{3_2}) \left(\sin(\theta_{3_1}) \cos(\theta_{3_4} - \alpha_4) - \cos(\theta_{3_1}) \sin(\theta_{3_4} - \alpha_4)\right) \\
& + l_4 \sin(\theta_{3_4}) \left(\cos(\theta_{3_1}) \sin(\theta_{3_2}) - \sin(\theta_{3_1}) \cos(\theta_{3_2})\right) = 0
\end{aligned} \tag{5.29}
$$

The general loop-closure equation found in Eq. (3.43) is also applicable for the fourth branch; i.e.,

$$
\begin{aligned}
f_i(x,\ y,\ \phi,\ \theta_{3_i}) = x^2 + y^2 & + (k_{1,i} \sin(\theta_{3_i}) + k_{2,i} \cos(\theta_{3_i}) + k_{3,i}) x \\
& + (k_{4,i} \sin(\theta_{3_i}) + k_{5,i} \cos(\theta_{3_i}) + k_{6,i}) y \\
& + (k_{7,i} \sin(\theta_{3_i}) + k_{8,i} \cos(\theta_{3_i}) + k_{9,i}) = 0
\end{aligned} \tag{5.30}
$$

where $k_{1,i}$ are shown in Appendix D.4.3.

5.5.3 Force-Unconstrained Poses

There are six equations ($|[^{\text{ref}}\mathbf{W}_k]| = 0$ and $f_i(x,\ y,\ \phi,\ \theta_{3_i}) = 0$, for $k = 1, 2$ and $i = 1, 2, 3, 4$) and seven variables (x, y, ϕ, and θ_{3_i}). This means that there is one 'free' variable. Let θ_{3_1} be the 'free' variable; i.e., θ_{3_1} will be considered as a constant. Thus, a problem of six non-linear equations in six unknowns results:

$$
\begin{aligned}
f_1(x,\ y,\ \phi) &= 0 \quad \text{Loop-Closure Equation of branch 1} \\
f_2(x,\ y,\ \phi,\ \theta_{3_2}) &= 0 \quad \text{Loop-Closure Equation of branch 2} \\
f_3(x,\ y,\ \phi,\ \theta_{3_3}) &= 0 \quad \text{Loop-Closure Equation of branch 3} \\
f_4(x,\ y,\ \phi,\ \theta_{3_4}) &= 0 \quad \text{Loop-Closure Equation of branch 4} \\
g_1(\theta_{3_2},\ \theta_{3_3}) &= 0 \quad \text{Determinant of sub-matrix composed by branches 1-2-3} \\
g_2(\theta_{3_2},\ \theta_{3_4}) &= 0 \quad \text{Determinant of sub-matrix composed by branches 1-2-4}
\end{aligned}
$$

This problem requires an elimination technique which is based on two similar procedures to eliminate variables θ_{3_3} and θ_{3_4}. A summary of the elimination process

is now described. First, half-angle substitution is applied to all the angles. Second, variables x and y are eliminated using the loop-closure equations. Third, variables θ_{3_3} and θ_{3_4} are eliminated separately using the determinant equations, leading to two equations in two unknowns (ϕ and θ_{3_2}). Fourth, more equations are generated to match the number of power products. These equations are written in matrix form $[\Psi]\,\mathbf{q}_2 = 0$. The elements of matrix $[\Psi]$ are a function of ϕ, while vector $\mathbf{q}_2$ contains power products of θ_{3_2}. Fifth, variable θ_{3_2} is eliminated by making matrix $[\Psi]$ singular, i.e., $|[\Psi]| = 0$. The determinant of $[\Psi]$ leads to a polynomial whose roots represent solutions of the force-unconstrained poses. The root finding problem is formulated as an eigenvalue problem. A discussion on numerical stability is presented, where the accuracy of the eigenvalues is achieved by scaling the dimensions of the manipulator. Sixth, the remaining variables are computed and unconstrained optimization techniques are employed to improve the accuracy of the results.

The first three steps involve the elimination of θ_{3_3} and θ_{3_4}. Given that the elimination procedure is similar, the elimination of θ_{3_3} is described in detail part a), while the elimination of θ_{3_4} is summarized in part b). Coefficients associated with θ_{3_3} have the superscript $^{(1)}$, while the superscript $^{(2)}$ is related to θ_{3_4}. Coefficients are systematically collected for further convenience in the elimination process and some of them are shown in Appendix D.4.3.

***Step 1*.- Applying Half-Angle Substitution**

a) Apply half-angle substitution to the joint angles, i.e.,

$$\sin(\theta_{3_i}) = \frac{2q_i}{1+q_i^2} \quad \text{and} \quad \cos(\theta_{3_i}) = \frac{1-q_i^2}{1+q_i^2}, \quad \text{where } q_i = \tan(\frac{\theta_{3_i}}{2}) \tag{5.31}$$

and where $i = 1, 2, 3$.

The new variables are substituted back into their respective equations and the denominators are cleared. For further convenience, the coefficients of the five power products of equation $g_1(q_2,\ q_3) = 0$ are collected as follows:

$$g_1(q_2,\ q_3) = {}^{(1)}a_1 q_3 q_2^2 + {}^{(1)}a_2 q_3^2 q_2 + {}^{(1)}a_3 q_3 q_2 + {}^{(1)}a_4 q_3 + {}^{(1)}a_5 q_2 = 0 \tag{5.32}$$

b) For the elimination regarding θ_{3_4}, half-angle substitution is applied to θ_{3_4} using Eq. (5.31) and the power product coefficients of equation $g_2(q_2,\ q_4) = 0$ are collected similarly,

$$g_2(q_2,\ q_4) = {}^{(2)}a_1 q_4 q_2^2 + {}^{(2)}a_2 q_4^2 q_2 + {}^{(2)}a_3 q_4 q_2 + {}^{(2)}a_4 q_4 + {}^{(2)}a_5 q_2 = 0 \tag{5.33}$$

Coefficients ${}^{(j)}a_k$, for $j = 1, 2$ and $k = 1, .., 5$ are shown in Appendix D.4.3.

Also, apply half-angle substitution to ϕ, i.e.,

$$\sin(\phi) = \frac{2t}{1+t^2} \quad \text{and} \quad \cos(\phi) = \frac{1-t^2}{1+t^2}, \quad \text{where } t = \tan(\frac{\phi}{2}) \tag{5.34}$$

***Step 2.*- Eliminating x and y**

a) Eliminate variables x and y from equations $f_1(x,\ y,\ t) = 0$, $f_2(x,\ y,\ t,\ q_2) = 0$, and $f_3(x,\ y,\ t,\ q_3) = 0$. Although two equations are required, one equation is used to linearize x and y, which appear as quadratic terms in the loop-closure equations and whose coefficients are one (as seen in Eqs. (3.43)). Thus new equations are generated by subtracting the loop-closure equations as follows:

$$f_1'(x, y, t, q_2) = f_1(x, y, t) - f_2(x, y, t, q_2) = 0 \tag{5.35a}$$

$$f_2'(x, y, t, q_3) = f_1(x, y, t) - f_3(x, y, t, q_3) = 0 \tag{5.35b}$$

Gosselin and Merlet (1994) used a similar elimination technique to solve the forward kinematics of the 3-RPR manipulator. This elimination technique does not

generate superfluous roots and the resulting polynomial maintains its canonical form. These equations can be also written as a system of linear equations:

$$f_1'(x, y, t, q_2) = {}^{(1)}\nu_{11}x + {}^{(1)}\nu_{12}y + {}^{(1)}\nu_{13} = 0 \tag{5.36a}$$

$$f_2'(x, y, t, q_3) = {}^{(1)}\nu_{21}x + {}^{(1)}\nu_{22}y + {}^{(1)}\nu_{23} = 0 \tag{5.36b}$$

where the coefficients of the power products are stored in two row vectors ${}^{(1)}\mathbf{b}_i$ of length 27 (shown in Appendix D.4.3), i.e.,

$${}^{(1)}\nu_{ij} = \sum_{h=0}^{2}\sum_{k=0}^{2} {}^{(1)}b_{ir}\, t^h q_{i+1}^k \tag{5.37}$$

for $i = 1, 2$, $j = 1, 2, 3$, and $r = 9(j-1) + 3h + k + 1$.

Notice that each element ${}^{(1)}\nu_{ij}$ is composed of nine terms, and the coefficients stored in vectors ${}^{(1)}\mathbf{b}_i$ contain the coefficients of all three ${}^{(1)}\nu_{ij}$ of one linear equation. Also, the term q_{i+1} is q_2, when $i = 1$, and q_3, when $i = 2$.

The solution of Eqs. (5.36a and 5.36b) is given by

$$\begin{bmatrix} {}^{(1)}\nu_{11} & {}^{(1)}\nu_{12} \\ {}^{(1)}\nu_{21} & {}^{(1)}\nu_{22} \end{bmatrix} \begin{bmatrix} {}^{(1)}x \\ {}^{(1)}y \end{bmatrix} = - \begin{bmatrix} {}^{(1)}\nu_{13} \\ {}^{(1)}\nu_{23} \end{bmatrix} \tag{5.38}$$

yielding

$${}^{(1)}x = \frac{{}^{(1)}\nu_{12}{}^{(1)}\nu_{23} - {}^{(1)}\nu_{22}{}^{(1)}\nu_{13}}{{}^{(1)}\nu_{11}{}^{(1)}\nu_{22} - {}^{(1)}\nu_{21}{}^{(1)}\nu_{12}} = \frac{{}^{(1)}num_x}{{}^{(1)}den} \tag{5.39a}$$

$${}^{(1)}y = \frac{{}^{(1)}\nu_{21}{}^{(1)}\nu_{13} - {}^{(1)}\nu_{11}{}^{(1)}\nu_{23}}{{}^{(1)}\nu_{11}{}^{(1)}\nu_{22} - {}^{(1)}\nu_{21}{}^{(1)}\nu_{12}} = \frac{{}^{(1)}num_y}{{}^{(1)}den} \tag{5.39b}$$

Coefficients of the power products involving the numerators (${}^{(1)}num_x$ and ${}^{(1)}num_y$)

and the denominator (${}^{(1)}den$) are collected as follows:

$$ {}^{(1)}num_x(t, q_2, q_3) = \sum_{h=0}^{4}\sum_{k=0}^{2}\sum_{l=0}^{2} {}^{(1)}n_{x_r}\, t^{\,h} q_2^k q_3^l \tag{5.40a} $$

$$ {}^{(1)}num_y(t, q_2, q_3) = \sum_{h=0}^{4}\sum_{k=0}^{2}\sum_{l=0}^{2} {}^{(1)}n_{y_r}\, t^{\,h} q_2^k q_3^l \tag{5.40b} $$

$$ {}^{(1)}den(t, q_2, q_3) = \sum_{h=0}^{4}\sum_{k=0}^{2}\sum_{l=0}^{2} {}^{(1)}dt_r\, t^{\,h} q_2^k q_3^l \tag{5.40c} $$

where $r = 9h + 3k + l + 1$ and the coefficients are stored in vectors of length 45: ${}^{(1)}\mathbf{n_x}$, ${}^{(1)}\mathbf{n_y}$, and ${}^{(1)}\mathbf{dt}$. These coefficients are shown in Appendix D.4.3.

Finally, the solutions of ${}^{(1)}x$ and ${}^{(1)}y$, which are function of t, q_2, and q_3, are substituted back into equation $f_1({}^{(1)}x, {}^{(1)}y, t) = 0$. After clearing the denominator the following equation results:

$$ f_1''(t, q_2, q_3) = \sum_{h=0}^{10}\sum_{k=0}^{4}\sum_{l=0}^{4} {}^{(1)}c_r\, t^{\,h} q_2^k q_3^l = 0 \tag{5.41} $$

where $r = 25h + 5k + l + 1$ and all coefficients are stored in a vector ${}^{(1)}\mathbf{c}$ whose length is 275. Due to the large length of this vector, coefficients ${}^{(1)}c_r$ are not presented in this dissertation.

b) For the second procedure (regarding θ_{3_4} or q_4), equation $f_4(x, y, t, q_4) = 0$ is used instead of $f_3(x, y, t, q_3) = 0$. This yields a new set of linear equations,

$$ \begin{aligned} f_1'(x, y, t, q_2) &= f_1(x, y, t) - f_2(x, y, t, q_2) \\ &= {}^{(2)}\nu_{11}x + {}^{(2)}\nu_{12}y + {}^{(2)}\nu_{13} = 0 \end{aligned} \tag{5.42a} $$

$$ \begin{aligned} f_3'(x, y, t, q_4) &= f_1(x, y, t) - f_4(x, y, t, q_4) \\ &= {}^{(2)}\nu_{21}x + {}^{(2)}\nu_{22}y + {}^{(2)}\nu_{23} = 0 \end{aligned} \tag{5.42b} $$

with the coefficients of the power products stored in two row vectors ${}^{(2)}\mathbf{b}_i$ of length

27, i.e.,

$$^{(2)}\nu_{ij} = \sum_{h=0}^{2}\sum_{k=0}^{2} {}^{(2)}b_{ir}\, t^{\,h} q_{i+2}^{k} \tag{5.43}$$

for $i = 1, 2$, $j = 1, 2, 3$, and $r = 9(j-1) + 3h + k + 1$. The term q_{i+2} is q_2, when $i = 1$, and q_4, when $i = 2$. Notice that the coefficients $^{(1)}\mathbf{b}_1 = {}^{(2)}\mathbf{b}_1$.

Solutions of $^{(2)}x$ and $^{(2)}y$ are obtained as follows:

$$^{(2)}x = \frac{^{(2)}\nu_{12}{}^{(2)}\nu_{23} - {}^{(2)}\nu_{22}{}^{(2)}\nu_{13}}{^{(2)}\nu_{11}{}^{(2)}\nu_{22} - {}^{(2)}\nu_{21}{}^{(2)}\nu_{12}} = \frac{^{(2)}num_x}{^{(2)}den} \tag{5.44a}$$

$$^{(2)}y = \frac{^{(2)}\nu_{21}{}^{(2)}\nu_{13} - {}^{(2)}\nu_{11}{}^{(2)}\nu_{23}}{^{(2)}\nu_{11}{}^{(2)}\nu_{22} - {}^{(2)}\nu_{21}{}^{(2)}\nu_{12}} = \frac{^{(2)}num_y}{^{(2)}den} \tag{5.44b}$$

The coefficients of the power products involving the numerators ($^{(2)}num_x$ and $^{(2)}num_y$) and the denominator ($^{(2)}den$) are collected in vectors of length 45: $^{(2)}\mathbf{n}_x$, $^{(2)}\mathbf{n}_y$ and $^{(2)}\mathbf{dt}$. The resulting solutions of $^{(2)}x$ and $^{(2)}y$ are substituted back into equation $f_1(^{(2)}x, {}^{(2)}y, t) = 0$. After clearing the denominator, the following equation results:

$$f_2''(t, q_2, q_4) = \sum_{h=0}^{10}\sum_{k=0}^{4}\sum_{l=0}^{4} {}^{(2)}c_r\, t^{\,h} q_2^k q_4^l = 0 \tag{5.45}$$

where $r = 25h + 5k + l + 1$ and all $^{(2)}c_r$ are stored in a vector $^{(2)}\mathbf{c}$ whose length is 275.

It is worthy of mention that the elimination of x and y was carried out in such a way that q_3 and q_4 were not contained in the same equation. This formulation simplifies further eliminations. Nevertheless, two sets of explicit solutions for x and y were generated and there will be some cases where $^{(1)}x \neq {}^{(2)}x$ and $^{(1)}y \neq {}^{(2)}y$. This is because of the quadratic nature of x and y in the loop-closure equations. In general, there are two solutions of x and y that satisfy $f_1(x, y, \phi) = 0$ and $f_2(x, y, \phi, \theta_{3_2}) = 0$. One solution satisfies $f_3(x, y, \phi, \theta_{3_3}) = 0$, but there is no restriction in the above formulation that the same solution has to satisfy $f_4(x, y, \phi, \theta_{3_4}) = 0$. If it did not,

the second solution of x and y would satisfy $f_4(x, y, \phi, \theta_{34}) = 0$. This situation will be addressed later when numerical values of x and y are computed.

***Step 3.*- Eliminating q_3 and q_4**

a) Eliminate variable q_3 by isolating it from equation $g_1(q_2, q_3) = 0$ and substituting it back into equation $f_1''(t, q_2, q_3) = 0$. This elimination is not simple because q_3 appears as a quadratic variable in $g_1(q_2, q_3) = 0$. To perform this elimination, it is important to write both equations $g_1(q_2, q_3) = 0$ and $f_1''(t, q_2, q_3) = 0$ in a simple form as single variable polynomials in q_3. The resulting simplified polynomials are defined as $g_1({}^{(1)}\eta, q_3) = 0$ and $f_1''({}^{(1)}\mu, q_3) = 0$, where ${}^{(1)}\eta$ and ${}^{(1)}\mu$ are sets of coefficients that are functions of q_2, and t and q_2, respectively. Thus,

$$g_1({}^{(1)}\eta, q_3) = {}^{(1)}\eta_0 q_3^2 + {}^{(1)}\eta_1 q_3 + {}^{(1)}\eta_2 = 0 \tag{5.46}$$

where ${}^{(1)}\eta_0 = {}^{(1)}a_2 q_2$, ${}^{(1)}\eta_1 = {}^{(1)}a_1 q_2^2 + {}^{(1)}a_3 q_2 + {}^{(1)}a_4$, and ${}^{(1)}\eta_2 = {}^{(1)}a_5 q_2$; and

$$f_1''({}^{(1)}\mu, q_3) = {}^{(1)}\mu_0 q_3^4 + {}^{(1)}\mu_1 q_3^3 + {}^{(1)}\mu_2 q_3^2 + {}^{(1)}\mu_3 q_3 + {}^{(1)}\mu_4 = 0 \tag{5.47}$$

where ${}^{(1)}\mu_s$ for $s = 4, ..., 0$ are multivariable polynomials in t (degree 10) and q_2 (degree 4), whose coefficients were previously stored in vector ${}^{(1)}\mathbf{c}$, and have the following structure

$${}^{(i)}\mu_s = \sum_{h=0}^{10} \sum_{k=0}^{4} {}^{(i)}c_r \, t^h q_2^k \tag{5.48}$$

where $r = 25h + 5k + s + 1$.

These simplified polynomials are a convenient set up for the elimination of q_3. If such simplification was not considered, an explosion of terms would have occurred. Next, q_3 is eliminated and ${}^{(1)}\eta$ and ${}^{(1)}\mu$ are considered as simple coefficients, after the elimination their polynomial structures will be restored.

A solution of q_3 is given as

$$q_3 = \frac{-{}^{(1)}\eta_1 \pm \sqrt{{}^{(1)}\eta_1^2 - 4\,{}^{(1)}\eta_0\,{}^{(1)}\eta_2}}{2\,{}^{(1)}\eta_0} = \frac{-{}^{(1)}\eta_1 + {}^{(1)}\lambda}{2\,{}^{(1)}\eta_0} \tag{5.49}$$

where ${}^{(1)}\lambda = \pm\sqrt{{}^{(1)}\eta_1^2 - 4\,{}^{(1)}\eta_0\,{}^{(1)}\eta_2}$.

Substitute Eq. (5.49) into Eq. (5.47) yielding an equation of the following form: $f_1^*({}^{(1)}\eta, {}^{(1)}\mu, {}^{(1)}\lambda) = 0$. The problem requires the elimination of the square root, ${}^{(1)}\lambda$, i.e., ${}^{(1)}\lambda$ must be squared. Let ${}^{(1)}\Lambda = {}^{(1)}\lambda^2 = {}^{(1)}\eta_1^2 - 4\,{}^{(1)}\eta_0\,{}^{(1)}\eta_2$. Therefore, equation $f_1^*({}^{(1)}\eta, {}^{(1)}\mu, {}^{(1)}\lambda) = 0$ may be written as follows:

$$\begin{aligned} f_1^*({}^{(1)}\eta, {}^{(1)}\mu, {}^{(1)}\lambda) &= {}^{(1)}\xi_0\,{}^{(1)}\lambda^4 + {}^{(1)}\xi_1\,{}^{(1)}\lambda^3 + {}^{(1)}\xi_2\,{}^{(1)}\lambda^2 + {}^{(1)}\xi_3\,{}^{(1)}\lambda + {}^{(1)}\xi_4 = 0 \\ &= {}^{(1)}\xi_0\,{}^{(1)}\Lambda^2 + {}^{(1)}\xi_1\,{}^{(1)}\Lambda\,{}^{(1)}\lambda + {}^{(1)}\xi_2\,{}^{(1)}\Lambda + {}^{(1)}\xi_3\,{}^{(1)}\lambda + {}^{(1)}\xi_4 = 0 \end{aligned} \tag{5.50}$$

where elements ${}^{(1)}\xi_k$ are a product combination of ${}^{(1)}\mu$ and ${}^{(1)}\eta$. Therefore,

$${}^{(1)}\xi_0\,{}^{(1)}\Lambda^2 + {}^{(1)}\xi_2\,{}^{(1)}\Lambda + {}^{(1)}\xi_4 = -\left({}^{(1)}\xi_1\,{}^{(1)}\Lambda + {}^{(1)}\xi_3\right){}^{(1)}\lambda \tag{5.51}$$

and squaring both sides yields

$$h_1({}^{(1)}\eta, {}^{(1)}\mu, {}^{(1)}\Lambda) = \left({}^{(1)}\xi_0\,{}^{(1)}\Lambda^2 + {}^{(1)}\xi_2\,{}^{(1)}\Lambda + {}^{(1)}\xi_4\right)^2 - \left({}^{(1)}\xi_1\,{}^{(1)}\Lambda + {}^{(1)}\xi_3\right)^2{}^{(1)}\Lambda = 0 \tag{5.52}$$

Substitute ${}^{(1)}\Lambda = {}^{(1)}\eta_1^2 - 4\,{}^{(1)}\eta_0\,{}^{(1)}\eta_2$, yielding

$$\begin{aligned} h_1({}^{(1)}\eta, {}^{(1)}\mu) = {}& {}^{(1)}\eta_2^{4(1)}\mu_0^2 + 2\,{}^{(1)}\eta_0^{2(1)}\eta_2^{2(1)}\mu_4\,{}^{(1)}\mu_0 - 2\,{}^{(1)}\eta_0\,{}^{(1)}\eta_2^{3(1)}\mu_2\,{}^{(1)}\mu_0 - {}^{(1)}\eta_1^{3(1)}\eta_2\,{}^{(1)}\mu_3\,{}^{(1)}\mu_0 \\ & -4\,{}^{(1)}\eta_0\,{}^{(1)}\eta_1^{2(1)}\eta_2\,{}^{(1)}\mu_4\,{}^{(1)}\mu_0 + {}^{(1)}\eta_1^{2(1)}\eta_2^{2(1)}\mu_2\,{}^{(1)}\mu_0 + 3\,{}^{(1)}\eta_0\,{}^{(1)}\eta_2^{2(1)}\eta_1\,{}^{(1)}\mu_3\,{}^{(1)}\mu_0 \\ & -2\,{}^{(1)}\eta_0^{3(1)}\eta_2\,{}^{(1)}\mu_4\,{}^{(1)}\mu_2 - {}^{(1)}\eta_0^{2(1)}\eta_1\,{}^{(1)}\eta_2\,{}^{(1)}\mu_3\,{}^{(1)}\mu_2 + 3\,{}^{(1)}\eta_0^{2(1)}\eta_1\,{}^{(1)}\eta_2\,{}^{(1)}\mu_1\,{}^{(1)}\mu_4 \\ & +{}^{(1)}\eta_0^{3(1)}\eta_2\,{}^{(1)}\mu_3^2 + {}^{(1)}\eta_0\,{}^{(1)}\eta_2^{3(1)}\mu_1^2 - {}^{(1)}\eta_2^{3(1)}\eta_1\,{}^{(1)}\mu_1\,{}^{(1)}\mu_0 - {}^{(1)}\eta_0\,{}^{(1)}\eta_1^{3(1)}\mu_1\,{}^{(1)}\mu_4 \\ & +{}^{(1)}\eta_0^{2(1)}\eta_1^{2(1)}\mu_2\,{}^{(1)}\mu_4 - {}^{(1)}\eta_0^{3(1)}\eta_1\,{}^{(1)}\mu_3\,{}^{(1)}\mu_4 + {}^{(1)}\eta_0^{2(1)}\eta_2^{2(1)}\mu_2^2 + {}^{(1)}\eta_1^{4(1)}\mu_4\,{}^{(1)}\mu_0 \\ & -2\,{}^{(1)}\eta_0^{2(1)}\eta_2^{2(1)}\mu_1\,{}^{(1)}\mu_3 + {}^{(1)}\eta_0\,{}^{(1)}\eta_1^{2(1)}\eta_2\,{}^{(1)}\mu_3\,{}^{(1)}\mu_1 - {}^{(1)}\eta_0\,{}^{(1)}\eta_1\,{}^{(1)}\eta_2^{2(1)}\mu_1\,{}^{(1)}\mu_2 \\ & +{}^{(1)}\eta_0^{4(1)}\mu_4^2 = 0 \end{aligned} \tag{5.53}$$

It is worth to mention that the resulting equation can be simplified by $256\eta_1^4$, a common factor among the resulting 22 terms of $h_1({}^{(1)}\eta, {}^{(1)}\mu) = 0$. Each term of $h_1({}^{(1)}\eta, {}^{(1)}\mu) = 0$ appears as a quartic expression in ${}^{(1)}\eta$, which are functions of q_2 (degree 2) as shown in Eq. (5.46), and a quadratic in ${}^{(1)}\mu$, which are polynomials in t (degree 10) and q_2 (degree 4) as shown in Eq. (5.48). If the polynomials of ${}^{(1)}\mu_i$ were substituted into Eq. (5.53), a bulky equation would result. As an alternative, each product ${}^{(1)}v_I = {}^{(1)}\mu_i {}^{(1)}\mu_{i'}$ (for $I = 1, ..., 15$; $i = 0, ..., 4$; and $i' = i, .., 4$) that appears in the terms of Eq. (5.53) are multiplied and the coefficients are collected.

$$ {}^{(1)}v_I = \sum_{h=0}^{20}\sum_{k=0}^{8} {}^{(1)}d_{I_r}\, t^h q_2^k; \qquad \text{for } I = 1, ..., 15 \tag{5.54} $$

where $r = 9h+k+1$. The coefficients are stored in a matrix ${}^{(1)}\mathbf{D}$ of size 189×15, i.e., ${}^{(1)}\mathbf{D} = [\ {}^{(1)}\mathbf{d}_1 \ \ {}^{(1)}\mathbf{d}_2 \ \ \cdots \ \ {}^{(1)}\mathbf{d}_{15}\ ]$, with ${}^{(1)}\mathbf{d}_I = [\ {}^{(1)}d_{I_1} \ \ {}^{(1)}d_{I_2} \ \ \cdots \ \ {}^{(1)}d_{I_{189}}\ ]^{\mathrm{T}}$. This substitution reduces considerably computation time. The new elements ${}^{(1)}v_I$ are substituted into Eq. (5.53) yielding

$$ \begin{aligned} h_1({}^{(1)}\eta, {}^{(1)}v) \;=\; & {}^{(1)}\eta_2^{4(1)}v_1 - {}^{(1)}\eta_2^{3(1)}\eta_1 {}^{(1)}v_2 + {}^{(1)}\eta_1^{2(1)}\eta_2^{2(1)}v_3 - 2^{(1)}\eta_0 {}^{(1)}\eta_2^{3(1)}v_3 - {}^{(1)}\eta_1^{3(1)}\eta_2 {}^{(1)}v_4 \\ & +3^{(1)}\eta_0 {}^{(1)}\eta_2^{2(1)}\eta_1 {}^{(1)}v_4 + 2^{(1)}\eta_0^{2(1)}\eta_2^{2(1)}v_5 - 4^{(1)}\eta_0 {}^{(1)}\eta_1^{2(1)}\eta_2 {}^{(1)}v_5 + {}^{(1)}\eta_1^{4(1)}v_5 \\ & +{}^{(1)}\eta_0 {}^{(1)}\eta_2^{3(1)}v_6 - {}^{(1)}\eta_0 {}^{(1)}\eta_1 {}^{(1)}\eta_2^{2(1)}v_7 - 2^{(1)}\eta_0^{2(1)}\eta_2^{2(1)}v_8 + {}^{(1)}\eta_0 {}^{(1)}\eta_1^{2(1)}\eta_2 {}^{(1)}v_8 \\ & +3^{(1)}\eta_0^{2(1)}\eta_1 {}^{(1)}\eta_2 {}^{(1)}v_9 - {}^{(1)}\eta_0 {}^{(1)}\eta_1^{3(1)}v_9 + {}^{(1)}\eta_0^{2(1)}\eta_2^{2(1)}v_{10} - {}^{(1)}\eta_0^{2(1)}\eta_1 {}^{(1)}\eta_2 {}^{(1)}v_{11} \\ & +{}^{(1)}\eta_0^{2(1)}\eta_1^{2(1)}v_{12} - 2^{(1)}\eta_0^{3(1)}\eta_2 {}^{(1)}v_{12} + {}^{(1)}\eta_0^{3(1)}\eta_2 {}^{(1)}v_{13} - {}^{(1)}\eta_0^{3(1)}\eta_1 {}^{(1)}v_{14} \\ & +{}^{(1)}\eta_0^{4(1)}v_{15} \;= 0 \end{aligned} \tag{5.55} $$

Finally, the corresponding values of ${}^{(1)}\eta_j$, Eq. (5.46), and ${}^{(1)}v_I$, Eq. (5.54), are substituted into $h_1({}^{(1)}\eta, {}^{(1)}v) = 0$ yielding

$$ h_1(t, q_2) = \sum_{h=0}^{20}\sum_{k=0}^{16} {}^{(1)}e_r\, t^h q_2^k = 0 \tag{5.56} $$

where $r = 17h + k + 1$. The coefficients are stored in vector ${}^{(1)}\mathbf{e}$ of length 357.

b) In a similar way, q_4 is eliminated with equations $f_2''(t, q_2, q_4) = 0$ and $g_2(q_2, q_4) = 0$, i.e.,

$$f_2''(t, q_2, q_4) = {}^{(2)}\mu_0 q_4^4 + {}^{(2)}\mu_1 q_4^3 + {}^{(2)}\mu_2 q_4^2 + {}^{(2)}\mu_3 q_4 + {}^{(2)}\mu_4 = 0 \tag{5.57}$$

$$g_2(q_2, q_4) = {}^{(2)}\eta_0 q_4^2 + {}^{(2)}\eta_1 q_4 + {}^{(2)}\eta_2 = 0 \tag{5.58}$$

Thus, q_4, which appears as a quadratic term in $g_2(q_2, q_4) = 0$, is solved from

$$q_4 = \frac{-{}^{(2)}\eta_1 \pm \sqrt{{}^{(2)}\eta_1^2 - 4\,{}^{(2)}\eta_0\,{}^{(2)}\eta_2}}{2\,{}^{(2)}\eta_0} = \frac{-{}^{(2)}\eta_1 + {}^{(2)}\lambda}{2\,{}^{(2)}\eta_0} \tag{5.59}$$

Then, q_4 is substituted into $f_2''(t, q_2, q_4) = 0$ and the square root term, ${}^{(2)}\lambda$, is eliminated using the method described above, i.e., squaring ${}^{(2)}\lambda$ and substituting ${}^{(2)}\lambda^2 = {}^{(2)}\eta_1^2 - 4\,{}^{(2)}\eta_0\,{}^{(2)}\eta_2$. The resulting equation, $h_2({}^{(2)}\eta, {}^{(2)}\mu) = 0$, is then simplified by collecting the coefficients of the terms ${}^{(2)}\upsilon_I = {}^{(2)}\mu_i\,{}^{(2)}\mu_{i'}$ in a matrix ${}^{(2)}\mathbf{D}$, i.e.,

$${}^{(2)}\upsilon_I = \sum_{h=0}^{20} \sum_{k=0}^{8} {}^{(2)}d_{I_r}\, t^h q_2^k; \qquad \text{for } I = 1, ..., 15 \tag{5.60}$$

where $r = 9h + k + 1$ and the coefficients are stored in a matrix ${}^{(2)}\mathbf{D}$ of size 189×15, i.e., ${}^{(2)}\mathbf{D} = [\ {}^{(2)}\mathbf{d}_1 \quad {}^{(2)}\mathbf{d}_2 \quad \cdots \quad {}^{(2)}\mathbf{d}_{15}\ ]$, with ${}^{(2)}\mathbf{d}_I = [\ {}^{(2)}d_{I_1} \quad {}^{(2)}d_{I_2} \quad \cdots \quad {}^{(2)}d_{I_{189}}\ ]^{\mathrm{T}}$.

Finally, the corresponding values of ${}^{(2)}\eta_j$, Eq. (5.58), and ${}^{(2)}\upsilon_I$, Eq. (5.60), are substituted into $h_2({}^{(2)}\eta, {}^{(2)}\mu) = 0$ yielding

$$h_2(t, q_2) = \sum_{h=0}^{20} \sum_{k=0}^{16} {}^{(2)}e_r\, t^h q_2^k = 0 \tag{5.61}$$

where $r = 17h + k + 1$. The coefficients are stored in vector ${}^{(2)}\mathbf{e}$ of length 357.

***Step 4*.- Generating More Equations**

Assemble a 2×17 matrix $[\Psi']$ by sorting the powers of q_2. This matrix is generated with equations $h_1(t,\, q_2) = 0$ and $h_2(t,\, q_2) = 0$, and its entries, $\psi_{i,j}$, are 20^{th}-order polynomials in t.

$$[\Psi']\ \mathbf{q}_2' = \begin{bmatrix} \psi_{1,1} & \psi_{1,2} & \cdots & \psi_{1,17} \\ \psi_{2,1} & \psi_{2,2} & \cdots & \psi_{2,17} \end{bmatrix} \begin{bmatrix} q_2^{16} \\ q_2^{15} \\ \vdots \\ q_2 \\ 1 \end{bmatrix} = \bar{\mathbf{0}} \tag{5.62}$$

Generate more equations, such that the number of equations matches the number of power products. Equations $h_1(t,\, q_2) = 0$ and $h_2(t,\, q_2) = 0$ are multiplied by q_2, q_2^2, ..., q_2^{14}, and q_2^{15}. This leads to a 32×32 matrix $[\Psi]$ whose entries are 20^{th}-order polynomials in t.

$$[\Psi]\ \mathbf{q}_2 = \bar{\mathbf{0}}$$

$$\begin{bmatrix} \psi_{1,1} & \psi_{1,2} & \cdots & \psi_{1,16} & \psi_{1,17} & 0 & \cdots & \cdots & 0 \\ \psi_{2,1} & \psi_{2,2} & \cdots & \psi_{2,16} & \psi_{2,17} & 0 & \cdots & \cdots & 0 \\ 0 & \psi_{1,1} & \psi_{1,2} & \cdots & \psi_{1,16} & \psi_{1,17} & 0 & \cdots & 0 \\ 0 & \psi_{2,1} & \psi_{2,2} & \cdots & \psi_{2,16} & \psi_{2,17} & 0 & \cdots & 0 \\ \vdots & 0 & \ddots & \ddots & \ddots & \ddots & \ddots & 0 & \vdots \\ 0 & \cdots & 0 & \psi_{1,1} & \psi_{1,2} & \cdots & \psi_{1,16} & \psi_{1,17} & 0 \\ 0 & \cdots & 0 & \psi_{2,1} & \psi_{2,2} & \cdots & \psi_{2,16} & \psi_{2,17} & 0 \\ 0 & \cdots & \cdots & 0 & \psi_{1,1} & \psi_{1,2} & \cdots & \psi_{1,16} & \psi_{1,17} \\ 0 & \cdots & \cdots & 0 & \psi_{2,1} & \psi_{2,2} & \cdots & \psi_{2,16} & \psi_{2,17} \end{bmatrix} \begin{bmatrix} q_2^{31} \\ q_2^{30} \\ q_2^{29} \\ \vdots \\ q_2^3 \\ q_2^2 \\ q_2 \\ 1 \end{bmatrix} = \bar{\mathbf{0}} \tag{5.63}$$

***Step 5*.- Solving for t**

A solution to this problem is solving $|[\Psi]| = 0$, but taking the determinant of such a complicated matrix, where every non-zero element is a 20^{th}-order polynomial in t, is not possible. As previously discussed for the 4-PRR manipulator, the eigenvalue problem should lead to better results.

Matrix $[\Psi]$ can be written as a matrix polynomial, i.e.,

$$[\Psi](t) = \sum_{i=0}^{20} [\Psi_i] t^i \tag{5.64}$$

where each entry of $[\Psi_i]$ corresponds to one of the coefficients ${}^{(1)}\mathbf{e}$ and ${}^{(2)}\mathbf{e}$ found in Eqs. (5.56 and 5.61).

The idea of this method is to assemble a 640×640 matrix $[\mathbf{K}]$ in the following form:

$$[\mathbf{K}] = \begin{bmatrix} \mathbf{0} & \mathbf{I} & \mathbf{0} & \cdots & \mathbf{0} \\ \mathbf{0} & \mathbf{0} & \mathbf{I} & \cdots & \mathbf{0} \\ \vdots & \vdots & \vdots & \ddots & \vdots \\ \mathbf{0} & \mathbf{0} & \mathbf{0} & \cdots & \mathbf{I} \\ -[\Psi_{20}]^{-1}[\Psi_0] & -[\Psi_{20}]^{-1}[\Psi_1] & -[\Psi_{20}]^{-1}[\Psi_2] & \cdots & -[\Psi_{20}]^{-1}[\Psi_{19}] \end{bmatrix} \tag{5.65}$$

where $\mathbf{0}$ and $\mathbf{I}$ are 32×32 null and identity matrices, respectively.

Matrix $[\mathbf{K}]$ is employed to formulate the standard eigenvalue problem as follows:

$$[\mathbf{K}]\,\mathbf{Q}_2 = \lambda \mathbf{Q}_2 \tag{5.66}$$

where λ is an eigenvalue and $\mathbf{Q}_2$ is the associated eigenvector with λ of the form $\mathbf{Q}_2 = [\ \mathbf{q}_2 \quad \mathbf{q}_2\lambda \quad \cdots \quad \mathbf{q}_2\lambda^{19}\ ]^{\mathrm{T}}$.

The eigenvalues of matrix $[\mathbf{K}]$ correspond precisely to the roots of the 640^{th}-order polynomial, i.e., $\lambda \equiv t$ for a given value of θ_{3_1}. A proof of this is shown in Appendix E.

Nonetheless, this method works if and only if matrix $[\Psi_{20}]$ is well-conditioned. In the implementation, different values of the design parameters (link lengths, arrangement of the bases, etc.) were considered but matrix $[\Psi_{20}]$ turned out to be always ill-conditioned. As an attempt to improve the condition of matrix $[\Psi_{20}]$, Singular Value Decomposition (SVD) was considered, $\mathbf{A} = \mathbf{U}\Sigma\mathbf{V}^{\mathrm{T}}$, (Golub and Van Loan, 1983). That is, SVD was implemented in matrices that contain the coefficients of polynomial systems of equations, i.e., starting with the original six equations, then with the resulting four equations after eliminating x and y, and finally with the remaining two equations $h_1(t, q_2) = 0$ and $h_2(t, q_2) = 0$. The idea was to verify the singular values of these matrices, and whenever a singular value was less than a predefined threshold, the singular value was set to zero. Finally, the elements of the matrices were computed as follows:

$$a_{ij} = \sum_{k=1}^{2} \sigma_k \, u_{ik} \, v_{jk} \tag{5.67}$$

In general, this small perturbation improves significantly the accuracy of further computations, in particular the elimination of potential catastrophic cancellation problems (Golub and Van Loan, 1983). Nevertheless, all considered matrices turned out to be well-conditioned. The problem arises when matrix $[\Psi]$ is separated in numerical matrices with Eq. (5.64) and the resulting $[\Psi_{20}]$ is always ill-conditioned.

As an alternative, the generalized eigenvalue problem, which is described in Appendix E.3.2, can be implemented as follows:

$$\lambda \, [\mathbf{K}_1] \, \mathbf{Q}_2 = [\mathbf{K}_2] \, \mathbf{Q}_2 \tag{5.68}$$

where λ is an eigenvalue which represents a solution of t, $\mathbf{Q}_2$ is the associated eigenvector with λ of the form $\mathbf{Q}_2 = [\ \mathbf{q}_2 \quad \mathbf{q}_2\lambda \quad \mathbf{q}_2\lambda^2 \quad \cdots \quad \mathbf{q}_2\lambda^{19}\ ]^{\mathrm{T}}$, and matrices $[\mathbf{K}_1]$

and $[\mathbf{K}_2]$ are defined as

$$[\mathbf{K}_1] = \begin{bmatrix} \mathbf{I} & \mathbf{0} & \cdots & \mathbf{0} & \mathbf{0} \\ \mathbf{0} & \mathbf{I} & \cdots & \mathbf{0} & \mathbf{0} \\ \vdots & \vdots & \ddots & \vdots & \vdots \\ \mathbf{0} & \mathbf{0} & \cdots & \mathbf{I} & \mathbf{0} \\ \mathbf{0} & \mathbf{0} & \cdots & \mathbf{0} & [\Psi_{20}] \end{bmatrix} \qquad [\mathbf{K}_2] = \begin{bmatrix} \mathbf{0} & \mathbf{I} & \mathbf{0} & \cdots & \mathbf{0} \\ \mathbf{0} & \mathbf{0} & \mathbf{I} & \cdots & \mathbf{0} \\ \vdots & \vdots & \ddots & \ddots & \vdots \\ \mathbf{0} & \mathbf{0} & \mathbf{0} & \cdots & \mathbf{I} \\ -[\Psi_0] & -[\Psi_1] & -[\Psi_2] & \cdots & -[\Psi_{19}] \end{bmatrix}$$

where $\mathbf{0}$ and $\mathbf{I}$ are 32×32 null and identity matrices, respectively.

The generalized eigenvalue problem, based on QZ factorization, determines all 640 eigenvalues. These eigenvalues can be either real or complex. The number of real eigenvalues represents a potential number of force-unconstrained poses for every assumed θ_{31} angle. The correct number of real eigenvalues, as well as, their accuracy depend on the precision of the numerical matrices $[\Psi_i]$, which have been significantly affected by a large number of computations. It was noticed that a very important element that allows matrices $[\Psi_i]$ to be numerically reliable is the scaling of the design parameters. The dimensions of the manipulator play a very important roll on the number and accuracy of the real eigenvalues. For instance, both large numbers (greater than one) or small numbers (less than 0.1) yielded incoherent results, while values within this range provided fairly accurate results. This is because, by setting the design parameters around this range, the coefficients of every term in the equations turn out to be similar. This assumption reduces relative errors due to the cancellation of significant digits relevant to the solutions. The inaccuracy increases when an affected solution is multiplied by large numbers.

In order to check a reliable scale of manipulator dimensions, which would provide the correct number and accuracy of the real eigenvalues, the aid of a graphical

representation of equations $h_1(t, q_2) = 0$ and $h_2(t, q_2) = 0$ was considered. The coefficients of these equations, ${}^{(1)}\mathbf{e}$ and ${}^{(2)}\mathbf{e}$, which have been previously determined in Eqs. (5.56 and 5.61), have been slightly perturbed through computations. Thus, the solutions of t and q_2 that satisfy these equations might be considered as an approximation of the solutions that satisfy the original problem of six equations in six unknowns. The graphical representation was carried out with a sequence of assumed values of one variable, say t. The roots of the second variable, q_2, were computed yielding two highly non-linear curves. The number of intersections between these curves represent the number of solutions of the polynomial system, i.e., the number of real eigenvalues.

For large manipulator dimensions, the number of real eigenvalues was less than the number of intersections. The number of solutions did not match because of the perturbed elements of matrices $[\Psi_i]$ which were extremely large yielding larger errors in the factorization. For small manipulator dimensions, the number of real eigenvalues was greater than the number of intersections. Nevertheless, the accuracy of the eigenvalues was very poor. The elements of matrices $[\Psi_i]$ were so small that for almost any eigenvalue λ the generalized eigenvalue problem of Eq. (5.68) was likely to converge.

In particular, the analysis was performed for a manipulator whose design parameters are as follows: both the fixed and the mobile platforms are squares, with the fixed platform being two-and-a-half times larger than the mobile platform, and all the links have the same dimensions as the sides of the mobile platform. These ratios happen to be the ones of the Reconfigurable Planar Parallel Manipulator (RPPM), shown in Figure 1.1. To determine an optimum scale of the sides of both platforms, several tests were performed for different values of θ_{31}. It was found that a very

reliable scale is when the side of the fixed platform equals 0.5 and consequentially the side of the mobile platform equals 0.2. To check the accuracy of the eigenvalues, another test was performed. The resulting eigenvalues were compared to solutions of t found using optimization methods, and the maximum relative error among the eigenvalues was less than 0.15 %. Other manipulator dimensions gave a much larger relative error.

***Step 6*.- Back-Substitution**

In spite of the fairly good accuracy of the eigenvalues, the associated eigenvectors turned out to be more sensitive to the compounded numerical errors. Therefore, solutions for q_2 could not be extracted from the eigenvectors $\mathbf{Q}_2$ of Eq. (5.68). For instance, the maximum relative error for the solutions of q_2 was over 3 %. Another way to solve for q_2 is with Eq. (5.63). For a given solution of t, matrix $[\Psi]$ can be evaluated numerically. Thus, a problem of the form $\mathbf{Ax} = \mathbf{b}$ results, where $\mathbf{A}$ contains any 31 rows and the first 31 columns of matrix $[\Psi]$, and $\mathbf{b}$ is formed with the negative of the 31 elements of the last column associated with the chosen rows. Nevertheless, every matrix $\mathbf{A}$ turned out to be ill-conditioned and Gauss elimination could not be performed. As an alternative, a given solution of t is substituted in equations $h_1(t, q_2) = 0$ and $h_2(t, q_2) = 0$ yielding two 16^{th}-order polynomials in q_2, i.e., $h_1'(q_2) = 0$ and $h_2'(q_2) = 0$. Thus, the solution of q_2 for a given t occurs when there is a repeated root in $h_1'(q_2) = 0$ and $h_2'(q_2) = 0$. Although, this approach is not computationally efficient a fairly decent solution of q_2 results. The maximum relative error for the solutions of q_2 was less than 1 %.

Solutions for q_3 and q_4 are determined with Eqs. (5.49 and 5.59), respectively. Two solutions for each variable exist. The solutions of q_3 and q_4 that better evaluate

equations $f_1''(t, q_2, q_3) = \epsilon$ and $f_2''(t, q_2, q_4) = \epsilon$ are captured, where $\epsilon \approx 0$. In general, there is a set of solutions of q_3 and q_4 that leads to $\epsilon < 10^{-3}$, while the other set of solutions leads to a considerably larger ϵ.

The obtained set of solutions, t, q_2, q_3 and q_4, are slightly inaccurate due to the compounded numerical errors. In order to improve the values of this set of solutions an optimization algorithm, such as MATLAB's function `fminsearch` (2001), is used. Let the objective function be the Euclidean norm of the four equations involving t, q_2, q_3 and q_4, i.e.,

$$f(t, q_2, q_3, q_4) = \left(g_1(q_2, q_3)^2 + g_2(q_2, q_4)^2 + f_1''(t, q_2, q_3)^2 + f_2''(t, q_2, q_4)^2\right)^{\frac{1}{2}} \tag{5.69}$$

yielding an unconstrained minimization problem of the form:

$$\min_{\varrho} f(\varrho) \tag{5.70}$$

where $\varrho = [t, q_2, q_3, q_4]$.

By assuming the starting point of ϱ as the obtained values of t, q_2, q_3 and q_4, the minimization problem converges quickly to zero after few iterations. Improving a set of solutions using optimization techniques has been applied in robotics. Manocha and Canny (1994) proposed using Newton-Raphson iterations to improve the accuracy of the solutions of the inverse kinematics of a general six revolute-jointed manipulator. The optimized solutions improve significantly towards the target solutions, although the coefficients of equations $f_1''(t, q_2, q_3) = 0$ and $f_2''(t, q_2, q_4) = 0$ are still a little bit perturbed.

The optimized values of t, q_2, q_3 and q_4 are then substituted into Eqs. (5.39a and 5.39b) and ${}^{(1)}x$ and ${}^{(1)}y$ are computed. Similarly, the optimized values are substituted into Eqs. (5.44a and 5.44b) and ${}^{(2)}x$ and ${}^{(2)}y$ are evaluated. As mentioned before, due

to the structure of the elimination technique, there are some cases where ${}^{(1)}x \neq {}^{(2)}x$ and ${}^{(1)}y \neq {}^{(2)}y$. Thus, a comparison of the x and y values is carried out and whenever the values are distinct, the solutions are filtered out.

Finally, a second optimization technique is performed using the original six equations. Each set of solutions is used as a starting point. The algorithm converges quickly to zero. This optimization ensures the accuracy of the solutions because the coefficients of the equations have no numerical problems and the starting point is very close to the target solution. The collinearity exception is verified by computing $det([\mathbf{W}_3])$, if $det([\mathbf{W}_3]) \neq 0$ the set of solutions is filtered out.

Example.

The force unconstrained poses of a 4-$\underline{\text{R}}$RR manipulator with the following characteristics is presented: Both the fixed and mobile platforms are squares, whose sides are 0.5 m and 0.2 m, respectively. The link lengths are $\rho_i = 0.2\ m$, for $i = 1, \ldots, 8$. In Figure 5.9, the force-unconstrained poses of the centre of the platform are presented. All 16 solutions of the inverse kinematics are considered in the plots. Figure 5.9a illustrates the loci of the single order of force-unconstrained poses in the $x-y-\phi$ space. Figure 5.9b is a projection of the curves in the xy plane. Figure 5.9c is a projection of the curves in the $x-\phi$ plane. Due to the symmetry of the manipulator design, this projection is identical to the projection in the $y-\phi$ plane.

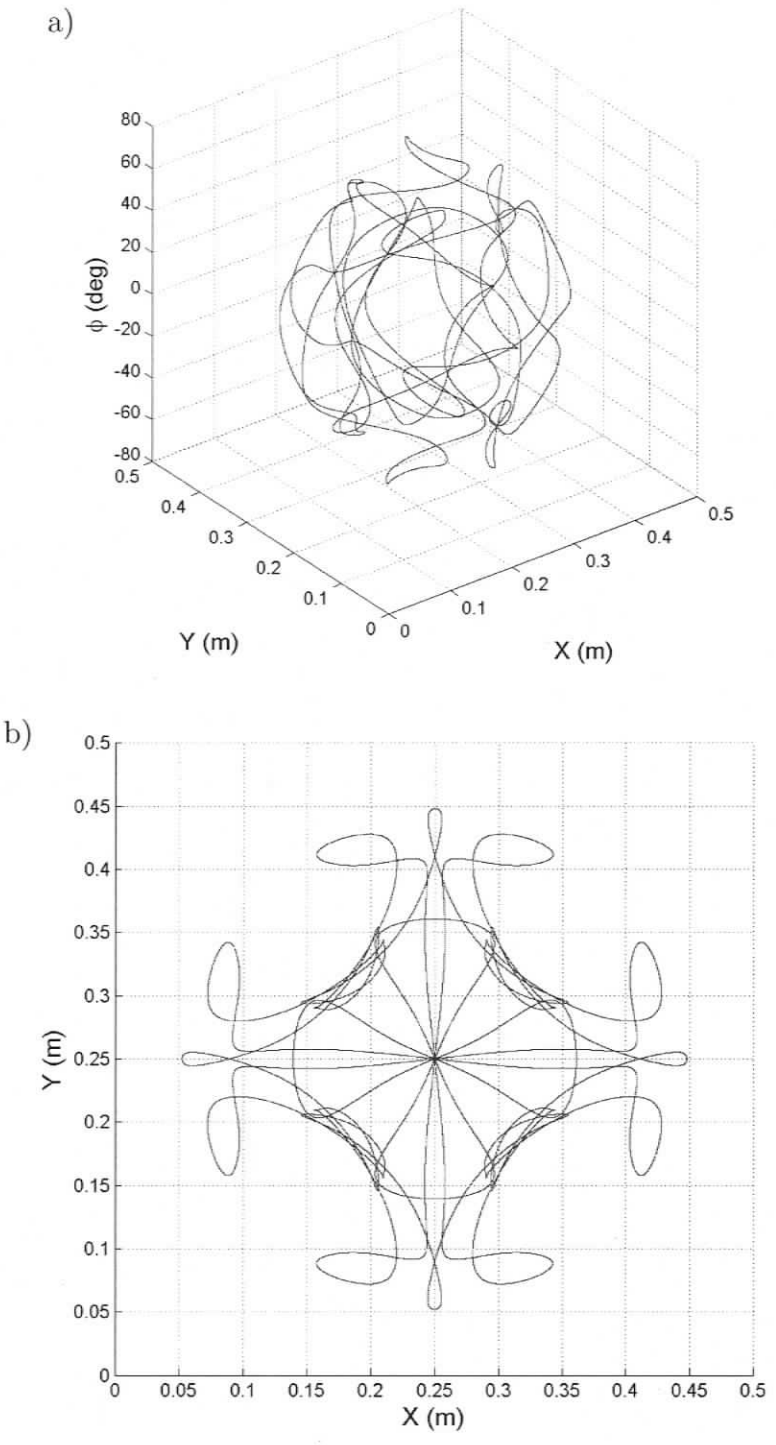

Figure 5.9: Force-Uncostrained Poses of the 4-RRR Manipulator.

c)

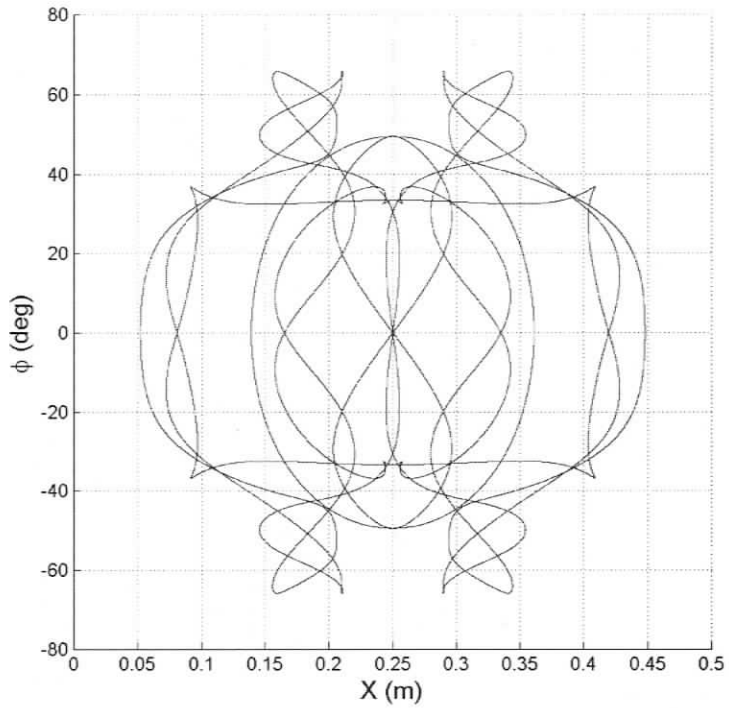

Figure 5.9 (cont'd): Force-Uncostrained Poses of the 4-RRR Manipulator.

It was noticed that some expected force-unconstrained poses were not obtained numerically. This occurred when the associated reciprocal screws intersect at or near infinity. A small variation of θ_{31} would lead to a rapid change of the intersection point (planar pencil). On these segments of the curves, finer intervals of θ_{31} allows finding more poses; however, numerical errors turned out to be larger, yielding no real solutions. This problem was fixed by interpolating among the obtained solutions and applying the optimization algorithm to ensure their accuracy.

As a result, four closed loops, all included in Figure 5.9, represent the force-unconstrained poses of this 4-RRR design.

5.6 Discussion

In this chapter, force-unconstrained poses of the 4-R$\underline{\text{P}}$R, 4-$\underline{\text{P}}$RR, and 4-$\underline{\text{R}}$RR manipulators were presented. The proposed solution is based on decoupling the redundant manipulators in four non-redundant mechanisms. The redundant manipulator is force unconstrained when the associated reciprocal screw matrices (sub-matrices of the redundant manipulator) of all four non-redundant manipulators are singular. Nevertheless, a dependency among the determinants of the sub-matrices was noticed. The number of non-linearly dependent determinants required to compute the force-unconstrained poses of a parallel manipulator with additional actuated branches is augmented by one for each additional branch added. For example, with the inclusion of one additional branch, two determinants are linearly independent. However, there are two exceptions: two associated reciprocal screws collinear and two passive joints coincident. These exceptions can be treated numerically by checking the condition of the remaining sub-matrices.

It was found that with the alternative approach, i.e., $det([\mathbf{W}]\,[\mathbf{W}]^{\mathrm{T}}) = 0$, a very large expression resulted. This yielded five equations in seven variables. However, two assigned variables would not generally solve the system of equations because a one-dimensional manifold was expected. This implies that the determinant required further factorization. Also with this approach, the *RPM* singularities of the 4-R$\underline{\text{P}}$R manipulator were not eliminated despite of having a non-singular sub-matrix. Therefore, the approach of analyzing all the sub-matrices turned out to be more effective.

The sub-matrix analysis led to polynomial systems of equations. Two elimination methods were employed to solve the polynomial systems: Gröbner bases and dialytic elimination. The first one is based on ordering the power products of the multivari-

able polynomials and creating new equations without generating superfluous power products. Nevertheless, when the system of non-linear equations is more complicated, the computation time tends to increase substantially, and algebraic software (such as Maple and Mathematica) are unable to compute the ideals. The second method is based on linearizing power products; i.e., the number of equations must match the number of power products of the polynomial system.

For the 4-R$\underline{P}$R manipulator, the time-derivative method was employed. Two quadratic polynomials resulted from the determinants of the Jacobian sub-matrices. Gröbner bases were used to solve the polynomial system of equations. The force-unconstrained poses of the 4-R$\underline{P}$R manipulator are represented by a quartic polynomial.

For the 4-$\underline{P}$RR manipulator, an elimination technique based on dialytic elimination was implemented. The method yielded an 8×8 matrix $[\Psi]$ that contains single-variable polynomials of degree 8 in each non-zero element. The determinant of $[\Psi]$ would lead to a 64^{th}-order polynomial. The computation of the roots of such a large polynomial may be susceptible to having floating point arithmetic problems. In addition, the computation of the coefficients of the resulting polynomial is required. As an alternative, the roots of this polynomial were found by formulating the problem as a standard eigenvalue problem, i.e., $[\mathbf{K}]\,\mathbf{T} = \lambda\mathbf{T}$, where matrix $[\mathbf{K}]$ is a 64×64 coefficient matrix and is formulated by expanding matrix $[\Psi]$ as a matrix polynomial. The eigenvalues of $[\mathbf{K}]$ correspond precisely to the roots of the mentioned 64^{th}-order polynomial. The eigenvalue problem reduces computation time considerably and makes the problem much more stable. However, it is prone to having erroneous solutions due to defective eigenvalues. The defective eigenvalues of a matrix are caused by repeated roots of the characteristic polynomial, i.e., the solution has a multiplicity

greater than one. Distinct eigenvalues yield linearly independent eigenvectors. Repeated eigenvalues lead to the same eigenvector and to complete the basis generalized eigenvectors are required. Thus, a matrix is defective when it has fewer linearly independent eigenvectors than eigenvalues. Golub and Van Loan (1983) remarked that defective or nearly defective matrices are not numerically stable. For instance, small changes in the nearly defective matrix can radically alter its Jordan form and it can also have a poorly conditioned matrix of eigenvectors in the eigenvalue problem. It was noticed that these eigenvalues came out as two identical real numbers (multiplicity of two) but did not correspond to any solution of the problem. As a result, these defective roots were filtered. The force-unconstrained poses of the 4-PRR manipulator are represented by a 64^{th}-order polynomial.

For the 4-RRR manipulator, a combination of both dialytic elimination and the elimination technique used by Gosselin and Merlet (1994) to solve the direct kinematics of planar parallel manipulators were implemented. The method led to a 32×32 matrix $[\Psi]$ that contains single-variable polynomials of degree 20 in each non-zero element. The determinant of $[\Psi]$ would yield a 640^{th}-order polynomial and its roots could be obtained by finding the eigenvalues of a 640×640 coefficient matrix, $[\mathbf{K}]$, as proposed for the 4-PRR manipulator. Nevertheless, matrix $[\mathbf{K}]$ requires the inversion of a matrix which turned out to be always ill-conditioned. As an alternative the problem was solved as a generalized eigenvalue problem, i.e., $\lambda\,[\mathbf{K}_1]\,\mathbf{Q}_2 = [\mathbf{K}_2]\,\mathbf{Q}_2$. Due to the large number of computations that were required to find the coefficients of matrices $[\mathbf{K}_1]$ and $[\mathbf{K}_2]$, the real eigenvalues were not fully accurate. In the back substitution process, two stages of optimization algorithms were employed to approximate the results to the precise solutions. In conclusion, a 640^{th}-order polynomial describes the singularity loci of the 4-RRR manipulator.

It is important to mention that the lengths of the links and the distance between bases must be scaled before solving these problems numerically. Both large and small dimensions may cause significant numerical errors.

Chapter 6

Conclusions and Recommendations for Future Work

6.1 Overview

Conclusions describing the overall accomplishments of this dissertation are presented. This is followed by the conclusions regarding to every chapter. In addition, recommendations for future work will be addressed.

6.2 Conclusions

Overall

Parallel manipulators may reach some configurations where the forces exerted by the actuators cannot sustain an arbitrary force acting on the mobile platform, i.e., the manipulator becomes force unconstrained. As a result, the manipulator gains one or more degree(s) of freedom of motion that are uncontrollable. Therefore, it is

important to avoid these configurations. The main objectives of this dissertation are the identification of all the poses (positions and orientations) of the mobile platform in which the manipulator is force unconstrained and the potential elimination of these poses by means of including redundant actuation.

The identification of force-unconstrained poses is often referred to in the literature as identifying the singularity loci of parallel manipulators, as a reference to an existing singular matrix. In this dissertation, this analysis is carried out for several actuation layouts. The considered problems are solved analytically allowing the force-unconstrained poses to be plotted in a three-dimensional space defined by the task space variables of the manipulator. These plots represent manifolds of singularities. Based on the analytical nature of this formulation, it is possible to modify some parameters of the manipulator and compare the singularity loci among different manipulator designs. Thus, the proposed analysis may be useful to determine the optimum design of a planar parallel manipulator. Whereas a numerical formulation, as often considered in the literature, would limit the analysis to a specific pose and design of the manipulator. For non-redundant manipulators an efficient technique, based upon having joint displacements as known values, is presented.

Two studies of actuation redundancy were considered: in-branch redundancy and additional actuated branches. In both studies, the force-unconstrained poses were reduced by one order of infinity ($O(\infty)$). This is, for non-redundant manipulators a two-dimensional manifold of singularities (surfaces) exists; while with the inclusion of redundancy, it is shown that the singularities are reduced to a one-dimensional manifold (curves). The in-branch redundancy case offers the same workspace of the corresponding non-redundant manipulator; however, the addition of an actuator within the mobile linkage implies an increment of inertia. The inclusion of additional

actuated branches may reduce the workspace of the manipulator; however, it would be possible to actuate all the joints attached to the fixed platform maintaining the inertia of the manipulator to a minimum. Small inertia of the mobile linkage allows the manipulator to be considered for high speed applications.

Next, conclusions for each chapter will be presented.

Chapter 2: Analysis of Force-Unconstrained Poses

In Chapter 2, force-unconstrained configurations of parallel manipulators were formulated with two methods: time derivative and screw theory. In addition, different techniques for identifying these configurations were described and discussed. The time derivative method may seem to be more appropriate, from the algebraic point of view, because the Jacobian matrix is expressed in terms of the position and orientation of the mobile platform. Whereas with the screw theory method, the entries of the associated reciprocal screw matrix are a function of joint displacements. Nevertheless, the physical meaning and geometric insight of screw theory allows for a better understanding of the singularity problem. In particular, for parallel manipulators, a force-unconstrained pose occurs when all associated reciprocal screws intersect at a common point (a planar pencil).

When either the Jacobian or the associated reciprocal screw matrix has been formulated, the identification of the force-unconstrained poses can be carried out either numerically or analytically. The numerical technique provides the information of how close a pose of the manipulator is from a singular configuration making this technique suitable for real-time applications. The analytical technique provides a mathematical and graphical representation of all singular configurations of a parallel

manipulator. The identification of all force-unconstrained poses is a crucial parameter for the manipulator's design as well as for the trajectory generation design.

Chapter 3: Force-Unconstrained Poses of Non-Redundant Planar Parallel Manipulators

In Chapter 3, an analysis of the force-unconstrained poses of the planar parallel manipulators most feasible for real applications, 3-R$\underline{P}$R, 3-$\underline{P}$RR, and 3-$\underline{R}$RR, was considered. The force-unconstrained poses of these non-redundant manipulators were plotted in a three-dimensional space defined by the position and orientation of the mobile platform yielding surfaces, or an order of two infinities ($O(\infty^2)$) of force-unconstrained poses.

In the literature, force-unconstrained poses have usually been presented through equations. In some cases, these poses have been reported for a constant payload orientation (Bonev et al., 2003). Their representation provides a clear understanding of the complexity of the curves on the xy plane; however, it does not show the nature of the surfaces for different payload orientations. The representation of these surfaces in a three-dimensional space, defined by the position and orientation of the mobile platform, has rarely been presented. As an example, Kong and Gosselin (2000), Husty et al. (1999), and Li et al. (2006), showed the singularity loci of the 3-R$\underline{P}$R manipulator. Attempts to represent the manifold of singularities of the 3-$\underline{R}$RR manipulator have been carried out (see for instance Chan and Ebert-Uphoff, 2001) yielding a single convex surface. In this dissertation, the force-unconstrained poses of the 3-$\underline{P}$RR and 3-$\underline{R}$RR manipulators were presented depending on their working mode and the combination of all of them. The identification of force-unconstrained poses

for each working mode is important because for a specific pose, the manipulator can be force unconstrained for one or two configurations but not for all of them. This allows a selection of a working mode that might be singularity free for a desired trajectory.

For each of the eight working modes, the nature of the singularity surfaces is very complicated, yielding non-convex surfaces. The use of a mesh to facilitate the generation of the singularity surface would involve points generated through interpolation; however, such points would not likely be part of the singularity surface. As an alternative, the poses were plotted with a large number of points. The combination of all working modes shows the association among the surfaces.

Chapter 4: Force-Unconstrained Poses of Planar Parallel Manipulators with In-Branch Redundancy

In Chapter 4, the inclusion of an extra actuator within the branches was considered. The force-unconstrained poses of the RRR-2RRR, PRR-2PRR, and RRR-2RRR actuation layouts, where the first branch contains the redundant actuator, were presented. The force-unconstrained poses of these mechanisms were plotted in the three-dimensional space $(x - y - \phi)$ yielding curves of force-unconstrained poses. Consequently, there was a reduction in the order of infinity of force-unconstrained poses from $O(\infty^2)$ for non-redundant planar parallel manipulators to $O(\infty)$ for planar parallel manipulators with one additional actuated joint. With further actuation, the force-unconstrained poses are reduced by one order of infinity for every additional actuated joint added into the system.

The methodology employed in this chapter is based on reciprocal screws associated

with the actuated joints. Since the associated reciprocal screw matrix is a non-square matrix, taking its determinant is not possible. As an alternative, the associated reciprocal screw matrix was divided into four square sub-matrices. The manipulator is force unconstrained if the determinant of all four sub-matrices is equal to zero.

For every actuation layout, two kinematic conditions were identified. Condition 1 occurs when the reciprocal screws associated with the actuated joints of branches 2 and 3 cross through the passive joint of the first branch; i.e., all four associated reciprocal screws intersect at a common point. The force-unconstrained poses under this condition can be represented by the path followed by a 1-dof mechanism composed of six bars. These equivalent mechanisms have the second link of branches 2 and 3 collinear with the respective edge of the mobile platform. Condition 2 occurs when the associated reciprocal screws of branch 1 are collinear and intersect the common point (intersection point) of the associated reciprocal screws of branches 2 and 3. With this condition, the above-mentioned actuation layouts can be considered as 2-dof seven-bar mechanisms. In addition, a discussion of the RPR-2RPR actuation layout was presented.

In-branch redundancy implies replacing passive joints with actuated joints. This leads to an improvement in the stiffness of the manipulator due to the passive joint clearances. Nonetheless, there is an increment in the linkage inertia and the need for a reliable control system.

Chapter 5: Force-Unconstrained Poses of Planar Parallel Manipulators with Additional Branches

In Chapter 5, the inclusion of an additional actuated branch was considered. The force-unconstrained poses of the 4-R$\underline{\text{P}}$R, 4-$\underline{\text{P}}$RR, and 4-$\underline{\text{R}}$RR manipulators were presented yielding curves in the $x - y - \phi$-dimensional space, i.e., $O(\infty)$ of force-unconstrained poses for planar parallel manipulators with one additional branch exist.

The non-square associated reciprocal screw matrix was divided into four square sub-matrices. A geometric analysis of the dependency among the determinants of the sub-matrices was presented. The number of nonlinearly dependent determinants required to compute the force-unconstrained poses of a parallel manipulator with additional actuated branches is augmented by one for each additional branch added. With the inclusion of one additional branch, the determinants of two of the sub-matrices must equal zero. Nonetheless, this is a necessary condition for the manipulator to be force unconstrained because an exception occurs when the two sub-matrices contain two associated reciprocal screws that are collinear. This exception, however, can be treated numerically by checking the condition of the remaining sub-matrices.

This analysis led to a system of polynomial equations. Elimination methods were employed. A thorough description of elimination methods is presented in Appendix C. For the 4-R$\underline{\text{P}}$R manipulator, Gröbner Bases, an elimination method embedded in algebraic software such as Maple and Mathematica, was primarily used to show the implementation of the method. Another elimination method could have been used instead. For the 4-$\underline{\text{P}}$RR, and 4-$\underline{\text{R}}$RR manipulators, Maple 7, was not capable of resolving the polynomial system. As an alternative, a labourious elimination process

was made yielding two equations in two variables. Dialytic elimination was then applied resulting in a square matrix whose elements are polynomials in one variable. To reduce floating-point arithmetic errors, the roots of the polynomial obtained from the determinant of this matrix, were solved as an eigenvalue problem.

6.3 Recommendations for Future Work

The identification of force-unconstrained poses in parallel manipulators is essential for their design. With this information, the next step to be considered is path generation design and architectural design. Path generation design can be implemented in existing manipulators with the objective of creating singularity-free paths. The architectural design aims to eliminate, or at least reduce, force-unconstrained poses within the workspace of the manipulator.

For the studied non-redundant manipulators with general geometry, singular configurations are encountered throughout the workspace. However, special architectures can be considered to eliminate force-unconstrained configurations. Bonev (2002) reported some of these special architectures.

For planar parallel manipulators with in-branch redundancy, further families of force-unconstrained poses could be eliminated with the inclusion of more actuators. Theoretically, a finite number of force-unconstrained poses will occur with the inclusion of two redundant actuators, while the manipulator will be free of force-unconstrained configurations with the inclusion of three redundant actuators. Based upon this, it would be interesting to demonstrate this statement with examples.

A similar analysis could be applied to planar parallel manipulators with additional branches. Nonetheless, the most appealing project that could be made out of planar

parallel manipulators with additional branches is the modification of the geometric parameters of the manipulators. As an example, the force-unconstrained poses of the 4-RPR manipulator, presented in this dissertation, correspond to the manipulator with a square fixed platform and a trapezoidal mobile platform. This choice was made to show all the force-unconstrained poses within the workspace. Nevertheless, other architectural designs were considered. In some cases, the force-unconstrained poses fell outside the reachable workspace.

Redundantly-actuated parallel manipulators require a reliable control system. That is, all actuators must be performing simultaneously otherwise the smallest variance in their displacements may cause severe damage to the manipulator. In order to develop a control scheme, an efficient dynamic model is also required. Making a reliable control system with an efficient dynamic model could be implemented on the Reconfigurable Planar Parallel Manipulator (RPPM), shown in Figure 1.1. This manipulator is currently equipped with force sensors and a fourth branch will be added in the near future, as well as a redesigned mobile platform. Therefore, a specific analysis of potential designs of the updated RPPM should be considered. As a requirement for this analysis, the identification of force-unconstrained poses would be possible based on the findings of this dissertation.

References

Adams, W. W., and Loustaunau, P., (1994), *An Introduction to Gröbner Bases.* Graduate Studies in Mathematics, Vol. 3, American Mathematical Society: Providence, RI, USA.

Albala, H., and Angeles, J., (1979), "Numerical Solution to the Input Output Displacement Equation of the General 7R Spatial Mechanism", in *Fifth World Congress on Theory of Machines and Mechanisms*, pp. 1008–1011.

Angeles, J., (1985), "On the Numerical Solution for the Inverse Kinematics Problem", *The International Journal of Robotics Research*, vol. 4, no. 2, pp. 21–37.

Antoniou, A., and Lu, W. S., (2002, preprint to appear in 2007), *Optimization: Methods, Algorithms and Applications.* Springer: New York, NY, USA.

Ball, R. S., (1900, reprinted in 1998), *A Treatise of the Theory of Screws.* Cambridge University Press: New York, NY, USA.

Bonev, I. A., (2002), *Geometric Analysis of Parallel Mechanisms.* Ph.D. Dissertation, Laval University, Department of Mechanical Engineering, Québec, QC, Canada, November.

Bonev, I. A., and Gosselin, C. M., (2001), "Singularity Loci of Planar Parallel Manipulators with Revolute Joints", in *Computational Kinematics*, F.C. Park, C.C. Iurascu editors, Seoul, South Korea, May, pp. 291–299.

Bonev, I. A., Zlatanov, D., and Gosselin, C. M., (2003), "Singularity Analysis of 3-DOF Planar Parallel Mechanisms via Screw Theory", *Transactions of the ASME, Journal of Mechanical Design*, vol. 125, no. 3, pp. 573–581.

Bruzzone, L. E., Molfino, R. M., and Razzoli, R. P., (2002), "Modelling and Design of a Parallel Robot for Laser-Cutting Applications", in *Proceedings of the IASTED International Conference Modelling, Identification and Control*, Innsbruck, Austria, February 18-21, pp. 518–522.

Buchberger, B., (1965), *Ein Algorithmus zum Auffinden der Basiselemente des Restklassenringes nach einem nulldimensionalen Polynomideal.* Ph.D. Dissertation, University of Innsbruck, Innsbruck, Austria.

Buchberger, B., and Winkler, F., (1998, editors), *Gröbner Bases and Applications.* Cambridge University Press: volume 251 of London Mathematical Society Lecture Note Series: Cambridge, England.

Carretero, J. A., Nahon, M., Gosselin, C. M., and Buckham, B. J., (1997), "Kinematic Analysis of a Three-DOF Parallel Mechanism for Telescope Applications", in *Proceedings of the ASME Design Engineering Technical Conference*, Sacramento, CA, USA, September, pp. 14–17.

Cayley, A., (1848), "On the Theory of Elimination", *Cambridge and Dublin Mathematical Journal*, pp. 116–120.

Ceccarelli, M., (2000), "Screw Axis Defined by Giulio Mozzi in 1763 and early Studies on Helicoidal Motion", *Mechanism and Machine Theory*, vol. 35, no. 6, pp. 761–770.

Chablat, D., and Wenger, P., (1998), "Working Modes and Aspects in Fully Parallel Manipulators", in *Proceedings of the 1998 IEEE International Conference on Robotics and Automation*, Leuven, Belgium, May, pp. 1964–1969.

Chan, V. K., (2001), *Singularity Analysis and Redundant Actuation of Parallel Manipulators.* M.A.Sc. Thesis, Georgia Institute of Technology, GA, USA, March.

Chan, V. K., and Ebert-Uphoff, I., (2001), "Investigation of the Deficiencies of Parallel Manipulators in Singular Configurations Through the Jacobian Nullspace", in *Proceedings of the 2001 IEEE International Conference on Robotics and Automation*, Seoul, Korea, May 21-26, pp. 1313–1320.

Chasles, M., (1830), "Note sur les Proprietes Generales du Systeme de Deux Corps Semblables entr'eux", in *Bullettin de Sciences Mathematiques, Astronomiques Physiques et Chimiques*, vol. 14, Baron de Ferussac, Paris, France, pp. 321–326.

Clavel, R., (1991), *Conception d'un robot parallèle rapide à 4 degrés de liberté.* Ph.D. Dissertation, Ecole Polytechnique Fédérale de Lausanne, Switzerland.

Cobb, R. G., Sullivan, J. M., Das, A., Davis, L. P., Hyde, T. T., Davis, T., Rahman, Z. H., and Spanos, J. T., (1999), "Vibration Isolation and Suppression System for Precision Payloads in Space", *Smart Materials and Structures*, vol. 8, pp. 798–812.

Collins, C. L., (1997), *Singularity Analysis and Design of Parallel Manipulators.* Ph.D. Dissertation, Mechanical and Aerospace Engineering, University of California, Irvine, CA, USA.

Collins, C. L., and Long, G. L., (1995), "The Singularity Analysis of an In-Parallel Hand Controller for Force-Reflected Teleoperation", *IEEE Transactions on Robotics and Automation*, vol. 11, no. 5, pp. 661–669.

Collins, C. L., and McCarthy, J. M., (1998), "The Quartic Singularity Surfaces of Planar Platforms in the Clifford Algebra of the Projective Plane", *Mechanism and Machine Theory*, vol. 33, no. 7, pp. 931–944.

Craig, J. J., (1987), *Introduction to Robotics, Mechanism and Control, second edition.* Addison-Wesley Publishing Company: Don Mills, ON, Canada.

Dandurand, A., (1984), "The Rigidity of Compound Spatial Grid", *Structural Topology*, vol. 10, pp. 41–56.

Dasgupta, B., and Mruthyunjaya, T. S., (1998), "Force Redundancy in Parallel Manipulators: Theoretical and Practical Issues", *Mechanism and Machine Theory*, vol. 33, no. 6, pp. 727–742.

Dasgupta, B., and Mruthyunjaya, T. S., (2000), "The Stewart Platform Manipulator: A Review", *Mechanism and Machine Theory*, vol. 35, no. 1, pp. 15–40.

Davidson, J. K., and Hunt, K. H., (2004), *Robots and Screw Theory: Applications of Kinematics and Statics to Robotics.* Oxford University Press: Toronto, ON, Canada.

Denavit, J., and Hartenberg, R. S., (1955), "A Kinematic Notation for Lower-Pair Mechanisms Based on Matrices", *Transactions of the ASME, Journal of Applied Mechanics*, June, pp. 215–221.

Destefani, J., (2003), "Return of the Hexapods", *Manufacturing Engineering*, vol. 130, no. 2, pp. 75–79.

Di Gregorio, R., and Parenti-Castelli, V., (2001), "Kinematics of a Six-dof Fixation Device for Long-Bone Fracture Reduction", *Journal of Robotic Systems*, vol. 18, no. 12, pp. 715–722.

Duffy, J., and Crane, C., (1980), "A Displacement Analysis of the General Spatial 7R Mechanism", *Mechanism and Machine Theory*, vol. 15, pp. 153–169.

Ebert-Uphoff, I., Lee, J.-K., and Lipkin, H., (2002), "Characteristic Tetrahedron of Wrench Singularities for Parallel Manipulators with Three Legs", *IMechE Journal of Mechanical Engineering Science*, vol. 216, no. 1, pp. 81–93.

Ebrahimi, I., Carretero, J. A., and Boudreau, R., (2006), "Singularity Analysis of a New Kinematically Redundant Planar Parallel Manipulator", in *Proceedings of the CSME Forum 2006*, Kananaskis, AB, Canada, May, 9 pages.

Erdman, A. G., Sandor, G. N., and Kota, S., (2001), *Mechanism Design: Analysis and Synthesis: Volume 1, Fourth Edition.* Prentice Hall: Toronto, ON, Canada.

Fajardo, P., and Rey-Bakaikoa, V., (1995), "Control of Six degree-of-freedom Parallel Manipulators for Synchrotron Radiation Applications", *Review of Scientific Instruments*, vol. 66, no. 2, pp. 1758–1761.

Fichter, E., (1986), "A Stewart Platform-Based Manipulator: General Theory and Practical Construction", *The International Journal of Robotics Research*, vol. 5, no. 2, pp. 157–182.

Firmani, F., (1999), *El Análisis Cinemático de un Hexápodo y su Aplicación para Controlar el Espejo Secundario de un Telescopio.* B.Eng. Thesis, Faculty of Engineering, National Autonomous University of Mexico (UNAM), Mexico City, Mexico, March.

Firmani, F., and Podhorodeski, R. P., (2002), "Force Degeneracies for a Redundantly Actuated Planar Parallel Manipulator", in *Proceedings of the CSME Forum 2002*, Kingston, ON, Canada, 9 pages.

Firmani, F., and Podhorodeski, R. P., (2004a), "Force-Unconstrained Poses for a Redundantly-Actuated Planar Parallel Manipulator", *Mechanism and Machine Theory*, vol. 39, no. 5, pp. 459–476.

Firmani, F., and Podhorodeski, R. P., (2004b), "Force-Unconstrained Poses for Parallel Manipulators with Redundant Actuated Branches", in *Proceedings of the CSME Forum 2004*, London, ON, Canada, 9 pages.

Firmani, F., and Podhorodeski, R. P., (2005a), "Force-Unconstrained Poses of the 3-PRR and 4-PRR Planar Parallel Manipulators", in *Proceedings of the 2005 CCToMM Symposium on Mechanisms, Machines, and Mechatronics*, Saint-Hubert, QC, Canada, 12 pages.

Firmani, F., and Podhorodeski, R. P., (2005b), "Force-Unconstrained Poses for Parallel Manipulators with Redundant Actuated Branches", *Transactions of the CSME*, vol. 29, no. 3, pp. 343–356.

Firmani, F., and Podhorodeski, R. P., (2005c), "Force-Unconstrained Poses of the 3-PRR and 4-PRR Planar Parallel Manipulators", *Transactions of the CSME*, vol. 29, no. 4, pp. 617–628.

Fisher, R., Podhorodeski, R. P., and Nokleby, S. B., (2001), "A Reconfigurable Planar Parallel Manipulator (RPPM)", in *Proceeding of the 2001 CCToMM Symposium*, St.-Hubert, QC, Canada, 2 pages.

Fisher, R., Podhorodeski, R. P., and Nokleby, S. B., (2004), "Design of a reconfigurable planar parallel manipulator", *Journal of Robotic Systems*, vol. 21, no. 12, pp. 665–675.

Fraleigh, J. B., (1976), *A First Course in Abstract Algebra, second edition.* Addison Wesley: Don Mills, ON, Canada.

Gohberg, I., Lancaster, P., and Rodman, L., (1982), *Matrix Polynomials.* Academic Press: New York, NY, USA.

Golub, H. G., and Van Loan, C. F., (1983), *Matrix Computations.* The Johns Hopkins University Press: Baltimore, MD, USA.

Gosselin, C. M., (1990a), "Determination of the Workspace of 6-DOF Parallel Manipulators", *Transactions of the ASME, Journal of Mechanisms, Transmissions, and Automation in Design*, vol. 112, no. 3, pp. 331–336.

Gosselin, C. M., (1990b), "Dexterity Indices for Planar and Spatial Manipulators", in *Proceedings of the 1990 IEEE International Conference on Robotics and Automation*, vol. 1, Cincinnati, OH, USA, May, pp. 650–655.

Gosselin, C. M., (1990c), "Stiffness Mapping for Parallel Manipulators", *IEEE Transactions on Robotics and Automation*, vol. 6, no. 3, pp. 377–382.

Gosselin, C. M., and Angeles, J., (1988), "The Optimum Kinematic Design of a Planar Three-Degree-of-Freedom Parallel Manipulator", *Transactions of the ASME,*

Journal of Mechanisms, Transmissions and Automation in Design, vol. 110, pp. 35–41.

Gosselin, C. M., and Angeles, J., (1990), "Singularity Analysis of Closed-Loop Kinematic Chains", *IEEE Transactions on Robotics and Automation*, vol. 6, June, pp. 281–290.

Gosselin, C. M., and Merlet, J. P., (1994), "The Direct Kinematics of Planar Parallel Manipulators: Special Architectures and Number of Solutions", *Mechanism and Machine Theory*, vol. 29, no. 8, pp. 1083–1097.

Gosselin, C. M., and Wang, J., (1997), "Singularity Loci of Planar Parallel Manipulators with Revolute Joints", *Robotics and Autonomous Systems*, vol. 21, no. 4, pp. 377–398.

Gosselin, C. M., Sefrioui, J., and Richard, M. J., (1992), "Solutions polynomiales au probleme de la cinematique directe des manipulateurs paralleles plans a trois degres de liberte: Polynomial solutions to the direct kinematic problem of planar three degree-of-freedom parallel manipulators", *Mechanism and Machine Theory*, vol. 27, no. 2, pp. 107–119.

Gosselin, C. M., Lemieux, S., and Merlet, J. P., (1996), "A New Architecture of Planar Three-Degree-of-Freedom Parallel Manipulator", in *Proceedings of the 1996 IEEE International Conference on Robotics and Automation*, vol. 4, Minneapolis, MN, USA, April, pp. 3738–3743.

Gough, V., (1956), "Contribution to Discussion of Papers on Research in Automobile Stability, Control and Tyre Performance", in *Proceedings of the Automotive Division of the Institution of Mechanical Engineers*, pp. 392–395.

Grace, K., Colgate, J., Glucksberg, M., and Chun, J., (1993), "A six degree of freedom micromanipulator for opthalmic surgery", in *Proceedings of the 1993 IEEE International Conference on Robotics and Automation*, Atlanta, GA, USA, May, pp. 630–635.

Griffis, M., and Duffy, J., (1989), "A Forward Displacement Analysis of a Class of Stewart Platform", *Journal of Robotic Systems*, vol. 6, no. 6, pp. 703–720.

Gupta, K., and Kazerounian, K., (1985), "Improved Numerical Solutions of the Inverse Kinematics of Robots", in *Proceedings of the 1985 IEEE International Conference on Robotics and Automation*, St. Louis, MS, USA, pp. 743–748.

Gupta, K., and Singh, V., (1989), "A Numerical Algorithm for Solving Robot Inverse Kinematics", *Robotica*, vol. 7, pp. 159–164.

Hao, F., and McCarthy, J. M., (1998), "Conditions for line-based singularities in spatial platform manipulators", *Journal of Robotic Systems*, vol. 15, no. 1, pp. 43–55.

Hunt, K. H., (1978, reprinted in 1990), *Kinematic Geometry of Mechanisms*. Oxford University Press: Toronto, ON, Canada.

Husty, M. L., (1996), "An Algorithm for Solving the Direct Kinematics of General Stewart-Gough Platforms", *Mechanism and Machine Theory*, vol. 31, no. 4, pp. 365–380.

Husty, M. L., Hayes, M. J. D., and Loibnegger, H., (1999), "The General Singularity Surface of Planar Three-Legged Platforms", in *Advances in Multibody Systems and Mechatronics*, Gerhard-Mercator-Universität, Duisburg, Germany, pp. 203–214.

Husty, M. L., Mielczarek, S., and Hiller, M., (2001), "Constructing an Overconstrained Planar 4RPR Manipulator with Maximal Forward Kinematics Solution Set", in *Proceedings of the RAAD '01 "Robotics in the Alpe-Adria-Danube Region"*, Vienna, Austria, 6 pages.

Innocenti, C., and Parenti-Castelli, V., (1990), "Direct Position Analysis of the Stewart Platform Mechanism", *Mechanism and Machine Theory*, vol. 25, no. 6, pp. 611–621.

Kazerounian, K., (1987), "On the Numerical Inverse Kinematics of Robotic Manipulators", *Transactions of the ASME, Journal of Mechanisms, Transmissions, and Automation in Design*, vol. 109, no. 1, pp. 8–13.

Kohli, D., and Osvatic, M., (1992), "Inverse Kinematics of General 4R2P, 3R3P, 4R1C, 2R2C, and 3C Serial Manipulators", in *American Society of Mechanical Engineers, Design Engineering Division (Publication) DE*, vol. 45, Scottsdale, AZ, USA, September, pp. 129–137.

Kohli, D., and Osvatic, M., (1993), "Inverse Kinematics of General 6R and 5R,P Serial Manipulators", *Transaction of the ASME, Journal of Mechanical Design*, vol. 115, no. 4, pp. 922–931.

Kong, X., and Gosselin, C. M., (2000), "Determination of the Uniqueness Domains of 3-RPR Parallel Manipulators with Similar Platforms", in *Proceedings of the ASME 26th Biennial Mechanisms Conference*, Baltimore, MD, USA, September 10-13, 8 pages.

Lazard, D., (1992), "Stewart platform and Gröbner basis", in *Proceedings of 3rd*

International Workshop on Advances in Robot Kinematic (ARK), Ferrara, Italy, September, pp. 136–142.

Lazard, D., (1993), *On the Representation of Rigid-Body Motions and its Application to Generalized Platform Manipulators.* In Computational Kinematics (J. Angeles, G. Hommel, and P. Kovács, eds.), Kluwer Academic Publishers: Dordrecht, The Netherlands, pp. 175-182.

Lazarevic, Z., (1997), *Feasibility of a Stewart Platform with Fixed Actuators as a Platform for CABG Surgery Device.* M.Sc. Thesis, Columbia University, Department of Bioengineering, October.

Lee, H., and Liang, C., (1988a), "A New Vector Theory for the Analysis of Spatial Mechanisms", *Mechanism and Machine Theory*, vol. 23, no. 3, pp. 209–217.

Lee, H., and Liang, C., (1988b), "Displacement Analysis of the General Spatial 7-Link 7R Mechanism", *Mechanism and Machine Theory*, vol. 23, no. 3, pp. 219–226.

Lee, J., Duffy, J., and Keler, J., (1999), "The Optimum Quality Index for the Stability of In Parallel Planar Platform Devices", *Transaction of the ASME, Journal of Mechanical Design*, vol. 121, pp. 15–20.

Lee, S., and Kim, S., (1993), "Kinematic Analysis of Generalized Parallel Manipulator Systems", in *Proceedings of the 32nd IEEE Conference on Decision and Control*, vol. 2, San Antonio, TX, USA, December 15-17, pp. 1097–1102.

Li, H., Gosselin, C. M., and Richard, M. J., (2006), "Determination of Maximal Singularity-Free Zones in the Workkspace of Planar Three-Degree-of-Freedom Parallel Mechanisms", *Mechanism and Machine Theory*, vol. 41, no. 10, pp. 1157–1167.

Li, T., (1997), "Numerical solution of multivariate polynomial systems by homotopy continuation methods", *Acta Numerica*, vol. 6, pp. 399–436.

Li, T., and Payandeh, S., (2002), "Design of Spherical Parallel Mechanisms for Application to Laparoscopic Surgery", *Robotica*, vol. 20, no. 2, pp. 133–138.

Liao, H., Li, T., and Tang, X., (2004), "Singularity Analysis of Redundant Parallel Manipulators", in *Proceedings of the 2004 IEEE International Conference on Systems, Man and Cybernetics*, vol. 5, The Hague, Netherlands, October 10-13, pp. 4214–4220.

Liu, G. F., Wu, Y. L., Wu, X. Z., Kuen, Y. Y., and Li, Z. X., (2001), "Analysis and Control of Redundant Parallel Manipulators", in *Proceedings of the 2001 IEEE International Conference on Robotics and Automation*, Seoul, Korea, May, 21-26, pp. 3748–3754.

Ma, O., and Angeles, J., (1991), "Architecture Singularities of Platform Manipulators", in *Proceedings of the 1991 IEEE International Conference on Robotics and Automation*, vol. 2, Sacramento, CA, USA, April 11-14, pp. 1542–1547.

Manocha, D., and Canny, J., (1992), "Real Time Inverse Kinematics for General 6R Manipulators", *Technical Report*, University of California, Berkeley, CA, USA.

Manocha, D., and Canny, J., (1994), "Efficient Inverse Kinematics for General 6R Manipulator", *IEEE Journal on Robotics and Automation*, vol. 10, no. 5, pp. 648–657.

Masory, O., and Wang, J., (1995), "Workspace Evaluation of Stewart Platforms", *Advanced Robotics*, vol. 9, no. 4, pp. 443–461.

MathWorks, (2001), *Optimization Toolbox User's Guide- Version 2.* The MathWorks, Inc.: Natick, MA, USA.

Mayer St-Onge, B., and Gosselin, C. M., (1996), "Singularity Analysis and Representation of Spatial Six-dof Parallel Manipulators", in *Proceedings of the 5th International Symposium on Advances in Robot Kinematics (ARK) Conference*, Portoroz-Bernardin, Slovenia, June, pp. 389–398.

Merlet, J. P., (1989), "Singular Configurations of Parallel Manipulators and Grassmann Geometry", *The International Journal of Robotics Research*, vol. 8, no. 5, pp. 45–56.

Merlet, J. P., (1996a), "Redundant Parallel Manipulators", *Journal of Laboratory Robotics and Automation*, vol. 8, pp. 17–24.

Merlet, J. P., (1996b), "Direct Kinematics of Planar Parallel Manipulators", in *Proceedings of the 1996 IEEE International Conference on Robotics and Automation*, vol. 4, Minneapolis, MN, USA, April, pp. 3744–3749.

Merlet, J. P., (2000), *Parallel Robots.* Kluwer Academic Publishers: The Netherlands.

Merlet, J. P., (2004), "Solving the Forward Kinematics of a Gough-Type Parallel Manipulator with Interval Analysis", *The International Journal of Robotics Research*, vol. 23, no. 3, pp. 221–23.

Merlet, J. P., Gosselin, C. M., and Mouly, N., (1998), "Workspaces of Planar Parallel Manipulators", *Mechanism and Machine Theory*, vol. 33, no. 1, pp. 7–20.

Miller, K., (2004), "Optimal Design and Modeling of Spatial Parallel Manipulators", *The International Journal of Robotics Research*, vol. 23, no. 2, pp. 127–140.

Mohamed, M., and Duffy, J., (1985), "A Direct Determination of the Instantaneous Kinematics of Fully Parallel Robot Manipulators", *Transactions of the ASME, Journal of Mechanisms, Transmissions, and Automation in Design*, vol. 107, no. 2, pp. 226–229.

Mohammadi-Daniali, H. R., Zsombor-Murray, P. J., and Angeles, J., (1995), "Singularity Analysis of Planar Parallel Manipulators", *Mechanism and Machine Theory*, vol. 30, no. 5, pp. 665–678.

Morgan, A., and Sommese, A., (1987), "Computing all solutions to polynomial systems using homotopy continuation", *Applied Mathematics and Computation*, vol. 24, no. 2, pp. 115–138.

Mozzi, G., (1763), "Discorso matematico sopra il rotamento momentaneo dei corpi", in *Stamperia di Donato Campo*, Naples, Italy.

Muller, A., (2005), "Internal Preload Control of Redundantly Actuated Parallel Manipulators-Its Application to Backlash Avoiding Control", *IEEE Transactions on Robotics*, vol. 21, no. 4, pp. 668–677.

Nanua, P., Waldron, K., and Murthy, V., (1990), "Direct Kinematic Solution of a Stewart Platform", *IEEE Transactions on Robotics and Automation*, vol. 6, no. 4, pp. 438–444.

Nokleby, S. B., (2003), *Identification and Utilization of Loss of Motion Capabilities of Robotic Manipulators*. Ph.D. dissertation, University of Victoria, Victoria, BC, Canada, April.

Nokleby, S. B., Fisher, R., Podhorodeski, R. P., and Firmani, F., (2005), "Force Capabilities of Redundantly-Actuated Parallel Manipulators", *Mechanism and Machine Theory*, vol. 40, no. 5, pp. 578–599.

Notash, L., (1998), "Uncertainty Configurations of Parallel Manipulators", *Mechanism and Machine Theory*, vol. 33, no. 1, pp. 123–138.

Notash, L., and Podhorodeski, R. P., (1994), "Uncertainty Configurations of Three-Branch Manipulators: Identification and Elimination", in *Proceedings of the ASME 23rd Biennial Mechanisms Conference*, vol. 72, Minneapolis, MN, USA, September 11-14, pp. 459–466.

Notash, L., and Podhorodeski, R. P., (1996), "Forward Displacement Analysis and Uncertainty Configurations of Parallel Manipulators With a Redundant Branch", *Journal of Robotic Systems*, vol. 13, no. 9, pp. 587–601.

O'Brien, J., and Wen, J., (1999), "Redundant Actuation for Improving Kinematic Manipulability", in *Proceedings of the 1999 IEEE International Conference on Robotics and Automation*, vol. 2, Detroit, MI, USA, May, pp. 1520–1525.

Park, F. C., and Kim, J. W., (1998), "Manipulability of Closed Kinematic Chains", *Transaction of the ASME, Journal of Mechanical Design*, vol. 120, no. 4, pp. 542–548.

Pieper, D., (1969), *The Kinematics of Manipulators under Computer Control.* Ph.D. Dissertation, Stanford University.

Pittens, K. H., and Podhorodeski, R. P., (1993), "A Family of Stewart Platforms with Optimal Dexterity", *Journal of Robotic Systems*, vol. 10, no. 4, pp. 463–479.

Plücker, J., (1868-9), *Neue Geometrie des Raumes gegründet auf die Betrachtung der geraden Linie als Raumelement.* Volumes 1 and 2. Teubner: Leipzig, Germany.

Poinsot, L., (1806), "Sur la Composition des Moments et la Composition des Aires", *Journal de l'Ecole Polytechnique*, vol. 6, no. 13, pp. 182–205.

Primrose, E., (1986), "On the Input-Output Equation of the General 7R-Mechanism", *Mechanism and Machine Theory*, vol. 21, pp. 509–510.

Raghavan, M., (1993), "The Stewart Platform of General Geometry has 40 Configurations", *Transactions of the ASME, Journal of Mechanical Design*, vol. 115, pp. 277–282.

Raghavan, M., and Roth, B., (1989), "Kinematic Analysis of the 6R Manipulator of General Geometry", in *International Symposium on Robotics Research*, Tokyo, Japan, pp. 314–320.

Raghavan, M., and Roth, B., (1993), "Inverse Kinematics of the General 6R Manipulator and Related Linkages", *Transaction of the ASME, Journal of Mechanical Design*, vol. 115, pp. 502–508.

Raghavan, M., and Roth, B., (1995), "Solving polynomial systems for the kinematic analysis and synthesis of mechanisms and robot manipulators", *Transactions of the ASME, Journal of Mechanical Design*, vol. 117, pp. 71–79.

Roth, B., (1984), "Screws, Motors, and Wrenches That Cannot be Bought in a Hardware Store", *Proceedings of the 1st International Symposium on Robotics Research*, June, pp. 679–693.

Roth, B., (1993), *Computation in Kinematics.* In Computational Kinematics (J. Angeles, G. Hommel, and P. Kovács, eds.), Kluwer Academic Publishers: Dordrecht, The Netherlands, pp. 3-14.

Roth, B., and Freudenstein, F., (1963), "Synthesis of path generating mechanisms by numerical methods", *Journal of Engineering for Industry, Transactions of the ASME*, vol. 85, pp. 298–307.

Roth, B., Rastegar, J., and Scheinman, V., (1973), "On the Design of Computer Controlled Manipulators", in *First CISM IFToMM Symposium on Theory and Practice of Robots and Manipulators*, pp. 93–113.

Saaty, T. L., (1981), *Modern Nonlinear Equations.* Dover: New York, NY, USA.

Salmon, G., (1885, reprinted in 1964), *Lessons Introductory to the Modern Higher Algebra, fifth edition.* Chelsea Publishing Company: New York, NY, USA.

Sefrioui, J., and Gosselin, C. M., (1994), "Étude et Représentation des Lieux de Singularités des Manipulateurs Parallèles Sphériques à Trois Degrés de Liberté avec Actionneurs Prismatiques", *Mechanism and Machine Theory*, vol. 29, no. 4, pp. 559–579.

Sefrioui, J., and Gosselin, C. M., (1995), "On the Quadratic Nature of the Singularity Curves of Planar Three-Degree-of-Freedom Parallel Manipulators", *Mechanism and Machine Theory*, vol. 30, no. 4, pp. 533–551.

Smith, D., (1997), "Kinematic Passive Correction of Errors in Active Surface Telescopes", *Smart Materials and Structures*, vol. 6, no. 4, pp. 498–503.

Smith III, W., and Nguyen, C., (1991), "Mechanical Analysis and Design of a Six Degree of Freedom Robotic Wrist for Space Assembly", in *Proceedings of the 23rd Southeastern Symposium on System Theory*, Columbia, SC, USA, March, pp. 177–181.

Sobejko, P., (2002), *Implementation of Redundantly-Sensed Parallel-Manipulator-Based 6-DOF Joysticks.* M.A.Sc. Thesis, University of Victoria, Victoria, BC, Canada, December.

Stewart, D., (1965), "A Platform with Six Degrees of Freedom", in *Proceedings of the Institution of Mechanical Engineers*, pp. 371–386.

Sylvester, J., (1841), "Examples of the dialytic method of elimination as applied to ternary systems of equations", *Cambridge Mathematical Journal*, pp. 232–236.

Tahmasebi, F., and Tsai, L. W., (1994), "Workspace and Singularity Analysis of a Novel Six-DOF Parallel Mini-Manipulator", *Journal of Applied Mechanisms and Robotics*, vol. 1, no. 2, pp. 31–40.

Tsai, L., and Morgan, A., (1985), "Solving the Kinematics of the most General Six and Five-Degree-of-Freedom Manipulators by Continuation Methods", *Transactions of the ASME, Journal of Mechanisms, Transmissions and Automation in Design*, vol. 107, pp. 189–200.

Tsai, L. W., (1999), *Robot Analysis, The Mechanics of Serial and Parallel Manipulators.* Wiley-Interscience: Toronto, ON, Canada.

Valasek, M., Bauma, V., Sika, Z., Belda, K., and Pisa, P., (2005), "Design-by-

Optimization and Control of Redundantly Actuated Parallel Kinematics Sliding Star", *Multibody System Dynamics*, vol. 14, no. 3-4, pp. 251–267.

Voglewede, P., and Ebert-Uphoff, I., (2004), "Measuring "Closenes" to Singularities for Parallel Manipulators", in *Proceedings of the 2004 IEEE International Conference on Robotics and Automation*, New Orleans, LA, USA, April, pp. 4539–4544.

Voglewede, P., and Ebert-Uphoff, I., (2002), "Two Viewpoints on the Unconstrained Motion of Parallel Manipulators at or Near Singular Configurations", in *Proceedings of the 2002 IEEE International Conference on Robotics and Automation*, Washington, DC, USA, May, pp. 503–510.

Voglewede, P. A., (2004), *Design of Redundant Actuation for Parallel Manipulators.* Ph.D. Dissertation, Georgia Institute of Technology, Atlanta, GA, USA, March.

Wampler, C. W., Morgan, A. P., and Sommese, A. J., (1990), "Numerical continuation methods for solving polynomial systems arising in kinematics", *Transactions of the ASME, Journal of Mechanical Design*, vol. 112, pp. 59–68.

Wang, J., and Gosselin, C. M., (2004), "Kinematic Analysis and Design of Kinematically Redundant Parallel Mechanisms", *Transactions of the ASME, Journal of Mechanical Design*, vol. 126, no. 1, pp. 109–118.

Watkins, D. S., (1991), *Fundamentals of Matrix Computations.* John Wiley and Sons Inc: Toronto, ON, Canada.

Wendlandt, J., and Sastry, S., (1994), "Design and Control of a Simplified Stewart Platform for Endoscopy", in *IEEE Conference on Decision and Control*, Lake Buena Vista, FL, USA, pp. 357–362.

Williams II, R. L., and Shelley, B. H., (1997), "Inverse Kinematics for Planar Parallel Manipulators", in *Proceedings of the 1997 ASME Design Technical Conferences, 23rd Design Automation Conference*, Sacramento, CA, USA, 6 pages.

Woo, L. S., and Freudenstein, F., (1970), "Application of Line Geometry to Theoretical Kinematics and the Kinematic Analysis of Mechanical Systems", *Transactions of the ASME, Journal Mechanisms*, vol. 5, pp. 417–460.

Wu, H., Handroos, H., Kovanen, J., Rouvinen, A., Hannukainen, P., Saira, T., and Jones, L., (2003), "Design of Parallel Intersector Weld/Cut Robot for Machining Processes in ITER Vacuum Vessel", *Fusion Engineering and Design*, vol. 69, no. 1, pp. 327–331.

Yoshikawa, T., (1990), *Foundations of Robotics: Analysis and Control.* The MIT Press: Cambridge, MA, USA.

Zhang, Y., and Duffy, J., (1998), "The Optimum Quality Index for a Redundant 4-4 In-Parallel Manipulator", in *Twelfth CISM-IFToMM Symposium on the Theory and Practice of Robots and Manipulators. RoManSy 98*, Paris, France, July, pp. 289–296.

Zhang, Y., Duffy, J., and Crane, C., (2000a), "The Optimum Quality Index for a Redundant 4-8 In-Parallel Manipulator", in *Proceedings of the Advances in Robot Kinematics (ARK) Conference*, Piran, Slovenia, June, pp. 239–248.

Zhang, Y., Duffy, J., and Crane, C., (2000b), "The Optimal Quality Index for a Spatial Redundant 8-8 In-Parallel Manipulator", in *Proceedings of the ASME Mechanisms Conference*, Baltimore, MD, USA, September.

Zibil, A., Firmani, F., Nokleby, S. B., and Podhorodeski, R. P., (2006), "An Explicit Method for Determining the Force-Moment Capabilities of Redundantly-Actuated Planar Parallel Manipulators", *accepted for publication in Transactions of the ASME, Journal of Mechanical Design.*

Zlatanov, D., Fenton, R. G., and Benhabib, B., (1994a), "Singularity Analysis of Mechanism and Robots Via a Motion-Space Model of the Instantaneous Kinematics", in *Proceedings of the 1994 IEEE International Conference on Robotics and Automation*, San Diego, CA, USA, pp. 980–985.

Zlatanov, D., Fenton, R. G., and Benhabib, B., (1994b), "Singularity Analysis of Mechanism and Robots Via a Velocity-Equation Model of the Instantaneous Kinematics", in *Proceedings of the 1994 IEEE International Conference on Robotics and Automation*, San Diego, CA, USA, pp. 986–991.

Zlatanov, D., Fenton, R. G., and Benhabib, B., (1994c), "Uncertainty Configurations of Three-Branch Manipulators: Identification and Elimination", in *Proceedings of the ASME 23rd Biennial Mechanisms Conference*, vol. 72, Minneapolis, MN, USA, September 11-14, pp. 467–476.

Zlatanov, D., Fenton, R. G., and Benhabib, B., (1998a), "Classification and Interpretation of the Singularities of Redundant Mechanisms", in *Proceedings of ASME Design Engineering Technical Conferences*, Atlanta, GA, USA, September 13-16, 11 pages.

Zlatanov, D., Fenton, R. G., and Benhabib, B., (1998b), "Identification and Classification of the Singular Configurations of Mechanisms", *Mechanism and Machine Theory*, vol. 33, no. 6, pp. 743–760.

Zlatanov, D., Bonev, I. A., and Gosselin, C. M., (2002), "Constraint Singularities of Parallel Mechanisms", in *Proceedings of the 2002 IEEE International Conference on Robotics and Automation*, Washington, DC, USA, pp. 496–502.

Appendix A

Kinematics of Manipulators Using Screw Theory

A.1 Overview

In this appendix, the velocity and static forces problems of serial and parallel manipulators using screw coordinates are presented.

A.2 Serial Manipulators

A.2.1 Velocity Solutions

Assume a serial manipulator with n joints. From Chasles Theorem, the velocity of a rigid body, in this case the end-effector of the manipulator, is composed of an angular velocity $\boldsymbol{\omega}$ and a translational velocity $\mathbf{v}$. In terms of screw quantities, the velocity can be considered as the twist about an instantaneous screw axis. Thus,

the end-effector velocity of the manipulator is the sum of all the twists about all the joints (Mohamed and Duffy, 1985), i.e.,

$$\mathbf{V} = \left\{ \begin{array}{c} \boldsymbol{\omega} \\ \mathbf{v} \end{array} \right\} = \sum_{j=1}^{n} \$_j \alpha_{\mathrm{T}_j} \tag{A.1}$$

where $\$_j$ are the screw coordinates of joint j, and α_{T_j} is the twist amplitude of joint j. Written in matrix form yields

$$\mathbf{V} = [\$]\, \boldsymbol{\alpha}_{\mathrm{T}} = [\$]\, \dot{\mathbf{q}} \tag{A.2}$$

where $[\$] = \left[\begin{array}{cccc} \$_1 & \$_2 & \cdots & \$_n \end{array} \right]$ is the screw matrix, also referred to as the Jacobian matrix, and $\boldsymbol{\alpha}_{\mathrm{T}} = \left[\begin{array}{cccc} \alpha_{\mathrm{T}_1} & \alpha_{\mathrm{T}_2} & \cdots & \alpha_{\mathrm{T}_n} \end{array} \right]^{\mathrm{T}}$ is the vector of twist amplitudes[1].

The forward velocity solution of a serial manipulator is defined as the problem that solves for the end-effector velocity $\mathbf{V}$ by knowing the joint rates $\dot{\mathbf{q}}$. This is achieved, for a serial manipulator, by solving Eq. (A.2).

The inverse velocity solution deals with the problem of solving for the joint rates by knowing a desired velocity of the end-effector. Assume that the problem is referred to a six jointed 6-dof manipulator; therefore, the resulting screw matrix $[\$]$ is a 6×6 square matrix. Thus, the inverse velocity problem can be solved by inverting $[\$]$ from Eq. (A.2),

$$\dot{\mathbf{q}} = [\$]^{-1}\, \mathbf{V} \tag{A.3}$$

[1]For serial manipulators, the twist amplitudes are commonly known as the vector of joint rates $\dot{\mathbf{q}}$.

A.2.2 Static Force Solutions

From Poinsot Theorem regarding forces and moments applied on a rigid body, applied forces can be modelled as a wrench applied on the end-effector of the manipulator. The static force problem can be solved using conservation of power; i.e., power in equals power out.

The power developed by the end-effector wrench on its twist must be equal to the power of all actuators (wrench intensities[2]) on the velocity of the joints (twist amplitudes); i.e.,

$$\boldsymbol{\tau}^{\mathrm{T}}\dot{\mathbf{q}} = \mathbf{F} \circledast \mathbf{V} \tag{A.4}$$

To simplify this expression, the screw coordinates of the wrench are interchanged to ray-coordinates (Plücker, 1868-9); i.e.,

$$\mathbf{F} \circledast \mathbf{V} = \mathbf{F'}^{\mathrm{T}}\,\mathbf{V} \tag{A.5}$$

where $\mathbf{F'} = \{\mathbf{m}^{\mathrm{T}}; \mathbf{f}^{\mathrm{T}}\}^{\mathrm{T}}$. Substituting Eq. (A.2) and Eq. (A.5) in Eq. (A.4) yields

$$\boldsymbol{\tau}^{\mathrm{T}}\dot{\mathbf{q}} = \mathbf{F'}^{\mathrm{T}}\,[\$]\,\dot{\mathbf{q}} \tag{A.6}$$

This is true for all $\dot{\mathbf{q}}$; therefore,

$$\boldsymbol{\tau}^{\mathrm{T}} = \mathbf{F'}^{\mathrm{T}}\,[\$] \tag{A.7}$$

Transposing both sides of Eq.(A.7) yields the solution to the inverse static force problem:

$$\boldsymbol{\tau} = [\$]^{\mathrm{T}}\,\mathbf{F'} \tag{A.8}$$

[2]For serial manipulators, the wrench intensities are also referred to as the force/torque vector $\boldsymbol{\tau}$.

The forward static force solution for a non-redundant serial manipulator, i.e., [$] is a square matrix, is obtained by inverting the transpose of the screw matrix, i.e.,

$$\mathbf{F}' = \left([\$]^{\mathrm{T}}\right)^{-1} \boldsymbol{\tau} \tag{A.9}$$

A.3 Parallel Manipulators

A.3.1 Velocity Solutions

Assume a manipulator with n_b branches, each branch containing n joints, and n_k being the actuated joints of the i^{th} branch. Let the platform velocity of the manipulator at the point where the platform is connected to the i^{th} branch be $\mathbf{V}$. Thus, $\mathbf{V}$ can be expressed as the sum of all the twists about all the joints of the i^{th} branch; i.e.,

$$\mathbf{V} = \left\{ \begin{array}{c} \boldsymbol{\omega} \\ \mathbf{v} \end{array} \right\} = \sum_{j=1}^{n} \$_{j_i} \alpha_{\mathrm{T}_{j_i}} \tag{A.10}$$

Let $\mathbf{W}_{k_i}$ be a wrench acting on a screw which is reciprocal to all joints of branch i except for joint k, which is being actuated, i.e.,

$$\$_{j_i} \circledast \mathbf{W}_{k_i} = 0, \text{ for } j \neq k \tag{A.11}$$

The twist amplitude of the k^{th} joint can be solved by taking the reciprocal product of both sides of Eq. (A.10) with $\mathbf{W}_{k_i}$; i.e.,

$$\mathbf{V} \circledast \mathbf{W}_{k_i} = \sum_{j=1}^{n} \$_{j_i} \alpha_{\mathrm{T}_{j_i}} \circledast \mathbf{W}_{k_i} \tag{A.12}$$

Since $\$_{j_i} \circledast \mathbf{W}_{k_i} = 0$ for $j \neq k$, the above expression can be simplified as follows:

$$\mathbf{V} \circledast \mathbf{W}_{k_i} = \$_{k_i} \alpha_{\mathrm{T}_{k_i}} \circledast \mathbf{W}_{k_i} \tag{A.13}$$

Hence,

$$\alpha_{T_{k_i}} = \frac{\mathbf{V} \circledast \mathbf{W}_{k_i}}{\$_{k_i} \circledast \mathbf{W}_{k_i}} \tag{A.14}$$

where $\dot{q}_{k_i} = \alpha_{T_{k_i}}$, with $\dot{q}_{k_i}$ being the joint rate of the k^{th} actuated joint of the i^{th} branch.

The general solution of the inverse velocity problem is presented next. Let $[\mathbf{W}] = [...\mathbf{W}_{k_i}...]$, for $k = 1, \ldots, n_k$, and $i = 1, \ldots, n_b$; i.e., all actuated joints of all branches. Define a diagonal matrix $[\mathbf{D}]$ that contains the inverse of the reciprocal products of the actuated joints and their associated reciprocal screw quantities; i.e.,

$$[\mathbf{D}] = \begin{bmatrix} \ddots & & 0 \\ & \frac{1}{\$_{k_i} \circledast \mathbf{W}_{k_i}} & \\ 0 & & \ddots \end{bmatrix} \tag{A.15}$$

hence,

$$\dot{\mathbf{q}} = [\mathbf{D}]\,[\mathbf{W}]^{T}\,\mathbf{V}' \tag{A.16}$$

where $\mathbf{V}' = \{\mathbf{v}^{T}; \boldsymbol{\omega}^{T}\}^{T}$.

The forward velocity problem of a non-redundantly actuated parallel manipulator, with $[\mathbf{D}]\,[\mathbf{W}]^{T}$ being a square matrix, is found as follows:

$$\mathbf{V}' = ([\mathbf{D}]\,[\mathbf{W}]^{T})^{-1}\,\dot{\mathbf{q}} \tag{A.17}$$

A.3.2 Static Force Solutions

The wrench $\mathbf{F}$ applied by the platform of a parallel manipulator is the sum of the wrenches applied by each actuated joint of the manipulator. A more detailed analysis

is shown in Section 2.4.

$$\mathbf{F} = \left\{ \begin{array}{c} \mathbf{f} \\ \mathbf{m} \end{array} \right\} = \sum_{i=1}^{n_b} \sum_{k=1}^{n_k} \mathbf{W}_{k_i} w_{k_i} = [\mathbf{W}] \ \mathbf{w} \tag{A.18}$$

The force/torque applied by the k^{th} actuated joint of the i^{th} branch can be modelled as follows:

$$\tau_{k_i} = w_{k_i} (\$_{k_i} \circledast \mathbf{W}_{k_i}) \tag{A.19}$$

Therefore, the wrench intensity is

$$w_{k_i} = \frac{\tau_{k_i}}{(\$_{k_i} \circledast \mathbf{W}_{k_i})} \tag{A.20}$$

and in matrix form

$$\mathbf{w} = [\mathbf{D}] \boldsymbol{\tau} \tag{A.21}$$

Substituting Eq. (A.21) in Eq. (A.18) yields the solution to the forward velocity problem, i.e.,

$$\mathbf{F} = [\mathbf{W}] [\mathbf{D}] \boldsymbol{\tau} \tag{A.22}$$

Finally, the inverse static force problem of a non-redundantly actuated parallel manipulator, with $[\mathbf{W}] [\mathbf{D}]$ being a square matrix, is found as follows:

$$\boldsymbol{\tau} = ([\mathbf{W}] [\mathbf{D}])^{-1} \mathbf{F} \tag{A.23}$$

Further details on screw quantities applied on serial and parallel manipulators may be found in Davidson and Hunt (2004).

Appendix B

Kinematics of Planar Parallel Manipulators

B.1 Overview

In this appendix, the inverse displacement problems of the non-redundant planar parallel manipulators studied in this dissertation are solved. In addition, the transformation of the resulting pose, from the origin of frame {ref} to a frame {cen} located at the centre of the mobile platform, is presented.

B.2 Inverse Displacement Solution

B.2.1 Mobile Platform Geometry

The inverse displacement solution of manipulators is referred to as the problem of solving for the three actuated joint displacements by knowing the end-effector's pose,

i.e., $\{ \; x \quad y \quad \phi \; \}^{\mathrm{T}}$. In general, the pose is described by a frame attached to the centre of mass of the mobile platform {cen}. This frame is referred to a global reference frame {0}, which in this case is located at $\{1_1\}$. The position of the connecting points between the mobile platform and the branches, $\{3_i\}$, with respect to {0} can be obtained from the geometry of the platform, as shown in Figure B.1.

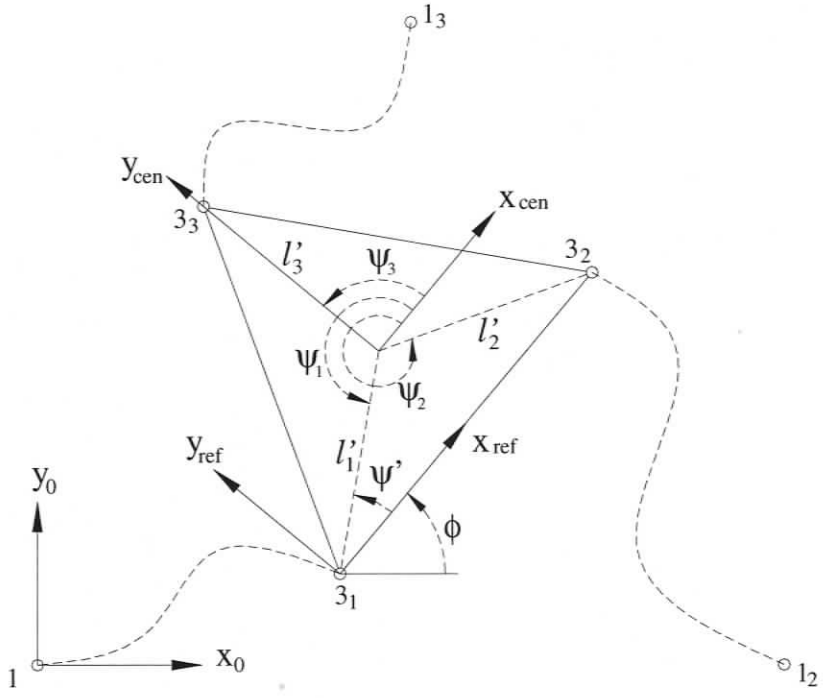

Figure B.1: Geometry of the Mobile Platform.

The position of each connecting point $\{3_i\}$ is found as follows:

$$\left\{ \begin{array}{c} x_{3_i} \\ y_{3_i} \end{array} \right\} = \left\{ \begin{array}{c} x + l'_i \cos(\phi + \psi_i) \\ y + l'_i \sin(\phi + \psi_i) \end{array} \right\} \tag{B.1}$$

B.2.2 Inverse Displacement Solution of the 3-RPR PPM

The displacement of the prismatic joint is obtained as follows:

$$d_{2_i} = \pm\sqrt{(x_{3_i} - bx_i)^2 + (y_{3_i} - by_i)^2} \tag{B.2}$$

yielding two solutions, though the negative solution may not be relevant in a real application.

The passive joints θ_{1_i} and θ_{3_i} are determined as follows:

$$\theta_{1_i} = \text{atan2}\,(y_{3_i} - by_i, x_{3_i} - bx_i) \tag{B.3}$$

and

$$\theta_{3_i} = \phi - \theta_{1_i} - \beta_i \tag{B.4}$$

where $\beta_1 = 0$, $\beta_2 = \pi$, and $\beta_3 = \pi - \alpha_3$.

B.2.3 Inverse Displacement Solution of the 3-PRR PPM

The equations that define the forward displacement problem of each branch are:

$$x_{3_i} = bx_i - d_{1_i}\sin(\gamma_i) + \rho_i\cos(\gamma_i + \theta_{2_i}) \tag{B.5a}$$

$$y_{3_i} = by_i + d_{1_i}\cos(\gamma_i) + \rho_i\sin(\gamma_i + \theta_{2_i}) \tag{B.5b}$$

where d_{1_i} and θ_{2_i} are the unknown values.

By squaring and adding both equations, the terms that involve θ_{2_i} can be eliminated, yielding a second order polynomial in terms of d_i; i.e.,

$$\begin{aligned} d_{1_i}^2 + 2((x_{3_i} - bx_i)\sin(\gamma_i) - (y_{3_i} - by_i)\cos(\gamma_i))d_{1_i} + \\ (x_{3_i} - bx_i)^2 + (y_{3_i} - by_i)^2 - \rho_i^2 = 0 \end{aligned} \tag{B.6}$$

There are up to two solutions for each d_{1_i}; i.e., the smaller root corresponds to the shorter configuration of the prismatic joint and the larger root represents the longer configuration of the prismatic joint.

The passive joints θ_{2_i} and θ_{3_i} can be computed as follows:

$$\theta_{2_i} = \text{atan2}(y_{3_i} - by_i - d_{1_i}\cos(\gamma_i), x_{3_i} - bx_i - d_{1_i}\sin(\gamma_i)) - \gamma_i \tag{B.7}$$

and

$$\theta_{3_i} = \phi - \theta_{2_i} - \gamma_i - \beta_i \tag{B.8}$$

where $\beta_1 = 0$, $\beta_2 = \pi$, and $\beta_3 = \pi - \alpha_3$.

Thus, for the overall manipulator, there are up to eight solutions of the inverse displacement problem or working modes.

B.2.4 Inverse Displacement Solution of the 3-RRR PPM

The equations that define the forward displacement problem of each branch are:

$$x_{3_i} = bx_i + \rho_{i+3}\cos(\theta_{1_i}) + \rho_i\cos(\theta_{1_i} + \theta_{2_i}) \tag{B.9a}$$

$$y_{3_i} = by_i + \rho_{i+3}\sin(\theta_{1_i}) + \rho_i\sin(\theta_{1_i} + \theta_{2_i}) \tag{B.9b}$$

where θ_{1_i} and θ_{2_i} are the unknown values.

Squaring and adding both equations yields

$$(x_{3_i} - bx_i)^2 + (y_{3_i} - by_i)^2 = \rho_{i+3}^2 + \rho_i^2 + 2\rho_{i+3}\rho_i\cos(\theta_{2_i}) \tag{B.10}$$

Thus,

$$\cos(\theta_{2_i}) = \frac{(x_{3_i} - bx_i)^2 + (y_{3_i} - by_i)^2 - \rho_{i+3}^2 - \rho_i^2}{2\rho_{i+3}\rho_i} \tag{B.11}$$

and

$$\sin(\theta_{2_i}) = \pm\sqrt{1 - \cos^2(\theta_{2_i})} \tag{B.12}$$

Hence, there are two solutions of θ_{2_i},

$$\theta_{2_i} = \text{atan2}(\sin(\theta_{2_i}), \cos(\theta_{2_i}))$$

Using Craig's solution (Craig, 1987), let the forward displacement equations be written as follows:

$$x_{3_i} - bx_i = k_{1_i}\cos(\theta_{1_i}) - k_{2_i}\sin(\theta_{1_i}) \tag{B.13a}$$

$$y_{3_i} - by_i = k_{1_i}\sin(\theta_{1_i}) + k_{2_i}\cos(\theta_{1_i}) \tag{B.13b}$$

where

$$k_{1_i} = \rho_{i+3} + \rho_i\cos(\theta_{2_i}) \tag{B.14a}$$

$$k_{2_i} = \rho_i\sin(\theta_{2_i}) \tag{B.14b}$$

Hence, the actuated joints θ_{1_i} and θ_{3_i} are given by

$$\theta_{1_i} = \text{atan2}(y_{3_i} - by_i, x_{3_i} - bx_i) - \text{atan2}(k_{2_i}, k_{1_i}) \tag{B.15}$$

and

$$\theta_{3_i} = \phi - \theta_{1_i} - \theta_{2_i} - \beta_i \tag{B.16}$$

where $\beta_1 = 0$, $\beta_2 = \pi$, and $\beta_3 = \pi - \alpha_3$.

All the combinations of θ_{2_i} lead to up to eight working modes.

B.3 Reference Frame Transformation

The obtained numerical value of the mobile platform position (x and y) is referred to as the origin of *{ref}*. Nevertheless, it can be transformed to a frame *{cen}* located at the centre of the platform and oriented as *{ref}* with the following homogeneous transform,

$$ {}^{0}\mathbf{P}_{0 \longrightarrow \text{cen}} = {}^{0}_{\text{ref}}[\mathbf{T}]\, {}^{\text{ref}}\mathbf{P}_{\text{ref} \longrightarrow \text{cen}} \tag{B.17} $$

where

$$ {}^{0}_{\text{ref}}[\mathbf{T}] = \begin{bmatrix} \cos(\phi) & -\sin(\phi) & 0 & x \\ \sin(\phi) & \cos(\phi) & 0 & y \\ 0 & 0 & 1 & 0 \\ 0 & 0 & 0 & 1 \end{bmatrix} \quad \text{and} \quad {}^{\text{ref}}\mathbf{P}_{\text{ref} \longrightarrow \text{cen}} = \begin{Bmatrix} l'_1 \cos(\psi') \\ l'_1 \sin(\psi') \\ 0 \\ 1 \end{Bmatrix}. $$

Appendix C

Elimination Methods

C.1 Overview

In this appendix, elimination methods are described. First, kinematic problems that require elimination methods are presented. Second, a prediction of the number of possible solutions in a polynomial system of equations is presented. Third, elimination methods are described, namely, numerical methods, continuation method, dialytic elimination, and Gröbner Bases.

C.2 Background

In general, kinematic problems of manipulators involve systems of nonlinear equations which can be reduced to a single polynomial in one variable. A common problem in robotics is the inverse kinematics of serial manipulators which leads to multiple solutions and the complexity of the problem depends on the architecture of the manipulator. For example, the inverse kinematics of manipulators with a spherical

group of joints at the wrist can be solved using the wrist partitioned method. An analytical solution of manipulators with this particular architecture was developed by Pieper (1969) yielding a 4^{th}-order polynomial in one variable. Nevertheless, when a manipulator has an arbitrary geometry, such as a link between the joints comprised in the wrist, the inverse kinematics problem becomes more complex.

Among early works related to the inverse kinematics of six revolute joint[1] ($6R$) manipulators, Pieper (1969) and Roth et al. (1973) appear to be the most significant. Albala and Angeles (1979) provided a determinant of a 12×12 matrix, whose entries were quadratic polynomials by substituting the tangent of the half-angle of one of the variables. Duffy and Crane (1980) found a 32 degree polynomial by following the same substitution. Tsai and Morgan (1985) claimed the existence of at most 16 solutions by using polynomial continuation of eight second-degree equations. Angeles (1985) applied the Gauss-Newton optimization method to minimize a function, which is the Euclidean norm of the end-effector between the actual and the desired position. Gupta and Kazerounian (1985) modified the Newton-Raphson method, which had been used previously on the governing kinematic equations, in order to make it more reliable and stable. Later on, Gupta and Singh (1989) reduced the computation time of the algorithm proposed by Gupta and Kazerounian (1985). Primrose (1986) confirmed the existence of at most 16 solutions and proved that the remaining 16 solutions found by Duffy and Crane (1980) were complex parts. Kazerounian (1987) developed an algorithm which is based on the sequential motion of joints.

The first attempts at solving the inverse kinematics of arbitrary geometry of 6R

[1]Manipulators with six revolute joints are considerd beacause, revolute joints (nonlinear) lead to more complicated equations than prismatic joints (linear).

manipulators were based on iterative techniques. However, these techniques have the weakness of not being efficient for practical applications and also being incapable of determining all solutions.

Using vector algebra, Lee and Liang (1988a and 1988b) derived a 16^{th} order polynomial for the input-output displacement equation of the general $7R$ spatial mechanism by applying half-angle substitution. Raghavan and Roth (1989 and 1993) presented the first method that may be used to calculate the characteristic polynomial of a $6R$ manipulator with general geometry. This was achieved using an elimination technique based on some implicit relations between the coefficients of independent loop-closure equations and dialytic elimination. This characteristic polynomial was obtained from 14 scalar equations. Manocha and Canny (1992 and 1994), and Kohli and Osvatic (1992 and 1993) successfully reduced the execution time of the Raghavan and Roth method.

The forward kinematics of parallel manipulators is another example of systems of nonlinear equations. For the Stewart-Gough platform (*6-3* layout), Innocenti and Parenti-Castelli (1990) determined forward displacement solutions by finding the roots of a single variable 16^{th} order polynomial based on the three loop-closure equations of an equivalent spatial mechanism. Similarly, 16 solutions of this layout were found by Nanua et al. (1990). For the 6-6 layout, or the general Stewart-Gough manipulator, Raghavan (1993) demonstrated with numerical examples, based on the continuation method, that the maximum number of solutions is 40. Husty (1996) determined a 40^{th} order univariable polynomial that describes all possible solutions of the general Stewart-Gough platform. Although a symbolic solution was obtained, this procedure seems to be difficult to automate (Merlet, 2004).

C.3 Polynomials and Number of Solutions

C.3.1 Definitions

A polynomial is an equation whose variable(s) appear in positive integer exponents. Assume a single variable polynomial, i.e.,

$$f(x) = a_0 x^n + a_1 x^{n-1} + \ldots + a_{n-1} x + a_n = 0 \tag{C.1}$$

The degree of a single variable polynomial is the largest integer power n, (Fraleigh, 1976). A fundamental theorem of algebra states that in a n^{th}-order polynomial there are n roots or solutions.

Now consider a multivariable polynomial, i.e.,

$$f(x_1, x_2) = a_0 x_1^n x_2^m + a_1 x_1^{n-1} x_2^m + a_2 x_1^{n-1} x_2^{m-1} + \ldots + a_r = 0 \tag{C.2}$$

where $r = (n+1)(m+1) - 1$. This polynomial is composed of terms (or monomials) in x_1 and x_2. Each monomial contains a coefficient a_i and a power product $x_1^{\eta} x_2^{\mu}$. The degree of each power product is the sum of its exponents $(\eta + \mu)$. The degree of a multivariable polynomial is equal to the largest degree of the power products $(n + m)$.

C.3.2 Bezout's Theorem

Let a system of n multivariable polynomials in n variables be

$$\begin{aligned} f_1(x_1, x_2, \ldots, x_n) &= 0 \\ f_2(x_1, x_2, \ldots, x_n) &= 0 \\ &\vdots \\ f_n(x_1, x_2, \ldots, x_n) &= 0 \end{aligned} \tag{C.3}$$

The degree of a system of multivariable polynomials is the product of the degrees of each multivariable polynomial. That is, if d_i is the degree of the i^{th} multivariable polynomial, the total degree of the system is given by

$$d_{\mathrm{T}} = \prod_{i=1}^{n} d_i \tag{C.4}$$

Bezout's Theorem (Tsai, 1999) states that a polynomial system of total degree d_{T} has at most d_{T} solutions. This number, also known as Bezout's number, is usually a loose upper bound on the number of finite solutions.

C.3.3 M-Homogeneous Bezout's Number

In order to reduce the number of superfluous solutions, Wampler et al. (1990) proposed a formulation to determine the total degree of a multivariable polynomial system using multihomogeneous variables. This formulation is based on associating the variables in groups and transforming each group into a corresponding homogenous set of variables (Tsai, 1999). The m-homogeneous formulation combines the variables of a polynomial system into m homogeneous groups. The combination of the variables in the groups will depend on the occurrence of the variables in the polynomial system. Given a set of n polynomials in n variables, as shown in Eq. (C.3), the system is divided into m groups, say $\{x_{11}, \ldots, x_{1k_1}\}$, $\{x_{21}, \ldots, x_{2k_2}\}$, $\ldots$,$\{x_{m1}, \ldots, x_{mk_m}\}$, where k_j is the number of variables in group j, with $k_1 + k_2 + \ldots + k_m = n$. Then, a homogeneous variable for each group is introduced, say y_{01}, $y_{02}, \ldots, y_{0m}$, by substituting $x_{ij} = y_{ij}/y_{0j}$. Denominators are then cleared. Let β_j for $j = 1$ to m denote the m groups of variables. Let the degree of equation i with respect to the variables of group j be d_{ji}. Bezout's number is computed by summing over j of the product $d_{ji}\beta_j$ for each m homogeneous equation, resulting in n linear equations in β_j with d_{ji}

as their coefficients. The product of these linear equations leads to a polynomial in β_j, i.e.,

$$\prod_{i=1}^{m}\left(\sum_{j=1}^{m} d_{ji}\beta_j\right) = (d_{11}\beta_1 + \ldots + d_{1m}\beta_m)(d_{21}\beta_1 + \ldots + d_{2m}\beta_m) \ldots (d_{n1}\beta_1 + \ldots + d_{nm}\beta_m) \quad \text{(C.5)}$$

Finally, the multihomogenous Bezout's number is equal to the coefficient of $\prod_{j=1}^{m}\beta_j^{k_j}$ obtained in Eq. (C.5).

Example.-

Assume the following polynomial system (Morgan and Sommese, 1987):

$$x_1^2 = 1$$

$$x_1 x_2 = 1$$

This system of two polynomials leads to the intersection of two vertical lines $x_1 = \pm 1$ with a parabola as shown in Figure C.1.

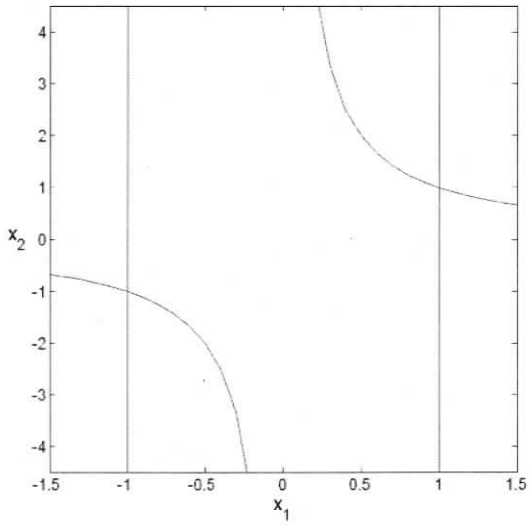

Figure C.1: Two Vertical Lines Intersecting a Parabola.

Despite Bezout's number, which is 4, there are only two finite solutions; i.e., $(x_1, x_2) = (1, 1)$ and $(x_1, x_2) = (-1, -1)$.

Separate the variables into two groups $\{x_1\}$ and $\{x_2\}$; hence, $k_1 = 1$, $k_2 = 1$, and $m = 2$. A homogenous set of variables is introduced, $x_1 = y_1/y_3$ and $x_2 = y_2/y_4$, and the denominators are cleared yielding:

$$\begin{aligned} y_1^2 &= y_3^2 \\ y_1 y_2 &= y_3 y_4 \end{aligned}$$

The degrees of the 2-homogenous system (2, because there are two homogeneous variables) are obtained and tabulated in Table C.1.

Table C.1: Degree of the 2-Homogeneous System.

Equation (i)	Group 1 ($j = 1$)	Group 2 ($j = 2$)
1	2	0
2	1	1

Then, Eq. (C.5) is computed yielding

$$\prod_{i=1}^{m} \left(\sum_{j=1}^{m} d_{ji} \beta_j \right) = (2\beta_1)(\beta_1 + \beta_2) = 2\beta_1^2 + 2\beta_1\beta_2 \tag{C.6}$$

where the coefficient of $\prod_{j=1}^{2} \beta_j^{k_j} = 2$ represents the 2-homogeneous Bezout's number. Therefore, this polynomial system results in, at most, 2 finite solutions. The reduction in the number of real solutions is due to a reduction in the number of solutions at infinity. It is important to mention that for a general polynomial system many different forms of grouping variables exist, each one leading to its associated m-homogeneous number (Raghavan and Roth, 1995).

The multi-homogeneous Bezout number, which is significantly smaller than the traditional Bezout's number, is still a bound for the number of solutions of the homogeneous polynomial system. That is, besides potential solutions, the m-homogeneous Bezout number includes solutions at infinity and extraneous solutions (Tsai, 1999).

C.4 Numerical Methods

Numerical methods are often considered to solve sets of nonlinear equations. Based on an iterative routine, these methods require an initial guess at a solution and through an optimization technique "the closest" solution to the initial guess can be found. Since kinematic problems of manipulators have multiple solutions, more initial guesses must be carried out to find the remaining solutions, but this does not guarantee that all solutions will be found.

C.5 Continuation Method

Roth and Freudenstein (1963) developed a numerical method known as the *bootstrap method* for solving problems associated with the synthesis of five-bar mechanisms. This numerical procedure was subsequently improved as the continuation method (Saaty, 1981). Based on this method, Tsai and Morgan (1985) solved the inverse kinematics of a general $6R$ serial manipulator. Raghavan (1993) identified up to 40 solutions for the general Stewart-Gough platform forward kinematics using the continuation method.

The continuation method is based on incorporating a reasonable initial guess and

solving for all possible solutions. Assume a set of n polynomials in n variables:

$$F(\mathbf{x}) = \begin{cases} f_1(x_1, x_2, \ldots, x_n) = 0 \\ f_2(x_1, x_2, \ldots, x_n) = 0 \\ \vdots \\ f_n(x_1, x_2, \ldots, x_n) = 0 \end{cases} \tag{C.7}$$

where $F(\mathbf{x}) = (f_1, f_2, \ldots, f_n)$ is referred to as the target system.

The continuation method requires the construction of a start system, $G(\mathbf{x}) = 0$. Any system can be used as a starting system for a given target system as long as it follows three basic rules:

- All the solutions of the start system must be known.
- All the solutions of the start system must be nonsingular.
- The start system must have the same multihomogeneous structure and degree as the target system $F(\mathbf{x})$; i.e., $G(\mathbf{x})$ must have exactly as many regular solutions as $F(\mathbf{x})$.

A simple start system for a 1-homogeneous transform is

$$G(\mathbf{x}) = \begin{cases} g_1(x_1) = p_1^{d_1} x_1^{d_1} - q_1^{d_1} = 0 \\ g_2(x_2) = p_2^{d_2} x_2^{d_2} - q_2^{d_2} = 0 \\ \vdots \\ g_n(x_n) = p_n^{d_n} x_n^{d_n} - q_n^{d_n} = 0 \end{cases} \tag{C.8}$$

where d_i is the degree of f_i; p_i and q_i are random non-zero numbers.

For multihomogeneous systems, it is desired to have a start system with the same m-homogeneous Bezout's number. An initial system with an identical polynomial

structure can be generated by a product of factors, i.e.,

$$g_i(\mathbf{x}) = \prod_{j=1}^{m} h_{ij}(x_{1j}, x_{2j}, \ldots, x_{k_j j}) = 0 \tag{C.9}$$

where h_{ij} is a polynomial of degree d_{ij}, and k_j denotes the number of variables in the j^{th} group.

The idea of the continuation method is based on "small changes in the parameters of the system of equations result in small changes in the numerical values of the solutions" (Raghavan and Roth, 1995). That is, if the solution of the start system ($G(\mathbf{x}) = 0$) is known, solutions of a similar system ($F(\mathbf{x})$) can be computed by tracking the solutions of $G(\mathbf{x})$ as its coefficients are gradually modified to those of $F(\mathbf{x})$ in small increments. This perturbation is carried out by a real parameter t, called the continuation parameter, which varies from 0 to 1. The relation between the solutions of the start system and the solutions of the target system is given by a homotopy function $H(\mathbf{x}, t) = 0$ of the form:

$$H(\mathbf{x}, t) = (1 - t)e^{i\theta}G(\mathbf{x}) + tF(\mathbf{x}) \tag{C.10}$$

where $e^{i\theta}$ is a random complex constant.

It is clear, from Eq. (C.10), that at $t = 0$ the homotopy function equals the start system, i.e., $H(\mathbf{x}, 0) = G(\mathbf{x})$ and at $t = 1$ the homotopy function equals the target system, i.e., $H(\mathbf{x}, 1) = F(\mathbf{x})$. Thus, the idea is to vary the continuation parameter t from 0 to 1 in small increments and to use an optimization iterative method (Antoniou and Lu, 2002) to obtain the solutions of the deformed polynomials at each step of the deformation. The solutions from the previous step are used as the initial guess for the current step. The transition of each solution follows a homotopy path. Finally, at $t = 1$ the numerical solutions of $H(\mathbf{x}, 1)$ match the solutions of the

original polynomial system $F(\mathbf{x})$. The term $e^{i\theta}$ is inserted into Eq. (C.10) for two reasons: existence of complex solutions and elimination of possible singular solutions. A system of polynomials with real coefficients may have complex solutions. Thus, it is important to consider a start system such that all the start solutions are complex-valued. Besides, the factor $e^{i\theta}$ changes the roots of the system when $t \neq 1$, but it does not affect the final solution when $t = 1$. Singular solutions may occur when using the Newton-Raphson iterative method, i.e., when the Jacobian of $H(\mathbf{x}, t)$ is singular. If the Jacobian of $H(\mathbf{x}, t)$ were singular, it would cause a failure in the Newton-Raphson iterative method and the solutions of $F(\mathbf{x})$ would not be possible to compute (Raghavan and Roth, 1995). Wampler et al. (1990) commented that in years of using this method, no randomly chosen θ has yielded a singular solution. In conclusion, the method satisfies the following properties of homotopy (Li, 1997):

- *Triviality.*- The solutions of $G(\mathbf{x}) = 0$ can be found in closed form.
- *Smoothness.*- No singularities along the solution of $H(\mathbf{x}, t) = 0$ due to $e^{i\theta}$.
- *Accessibility.*- Every isolated solution of $F(\mathbf{x}) = 0$ is found from a solution of $G(\mathbf{x}) = 0$.

Example.-

Assume the following polynomials:

$$f_1(x, y) = (6x - 6)^2 + (2y - 1)^2 - 169 = 0 \quad \text{(C.11a)}$$

$$f_2(x, y) = (x - 1)^2(8 - y)^2 + 16y^3 - 48y^2 - 256 = 0 \quad \text{(C.11b)}$$

where, $f_1(x, y) = 0$ is an ellipse and $f_2(x, y) = 0$ is a complicated cubic polynomial, as shown in Figure C.2.

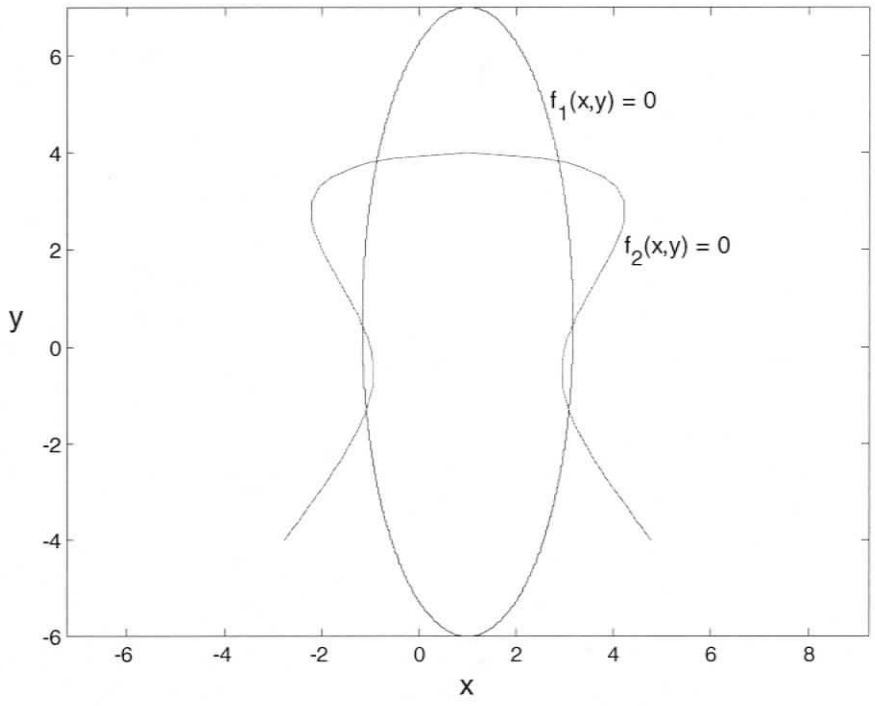

Figure C.2: Example of Two Polynomials Intersecting at Six Points.

According to Bezout's number, there is a maximum of eight possible solutions. However, as shown in Figure C.2, there are six real solutions and one pair of complex solutions.

Assume the following start system:

$$g_1(x) = (x+1)(x-3) = 0 \tag{C.12a}$$

$$g_2(y) = (y-1)(y+1)(y-3)(y+2) = 0 \tag{C.12b}$$

It is clear that the solutions for the start system polynomials are $x = -1$ and $x = 3$ for $g_1(x) = 0$, and $y = 1$, $y = -1$, $y = 3$, and $y = -2$ for $g_2(x) = 0$. Thus, there are eight combinations among the solutions of the start system: $(-1, 1)$, $(-1, -1)$,

$(-1,3)$, $(-1,-2)$, $(3,1)$, $(3,-1)$, $(3,3)$, and $(3,-2)$. The homotopy function is generated as follows:

$$H(x,y,t) = (1-t)e^{i\theta}\begin{bmatrix} g_1(x) \\ g_2(y) \end{bmatrix} + t\begin{bmatrix} f_1(x,y) \\ f_2(x,y) \end{bmatrix} = \bar{0} \tag{C.13}$$

The complex parameter is arbitrarily chosen $\theta = \pi/2$, i.e., $e^{i\theta} = i$, yielding

$$H(x,y,t) = \begin{bmatrix} h_1(x,y,t) \\ h_2(x,y,t) \end{bmatrix} = \bar{0} \tag{C.14}$$

where

$$h_1(x,y,t) = 9x^2t - 18xt - 33t + y^2t - yt + (x^2 - x^2t - 2x + 2xt - 3 + 3t)\,i = 0$$

$$h_2(x,y,t) = 64x^2t + y^2x^2t - 16yx^2t - 128xt - 2y^2xt + 32yxt + 16y^3t - 192t$$
$$-16yt - 47y^2t + (1-t)\,(y^4 - y^3 - 7y^2 + y + 6)\,i = 0$$

The continuation parameter (t) is varied from 0 to 1 with an increment of 0.01. The MATLAB function `fminsearch` (MathWorks, 2001) is employed to minimize $H(x,y,t) = \bar{0}$ at each interval of t for every combination of the solutions. The results, for $\Delta t = 0.01$ and optimset('TolX',$1e-6$,'TolFun',$1e-12$), are shown in Table C.2.

All six real solutions were obtained; however, the expected pair of complex solutions diverged from its homotopy path and turned out to follow a different path yielding two repeated real solutions, i.e., solutions 2 and 4, and solutions 6 and 8 are the repeated roots.

Table C.2: Solutions of the Polynomial System Using the Continuation Method.

Solution	Initial x_0	Initial y_0	Solution x	Solution y	$H(x, y, t) = 0$
1	-1	1	-1.1666581	0.4817119	5.371e-12
2	-1	-1	-1.0803741	-1.3161476	7.79e-12
3	-1	3	-0.8600698	3.8333562	1.618e-11
4	-1	-2	-1.0803741	-1.3161476	3.10e-12
5	3	1	3.1666581	0.4817119	2.57e-12
6	3	-1	3.0803741	-1.3161476	2.603e-11
7	3	3	2.8600698	3.8333562	2.02e-12
8	3	-2	3.0803741	-1.3161476	2.44e-11

C.6 Dialytic Elimination

A well known technique for reduction of polynomial systems is the Sylvester dialytic elimination method. This method is attributed to Sylvester (1841) and Cayley (1848). It is based on Sylvester matrices whose entries are either zeroes or coefficients of polynomials. The method requires the derivation of an equation known as the eliminant. Salmon (1885) developed various methods to formulate the eliminant. Roth (1993) modified the dialytic method to make it more suitable for kinematic problems. This method has been used to find the solutions of the inverse kinematics of serial manipulators by Lee and Liang (1988a and 1988b) and Raghavan and Roth (1989 and 1993). Also, Innocenti and Parenti-Castelli (1990) and Nanua et al. (1990) applied this method to find the solutions of the forward kinematics for the Stewart-Gough platform (*6-3* layout).

Assume a set of two polynomials in terms of two variables, x and y. The dialytic elimination method can be summarized in six steps:

1. Suppress one of the variables, say y (consider it as a constant).
2. Linearize the power products of the remaining variable (x).
3. Generate new linear equations, so that the number of power products matches the number of linear equations, and write these equations in matrix form.
4. Set the determinant of the coefficient matrix to zero and obtain the characteristic polynomial in terms of the suppressed variable (y).
5. Determine the roots of the polynomial.
6. Substitute the roots of the polynomial and solve the linear system for the remaining unknowns.

Steps 4 and 5 can be combined by computing the eigenvalues of the coefficient matrix.

This method can be applied to a relatively small set of variables in the polynomials because the resulting polynomial can increase its degree exponentially introducing a large number of superfluous solutions.

Example.-

Assume the same polynomials used in Section C.4,

$$f_1(x,y) = (6x-6)^2 + (2y-1)^2 - 169 = 0 \tag{C.15a}$$

$$f_2(x,y) = (x-1)^2(8-y)^2 + 16y^3 - 48y^2 - 256 = 0 \tag{C.15b}$$

which are expanded:

$$f_1(x,y) = 9x^2 - 18x + y^2 - y - 33 = 0 \tag{C.16a}$$

$$f_2(x,y) = \left(y^2 - 16y + 64\right)x^2 + \left(-2y^2 + 32y - 128\right)x + 16y^3 - 47y^2 - 16y - 192 = 0 \tag{C.16b}$$

Suppress one variable (y) yielding

$$f_1(x,y) = a_{10}x^2 + a_{11}x + a_{12} = 0 \tag{C.17a}$$

$$f_2(x,y) = a_{20}x^2 + a_{21}x + a_{22} = 0 \tag{C.17b}$$

where

$a_{10} = 9$ $\quad a_{12} = y^2 - y - 33$ $\quad a_{21} = -2y^2 + 32y - 128$

$a_{11} = -18$ $\quad a_{20} = y^2 - 16y + 64$ $\quad a_{22} = 16y^3 - 47y^2 - 16y - 192$

Write Eqs.(C.17a) and (C.17b) in matrix form:

$$\begin{bmatrix} a_{10} & a_{11} & a_{12} \\ a_{20} & a_{21} & a_{22} \end{bmatrix} \begin{bmatrix} x^2 \\ x \\ 1 \end{bmatrix} = \begin{bmatrix} 0 \\ 0 \end{bmatrix} \tag{C.18}$$

Generate more equations such that the number of equations is as many as the number of power products, which are considered as linear terms. This is carried out by multiplying both equations of Eq. (C.18) by x, yielding

$$\begin{bmatrix} a_{10} & a_{11} & a_{12} & 0 \\ a_{20} & a_{21} & a_{22} & 0 \\ 0 & a_{10} & a_{11} & a_{12} \\ 0 & a_{20} & a_{21} & a_{22} \end{bmatrix} \begin{bmatrix} x^3 \\ x^2 \\ x \\ 1 \end{bmatrix} = \begin{bmatrix} 0 \\ 0 \\ 0 \\ 0 \end{bmatrix} \tag{C.19}$$

Set the determinant of the coefficient matrix, which is a function of y, to zero. This leads to a polynomial in y of the form:

$$-16(y^4 - 161y^3 + 470y^3 + 608y - 384)^2 = 0 \tag{C.20}$$

Due to the nature of the polynomials, there are two solutions of x for each real solution of y, as shown in Figure C.2. Determine the roots of the polynomial and substitute them in Eq. (C.16a) to obtain the corresponding two solutions of x for each solution of y. As an alternative, the substitution can be performed using Gauss elimination, i.e., Eq. (C.18) may be written in the following form $\mathbf{Ax} = \mathbf{b}$; however, due to the nature of the polynomials matrix $\mathbf{A}$ turned out to be rank deficient. The solutions of x and y are presented in Table C.3.

Table C.3: Solutions of the Polynomial System Using the Dialytic Elimination.

Solution	Solution y	Solution x
1	158.00108	$1 + 52.45563i$
2		$1 - 52.45563i$
3	3.8333562	2.8600698
4		-0.8600698
5	-1.3161476	3.0803741
6		-1.0803741
7	0.4817119	3.1666581
8		-1.1666581

C.7 Gröbner Bases

C.7.1 Introduction

Gröbner Bases (Buchberger, 1965) is another analytic method based on converting a set of polynomial equations $F(\mathbf{x}) = 0$ into an equivalent system $G(\mathbf{x}) = 0$, where $G(\mathbf{x}) = 0$ is structured in a triangular form, analogous to the Gauss elimination method applied to linear equations. Both sets of polynomials, $F(\mathbf{x}) = 0$ and $G(\mathbf{x}) = 0$, are equivalent bases; that is, they generate the same ideal.

C.7.2 Definitions

A polynomial has real coefficients and non-negative integer exponents. A set of polynomials in n variables is denoted as $R[x_1, \ldots, x_n]$.

A *ring* $(k[x_1, \ldots, x_n])$ is a set of elements that satisfies basic algebraic properties of addition and multiplication (binary operations): associative, commutative, distributive, identity, and inverse; i.e., for a, b, $c \in k$:

$a + b \in k$	for $0 \in k$ then $a + 0 = a$
$(a + b) + c = a + (b + c)$	for $1 \in k$ then $1 * a = a * 1 = a$
$a + b = b + a$	for $-a \in k$ then $a + (-a) = 0$
$a * b \in k$	$a * (b * c) = (a * b) * c$
$a * (b + c) = a * b + a * c$ and	$(b + c) * a = b * a + c * a$

The most common types of rings are integers $(\mathbb{Z})$ and polynomials.

A *field* (k) is a commutative ring that has an additional property, the multiplicative inverse, i.e., $(a * a^{-1} = 1)$. Neither integers nor polynomials have this property.

Examples of fields are complex numbers ($\mathbb{C}$), rational numbers ($\mathbb{Q}$), and real numbers ($\mathbb{R}$).

The *variety*, $V(f_1, \ldots, f_n)$ defined by polynomials $\{f_1, \ldots, f_n\} \in k[x_1, \ldots, x_n]$ can be expressed as the common roots of a set of polynomials.

An ideal (I) is contained in the set of polynomials, i.e., $I \subset R[x_1, \ldots, x_n]$, if the following conditions are satisfied:

i) $f_1 + f_2 \in I$ for all $f_1, f_2 \in I$

ii) $f\,h \in I$ for all $f \in I$ and $h \in k[x_1, \ldots, x_n]$

Therefore, the ideal of a set of polynomials $\langle f_1, \ldots, f_n \rangle$ is defined as

$$\langle f_1, \ldots, f_n \rangle = \left\{ \sum_{i=1}^{n} h_i f_i \mid h_i \in k[x_1, \ldots, x_n], i = 1, \ldots, n \right\} \tag{C.21}$$

The set $\{f_1, \ldots, f_n\}$ is called a *generating set*, or generator, of the ideal I. The desired "better" representation of the variety is the desired "better" generating set for the ideal $\langle f_1, \ldots, f_n \rangle$. A "better" generating set for I is called a Gröbner Basis for I. For instance, a matrix that has undergone Gaussian elimination is said to be in row echelon form and this is the "better" generating set of a linear system of equations (Adams and Loustaunau, 1994).

Theorem C.1- (Hilbert Basis Theorem). If I is any ideal of the ring $k[x_1, \ldots, x_n]$, then there exist polynomials $\{f_1, \ldots, f_s\}$ such that $I = \langle f_1, \ldots, f_s \rangle$. That is, every ideal in $k[x_1, \ldots, x_n]$ is finitely generated.

C.7.3 Fundamentals

Lexicographic Order and Terminology

To solve for the roots of a set of polynomials, it is important to specify an order on the power products. There are many ways to order power products. First, the order of the variables has to be specified. For instance, if $x > y > z$, then x is maximal to y, and similarly x and y are maximal to z.

There are three types of orders, lexicographical order (*lex*), degree lexicographical order (*deglex*), and reverse lexicographical order (*degrevlex*), which are defined as:

lex. - The variable order ($x > y$) and the power of the variables, e.g.,

$$1 < y < y^2 < y^3 < ... < x < xy < xy^2 ... < x^2 < ... \tag{C.22}$$

deglex. - The degree of the term and in case of a tie *lex* (say $x > y$) breaks it, e.g.,

$$1 < y < x < y^2 < xy < x^2 < y^3 < xy^2 < x^2y < x^3 < ... \tag{C.23}$$

degrevlex. - The degree of the term and in case of a tie, for the terms $x^{\mu_1}y^{\mu_2}z^{\mu_3} < x^{\eta_1}y^{\eta_2}z^{\eta_3}$, the first coordinates μ_i and η_i from the right that are different satisfy $\mu_i > \eta_i$. That is, the rightmost variable is the least maximal, so a less maximal variable with a larger power makes the entire power product less than another term with the same degree, e.g.,

$$x^2yz < xy^3 \qquad \begin{matrix}(2,1,1) < (1,3,0) \\ \mu_3 > \eta_3\end{matrix} \tag{C.24}$$

The reason that three variables were considered for this term order is because two variables would have led to the same order as *deglex* (Adams and Loustaunau, 1994). Note that the order in Eq. (C.24) would have been the opposite of the *deglex* order.

In a polynomial, the order of the terms is defined in decreasing order in the maximal variable, e.g.,

$$f(x,y,z) = \underbrace{4x^3yz}_{x^3} - \underbrace{2x^2y^2z^3 + 6x^2y}_{x^2} - \underbrace{3xy^2z^2}_{x^1} + \underbrace{5y^2z}_{x^0} \tag{C.25}$$

The leading term $lt(f)$ of a polynomial f is the term that is maximal in the polynomial. The leading coefficient $lc(f)$ of the polynomial f is the coefficient of the leading term in f. The leading power product $lp(f)$ of f is the power product of the leading term. Thus, $lt(f) = lc(f)lp(f)$. For the polynomial of Eq. (C.25), the leading elements are:

$$lt(f) = 4x^3yz \qquad lc(f) = 4 \qquad lp(f) = x^3yz \tag{C.26}$$

The least common multiple (lcm) of monomials $x_1^{\mu_1}x_2^{\mu_2}x_3^{\mu_3}...$ and $x_1^{\eta_1}x_2^{\eta_2}x_3^{\eta_3}...$ is $x_1^{\gamma_1}x_2^{\gamma_2}x_3^{\gamma_3}...$, where $\gamma_i = \max(\mu_i, \eta_i)$, e.g., the $lcm\,(x^6y^2z^2, x^3y^4z^2) = x^6y^4z^2$.

Polynomial Division

Assume the set of polynomials described in Section C4 ordered in a lexicographical order form $x > y$, with $g = f_1(x,y)$ and $f = f_2(x,y)$ as follows:

$$g = 9x^2 - 18x + y^2 - y - 33 = 0 \tag{C.27a}$$

$$f = \left(y^2 - 16y + 64\right)x^2 + \left(-2y^2 + 32y - 128\right)x + 16y^3 - 47y^2 - 16y - 192 = 0 \tag{C.27b}$$

Perform the polynomial division to eliminate the terms that contain variable x, but first, for convenience through the division process, multiply Eq. (C.27b) by 9,

which is the leading coefficient in Eq. (C.27a), i.e., $lc(g) = 9$.

$$
\begin{array}{r|l}
 & \overbrace{y^2 - 16y + 64}^{\text{quotient } (q)} \\
9x^2 - 18x + y^2 - y - 33 & 9y^2x^2 - 144yx^2 + 576x^2 - 18y^2x + 288yx - 1152x + 144y^3 - 423y^2 - 144y - 1728 \\
 & \underline{9y^2x^2 - 18xy^2 + y^4 - y^3 - 33y^2} \\
 & \quad -144yx^2 + 576x^2 + 288yx - 1152x - y^4 + 145y^3 - 390y^2 - 144y - 1728 \\
 & \quad \underline{-144yx^2 + 288yx - 16y^3 + 16y^2 + 528y} \\
 & \quad\quad 576x^2 - 1152x - y^4 + 161y^3 - 406y^2 - 672y - 1728 \\
 & \quad\quad \underline{576x^2 - 1152x + 64y^2 - 64y - 2112} \\
 & \quad\quad\quad \underbrace{-y^4 + 161y^3 - 470y^2 - 608y + 384}_{\text{remainder } (r)}
\end{array}
$$

In the case that there are more than two polynomials, polynomial f can be divided by multiple polynomials $g_1, \ldots, g_m$.

In summary, the division was performed by eliminating the leading term of x in f. This process can be generalized as

$$h = f - \frac{lt(f)}{lt(g)}g \tag{C.28}$$

where h, the remainder at every step, is called a reduction of f by g.

Theorem C.2- Let g be a non-zero polynomial in $k[x_1, \ldots, x_n]$. Then for any $f \in k[x_1, \ldots, x_n]$, there exists a quotient, q, and remainder, r, in $k[x_1, \ldots, x_n]$ such that

$$f = qg + r, \text{ with } r = 0 \tag{C.29}$$

or for more than two polynomials, i.e., $\{g_1, \ldots, g_m\} \in k[x_1, \ldots, x_n]$,

$$f = q_1g_1 + \ldots + q_mg_m + r, \text{ with } r = 0 \tag{C.30}$$

Clearly, if $r = 0$ then f is related to the ideal of $\{g_1, \ldots, g_m\}$, i.e., $f \in \langle g_1, \ldots, g_m \rangle$, as given by the definition of the ideal of a set of polynomials in Eq. (C.21). If $r \neq 0$

then the chosen $\{g_1, \ldots, g_m\}$ implies that $f \notin \langle g_1, \ldots, g_m \rangle$. Therefore, it is necessary to find a special generating set for the ideal called a Gröbner basis.

Theorem C.3- A polynomial r is called reduced with respect to a set of nonzero polynomials $\{g_1, \ldots, g_m\}$ if $r = 0$ or no power product that appears in r is divisible by any one of the $lp(g_i)$ for $i = 1, \ldots, m$. Mathematically, r cannot be reduced modulo $\{g_1, \ldots, g_m\}$ and f is in a normal form modulo $\{g_1, \ldots, g_m\}$. Thus, Eq. (C.28) can also be written as

$$f \xrightarrow{g} h \tag{C.31}$$

after the first reduction or

$$f \xrightarrow{g} h \xrightarrow{g} r \quad \text{or} \quad f \xrightarrow{g+} r \tag{C.32}$$

after all possible reductions.

An algorithm to compute multivariable polynomial divisions is presented in Section C.7.5.

In the previous example, the leading power product of g is $lp(g) = x^2$, and the remainder is

$$r = -y^4 + 161y^3 - 470y^2 - 608y + 384 \tag{C.33}$$

Thus, r is reduced with respect to g, and $f = qg + r$, where $q = y^2 - 16y + 64$.

Since the remainder turned out to be an equation in a single variable, it can be set equal to zero and the roots of y correspond to the solutions of the polynomial system that would make $r = 0$. Having $r = 0$, for any solution of y, f is therefore related to an ideal of g, i.e., $f \in \langle g \rangle$. Thus, an ideal of the set of polynomials is

$$\begin{aligned} \langle f_1(x,y), f_2(x,y) \rangle &= \langle f_1(x,y), r \rangle \\ &= \langle 9x^2 - 18x + y^2 - y - 33, -y^4 + 161y^3 - 470y^2 - 608y + 384 \rangle \end{aligned} \tag{C.34}$$

This trivial solution was achieved because of the nature of the problem. However, this is not a unique ideal, if the term order was inverted, i.e., $y > x$, a different ideal would have resulted. For instance, the remainder after the division polynomial is

$$r = -159x^2y + 318xy + 481y - 9x^4 + 340x^2 + 36x^3 - 752x - 1215 \qquad \text{(C.35)}$$

which cannot reduce modulo $\{g\}$, and since $r \neq 0$ the chosen generating set does not yield an ideal of $\{f_1(x,y), f_2(x,y)\}$. This kind of problem turns out to be more general and will be addressed in the next section.

It is worthy of mention that Eq. (C.33) turns out to be the same equation as Eq.(C.16a), which was found through the determinant of the coefficient matrix using the dialytic elimination method. Similarly, the roots of Eq. (C.33) are substituted in Eq. (C.27a) to find the solutions of x.

C.7.4 Gröbner Bases

A set of polynomials is related to a ring $k[x_1, \ldots, x_n]$, which can perform binary operations. According to Hilbert Basis Theorem (Theorem C.1), there is a set of polynomials that generates an ideal of the ring $k[x_1, \ldots, x_n]$. This set of polynomials, or Gröbner basis, provides the "better" representation of the variety, or the common roots of the set of polynomials. The following theorems define the existence and uniqueness of a Gröbner basis:

Theorem C.4- A set of non-zero polynomials $G = \{g_1, \ldots, g_t\} \in k[x_1, \ldots, x_n]$ is called a Gröbner basis for I if and only if for all $f \in I$ such that $f \neq 0$, there exists $i \in \{1, ..., t\}$ such that $lp(g_i)$ divides $lp(f)$.

Theorem C.5- Let $G = \{g_1, \ldots, g_t\}$ be a set of non-zero polynomials of the ring $k[x_1, \ldots, x_n]$. Then G is a Gröbner basis if and only if for all $f \in k[x_1, \ldots, x_n]$ the remainder of the division f by G is unique.

It is important to mention that the uniqueness of a Gröbner basis is related to a specific term order.

One of the problems in the polynomial division is the cancelation of the leading terms. A very effective method to generate a Gröbner basis is through a syzygy polynomial, better known as S-polynomial. Let $0 \neq f\ ,\ g \in k[x_1, \ldots, x_n]$. Let $L = lcm(lp(f), lp(g))$, where lcm denotes the least common multiple. Thus, the S-polynomial is defined as:

$$S(f,g) = \frac{L}{lt(f)}f - \frac{L}{lt(g)}g \tag{C.36}$$

Buchberger (1965) and Buchberger and Winkler (1998) proved that S-polynomials actually remove all the ambiguity caused by the division algorithm.

Theorem C.6- (Buchberger's Theorem). Let $G = \{g_1, \ldots, g_t\}$ be a set of non-zero polynomials in $k[x_1, \ldots, x_n]$. Then G is a Gröbner basis for the ideal $I = \langle G \rangle$ if and only if for all $i \neq j$,

$$S(g_i, g_j) \xrightarrow{G_+} 0 \tag{C.37}$$

The strategy for computing Gröbner bases is to reduce the S-polynomials. If a remainder is non-zero, add this remainder to the list of polynomials in the generating set, and repeat this process until there are enough polynomials to make all S-polynomials reduce to zero (Adams and Loustaunau, 1994). Buchberger's algorithm to compute Gröbner Bases is presented in Section C.7.5.

There are two considerations that should be taken into account to have a unique Gröbner basis. This is because two choices have been made arbitrarily. First, the order in which the polynomials are incorporated, which affects the Algorithm Division. Second, the random choice of $\{f, g\} \in \Gamma$ in Buchberger's Algorithm. A proposition for a Reduced Gröbner Bases is presented in Adams and Loustaunau (1994), where the term order is fixed and reduction process is constrained to follow a specific order.

C.7.5 Algorithms

The following algorithms were extracted from Adams and Loustaunau (1994), and slightly modified to be consistent with the notation carried out through this Section.

Multivariable Division Algorithm

INPUT: $f, g_1, ..., g_m \in k[x_1, \ldots, x_n]$ with $g_i \neq 0$ for $i = 1, ..., m$

OUTPUT: $q_1, ..., q_m, r$ such that $f = q_1 g_1 + ... + q_m g_m + r$ and $f \xrightarrow{g+} r$

INITIALIZATION: $q_i = 0$, for $i = 1, ..., m$, $r = 0$, and $h = f$

WHILE $h \neq 0$ **DO**

IF there exists i such that $lp(g_i)$ divides $lp(h)$ **THEN**

choose i least such that $lp(g_i)$ divides $lp(h)$

$q_i = q_i + \frac{lt(h)}{lt(g_i)}$

$h = h - \frac{lt(h)}{lt(g_i)} g_i$

ELSE

$r = r + lt(h)$

$h = h - lt(h)$

Buchberger's Algorithm for Computing Gröbner Bases

INPUT: $F = \{f_1, ..., f_s\} \subseteq k[x_1, \ldots, x_n]$ with $f_i \neq 0$ for $i = 1, ..., s$

OUTPUT: $G = \{g_1, ..., g_t\}$, a Gröbner basis for $\langle f_1, ..., f_s \rangle$

INITIALIZATION: $G = F$, $\Gamma = \{\{f_i, f_j\} \mid f_i \neq f_j \in G\}$

WHILE $\Gamma \neq 0$ **DO**

Choose any $\{f, g\} \in \Gamma$

$\Gamma = \Gamma - \{\{f_i, f_j\}\}$

$S(f, g) \xrightarrow{G_+} h$

IF $h \neq 0$ **THEN**

$\Gamma = \Gamma \cup \{\{q, h\} \text{ |for all } q \in G\}$

$G = G \cup \{h\}$

where Γ keeps track of the combinations of the generating sets.

Example.-

Assume the set of polynomials described in Section C4 and determine the Gröbner Bases with a term order *lex* $x > y$.

$$f_1 = 9x^2 - 18x + y^2 - y - 33 = 0$$

$$f_2 = \left(y^2 - 16y + 64\right) x^2 + \left(-2y^2 + 32y - 128\right) x + 16y^3 - 47y^2 - 16y - 192 = 0$$

INITIALIZATION: $G = \{f_2, f_1\}$, $\Gamma = \{f_2, f_1\}$

First pass through the WHILE Loop

Choose $\{f, g\} = \{f_2, f_1\}$

$\Gamma = \Gamma - \{f_2, f_1\} = 0$

$S(f_2, f_1) \xrightarrow{G_+} h$, this step is shown in detail as follows.

S-Polynomial, with $L = lmc(f_2, f_1) = x^2y^2$

$S(f_2, f_1) = \frac{L}{lt(f_2)} f_2 - \frac{L}{lt(f_1)} f_1 = \frac{x^2y^2}{x^2y^2} f_2 - \frac{x^2y^2}{9x^2} f_1 =$

$= -16yx^2 + 64x^2 + 32yx - 128x - \frac{1}{9}y^4 + \frac{145}{9}y^3 - \frac{130}{3}y^2 - 16y - 192$

Reduction $S(f_1, f_2)$ modulo G, with $q_1 = 0$, $q_2 = 0$, and $h = S(f_2, f_1)$

$q_1 = q_1 + \frac{lt(h)}{lt(f_1)} = 0 + \frac{-16yx^2}{9x^2} = \frac{-16}{9}y$

$h = h - \frac{lt(h)}{lt(f_1)}f_1 = S(f_1, f_2) - \frac{-16}{9}y(f_1)$

$= 64x^2 - 128x - \frac{1}{9}y^4 + \frac{161}{9}y^3 - \frac{406}{9}y^2 - \frac{224}{3}y - 192$

$q_1 = q_1 + \frac{lt(h)}{lt(f_1)} = \frac{-16}{9}y + \frac{64x^2}{9x^2} = \frac{-16}{9}y + \frac{64}{9}$

$h = h - \frac{lt(h)}{lt(f_1)}f_1 = h - \frac{64}{9}f_1$

$= -\frac{1}{9}y^4 + \frac{161}{9}y^3 - \frac{470}{9}y^2 - \frac{608}{9}y + \frac{128}{3}$

h cannot be reduced modulo[2] G.

Thus, $S(f_2, f_1) \xrightarrow{G_+} -\frac{1}{9}y^4 + \frac{161}{9}y^3 - \frac{470}{9}y^2 - \frac{608}{9}y + \frac{128}{3} = h$.

Since, $h \neq 0$, let $f_3 = -y^4 + 161y^3 - 470y^2 - 608y + 384$, which has been scaled for convenience. Let $\Gamma = \{\{f_1, f_3\}, \{f_2, f_3\}\}$ and $G = \{f_1, f_2, f_3\}$.

Second pass through the WHILE Loop

Choose $\{f, g\} = \{f_3, f_1\}$

$\Gamma = \{\{f_3, f_1\}, \{f_3, f_2\}\} - \{f_3, f_1\} = \{f_3, f_2\}$

$S(f_3, f_1) \xrightarrow{G_+} h$; this step is shown below:

S-Polynomial, with $L = lmc(f_3, f_2) = x^2y^4$

$S(f_3, f_1) = -161y^3x^2 + 470y^2x^2 + 608yx^2 - 384x^2 + 2y^4x - \frac{1}{9}y^6 + \frac{1}{9}y^5 + \frac{11}{3}y^4$

Reduction $S(f_3, f_1)$ modulo G, with $q_1 = 0$, $q_3 = 0$, and $h = S(f_3, f_1)$

After eight loops in the Multivariable Division Algorithm using both generating set polynomials, f_1 and f_3, the remainder $h = 0$.

Thus, $S(f_3, f_1) \xrightarrow{G_+} 0 = h$

---

[2] In this reduction, $g_2 = f_2$ was not used, but the algorithm can choose either polynomial of the generating set, as long as $lp(g_i)$ divides $lp(h)$.

Third pass through the WHILE Loop

Choose $\{f, g\} = \{f_3, f_2\}$

$\Gamma = \{f_3, f_2\} - \{f_3, f_2\} = 0$

$S(f_3, f_2) \xrightarrow{G_+} h$; this step is shown below:

S-Polynomial, with $L = lmc(f_3, f_2) = x^2y^4$

$$S(f_3, f_2) = -145y^3x^2 + 406y^2x^2 + 608yx^2 - 384x^2 + 2y^4x - 32y^3x + 128y^2x$$
$$-16y^5 + 47y^4 + 16y^3 + 192y^2$$

Reduction $S(f_3, f_2)$ modulo G, with $q_2 = 0$, $q_3 = 0$, and $h = S(f_3, f_2)$

After seven loops in the Multivariable Division Algorithm using both generating set polynomials f_2 and f_3, the remainder $h = 0$.

Thus, $S(f_3, f_2) \xrightarrow{G_+} 0 = h$

Since $h = 0$ and $\Gamma = 0$ the WHILE loop stops.

So, the Gröbner basis, $G = \{f_1, f_2, f_3\}$, is contained in the ideal of the original set of polynomials, i.e., $\langle f_1, f_2 \rangle$. Notice that f_3 is the same as the remainder of the division polynomial Eq. (C.33). Therefore, solutions of y are found with f_3 and then substituted in f_1 to find the corresponding solution of x. One question may arise, why is $G = \{f_1, f_2, f_3\}$ not structured in a triangular form like the Gauss elimination method as stated before? The answer is due to the repeatability of the roots in y.

Assume the same problem but now the term and variable order are *deglex* and $y > x$, respectively[3]. The polynomials are incorporated in Buchberger's Algorithm

[3]Also, it is important to mention that through the polynomial division, this variable order did not yield r=0, as shown in Eq. (C.35).

which yields the following results:

$$g_1 = 81x^8 - 648x^7 + 224136x^6 - 1335744x^5 + 555838x^4 + 6669512x^3 - 1856824x^2 - 13180448x - 6743103 = 0$$

$$g_2 = -4293x^6 + 25758x^5 - 11840679x^4 + 47190996x^3 + 29178937x^2 - 152671178x - 121541301 + 1347520y = 0$$

In this example, the resulting Gröbner basis, $G = \{g_1, g_2\}$, is structured in a triangular form like the Gauss elimination method; g_1 is an 8^{th}-order polynomial in x and g_2 is a linear equation in y. That is, for each solution of x, there is a corresponding solution of y.

Gröbner Bases have been used in kinematics. For instance, Lazard (1992 and 1993) solved the forward displacement problem of the Stewart-Gough platform.

Appendix D

Coefficients of Equations

D.1 Overview

The coefficients of polynomials, vectors, and matrices, that for space reasons were not included within the Chapters, are presented in this appendix.

D.2 Coefficients of Non-Redundant Manipulators

3-PRR Manipulator, coefficients of Eq. (3.34):

$$\psi_{i1} = c(\gamma_i)t^2 + c(\gamma_i)$$

$$\psi_{i2} = s(\gamma_i)t^2 + s(\gamma_i)$$

$$\begin{aligned}\psi_{i3} = &\left(-\left(\rho_i c(\theta_{3_i}) + l_i\right) c(-\gamma_i + \alpha_i) - c(\gamma_i)bx_i - s(\gamma_i)by_i - \rho_i s(\theta_{3_i})s(-\gamma_i + \alpha_i)\right) t^2 \\ &+ \left(-2\left(\rho_i c(\theta_{3_i}) + l_i\right) s(-\gamma_i + \alpha_i) + 2\rho_i s(\theta_{3_i})c(-\gamma_i + \alpha_i)\right) t \\ &+ \rho_i s(\theta_{3_i})s(-\gamma_i + \alpha_i) + \left(\rho_i c(\theta_{3_i}) + l_i\right) c(-\gamma_i + \alpha_i) - s(\gamma_i)by_i - c(\gamma_i)bx_i\end{aligned}$$

for $i = 1, 2, 3$.

3-RPR Manipulator, coefficients of Eq. (3.26):

$$
\begin{aligned}
a_0 &= -y^2 b x_2 l_3 c\alpha_3 + y x b x_2 l_3 s\alpha_3 - y b x_2 b x_3 l_3 s\alpha_3 + y b x_2 l_3 b y_3 c\alpha_3 - y l_2 b x_3 l_3 s\alpha_3 \\
&\quad + y l_2 l_3 b y_3 c\alpha_3 + y^2 l_2 b x_3 - y x l_2 b y_3 \\
a_1 &= -2y^2 b x_2 l_3 s\alpha_3 - 2y x b x_2 l_3 c\alpha_3 - 2y b x_2 l_2 l_3 c\alpha_3 + 2y b x_2 b x_3 l_3 c\alpha_3 + 2y b x_2 l_3 b y_3 s\alpha_3 \\
&\quad + 2y l_2 b x_3 l_3 c\alpha_3 + 2y l_2 l_3 b y_3 s\alpha_3 + 2x b x_2 l_2 l_3 s\alpha_3 - 2x l_2 b x_3 l_3 s\alpha_3 + 2x l_2 l_3 b y_3 c\alpha_3 \\
&\quad + 2y x l_2 b x_3 - 2y b x_2 l_2 b x_3 - 2x^2 l_2 b y_3 + 2x b x_2 l_2 b y_3 \\
a_2 &= -4y b x_2 l_2 l_3 s\alpha_3 + 2y l_2 b x_3 l_3 s\alpha_3 - 2y l_2 l_3 b y_3 c\alpha_3 - 4x b x_2 l_2 l_3 c\alpha_3 + 4x l_2 b x_3 l_3 c\alpha_3 \\
&\quad + 4x l_2 l_3 b y_3 s\alpha_3 \\
a_3 &= -2y^2 b x_2 l_3 s\alpha_3 - 2y x b x_2 l_3 c\alpha_3 + 2y b x_2 l_2 l_3 c\alpha_3 + 2y b x_2 b x_3 l_3 c\alpha_3 + 2y b x_2 l_3 b y_3 s\alpha_3 \\
&\quad - 2y l_2 b x_3 l_3 c\alpha_3 - 2y l_2 l_3 b y_3 s\alpha_3 - 2x b x_2 l_2 l_3 s\alpha_3 + 2x l_2 b x_3 l_3 s\alpha_3 - 2x l_2 l_3 b y_3 c\alpha_3 \\
&\quad + 2y x l_2 b x_3 - 2y b x_2 l_2 b x_3 - 2x^2 l_2 b y_3 + 2x b x_2 l_2 b y_3 \\
a_4 &= y^2 b x_2 l_3 c\alpha_3 - y x b x_2 l_3 s\alpha_3 + y b x_2 b x_3 l_3 s\alpha_3 - y b x_2 l_3 b y_3 c\alpha_3 - y l_2 b x_3 l_3 s\alpha_3 \\
&\quad + y l_2 l_3 b y_3 c\alpha_3 - y^2 l_2 b x_3 + y x l_2 b y_3
\end{aligned}
$$

3-RRR Manipulator, coefficients of Eq. (3.44):

$$
\begin{aligned}
k_{1,i} &= -2l_i c(\phi - \beta_i) - 2\rho_{i+3} c(\phi - \theta_{3_i} - \beta_i) - 2bx_i \\
k_{2,i} &= -2l_i s(\phi - \beta_i) - 2\rho_{i+3} s(\phi - \theta_{3_i} - \beta_i) - 2by_i \\
k_{3,i} &= 2l_i \rho_{i+3} c(\phi - \beta_i) c(\phi - \theta_{3_i} - \beta_i) + 2l_i \rho_{i+3} s(\phi - \beta_i) s(\phi - \theta_{3_i} - \beta_i) + \\
&\quad 2l_i bx_i c(\phi - \beta_i) + 2l_i by_i s(\phi - \beta_i) + bx_i^2 + by_i^2 + l_i^2 + \rho_{i+3}^2 - \rho_i^2 + \\
&\quad + 2\rho_{i+3} bx_i c(\phi - \theta_{3_i} - \beta_i) + 2\rho_{i+3} by_i s(\phi - \theta_{3_i} - \beta_i)
\end{aligned}
$$

for $i = 1, 2, 3$.

D.3 Coefficients of Manipulators with In-Branch Redundancy

D.3.1 Coefficients of the RRR-2RRR Manipulator

Coefficients of the 4^{th}-order polynomial in Eq. (4.25):

$$a_0 = y^2 l_2 b x_3 - y l_3 b x_2 b x_3 s\alpha_3 - y^2 l_3 b x_2 c\alpha_3 + y l_3 b x_2 b y_3 c\alpha_3 + y l_3 l_2 b y_3 c\alpha_3 - y l_2 b y_3 x$$
$$- y l_3 l_2 b x_3 s\alpha_3 + y l_3 b x_2 x s\alpha_3$$

$$a_1 = -2x^2 l_2 b y_3 + 2y l_2 b x_3 x + 2y l_3 l_2 b x_3 c\alpha_3 + 2x l_2 s\alpha_3 l_3 b x_2 + 2y l_3 l_2 b y_3 s\alpha_3$$
$$- 2y l_3 b x_2 x c\alpha_3 - 2y l_2 b x_2 c\alpha_3 l_3 - 2y^2 l_3 b x_2 s\alpha_3 - 2y l_2 b x_3 b x_2 + 2y l_3 b x_2 b y_3 s\alpha_3$$
$$+ 2x l_3 l_2 b y_3 c\alpha_3 - 2x l_3 l_2 b x_3 s\alpha_3 + 2y l_3 b x_2 b x_3 c\alpha_3 + 2x l_2 b x_2 b y_3$$

$$a_2 = 2y l_3 l_2 b x_3 s\alpha_3 - 4y l_2 s\alpha_3 l_3 b x_2 + 4x l_3 l_2 b x_3 c\alpha_3 - 4x l_2 b x_2 c\alpha_3 l_3 - 2y l_3 l_2 b y_3 c\alpha_3$$
$$+ 4x l_3 l_2 b y_3 s\alpha_3$$

$$a_3 = 2x l_3 l_2 b x_3 s\alpha_3 - 2y l_3 l_2 b x_3 c\alpha_3 + 2y l_3 b x_2 b x_3 c\alpha_3 + 2x l_2 b x_2 b y_3 - 2x l_3 l_2 b y_3 c\alpha_3$$
$$- 2y l_2 b x_3 b x_2 + 2y l_2 b x_3 x - 2x l_2 s\alpha_3 l_3 b x_2 - 2x^2 l_2 b y_3 + 2y l_2 b x_2 c\alpha_3 l_3$$
$$- 2y l_3 b x_2 x c\alpha_3 + 2y l_3 b x_2 b y_3 s\alpha_3 - 2y l_3 l_2 b y_3 s\alpha_3 - 2y^2 l_3 b x_2 s\alpha_3$$

$$a_4 = y^2 l_3 b x_2 c\alpha_3 + y l_3 l_2 b y_3 c\alpha_3 - y l_3 l_2 b x_3 s\alpha_3 + y l_3 b x_2 b x_3 s\alpha_3 - y^2 l_2 b x_3 - y l_3 b x_2 x s\alpha_3$$
$$- y l_3 b x_2 b y_3 c\alpha_3 + y l_2 b y_3 x$$

D.3.2 Coefficients of the PRR-2PRR Manipulator

Coefficients of the determinant of the associated reciprocal screw matrix, Eq. (4.40):

$$a_1 = 2l_3 s\gamma_1$$
$$a_2 = 4l_3 c\gamma_1$$
$$a_3 = -2l_3 s\gamma_1$$
$$a_4 = 2\left(l_2 c\gamma_1 s\alpha_3 - l_2 s\gamma_1 c\alpha_3\right)$$
$$a_5 = -4\left(l_2 c\gamma_1 c\alpha_3 + l_2 s\gamma_1 s\alpha_3\right)$$
$$a_6 = 2\left(l_2 s\gamma_1 c\alpha_3 - l_2 c\gamma_1 s\alpha_3\right)$$
$$a_7 = 4\left(l_2 c\gamma_1 c\alpha_3 + l_2 s\gamma_1 s\alpha_3 - l_3 c\gamma_1\right)$$
$$a_8 = 8\left(l_2 c\gamma_1 s\alpha_3 + l_3 s\gamma_1 - l_2 s\gamma_1 c\alpha_3\right)$$
$$a_9 = 4\left(l_3 c\gamma_1 - l_2 c\gamma_1 c\alpha_3 - l_2 s\gamma_1 s\alpha_3\right)$$
$$a_{10} = 2\left(l_2 s\gamma_1 c\alpha_3 - l_2 c\gamma_1 s\alpha_3\right)$$
$$a_{11} = 4\left(l_2 c\gamma_1 c\alpha_3 + l_2 s\gamma_1 s\alpha_3\right)$$
$$a_{12} = 2\left(l_2 c\gamma_1 s\alpha_3 - l_2 s\gamma_1 c\alpha_3\right)$$
$$a_{13} = -2l_3 s\gamma_1$$
$$a_{14} = -4l_3 c\gamma_1$$
$$a_{15} = 2l_3 s\gamma_1$$

Coefficients of the loop-closure equation of branch 2, Eq. (4.41):

$$b_1 = s\gamma_2 y + c\gamma_2 x - c\gamma_2 b x_2 - c\gamma_2 l_2 + c\gamma_2 \rho_2$$
$$b_2 = 2s\gamma_2 l_2 - 2s\gamma_2 \rho_2$$
$$b_3 = s\gamma_2 y + c\gamma_2 l_2 + c\gamma_2 x - c\gamma_2 \rho_2 - c\gamma_2 b x_2$$
$$b_4 = 2s\gamma_2 \rho_2$$
$$b_5 = 4c\gamma_2 \rho_2$$
$$b_6 = -2s\gamma_2 \rho_2$$
$$b_7 = c\gamma_2 x - c\gamma_2 \rho_2 - c\gamma_2 b x_2 - c\gamma_2 l_2 + s\gamma_2 y$$
$$b_8 = 2s\gamma_2 \rho_2 + 2s\gamma_2 l_2$$
$$b_9 = s\gamma_2 y + c\gamma_2 x - c\gamma_2 b x_2 + c\gamma_2 l_2 + c\gamma_2 \rho_2$$

Coefficients of the loop-closure equation of branch 3, Eq. (4.42):

$$c_1 = s\gamma_3\rho_3 s\alpha_3 - s\gamma_3 l_3 s\alpha_3 - c\gamma_3 l_3 c\alpha_3 + c\gamma_3\rho_3 c\alpha_3 + c\gamma_3 x - s\gamma_3 by_3 + s\gamma_3 y - c\gamma_3 bx_3$$

$$c_2 = 2s\gamma_3 l_3 c\alpha_3 - 2c\gamma_3 l_3 s\alpha_3 + 2c\gamma_3\rho_3 s\alpha_3 - 2s\gamma_3\rho_3 c\alpha_3$$

$$c_3 = s\gamma_3 l_3 s\alpha_3 + c\gamma_3 x - c\gamma_3 bx_3 + s\gamma_3 y + c\gamma_3 l_3 c\alpha_3 - c\gamma_3\rho_3 c\alpha_3 - s\gamma_3\rho_3 s\alpha_3 - s\gamma_3 by_3$$

$$c_4 = -2c\gamma_3\rho_3 s\alpha_3 + 2s\gamma_3\rho_3 c\alpha_3$$

$$c_5 = 4s\gamma_3\rho_3 s\alpha_3 + 4c\gamma_3\rho_3 c\alpha_3$$

$$c_6 = -2s\gamma_3\rho_3 c\alpha_3 + 2c\gamma_3\rho_3 s\alpha_3$$

$$c_7 = -c\gamma_3 bx_3 - s\gamma_3 by_3 + c\gamma_3 x + s\gamma_3 y - c\gamma_3 l_3 c\alpha_3 - s\gamma_3 l_3 s\alpha_3 - s\gamma_3\rho_3 s\alpha_3 - c\gamma_3\rho_3 c\alpha_3$$

$$c_8 = 2s\gamma_3\rho_3 c\alpha_3 - 2c\gamma_3\rho_3 s\alpha_3 - 2c\gamma_3 l_3 s\alpha_3 + 2s\gamma_3 l_3 c\alpha_3$$

$$c_9 = c\gamma_3\rho_3 c\alpha_3 + s\gamma_3\rho_3 s\alpha_3 + c\gamma_3 l_3 c\alpha_3 + s\gamma_3 l_3 s\alpha_3 + s\gamma_3 y - s\gamma_3 by_3 + c\gamma_3 x - c\gamma_3 bx_3$$

Elements of the polynomial matrices, Eq. (4.45):

$$[\Psi_j] = \begin{bmatrix}
a_i & 0 & a_{i+3} & a_{i+6} & a_{i+9} & 0 & 0 & a_{i+12} & 0 & 0 & 0 & 0 \\
b_i & 0 & 0 & b_{i+3} & 0 & 0 & 0 & b_{i+6} & 0 & 0 & 0 & 0 \\
0 & a_i & 0 & a_{i+3} & a_{i+6} & a_{i+9} & 0 & 0 & a_{i+12} & 0 & 0 & 0 \\
0 & b_i & 0 & 0 & b_{i+3} & 0 & 0 & 0 & b_{i+6} & 0 & 0 & 0 \\
0 & 0 & c_i & c_{i+3} & c_{i+6} & 0 & 0 & 0 & 0 & 0 & 0 & 0 \\
0 & 0 & 0 & a_i & 0 & a_{i+3} & a_{i+6} & a_{i+9} & 0 & 0 & a_{i+12} & 0 \\
0 & 0 & 0 & c_i & c_{i+3} & c_{i+6} & 0 & 0 & 0 & 0 & 0 & 0 \\
0 & 0 & 0 & b_i & 0 & 0 & b_{i+3} & 0 & 0 & 0 & b_{i+6} & 0 \\
0 & 0 & 0 & 0 & a_i & 0 & a_{i+3} & a_{i+6} & a_{i+9} & 0 & 0 & a_{i+12} \\
0 & 0 & 0 & 0 & b_i & 0 & 0 & b_{i+3} & 0 & 0 & 0 & b_{i+6} \\
0 & 0 & 0 & 0 & 0 & 0 & c_i & c_{i+3} & c_{i+6} & 0 & 0 & 0 \\
0 & 0 & 0 & 0 & 0 & 0 & 0 & c_i & c_{i+3} & c_{i+6} & 0 & 0
\end{bmatrix}$$

where $i = 1, 2, 3$ and $j = 3 - i$.

D.3.3 Coefficients of the RRR-2RRR Manipulator

Condition 1

Coefficients of the polynomials shown in Eqs. (4.57a and 4.57b):

$$a_1 = -2bx_2 + 2(l_2 + \rho_2 c\theta_{3_2})c\phi$$

$$a_2 = 2(l_2 + \rho_2 c\theta_{3_2})s\phi$$

$$a_3 = bx_2^2 + \rho_2^2 + l_2^2 - \rho_5^2 + 2\rho_2 l_2 c\theta_{3_2} - 2bx_2(l_2 + \rho_2 c\theta_{3_2})c\phi$$

$$b_1 = -2bx_3 + 2(l_3 + \rho_3 c\theta_{3_3})c(\phi + \alpha_3)$$

$$b_2 = -2by_3 + 2(l_3 + \rho_3 c\theta_{3_3})s(\phi + \alpha_3)$$

$$b_3 = -2bx_3(l_3 + \rho_3 c\theta_{3_3})c(\phi + \alpha_3) - 2by_3(l_3 + \rho_3 c\theta_{3_3})s(\phi + \alpha_3)$$
$$+bx_3^2 + by_3^2 + \rho_3^2 + l_3^2 - \rho_6^2 + 2\rho_3 l_3 c\theta_{3_3}$$

Condition 2

Coefficients of the determinant of the associated reciprocal screw matrix, Eq. (4.63):

$$a_1 = -2l_3 y \qquad a_6 = -2l_2 c\alpha_3 y + 2l_2 s\alpha_3 x \qquad a_{11} = -4l_2 s\alpha_3 y - 4l_2 c\alpha_3 x$$

$$a_2 = -4l_3 x \qquad a_7 = 4(l_3 x - l_2 c\alpha_3 x - l_2 s\alpha_3 y) \qquad a_{12} = 2l_2 c\alpha_3 y - 2l_2 s\alpha_3 x$$

$$a_3 = 2l_3 y \qquad a_8 = 8(l_2 c\alpha_3 y - l_3 y - l_2 s\alpha_3 x) \qquad a_{13} = 2l_3 y$$

$$a_4 = 2l_2 c\alpha_3 y - 2l_2 s\alpha_3 x \qquad a_9 = 4(l_2 s\alpha_3 y + l_2 c\alpha_3 x - l_3 x) \qquad a_{14} = 4l_3 x$$

$$a_5 = 4l_2 c\alpha_3 x + 4l_2 s\alpha_3 y \qquad a_{10} = -2l_2 c\alpha_3 y + 2l_2 s\alpha_3 x \qquad a_{15} = -2l_3 y$$

Coefficients of the loop-closure equation of branch 2, Eq. (4.64):

$$b_1 = bx_2^2 + y^2 + l_2^2 - 2bx_2x - \rho_5^2 - 2l_2\rho_2 - 2\rho_2bx_2 + 2\rho_2x + x^2 + 2l_2bx_2 - 2l_2x + \rho_2^2$$

$$b_2 = -4\rho_2y + 4l_2y$$

$$b_3 = -2\rho_2x + y^2 + x^2 - \rho_5^2 + bx_2^2 - 2bx_2x + l_2^2 + \rho_2^2 + 2l_2x - 2l_2\rho_2 + 2\rho_2bx_2 - 2l_2bx_2$$

$$b_4 = 4\rho_2y$$

$$b_5 = 8\rho_2x - 8\rho_2bx_2$$

$$b_6 = -4\rho_2y$$

$$b_7 = -\rho_5^2 + 2\rho_2bx_2 - 2\rho_2x + 2l_2\rho_2 + bx_2^2 + 2l_2bx_2 - 2l_2x + \rho_2^2 + l_2^2 + x^2 + y^2 - 2bx_2x$$

$$b_8 = 4\rho_2y + 4l_2y$$

$$b_9 = 2\rho_2x + y^2 + x^2 - \rho_5^2 + bx_2^2 - 2bx_2x + l_2^2 + \rho_2^2 + 2l_2x + 2l_2\rho_2 - 2\rho_2bx_2 - 2l_2bx_2$$

Coefficients of the loop-closure equation of branch 3, Eq. (4.65):

$$c_1 = x^2 + y^2 + l_3^2 - \rho_6^2 + \rho_3^2 + by_3^2 + bx_3^2 + 2(l_3bx_3c\alpha_3 - l_3xc\alpha_3 - l_3\rho_3c\alpha_3^2 - \rho_3by_3s\alpha_3$$
$$-\rho_3bx_3c\alpha_3 + \rho_3ys\alpha_3 - l_3ys\alpha_3 + l_3by_3s\alpha_3 - l_3\rho_3s\alpha_3^2 + \rho_3xc\alpha_3 - bx_3x - by_3y)$$

$$c_2 = 4((l_3bx_3 - l_3x - \rho_3bx_3 + \rho_3x)\, s\alpha_3 + (l_3y - l_3by_3 - \rho_3y + \rho_3by_3)\, c\alpha_3)$$

$$c_3 = \rho_3^2 + l_3^2 - \rho_6^2 + x^2 + bx_3^2 + y^2 + by_3^2 + 2(l_3xc\alpha_3 - by_3y - bx_3x - l_3\rho_3s\alpha_3^2 - \rho_3ys\alpha_3$$
$$-l_3by_3s\alpha_3 + l_3ys\alpha_3 + \rho_3by_3s\alpha_3 - l_3bx_3c\alpha_3 + \rho_3bx_3c\alpha_3 - \rho_3xc\alpha_3 - l_3\rho_3c\alpha_3^2)$$

$$c_4 = 4(\rho_3yc\alpha_3 - \rho_3by_3c\alpha_3 - \rho_3xs\alpha_3 + \rho_3bx_3s\alpha_3)$$

$$c_5 = 8(\rho_3ys\alpha_3 - \rho_3bx_3c\alpha_3 - \rho_3by_3s\alpha_3 + \rho_3xc\alpha_3)$$

$$c_6 = 4(\rho_3by_3c\alpha_3 - \rho_3bx_3s\alpha_3 - \rho_3yc\alpha_3 + \rho_3xs\alpha_3)$$

$$c_7 = x^2 + y^2 + l_3^2 - \rho_6^2 + \rho_3^2 + by_3^2 + bx_3^2 + 2(l_3bx_3c\alpha_3 - l_3xc\alpha_3 + l_3\rho_3c\alpha_3^2 + \rho_3by_3s\alpha_3$$
$$+\rho_3bx_3c\alpha_3 - \rho_3ys\alpha_3 - l_3ys\alpha_3 + l_3by_3s\alpha_3 + l_3\rho_3s\alpha_3^2 - \rho_3xc\alpha_3 - bx_3x - by_3y)$$

$$c_8 = 4((l_3bx_3 - l_3x + \rho_3bx_3 - \rho_3x)\, s\alpha_3 + (l_3y - l_3by_3 + \rho_3y - \rho_3by_3)\, c\alpha_3)$$

$$c_9 = \rho_3^2 + l_3^2 - \rho_6^2 + y^2 + by_3^2 + x^2 + bx_3^2 + 2(l_3\rho_3s\alpha_3^2 - by_3y - bx_3x + l_3xc\alpha_3 + \rho_3ys\alpha_3$$
$$-l_3by_3s\alpha_3 + l_3ys\alpha_3 - \rho_3by_3s\alpha_3 - l_3bx_3c\alpha_3 - \rho_3bx_3c\alpha_3 + \rho_3xc\alpha_3 + l_3\rho_3c\alpha_3^2)$$

D.4 Coefficients of Redundant Manipulators with Additional Branches

D.4.1 Coefficients of the 4-RPR Manipulator

Coefficients of the polynomials obtained from the determinants of the sub-matrices.

Coefficients of Eq. (5.2a):

$$g_1 = -l_2 b y_3 s\phi$$

$$g_2 = -l_2 c\phi b x_3 + l_3 b x_2 c\phi c\alpha_3 - l_3 b x_2 s\phi s\alpha_3$$

$$g_3 = l_2 s\phi b x_3 + l_2 b y_3 c\phi - l_3 b x_2 s\phi c\alpha_3 - l_3 b x_2 c\phi s\alpha_3$$

$$g_4 = l_3 l_2 s\phi^2 b x_3 c\alpha_3 + l_3 l_2 s\phi b x_3 c\phi s\alpha_3 + l_2 b y_3 s\phi b x_2 - l_2 s\phi^2 b x_2 l_3 c\alpha_3 - l_2 s\phi b x_2 l_3 c\phi s\alpha_3$$
$$- l_3 l_2 s\phi b y_3 c\phi c\alpha_3 + l_3 l_2 s\phi^2 b y_3 s\alpha_3$$

$$g_5 = -l_2 s\phi b x_2 b x_3 - l_3 l_2 c\phi^2 b x_3 s\alpha_3 + l_3 b x_2 b y_3 s\phi s\alpha_3 - l_3 l_2 c\phi b y_3 s\phi s\alpha_3 + l_2 s\phi b x_2 l_3 c\phi c\alpha_3$$
$$+ l_3 l_2 c\phi^2 b y_3 c\alpha_3 - l_2 s\phi^2 b x_2 l_3 s\alpha_3 + l_3 b x_2 b x_3 c\phi s\alpha_3 - l_3 l_2 c\phi b x_3 s\phi c\alpha_3$$
$$+ l_3 b x_2 b x_3 s\phi c\alpha_3 - l_3 b x_2 b y_3 c\phi c\alpha_3$$

Coefficients of Eq. (5.2b):

$$h_1 = -l_2 b y_4 s\phi$$

$$h_2 = -l_2 c\phi b x_4 + l_4 b x_2 c\phi c\alpha_4 - l_4 b x_2 s\phi s\alpha_4$$

$$h_3 = l_2 s\phi b x_4 + l_2 b y_4 c\phi - l_4 b x_2 s\phi c\alpha_4 - l_4 b x_2 c\phi s\alpha_4$$

$$h_4 = l_4 l_2 s\phi^2 b x_4 c\alpha_4 + l_4 l_2 s\phi b x_4 c\phi s\alpha_4 + l_2 b y_4 s\phi b x_2 - l_2 s\phi^2 b x_2 l_4 c\alpha_4 - l_2 s\phi b x_2 l_4 c\phi s\alpha_4$$
$$- l_4 l_2 s\phi b y_4 c\phi c\alpha_4 + l_4 l_2 s\phi^2 b y_4 s\alpha_4$$

$$h_5 = -l_2 s\phi b x_2 b x_4 - l_4 l_2 c\phi^2 b x_4 s\alpha_4 + l_4 b x_2 b y_4 s\phi s\alpha_4 - l_4 l_2 c\phi b y_4 s\phi s\alpha_4 + l_2 s\phi b x_2 l_4 c\phi c\alpha_4$$
$$+ l_4 l_2 c\phi^2 b y_4 c\alpha_4 - l_2 s\phi^2 b x_2 l_4 s\alpha_4 + l_4 b x_2 b x_4 c\phi s\alpha_4 - l_4 l_2 c\phi b x_4 s\phi c\alpha_4$$
$$+ l_4 b x_2 b x_4 s\phi c\alpha_4 - l_4 b x_2 b y_4 c\phi c\alpha_4$$

Coefficients of the fourth-order polynomial $\mathbf{Q}_\mu$ in x, Eq. (5.3a):

$$\mu_1 = h_1^2\, g_2^2 + g_2 g_1 h_3^2 - g_2 g_3 h_1 h_3 - 2 g_2 h_1 h_2 g_1 - g_1 h_2 g_3 h_3 + h_2^2\, g_1^2 + h_2 g_3^2\, h_1$$

$$\mu_2 = 2(g_5 h_2 g_3 h_1 + g_2^2\, h_1 h_4 + h_2^2\, g_1 g_4 + g_2 h_3 h_5 g_1 - g_2 h_1 h_2 g_4 - g_2 h_2 g_1 h_4) - g_2 h_3 g_3 h_4$$
$$+ g_2 h_3^2\, g_4 - h_2 g_3 h_5 g_1 - g_2 h_5 g_3 h_1 - h_3 g_4 h_2 g_3 - g_2 h_3 g_5 h_1 + h_2 g_3^2\, h_4 - h_3 h_2 g_5 g_1$$

$$\mu_3 = 2(g_5 h_2 g_3 h_4 + g_2 h_3 g_4 h_5 - g_2 h_4 h_2 g_4) + h_2 g_5^2\, h_1 + g_2^2\, h_4^2 - h_2 g_5 h_5 g_1 - h_2 g_3 h_5 g_4$$
$$- h_3 h_2 g_5 g_4 - g_2 h_5 g_3 h_4 - g_2 h_5 g_5 h_1 + g_2 h_5^2\, g_1 - g_2 h_3 h_4 g_5 + h_2^2\, g_4^2$$

$$\mu_4 = g_2 g_4 h_5^2 - h_2 g_5 h_5 g_4 + h_2 g_5^2\, h_4 - g_2 h_4 g_5 h_5$$

Coefficients of the first-order polynomial $\mathbf{Q}_\eta$ in y, Eq. (5.3b):

$$\eta_1 = 2(a_2^2\, h_1 h_5 h_2 a_5 - a_2 h_2^2\, a_1 h_5 a_5) - a_2^3\, h_1 h_5^2 + a_2^2\, h_2 a_1 h_5^2 - h_2 a_3 a_2^2\, h_4 h_5 + h_2^3\, a_1 a_5^2$$
$$+ h_2^2\, a_3 a_2 a_4 h_5 - h_2^3\, a_3 a_4 a_5 + a_2^3\, h_3 h_4 h_5 - a_2^2\, h_3 h_4 h_2 a_5 - a_2^2\, h_3 h_2 a_4 h_5 - a_2 h_1 h_2^2\, a_5^2$$
$$+ a_2 h_3 h_2^2\, a_4 a_5 + h_2^2\, a_3 a_2 h_4 a_5$$

$$\eta_2 = (2(a_2 h_3 h_2 a_3^2\, h_1 + a_2 h_2^2\, a_3 h_1 a_1 - a_2^2\, h_3 h_1 h_2 a_1 - a_2 h_3^2\, a_1 h_2 a_3) - h_2^2\, a_3^3\, h_1 - h_2^3\, a_3 a_1^2$$
$$+ h_3 h_1^2\, a_2^3 + a_2^2\, h_3^3\, a_1 + a_2 h_3 h_2^2\, a_1^2 + h_2^2\, a_3^2\, h_3 a_1 - a_2^2\, h_3^2\, a_3 h_1 - a_2^2\, h_2 a_3 h_1^2) x^3$$
$$+ (2(a_2^2\, h_2 a_1 h_5 h_1 + a_2 h_3 a_5 h_2 a_3 h_1 - a_2^2\, h_3 h_2 a_1 h_4 - a_2^2\, h_2 a_3 h_1 h_4 - a_2^2\, h_3 h_1 h_2 a_4$$
$$+ a_2 h_2^2\, a_3 a_1 h_4 - h_2^3\, a_3 a_1 a_4 + a_2 h_3 h_2^2\, a_1 a_4 + a_2 h_2^2\, a_3 h_1 a_4 - a_2 h_3 h_2 a_3 h_5 a_1$$
$$+ a_2^3\, h_3 h_1 h_4 + a_2 h_3 h_2 a_3^2\, h_4 - a_2 h_3^2\, a_4 h_2 a_3 - a_2 h_2^2\, a_1 a_5 h_1) + h_2^3\, a_1^2\, a_5 + h_2^2\, a_3^2\, h_5 a_1$$
$$+ h_2^2\, a_3^2\, h_3 a_4 - h_2^2\, a_3^2\, a_5 h_1 - a_2^2\, h_3^2\, a_5 h_1 - a_2^2\, h_3^2\, a_3 h_4 + a_2^2\, h_3^2\, h_5 a_1 - a_2 h_2^2\, a_1^2\, h_5$$
$$- a_2^3\, h_1^2\, h_5 + a_2^2\, h_3^3\, a_4 + a_2^2\, h_1^2\, h_2 a_5 - h_2^2\, a_3^3\, h_4) x^2 + (2(a_2 h_3 a_5 h_2 a_3 h_4$$
$$+ h_2^2\, a_3 a_2 h_4 a_4 - a_2^2\, h_3 h_4 h_2 a_4 - a_2 h_3 h_2 a_3 h_5 a_4) + a_2^2\, h_1 h_5 h_2 a_4 + a_2^2\, h_1 h_2 a_5 h_4$$
$$+ a_2 h_3 h_2^2\, a_4^2 - h_2 a_3 a_2^2\, h_4^2 - a_2^3\, h_1 h_5 h_4 - a_2 h_1 h_2^2\, a_5 a_4 - a_2^2\, h_3^2\, a_5 h_4 - h_2^3\, a_3 a_4^2$$
$$+ a_2^2\, h_2 a_1 h_5 h_4 - a_2 h_2^2\, a_1 h_5 a_4 + h_2^2\, a_3^2\, h_5 a_4 + a_2^2\, h_3^2\, h_5 a_4 - h_2^2\, a_3^2\, a_5 h_4 + a_2^3\, h_3 h_4^2$$
$$- a_2 h_2^2\, a_1 a_5 h_4 + h_2^3\, a_1 a_5 a_4) x$$

D.4.2 Coefficients of the 4-PRR Manipulator

Coefficients of power products in step 1, Eqs. (5.12 and 5.13):

$$[\mathbf{A}] = \begin{bmatrix} a_{1,1} & a_{1,2} & a_{1,3} & a_{1,4} & a_{1,5} \\ a_{2,1} & a_{2,2} & a_{2,3} & a_{2,4} & a_{2,5} \end{bmatrix}$$

$a_{i,1} = -2s_{3_1} l_j$

$a_{i,2} = 2c_{3_1} l_2 s\alpha_j + 2s_{3_1} l_2 c\alpha_j$

$a_{i,3} = -4c_{3_1} l_j + 4c_{3_1} l_2 c\alpha_j - 4s_{3_1} l_2 s\alpha_j$

$a_{i,4} = 2s_{3_1} l_j$

$a_{i,5} = -2c_{3_1} l_2 s\alpha_j - 2s_{3_1} l_2 c\alpha_j$

where $s_{3_1} = \sin(\theta_{3_1})$, $c_{3_1} = \cos(\theta_{3_1})$, $s\alpha_j = \sin(\alpha_j)$, and $c\alpha_j = \cos(\alpha_j)$, for $i = 1, 2$ and $j = 3, 4$.

Coefficients of power products in step 2, Eq. (5.15):

$$[\mathbf{B}] = \begin{bmatrix} b_{1,1} & b_{1,2} & b_{1,3} & b_{1,4} & b_{1,5} & b_{1,6} & b_{1,7} & b_{1,8} & b_{1,9} & b_{1,10} \\ b_{2,1} & b_{2,2} & b_{2,3} & b_{2,4} & b_{2,5} & b_{2,6} & b_{2,7} & b_{2,8} & b_{2,9} & b_{2,10} \\ b_{3,1} & b_{3,2} & b_{3,3} & b_{3,4} & b_{3,5} & b_{3,6} & b_{3,7} & b_{3,8} & b_{3,9} & b_{3,10} \end{bmatrix}$$

$b_{i,1} = s(\gamma_j - \gamma_1)$

$b_{i,2} = \rho_1 c(\gamma_j) s(\gamma_1 - \alpha_1) s_{3_1} - (\rho_1 c_{3_1} + l_1) c(\gamma_j) c(\gamma_1 - \alpha_1) - (\rho_j - l_j) c(\gamma_1) c(\gamma_j - \alpha_j)$

$b_{i,3} = -\rho_1 c(\gamma_j) c(\gamma_1 - \alpha_1) s_{3_1} - (\rho_1 c_{3_1} + l_1) c(\gamma_j) s(\gamma_1 - \alpha_1) - (\rho_j - l_j) c(\gamma_1) s(\gamma_j - \alpha_j)$

$b_{i,4} = -s\left(\gamma_j\right) c\left(\gamma_1\right) by_j + c\left(\gamma_j\right) s\left(\gamma_1\right) by_1 - \left(bx_j - bx_1\right) c\left(\gamma_j\right) c\left(\gamma_1\right)$

$b_{i,5} = -2\rho_j c\left(\gamma_1\right) s(\gamma_j - \alpha_j)$

$b_{i,6} = 2\rho_j c\left(\gamma_1\right) c(\gamma_j - \alpha_j)$

$b_{i,7} = \rho_1 c(\gamma_j) s(\gamma_1 - \alpha_1) s_{3_1} - (\rho_1 c_{3_1} + l_1) c(\gamma_j) c(\gamma_1 - \alpha_1) + (\rho_j + l_j) c(\gamma_1) c(\gamma_j - \alpha_j)$

$b_{i,8} = -\rho_1 c(\gamma_j) c(\gamma_1 - \alpha_1) s_{3_1} - (\rho_1 c_{3_1} + l_1) c(\gamma_j) s(\gamma_1 - \alpha_1) + (\rho_j + l_j) c(\gamma_1) s(\gamma_j - \alpha_j)$

$b_{i,9} = s(\gamma_j - \gamma_1)$

$b_{i,10} = -s\left(\gamma_j\right) c\left(\gamma_1\right) by_j + c\left(\gamma_j\right) s\left(\gamma_1\right) by_1 - \left(bx_j - bx_1\right) c\left(\gamma_j\right) c\left(\gamma_1\right)$

for $i = 1, 2, 3$ and $j = i + 1$.

Coefficients of power products in step 3, Eq. (5.17):

$$[\mathbf{C}] = \begin{bmatrix} c_{1,1} & c_{1,2} & \cdots & c_{1,19} & c_{1,20} \\ c_{2,1} & c_{2,2} & \cdots & c_{2,19} & c_{2,20} \end{bmatrix}$$

$c_{i,1} = -b_{j,1}b_{1,2} + b_{j,2}b_{1,1}$

$c_{i,2} = -b_{j,1}b_{1,3} + b_{j,3}b_{1,1}$

$c_{i,3} = b_{j,5}b_{1,1}$

$c_{i,4} = b_{j,6}b_{1,1}$

$c_{i,5} = b_{j,7}b_{1,1} - b_{j,9}b_{1,2}$

$c_{i,6} = -b_{j,9}b_{1,3} + b_{j,8}b_{1,1}$

$c_{i,7} = -b_{j,1}b_{1,4} + b_{j,4}b_{1,1}$

$c_{i,8} = b_{j,10}b_{1,1} - b_{j,9}b_{1,4}$

$c_{i,9} = -b_{j,1}b_{1,5}$

$c_{i,10} = -b_{j,1}b_{1,6}$

$c_{i,11} = -b_{j,9}b_{1,5}$

$c_{i,12} = -b_{j,9}b_{1,6}$

$c_{i,13} = -b_{j,1}b_{1,7} + b_{j,2}b_{1,9}$

$c_{i,14} = -b_{j,1}b_{1,8} + b_{j,3}b_{1,9}$

$c_{i,15} = b_{j,5}b_{1,9}$

$c_{i,16} = b_{j,6}b_{1,9}$

$c_{i,17} = b_{j,7}b_{1,9} - b_{j,9}b_{1,7}$

$c_{i,18} = -b_{j,9}b_{1,8} + b_{j,8}b_{1,9}$

$c_{i,19} = -b_{j,1}b_{1,10} + b_{j,4}b_{1,9}$

$c_{i,20} = b_{j,10}b_{1,9} - b_{j,9}b_{1,10}$

for $i = 1, 2$ and $j = i + 1$.

D.4.3 Coefficients of the 4-RRR Manipulator

Coefficients of the simplified loop-closure equations, Eq. (5.30):

$$k_{1,i} = -2\rho_{i+4}\sin(\phi - \beta_i)$$

$$k_{2,i} = -2\rho_{i+4}\cos(\phi - \beta_i)$$

$$k_{3,i} = -2l_i\cos(\phi - \beta_i) - 2bx_i$$

$$k_{4,i} = 2\rho_{i+4}\cos(\phi - \beta_i)$$

$$k_{5,i} = -2\rho_{i+4}\sin(\phi - \beta_i)$$

$$k_{6,i} = -2l_i\sin(\phi - \beta_i) - 2by_i$$

$$k_{7,i} = -2\rho_{i+4}by_i\cos(\phi - \beta_i) + 2\rho_{i+4}bx_i\sin(\phi - \beta_i)$$

$$k_{8,i} = 2\rho_{i+4}by_i\sin(\phi - \beta_i) + 2\rho_{i+4}bx_i\cos(\phi - \beta_i) + 2l_i\rho_{i+4}$$

$$k_{9,i} = 2l_iby_i\sin(\phi - \beta_i) + 2l_ibx_i\cos(\phi - \beta_i)bx_i - \rho_i^2 + \rho_{i+4}^2 + bx_i^2 + by_i^2 + l_i^2$$

for $i = 1, 2, 3, 4$

Coefficients of power products in step 1, Eqs. (5.32 and 5.33):

$${}^{(i)}a_1 = -2s_{3_1}l_j$$

$${}^{(i)}a_2 = 2c_{3_1}l_2s\alpha_j + 2s_{3_1}l_2c\alpha_j$$

$${}^{(i)}a_3 = -4c_{3_1}l_j + 4c_{3_1}l_2c\alpha_j - 4s_{3_1}l_2s\alpha_j$$

$${}^{(i)}a_4 = 2s_{3_1}l_j$$

$${}^{(i)}a_5 = -2c_{3_1}l_2s\alpha_j - 2s_{3_1}l_2c\alpha_j$$

for $i = 1, 2$ and $j = i + 2$.

Coefficients of power products in step 2, Eq. (5.37):

$$
\begin{aligned}
{}^{(1)}\mathbf{b}_1 = [&2\left(\rho_6 - \rho_5 c_{3_1} - l_2 - bx_2\right), \quad 0, \quad -2\left(l_2 + \rho_5 c_{3_1} + \rho_6 + bx_2\right), \quad 4\rho_5 s_{3_1}, \quad 8\rho_6, \\
&4\rho_5 s_{3_1}, \quad 2\left(\rho_5 c_{3_1} - \rho_6 + l_2 - bx_2\right), \quad 0, \quad 2\left(l_2 + \rho_6 + \rho_5 c_{3_1} - bx_2\right), \quad 2\rho_5 s_{3_1}, \quad 4\rho_6, \\
&2\rho_5 s_{3_1}, \quad 4\left(l_2 - \rho_6 + \rho_5 c_{3_1}\right), \quad 0, \quad 4\left(l_2 + \rho_6 + \rho_5 c_{3_1}\right), \quad -2\rho_5 s_{3_1}, \quad -4\rho_6, \quad -2\rho_5 s_{3_1}, \\
&\left(\rho_6 - bx_2 - l_2\right)^2 + \rho_1^2 - \rho_2^2 - \rho_5^2, \quad 0, \quad \left(\rho_6 + bx_2 + l_2\right)^2 + \rho_1^2 - \rho_2^2 - \rho_5^2, \quad 0, \quad -8\rho_6 bx_2, \\
&0, \quad \left(\rho_6 + bx_2 - l_2\right)^2 + \rho_1^2 - \rho_2^2 - \rho_5^2, \quad 0, \quad \left(\rho_6 - bx_2 + l_2\right)^2 + \rho_1^2 - \rho_2^2 - \rho_5^2]
\end{aligned}
$$

and

$$
\begin{aligned}
{}^{(1)}\mathbf{b}_2 = [&2\left(\left(\rho_7 - l_3\right) c\alpha_3 - \rho_5 c_{3_1} - bx_3\right), \quad -4\rho_7 s\alpha_3, \quad -2\left(\rho_5 c_{3_1} + \left(l_3 + \rho_7\right) c\alpha_3 + bx_3\right), \\
&4\left(\left(\rho_7 - l_3\right) s\alpha_3 + \rho_5 s_{3_1}\right), \quad 8\rho_7 c\alpha_3, \quad 4\left(\rho_5 s_{3_1} - \left(\rho_7 + l_3\right) s\alpha_3\right), \quad 2(\rho_5 c_{3_1} + (l_3 - \rho_7) c\alpha_3 - \\
&bx_3), \quad 4\rho_7 s\alpha_3, \quad 2\left(\left(\rho_7 + l_3\right) c\alpha_3 + \rho_5 c_{3_1} - bx_3\right), \quad 2\left(\rho_5 s_{3_1} - by_3 + \left(\rho_7 - l_3\right) s\alpha_3\right), \\
&4\rho_7 c\alpha_3, \quad 2\left(\rho_5 s_{3_1} - \left(l_3 + \rho_7\right) s\alpha_3 - by_3\right), \quad 4\left(\rho_5 c_{3_1} + \left(l_3 - \rho_7\right) c\alpha_3\right), \quad 8\rho_7 s\alpha_3, \quad 4(\rho_5 c_{3_1} + \\
&\left(l_3 + \rho_7\right) c\alpha_3), \quad 2\left(\left(l_3 - \rho_7\right) s\alpha_3 - \rho_5 s_{3_1} - by_3\right), \quad -4\rho_7 c\alpha_3, \quad 2((\rho_7 + l_3) s\alpha_3 - by_3 - \rho_5 s_{3_1}), \\
&\xi + \left(\rho_7 - l_3\right)^2 - 2\left(\rho_7 - l_3\right)\left(by_3 s\alpha_3 + bx_3 c\alpha_3\right), \quad 4\rho_7\left(bx_3 s\alpha_3 - by_3 c\alpha_3\right), \quad \xi + \left(\rho_7 + l_3\right)^2 + \\
&2\left(\rho_7 + l_3\right)\left(by_3 s\alpha_3 + bx_3 c\alpha_3\right), \quad 4\left(\rho_7 - l_3\right)\left(by_3 c\alpha_3 - bx_3 s\alpha_3\right), \quad -8\rho_7(by_3 s\alpha_3 + bx_3 c\alpha_3), \\
&4\left(l_3 + \rho_7\right)\left(bx_3 s\alpha_3 - by_3 c\alpha_3\right), \quad \xi + \left(\rho_7 - l_3\right)^2 + 2\left(\rho_7 - l_3\right)\left(by_3 s\alpha_3 + bx_3 c\alpha_3\right), \\
&4\rho_7(by_3 c\alpha_3 - bx_3 s\alpha_3), \quad \xi + \left(\rho_7 + l_3\right)^2 - 2\left(\rho_7 + l_3\right)\left(by_3 s\alpha_3 + bx_3 c\alpha_3\right)]
\end{aligned}
$$

where $\xi = bx_3^2 + by_3^2 + \rho_1^2 - \rho_3^2 - \rho_5^2$

For Eq. (5.43); when $i = 1$, ${}^{(2)}\mathbf{b}_1 = {}^{(1)}\mathbf{b}_1$; and when $i = 2$, ${}^{(2)}\mathbf{b}_2$ is found by substituting, from ${}^{(1)}\mathbf{b}_2$, subscripts $_3$ for $_4$ and also ρ_7 for ρ_8.

Coefficients of the numerator involving the solution for x, Eq. (5.40a):

$$
\begin{aligned}
{}^{(i)}\mathbf{n}_{\mathbf{x}} = [\ & {}^{(i)}b_{1,10}\,{}^{(i)}b_{2,19} - {}^{(i)}b_{2,10}\,{}^{(i)}b_{1,19}, \\
& {}^{(i)}b_{1,10}\,{}^{(i)}b_{2,20} - {}^{(i)}b_{2,11}\,{}^{(i)}b_{1,19}, \\
& {}^{(i)}b_{1,10}\,{}^{(i)}b_{2,21} - {}^{(i)}b_{2,12}\,{}^{(i)}b_{1,19}, \\
& {}^{(i)}b_{1,11}\,{}^{(i)}b_{2,19} - {}^{(i)}b_{2,10}\,{}^{(i)}b_{1,20}, \\
& {}^{(i)}b_{1,11}\,{}^{(i)}b_{2,20} - {}^{(i)}b_{2,11}\,{}^{(i)}b_{1,20}, \\
& {}^{(i)}b_{1,11}\,{}^{(i)}b_{2,21} - {}^{(i)}b_{2,12}\,{}^{(i)}b_{1,20}, \\
& {}^{(i)}b_{1,12}\,{}^{(i)}b_{2,19} - {}^{(i)}b_{2,10}\,{}^{(i)}b_{1,21}, \\
& {}^{(i)}b_{1,12}\,{}^{(i)}b_{2,20} - {}^{(i)}b_{2,11}\,{}^{(i)}b_{1,21}, \\
& - {}^{(i)}b_{2,12}\,{}^{(i)}b_{1,21} + {}^{(i)}b_{1,12}\,{}^{(i)}b_{2,21}, \\
& - {}^{(i)}b_{2,13}\,{}^{(i)}b_{1,19} + {}^{(i)}b_{1,10}\,{}^{(i)}b_{2,22} + {}^{(i)}b_{1,13}\,{}^{(i)}b_{2,19} - {}^{(i)}b_{2,10}\,{}^{(i)}b_{1,22}, \\
& - {}^{(i)}b_{2,14}\,{}^{(i)}b_{1,19} + {}^{(i)}b_{1,13}\,{}^{(i)}b_{2,20} + {}^{(i)}b_{1,10}\,{}^{(i)}b_{2,23} - {}^{(i)}b_{2,11}\,{}^{(i)}b_{1,22}, \\
& {}^{(i)}b_{1,13}\,{}^{(i)}b_{2,21} - {}^{(i)}b_{2,15}\,{}^{(i)}b_{1,19} + {}^{(i)}b_{1,10}\,{}^{(i)}b_{2,24} - {}^{(i)}b_{2,12}\,{}^{(i)}b_{1,22}, \\
& - {}^{(i)}b_{2,10}\,{}^{(i)}b_{1,23} - {}^{(i)}b_{2,13}\,{}^{(i)}b_{1,20} + {}^{(i)}b_{1,14}\,{}^{(i)}b_{2,19} + {}^{(i)}b_{1,11}\,{}^{(i)}b_{2,22}, \\
& - {}^{(i)}b_{2,14}\,{}^{(i)}b_{1,20} - {}^{(i)}b_{2,11}\,{}^{(i)}b_{1,23} + {}^{(i)}b_{1,14}\,{}^{(i)}b_{2,20} + {}^{(i)}b_{1,11}\,{}^{(i)}b_{2,23}, \\
& - {}^{(i)}b_{2,15}\,{}^{(i)}b_{1,20} + {}^{(i)}b_{1,14}\,{}^{(i)}b_{2,21} + {}^{(i)}b_{1,11}\,{}^{(i)}b_{2,24} - {}^{(i)}b_{2,12}\,{}^{(i)}b_{1,23}, \\
& - {}^{(i)}b_{2,13}\,{}^{(i)}b_{1,21} - {}^{(i)}b_{2,10}\,{}^{(i)}b_{1,24} + {}^{(i)}b_{1,15}\,{}^{(i)}b_{2,19} + {}^{(i)}b_{1,12}\,{}^{(i)}b_{2,22}, \\
& - {}^{(i)}b_{2,14}\,{}^{(i)}b_{1,21} - {}^{(i)}b_{2,11}\,{}^{(i)}b_{1,24} + {}^{(i)}b_{1,15}\,{}^{(i)}b_{2,20} + {}^{(i)}b_{1,12}\,{}^{(i)}b_{2,23}, \\
& {}^{(i)}b_{1,15}\,{}^{(i)}b_{2,21} - {}^{(i)}b_{2,15}\,{}^{(i)}b_{1,21} - {}^{(i)}b_{2,12}\,{}^{(i)}b_{1,24} + {}^{(i)}b_{1,12}\,{}^{(i)}b_{2,24}, \\
& - {}^{(i)}b_{2,13}\,{}^{(i)}b_{1,22} + {}^{(i)}b_{1,10}\,{}^{(i)}b_{2,25} - {}^{(i)}b_{2,16}\,{}^{(i)}b_{1,19} + {}^{(i)}b_{1,13}\,{}^{(i)}b_{2,22} + {}^{(i)}b_{1,16}\,{}^{(i)}b_{2,19} - {}^{(i)}b_{2,10}\,{}^{(i)}b_{1,25}, \\
& - {}^{(i)}b_{2,11}\,{}^{(i)}b_{1,25} - {}^{(i)}b_{2,17}\,{}^{(i)}b_{1,19} + {}^{(i)}b_{1,10}\,{}^{(i)}b_{2,26} + {}^{(i)}b_{1,13}\,{}^{(i)}b_{2,23} + {}^{(i)}b_{1,16}\,{}^{(i)}b_{2,20} - {}^{(i)}b_{2,14}\,{}^{(i)}b_{1,22}, \\
& - {}^{(i)}b_{2,18}\,{}^{(i)}b_{1,19} + {}^{(i)}b_{1,13}\,{}^{(i)}b_{2,24} + {}^{(i)}b_{1,16}\,{}^{(i)}b_{2,21} - {}^{(i)}b_{2,15}\,{}^{(i)}b_{1,22} + {}^{(i)}b_{1,10}\,{}^{(i)}b_{2,27} - {}^{(i)}b_{2,12}\,{}^{(i)}b_{1,25}, \\
& - {}^{(i)}b_{2,10}\,{}^{(i)}b_{1,26} - {}^{(i)}b_{2,13}\,{}^{(i)}b_{1,23} + {}^{(i)}b_{1,14}\,{}^{(i)}b_{2,22} + {}^{(i)}b_{1,17}\,{}^{(i)}b_{2,19} - {}^{(i)}b_{2,16}\,{}^{(i)}b_{1,20} + {}^{(i)}b_{1,11}\,{}^{(i)}b_{2,25}, \\
& - {}^{(i)}b_{2,11}\,{}^{(i)}b_{1,26} + {}^{(i)}b_{1,14}\,{}^{(i)}b_{2,23} - {}^{(i)}b_{2,17}\,{}^{(i)}b_{1,20} + {}^{(i)}b_{1,17}\,{}^{(i)}b_{2,20} - {}^{(i)}b_{2,14}\,{}^{(i)}b_{1,23} + {}^{(i)}b_{1,11}\,{}^{(i)}b_{2,26},
\end{aligned}
$$

$$
\begin{aligned}
&-{}^{(i)}b_{2,12}\,{}^{(i)}b_{1,26}-{}^{(i)}b_{2,15}\,{}^{(i)}b_{1,23}-{}^{(i)}b_{2,18}\,{}^{(i)}b_{1,20}+{}^{(i)}b_{1,11}\,{}^{(i)}b_{2,27}+{}^{(i)}b_{1,14}\,{}^{(i)}b_{2,24}+{}^{(i)}b_{1,17}\,{}^{(i)}b_{2,21},\\
&-{}^{(i)}b_{2,10}\,{}^{(i)}b_{1,27}+{}^{(i)}b_{1,12}\,{}^{(i)}b_{2,25}+{}^{(i)}b_{1,15}\,{}^{(i)}b_{2,22}-{}^{(i)}b_{2,16}\,{}^{(i)}b_{1,21}+{}^{(i)}b_{1,18}\,{}^{(i)}b_{2,19}-{}^{(i)}b_{2,13}\,{}^{(i)}b_{1,24},\\
&-{}^{(i)}b_{2,14}\,{}^{(i)}b_{1,24}+{}^{(i)}b_{1,15}\,{}^{(i)}b_{2,23}+{}^{(i)}b_{1,12}\,{}^{(i)}b_{2,26}+{}^{(i)}b_{1,18}\,{}^{(i)}b_{2,20}-{}^{(i)}b_{2,17}\,{}^{(i)}b_{1,21}-{}^{(i)}b_{2,11}\,{}^{(i)}b_{1,27},\\
&-{}^{(i)}b_{2,18}\,{}^{(i)}b_{1,21}-{}^{(i)}b_{2,12}\,{}^{(i)}b_{1,27}+{}^{(i)}b_{1,15}\,{}^{(i)}b_{2,24}+{}^{(i)}b_{1,18}\,{}^{(i)}b_{2,21}+{}^{(i)}b_{1,12}\,{}^{(i)}b_{2,27}-{}^{(i)}b_{2,15}\,{}^{(i)}b_{1,24},\\
&-{}^{(i)}b_{2,16}\,{}^{(i)}b_{1,22}+{}^{(i)}b_{1,13}\,{}^{(i)}b_{2,25}+{}^{(i)}b_{1,16}\,{}^{(i)}b_{2,22}-{}^{(i)}b_{2,13}\,{}^{(i)}b_{1,25},\\
&-{}^{(i)}b_{2,14}\,{}^{(i)}b_{1,25}-{}^{(i)}b_{2,17}\,{}^{(i)}b_{1,22}+{}^{(i)}b_{1,16}\,{}^{(i)}b_{2,23}+{}^{(i)}b_{1,13}\,{}^{(i)}b_{2,26},\\
&{}^{(i)}b_{1,16}\,{}^{(i)}b_{2,24}+{}^{(i)}b_{1,13}\,{}^{(i)}b_{2,27}-{}^{(i)}b_{2,15}\,{}^{(i)}b_{1,25}-{}^{(i)}b_{2,18}\,{}^{(i)}b_{1,22},\\
&{}^{(i)}b_{1,17}\,{}^{(i)}b_{2,22}+{}^{(i)}b_{1,14}\,{}^{(i)}b_{2,25}-{}^{(i)}b_{2,16}\,{}^{(i)}b_{1,23}-{}^{(i)}b_{2,13}\,{}^{(i)}b_{1,26},\\
&{}^{(i)}b_{1,14}\,{}^{(i)}b_{2,26}-{}^{(i)}b_{2,17}\,{}^{(i)}b_{1,23}+{}^{(i)}b_{1,17}\,{}^{(i)}b_{2,23}-{}^{(i)}b_{2,14}\,{}^{(i)}b_{1,26},\\
&-{}^{(i)}b_{2,18}\,{}^{(i)}b_{1,23}-{}^{(i)}b_{2,15}\,{}^{(i)}b_{1,26}+{}^{(i)}b_{1,17}\,{}^{(i)}b_{2,24}+{}^{(i)}b_{1,14}\,{}^{(i)}b_{2,27},\\
&-{}^{(i)}b_{2,13}\,{}^{(i)}b_{1,27}+{}^{(i)}b_{1,15}\,{}^{(i)}b_{2,25}+{}^{(i)}b_{1,18}\,{}^{(i)}b_{2,22}-{}^{(i)}b_{2,16}\,{}^{(i)}b_{1,24},\\
&-{}^{(i)}b_{2,14}\,{}^{(i)}b_{1,27}+{}^{(i)}b_{1,15}\,{}^{(i)}b_{2,26}+{}^{(i)}b_{1,18}\,{}^{(i)}b_{2,23}-{}^{(i)}b_{2,17}\,{}^{(i)}b_{1,24},\\
&{}^{(i)}b_{1,15}\,{}^{(i)}b_{2,27}-{}^{(i)}b_{2,15}\,{}^{(i)}b_{1,27}-{}^{(i)}b_{2,18}\,{}^{(i)}b_{1,24}+{}^{(i)}b_{1,18}\,{}^{(i)}b_{2,24},\\
&-{}^{(i)}b_{2,16}\,{}^{(i)}b_{1,25}+{}^{(i)}b_{1,16}\,{}^{(i)}b_{2,25},\\
&{}^{(i)}b_{1,16}\,{}^{(i)}b_{2,26}-{}^{(i)}b_{2,17}\,{}^{(i)}b_{1,25},\\
&{}^{(i)}b_{1,16}\,{}^{(i)}b_{2,27}-{}^{(i)}b_{2,18}\,{}^{(i)}b_{1,25},\\
&-{}^{(i)}b_{2,16}\,{}^{(i)}b_{1,26}+{}^{(i)}b_{1,17}\,{}^{(i)}b_{2,25},\\
&{}^{(i)}b_{1,17}\,{}^{(i)}b_{2,26}-{}^{(i)}b_{2,17}\,{}^{(i)}b_{1,26},\\
&{}^{(i)}b_{1,17}\,{}^{(i)}b_{2,27}-{}^{(i)}b_{2,18}\,{}^{(i)}b_{1,26},\\
&-{}^{(i)}b_{2,16}\,{}^{(i)}b_{1,27}+{}^{(i)}b_{1,18}\,{}^{(i)}b_{2,25},\\
&-{}^{(i)}b_{2,17}\,{}^{(i)}b_{1,27}+{}^{(i)}b_{1,18}\,{}^{(i)}b_{2,26},\\
&{}^{(i)}b_{1,18}\,{}^{(i)}b_{2,27}-{}^{(i)}b_{2,18}\,{}^{(i)}b_{1,27}]
\end{aligned}
$$

for $i = 1, 2$.

Coefficients of the numerator involving the solution for y, Eq. (5.40b):

$$
\begin{aligned}
{}^{(i)}\mathbf{n_y} = [& -{}^{(i)}b_{1,1}\,{}^{(i)}b_{2,19}+{}^{(i)}b_{2,1}\,{}^{(i)}b_{1,19}, \\
& -{}^{(i)}b_{1,1}\,{}^{(i)}b_{2,20}+{}^{(i)}b_{2,2}\,{}^{(i)}b_{1,19}, \\
& -{}^{(i)}b_{1,1}\,{}^{(i)}b_{2,21}+{}^{(i)}b_{2,3}\,{}^{(i)}b_{1,19}, \\
& -{}^{(i)}b_{1,2}\,{}^{(i)}b_{2,19}+{}^{(i)}b_{2,1}\,{}^{(i)}b_{1,20}, \\
& -{}^{(i)}b_{1,2}\,{}^{(i)}b_{2,20}+{}^{(i)}b_{2,2}\,{}^{(i)}b_{1,20}, \\
& -{}^{(i)}b_{1,2}\,{}^{(i)}b_{2,21}+{}^{(i)}b_{2,3}\,{}^{(i)}b_{1,20}, \\
& {}^{(i)}b_{2,1}\,{}^{(i)}b_{1,21}-{}^{(i)}b_{1,3}\,{}^{(i)}b_{2,19}, \\
& -{}^{(i)}b_{1,3}\,{}^{(i)}b_{2,20}+{}^{(i)}b_{2,2}\,{}^{(i)}b_{1,21}, \\
& -{}^{(i)}b_{1,3}\,{}^{(i)}b_{2,21}+{}^{(i)}b_{2,3}\,{}^{(i)}b_{1,21}, \\
& -{}^{(i)}b_{1,1}\,{}^{(i)}b_{2,22}+{}^{(i)}b_{2,4}\,{}^{(i)}b_{1,19}+{}^{(i)}b_{2,1}\,{}^{(i)}b_{1,22}-{}^{(i)}b_{1,4}\,{}^{(i)}b_{2,19}, \\
& -{}^{(i)}b_{1,1}\,{}^{(i)}b_{2,23}+{}^{(i)}b_{2,2}\,{}^{(i)}b_{1,22}-{}^{(i)}b_{1,4}\,{}^{(i)}b_{2,20}+{}^{(i)}b_{2,5}\,{}^{(i)}b_{1,19}, \\
& {}^{(i)}b_{2,6}\,{}^{(i)}b_{1,19}+{}^{(i)}b_{2,3}\,{}^{(i)}b_{1,22}-{}^{(i)}b_{1,4}\,{}^{(i)}b_{2,21}-{}^{(i)}b_{1,1}\,{}^{(i)}b_{2,24}, \\
& {}^{(i)}b_{2,1}\,{}^{(i)}b_{1,23}+{}^{(i)}b_{2,4}\,{}^{(i)}b_{1,20}-{}^{(i)}b_{1,5}\,{}^{(i)}b_{2,19}-{}^{(i)}b_{1,2}\,{}^{(i)}b_{2,22}, \\
& -{}^{(i)}b_{1,2}\,{}^{(i)}b_{2,23}+{}^{(i)}b_{2,2}\,{}^{(i)}b_{1,23}-{}^{(i)}b_{1,5}\,{}^{(i)}b_{2,20}+{}^{(i)}b_{2,5}\,{}^{(i)}b_{1,20}, \\
& {}^{(i)}b_{2,6}\,{}^{(i)}b_{1,20}+{}^{(i)}b_{2,3}\,{}^{(i)}b_{1,23}-{}^{(i)}b_{1,2}\,{}^{(i)}b_{2,24}-{}^{(i)}b_{1,5}\,{}^{(i)}b_{2,21}, \\
& {}^{(i)}b_{2,1}\,{}^{(i)}b_{1,24}+{}^{(i)}b_{2,4}\,{}^{(i)}b_{1,21}-{}^{(i)}b_{1,3}\,{}^{(i)}b_{2,22}-{}^{(i)}b_{1,6}\,{}^{(i)}b_{2,19}, \\
& {}^{(i)}b_{2,5}\,{}^{(i)}b_{1,21}-{}^{(i)}b_{1,3}\,{}^{(i)}b_{2,23}-{}^{(i)}b_{1,6}\,{}^{(i)}b_{2,20}+{}^{(i)}b_{2,2}\,{}^{(i)}b_{1,24}, \\
& -{}^{(i)}b_{1,3}\,{}^{(i)}b_{2,24}+{}^{(i)}b_{2,3}\,{}^{(i)}b_{1,24}-{}^{(i)}b_{1,6}\,{}^{(i)}b_{2,21}+{}^{(i)}b_{2,6}\,{}^{(i)}b_{1,21}, \\
& {}^{(i)}b_{2,4}\,{}^{(i)}b_{1,22}+{}^{(i)}b_{2,1}\,{}^{(i)}b_{1,25}-{}^{(i)}b_{1,1}\,{}^{(i)}b_{2,25}-{}^{(i)}b_{1,4}\,{}^{(i)}b_{2,22}+{}^{(i)}b_{2,7}\,{}^{(i)}b_{1,19}-{}^{(i)}b_{1,7}\,{}^{(i)}b_{2,19}, \\
& -{}^{(i)}b_{1,1}\,{}^{(i)}b_{2,26}+{}^{(i)}b_{2,2}\,{}^{(i)}b_{1,25}+{}^{(i)}b_{2,8}\,{}^{(i)}b_{1,19}-{}^{(i)}b_{1,4}\,{}^{(i)}b_{2,23}-{}^{(i)}b_{1,7}\,{}^{(i)}b_{2,20}+{}^{(i)}b_{2,5}\,{}^{(i)}b_{1,22}, \\
& -{}^{(i)}b_{1,1}\,{}^{(i)}b_{2,27}+{}^{(i)}b_{2,6}\,{}^{(i)}b_{1,22}+{}^{(i)}b_{2,3}\,{}^{(i)}b_{1,25}-{}^{(i)}b_{1,4}\,{}^{(i)}b_{2,24}-{}^{(i)}b_{1,7}\,{}^{(i)}b_{2,21}+{}^{(i)}b_{2,9}\,{}^{(i)}b_{1,19}, \\
& -{}^{(i)}b_{1,2}\,{}^{(i)}b_{2,25}-{}^{(i)}b_{1,8}\,{}^{(i)}b_{2,19}+{}^{(i)}b_{2,1}\,{}^{(i)}b_{1,26}+{}^{(i)}b_{2,4}\,{}^{(i)}b_{1,23}-{}^{(i)}b_{1,5}\,{}^{(i)}b_{2,22}+{}^{(i)}b_{2,7}\,{}^{(i)}b_{1,20}, \\
& -{}^{(i)}b_{1,8}\,{}^{(i)}b_{2,20}-{}^{(i)}b_{1,2}\,{}^{(i)}b_{2,26}+{}^{(i)}b_{2,2}\,{}^{(i)}b_{1,26}-{}^{(i)}b_{1,5}\,{}^{(i)}b_{2,23}+{}^{(i)}b_{2,8}\,{}^{(i)}b_{1,20}+{}^{(i)}b_{2,5}\,{}^{(i)}b_{1,23},
\end{aligned}
$$

$$
\begin{aligned}
&{}^{(i)}b_{2,3}\,{}^{(i)}b_{1,26}+{}^{(i)}b_{2,6}\,{}^{(i)}b_{1,23}-{}^{(i)}b_{1,8}\,{}^{(i)}b_{2,21}+{}^{(i)}b_{2,9}\,{}^{(i)}b_{1,20}-{}^{(i)}b_{1,5}\,{}^{(i)}b_{2,24}-{}^{(i)}b_{1,2}\,{}^{(i)}b_{2,27},\\
&{}^{(i)}b_{2,7}\,{}^{(i)}b_{1,21}+{}^{(i)}b_{2,4}\,{}^{(i)}b_{1,24}-{}^{(i)}b_{1,9}\,{}^{(i)}b_{2,19}+{}^{(i)}b_{2,1}\,{}^{(i)}b_{1,27}-{}^{(i)}b_{1,6}\,{}^{(i)}b_{2,22}-{}^{(i)}b_{1,3}\,{}^{(i)}b_{2,25},\\
&{}^{(i)}b_{2,5}\,{}^{(i)}b_{1,24}+{}^{(i)}b_{2,8}\,{}^{(i)}b_{1,21}-{}^{(i)}b_{1,3}\,{}^{(i)}b_{2,26}-{}^{(i)}b_{1,9}\,{}^{(i)}b_{2,20}+{}^{(i)}b_{2,2}\,{}^{(i)}b_{1,27}-{}^{(i)}b_{1,6}\,{}^{(i)}b_{2,23},\\
&{}^{(i)}b_{2,3}\,{}^{(i)}b_{1,27}-{}^{(i)}b_{1,6}\,{}^{(i)}b_{2,24}+{}^{(i)}b_{2,9}\,{}^{(i)}b_{1,21}-{}^{(i)}b_{1,3}\,{}^{(i)}b_{2,27}+{}^{(i)}b_{2,6}\,{}^{(i)}b_{1,24}-{}^{(i)}b_{1,9}\,{}^{(i)}b_{2,21},\\
&{}^{(i)}b_{2,7}\,{}^{(i)}b_{1,22}+{}^{(i)}b_{2,4}\,{}^{(i)}b_{1,25}-{}^{(i)}b_{1,4}\,{}^{(i)}b_{2,25}-{}^{(i)}b_{1,7}\,{}^{(i)}b_{2,22},\\
&{}^{(i)}b_{2,5}\,{}^{(i)}b_{1,25}+{}^{(i)}b_{2,8}\,{}^{(i)}b_{1,22}-{}^{(i)}b_{1,4}\,{}^{(i)}b_{2,26}-{}^{(i)}b_{1,7}\,{}^{(i)}b_{2,23},\\
&{}^{(i)}b_{2,6}\,{}^{(i)}b_{1,25}-{}^{(i)}b_{1,4}\,{}^{(i)}b_{2,27}-{}^{(i)}b_{1,7}\,{}^{(i)}b_{2,24}+{}^{(i)}b_{2,9}\,{}^{(i)}b_{1,22},\\
&-{}^{(i)}b_{1,8}\,{}^{(i)}b_{2,22}+{}^{(i)}b_{2,4}\,{}^{(i)}b_{1,26}-{}^{(i)}b_{1,5}\,{}^{(i)}b_{2,25}+{}^{(i)}b_{2,7}\,{}^{(i)}b_{1,23},\\
&{}^{(i)}b_{2,5}\,{}^{(i)}b_{1,26}-{}^{(i)}b_{1,5}\,{}^{(i)}b_{2,26}+{}^{(i)}b_{2,8}\,{}^{(i)}b_{1,23}-{}^{(i)}b_{1,8}\,{}^{(i)}b_{2,23},\\
&{}^{(i)}b_{2,6}\,{}^{(i)}b_{1,26}-{}^{(i)}b_{1,8}\,{}^{(i)}b_{2,24}-{}^{(i)}b_{1,5}\,{}^{(i)}b_{2,27}+{}^{(i)}b_{2,9}\,{}^{(i)}b_{1,23},\\
&{}^{(i)}b_{2,7}\,{}^{(i)}b_{1,24}-{}^{(i)}b_{1,9}\,{}^{(i)}b_{2,22}+{}^{(i)}b_{2,4}\,{}^{(i)}b_{1,27}-{}^{(i)}b_{1,6}\,{}^{(i)}b_{2,25},\\
&{}^{(i)}b_{2,8}\,{}^{(i)}b_{1,24}+{}^{(i)}b_{2,5}\,{}^{(i)}b_{1,27}-{}^{(i)}b_{1,6}\,{}^{(i)}b_{2,26}-{}^{(i)}b_{1,9}\,{}^{(i)}b_{2,23},\\
&-{}^{(i)}b_{1,6}\,{}^{(i)}b_{2,27}+{}^{(i)}b_{2,9}\,{}^{(i)}b_{1,24}-{}^{(i)}b_{1,9}\,{}^{(i)}b_{2,24}+{}^{(i)}b_{2,6}\,{}^{(i)}b_{1,27},\\
&-{}^{(i)}b_{1,7}\,{}^{(i)}b_{2,25}+{}^{(i)}b_{2,7}\,{}^{(i)}b_{1,25},\\
&-{}^{(i)}b_{1,7}\,{}^{(i)}b_{2,26}+{}^{(i)}b_{2,8}\,{}^{(i)}b_{1,25},\\
&{}^{(i)}b_{2,9}\,{}^{(i)}b_{1,25}-{}^{(i)}b_{1,7}\,{}^{(i)}b_{2,27},\\
&-{}^{(i)}b_{1,8}\,{}^{(i)}b_{2,25}+{}^{(i)}b_{2,7}\,{}^{(i)}b_{1,26},\\
&-{}^{(i)}b_{1,8}\,{}^{(i)}b_{2,26}+{}^{(i)}b_{2,8}\,{}^{(i)}b_{1,26},\\
&{}^{(i)}b_{2,9}\,{}^{(i)}b_{1,26}-{}^{(i)}b_{1,8}\,{}^{(i)}b_{2,27},\\
&-{}^{(i)}b_{1,9}\,{}^{(i)}b_{2,25}+{}^{(i)}b_{2,7}\,{}^{(i)}b_{1,27},\\
&-{}^{(i)}b_{1,9}\,{}^{(i)}b_{2,26}+{}^{(i)}b_{2,8}\,{}^{(i)}b_{1,27},\\
&{}^{(i)}b_{2,9}\,{}^{(i)}b_{1,27}-{}^{(i)}b_{1,9}\,{}^{(i)}b_{2,27}]
\end{aligned}
$$

for $i = 1, 2$.

Coefficients of the denominators involving the solutions for x and y, Eq. (5.40c):

$$
\begin{aligned}
{}^{(i)}\mathbf{dt} = [&- {}^{(i)}b_{2,1}\,{}^{(i)}b_{1,10} + {}^{(i)}b_{1,1}\,{}^{(i)}b_{2,10},\\
&- {}^{(i)}b_{2,2}\,{}^{(i)}b_{1,10} + {}^{(i)}b_{1,1}\,{}^{(i)}b_{2,11},\\
&{}^{(i)}b_{1,1}\,{}^{(i)}b_{2,12} - {}^{(i)}b_{2,3}\,{}^{(i)}b_{1,10},\\
&- {}^{(i)}b_{2,1}\,{}^{(i)}b_{1,11} + {}^{(i)}b_{1,2}\,{}^{(i)}b_{2,10},\\
&- {}^{(i)}b_{2,2}\,{}^{(i)}b_{1,11} + {}^{(i)}b_{1,2}\,{}^{(i)}b_{2,11},\\
&{}^{(i)}b_{1,2}\,{}^{(i)}b_{2,12} - {}^{(i)}b_{2,3}\,{}^{(i)}b_{1,11},\\
&{}^{(i)}b_{1,3}\,{}^{(i)}b_{2,10} - {}^{(i)}b_{2,1}\,{}^{(i)}b_{1,12},\\
&{}^{(i)}b_{1,3}\,{}^{(i)}b_{2,11} - {}^{(i)}b_{2,2}\,{}^{(i)}b_{1,12},\\
&{}^{(i)}b_{1,3}\,{}^{(i)}b_{2,12} - {}^{(i)}b_{2,3}\,{}^{(i)}b_{1,12},\\
&{}^{(i)}b_{1,1}\,{}^{(i)}b_{2,13} - {}^{(i)}b_{2,1}\,{}^{(i)}b_{1,13} + {}^{(i)}b_{1,4}\,{}^{(i)}b_{2,10} - {}^{(i)}b_{2,4}\,{}^{(i)}b_{1,10},\\
&- {}^{(i)}b_{2,2}\,{}^{(i)}b_{1,13} - {}^{(i)}b_{2,5}\,{}^{(i)}b_{1,10} + {}^{(i)}b_{1,1}\,{}^{(i)}b_{2,14} + {}^{(i)}b_{1,4}\,{}^{(i)}b_{2,11},\\
&{}^{(i)}b_{1,1}\,{}^{(i)}b_{2,15} + {}^{(i)}b_{1,4}\,{}^{(i)}b_{2,12} - {}^{(i)}b_{2,3}\,{}^{(i)}b_{1,13} - {}^{(i)}b_{2,6}\,{}^{(i)}b_{1,10},\\
&- {}^{(i)}b_{2,1}\,{}^{(i)}b_{1,14} - {}^{(i)}b_{2,4}\,{}^{(i)}b_{1,11} + {}^{(i)}b_{1,5}\,{}^{(i)}b_{2,10} + {}^{(i)}b_{1,2}\,{}^{(i)}b_{2,13},\\
&- {}^{(i)}b_{2,2}\,{}^{(i)}b_{1,14} - {}^{(i)}b_{2,5}\,{}^{(i)}b_{1,11} + {}^{(i)}b_{1,5}\,{}^{(i)}b_{2,11} + {}^{(i)}b_{1,2}\,{}^{(i)}b_{2,14},\\
&{}^{(i)}b_{1,2}\,{}^{(i)}b_{2,15} + {}^{(i)}b_{1,5}\,{}^{(i)}b_{2,12} - {}^{(i)}b_{2,6}\,{}^{(i)}b_{1,11} - {}^{(i)}b_{2,3}\,{}^{(i)}b_{1,14},\\
&{}^{(i)}b_{1,3}\,{}^{(i)}b_{2,13} + {}^{(i)}b_{1,6}\,{}^{(i)}b_{2,10} - {}^{(i)}b_{2,4}\,{}^{(i)}b_{1,12} - {}^{(i)}b_{2,1}\,{}^{(i)}b_{1,15},\\
&{}^{(i)}b_{1,6}\,{}^{(i)}b_{2,11} + {}^{(i)}b_{1,3}\,{}^{(i)}b_{2,14} - {}^{(i)}b_{2,2}\,{}^{(i)}b_{1,15} - {}^{(i)}b_{2,5}\,{}^{(i)}b_{1,12},\\
&- {}^{(i)}b_{2,6}\,{}^{(i)}b_{1,12} - {}^{(i)}b_{2,3}\,{}^{(i)}b_{1,15} + {}^{(i)}b_{1,6}\,{}^{(i)}b_{2,12} + {}^{(i)}b_{1,3}\,{}^{(i)}b_{2,15},\\
&- {}^{(i)}b_{2,1}\,{}^{(i)}b_{1,16} - {}^{(i)}b_{2,4}\,{}^{(i)}b_{1,13} + {}^{(i)}b_{1,4}\,{}^{(i)}b_{2,13} - {}^{(i)}b_{2,7}\,{}^{(i)}b_{1,10} + {}^{(i)}b_{1,1}\,{}^{(i)}b_{2,16} + {}^{(i)}b_{1,7}\,{}^{(i)}b_{2,10},\\
&- {}^{(i)}b_{2,8}\,{}^{(i)}b_{1,10} - {}^{(i)}b_{2,2}\,{}^{(i)}b_{1,16} - {}^{(i)}b_{2,5}\,{}^{(i)}b_{1,13} + {}^{(i)}b_{1,1}\,{}^{(i)}b_{2,17} + {}^{(i)}b_{1,4}\,{}^{(i)}b_{2,14} + {}^{(i)}b_{1,7}\,{}^{(i)}b_{2,11},\\
&- {}^{(i)}b_{2,3}\,{}^{(i)}b_{1,16} + {}^{(i)}b_{1,1}\,{}^{(i)}b_{2,18} + {}^{(i)}b_{1,7}\,{}^{(i)}b_{2,12} + {}^{(i)}b_{1,4}\,{}^{(i)}b_{2,15} - {}^{(i)}b_{2,9}\,{}^{(i)}b_{1,10} - {}^{(i)}b_{2,6}\,{}^{(i)}b_{1,13},\\
&- {}^{(i)}b_{2,4}\,{}^{(i)}b_{1,14} - {}^{(i)}b_{2,1}\,{}^{(i)}b_{1,17} + {}^{(i)}b_{1,5}\,{}^{(i)}b_{2,13} - {}^{(i)}b_{2,7}\,{}^{(i)}b_{1,11} + {}^{(i)}b_{1,2}\,{}^{(i)}b_{2,16} + {}^{(i)}b_{1,8}\,{}^{(i)}b_{2,10},\\
&- {}^{(i)}b_{2,8}\,{}^{(i)}b_{1,11} - {}^{(i)}b_{2,5}\,{}^{(i)}b_{1,14} - {}^{(i)}b_{2,2}\,{}^{(i)}b_{1,17} + {}^{(i)}b_{1,5}\,{}^{(i)}b_{2,14} + {}^{(i)}b_{1,2}\,{}^{(i)}b_{2,17} + {}^{(i)}b_{1,8}\,{}^{(i)}b_{2,11},
\end{aligned}
$$

$$-{}^{(i)}b_{2,3}\,{}^{(i)}b_{1,17}+{}^{(i)}b_{1,2}\,{}^{(i)}b_{2,18}+{}^{(i)}b_{1,5}\,{}^{(i)}b_{2,15}+{}^{(i)}b_{1,8}\,{}^{(i)}b_{2,12}-{}^{(i)}b_{2,9}\,{}^{(i)}b_{1,11}-{}^{(i)}b_{2,6}\,{}^{(i)}b_{1,14},$$

$${}^{(i)}b_{1,6}\,{}^{(i)}b_{2,13}-{}^{(i)}b_{2,7}\,{}^{(i)}b_{1,12}+{}^{(i)}b_{1,9}\,{}^{(i)}b_{2,10}+{}^{(i)}b_{1,3}\,{}^{(i)}b_{2,16}-{}^{(i)}b_{2,1}\,{}^{(i)}b_{1,18}-{}^{(i)}b_{2,4}\,{}^{(i)}b_{1,15},$$

$$-{}^{(i)}b_{2,8}\,{}^{(i)}b_{1,12}+{}^{(i)}b_{1,9}\,{}^{(i)}b_{2,11}+{}^{(i)}b_{1,3}\,{}^{(i)}b_{2,17}+{}^{(i)}b_{1,6}\,{}^{(i)}b_{2,14}-{}^{(i)}b_{2,2}\,{}^{(i)}b_{1,18}-{}^{(i)}b_{2,5}\,{}^{(i)}b_{1,15},$$

$$-{}^{(i)}b_{2,6}\,{}^{(i)}b_{1,15}+{}^{(i)}b_{1,3}\,{}^{(i)}b_{2,18}-{}^{(i)}b_{2,9}\,{}^{(i)}b_{1,12}-{}^{(i)}b_{2,3}\,{}^{(i)}b_{1,18}+{}^{(i)}b_{1,6}\,{}^{(i)}b_{2,15}+{}^{(i)}b_{1,9}\,{}^{(i)}b_{2,12},$$

$$-{}^{(i)}b_{2,4}\,{}^{(i)}b_{1,16}+{}^{(i)}b_{1,4}\,{}^{(i)}b_{2,16}-{}^{(i)}b_{2,7}\,{}^{(i)}b_{1,13}+{}^{(i)}b_{1,7}\,{}^{(i)}b_{2,13},$$

$$-{}^{(i)}b_{2,8}\,{}^{(i)}b_{1,13}-{}^{(i)}b_{2,5}\,{}^{(i)}b_{1,16}+{}^{(i)}b_{1,4}\,{}^{(i)}b_{2,17}+{}^{(i)}b_{1,7}\,{}^{(i)}b_{2,14},$$

$${}^{(i)}b_{1,4}\,{}^{(i)}b_{2,18}+{}^{(i)}b_{1,7}\,{}^{(i)}b_{2,15}-{}^{(i)}b_{2,9}\,{}^{(i)}b_{1,13}-{}^{(i)}b_{2,6}\,{}^{(i)}b_{1,16},$$

$${}^{(i)}b_{1,5}\,{}^{(i)}b_{2,16}-{}^{(i)}b_{2,7}\,{}^{(i)}b_{1,14}+{}^{(i)}b_{1,8}\,{}^{(i)}b_{2,13}-{}^{(i)}b_{2,4}\,{}^{(i)}b_{1,17},$$

$$-{}^{(i)}b_{2,8}\,{}^{(i)}b_{1,14}-{}^{(i)}b_{2,5}\,{}^{(i)}b_{1,17}+{}^{(i)}b_{1,5}\,{}^{(i)}b_{2,17}+{}^{(i)}b_{1,8}\,{}^{(i)}b_{2,14},$$

$${}^{(i)}b_{1,5}\,{}^{(i)}b_{2,18}+{}^{(i)}b_{1,8}\,{}^{(i)}b_{2,15}-{}^{(i)}b_{2,9}\,{}^{(i)}b_{1,14}-{}^{(i)}b_{2,6}\,{}^{(i)}b_{1,17},$$

$${}^{(i)}b_{1,9}\,{}^{(i)}b_{2,13}-{}^{(i)}b_{2,7}\,{}^{(i)}b_{1,15}+{}^{(i)}b_{1,6}\,{}^{(i)}b_{2,16}-{}^{(i)}b_{2,4}\,{}^{(i)}b_{1,18},$$

$$-{}^{(i)}b_{2,8}\,{}^{(i)}b_{1,15}+{}^{(i)}b_{1,9}\,{}^{(i)}b_{2,14}+{}^{(i)}b_{1,6}\,{}^{(i)}b_{2,17}-{}^{(i)}b_{2,5}\,{}^{(i)}b_{1,18},$$

$${}^{(i)}b_{1,9}\,{}^{(i)}b_{2,15}-{}^{(i)}b_{2,9}\,{}^{(i)}b_{1,15}-{}^{(i)}b_{2,6}\,{}^{(i)}b_{1,18}+{}^{(i)}b_{1,6}\,{}^{(i)}b_{2,18},$$

$$-{}^{(i)}b_{2,7}\,{}^{(i)}b_{1,16}+{}^{(i)}b_{1,7}\,{}^{(i)}b_{2,16},$$

$$-{}^{(i)}b_{2,8}\,{}^{(i)}b_{1,16}+{}^{(i)}b_{1,7}\,{}^{(i)}b_{2,17},$$

$$-{}^{(i)}b_{2,9}\,{}^{(i)}b_{1,16}+{}^{(i)}b_{1,7}\,{}^{(i)}b_{2,18},$$

$$-{}^{(i)}b_{2,7}\,{}^{(i)}b_{1,17}+{}^{(i)}b_{1,8}\,{}^{(i)}b_{2,16},$$

$${}^{(i)}b_{1,8}\,{}^{(i)}b_{2,17}-{}^{(i)}b_{2,8}\,{}^{(i)}b_{1,17},$$

$${}^{(i)}b_{1,8}\,{}^{(i)}b_{2,18}-{}^{(i)}b_{2,9}\,{}^{(i)}b_{1,17},$$

$$-{}^{(i)}b_{2,7}\,{}^{(i)}b_{1,18}+{}^{(i)}b_{1,9}\,{}^{(i)}b_{2,16},$$

$$-{}^{(i)}b_{2,8}\,{}^{(i)}b_{1,18}+{}^{(i)}b_{1,9}\,{}^{(i)}b_{2,17},$$

$${}^{(i)}b_{1,9}\,{}^{(i)}b_{2,18}-{}^{(i)}b_{2,9}\,{}^{(i)}b_{1,18}]$$

for $i = 1, 2$.

Appendix E

Polynomial Eigenvalue Problem

E.1 Overview

In this subsection, a brief introduction of matrix polynomials is presented. This is followed by the roots of a polynomial matrix solved as an eigenvalue problem.

E.2 Matrix Polynomial

The elimination method has led to a problem of the form:

$$\Psi \, \mathbf{t} = \bar{\mathbf{0}} \tag{E.1}$$

where Ψ is an $m \times m$ matrix, whose elements are polynomials in terms of q_2, and $\mathbf{t}$ is a nontrivial vector, whose elements are of the form t^i, where $i = 0, ..., n$, with $n = m - 1$. A solution to this problem occurs when matrix Ψ is singular.

A matrix polynomial may be written as:

$$\Psi(q_2) = \sum_{i=0}^{k} \Psi_i \boldsymbol{\lambda}^i \tag{E.2}$$

where Ψ_i are $m \times m$ numerical matrices defined by the geometrical parameters of the manipulator, λ is the variable of the matrix polynomial ($\lambda \equiv q_2$), and k is the largest degree of the variable λ in the polynomial matrix. For the case of the 4-PRR manipulator $k = 8$ and for the 4-RRR manipulator $k = 20$. The aim is to find the roots of the polynomial equation,

$$\mathbf{f}(\boldsymbol{\lambda}) = |\Psi(\boldsymbol{\lambda})| = 0 \tag{E.3}$$

A matrix polynomial of degree k is said to be monic if $\Psi_k = \mathbf{I}$, $\mathbf{I}$ being the identity matrix. Let Ψ_k be a non-singular and well-conditioned matrix. As a result, the inversion of Ψ_k does not introduce severe numerical errors. Thus, the following expression can be written as:

$$\tilde{\Psi}(\boldsymbol{\lambda}) = \Psi_k^{-1}\Psi(\boldsymbol{\lambda}) = \sum_{i=0}^{k} \Psi_k^{-1}\Psi_i \boldsymbol{\lambda}^i \tag{E.4}$$

where $\tilde{\Psi}(\boldsymbol{\lambda})$ is a monic matrix polynomial and its determinant has the same roots as $\mathbf{f}(\boldsymbol{\lambda})$. Let λ_0 be a root of the polynomial; therefore, $\tilde{\Psi}(\lambda_0)$ is a singular matrix and there is at least one non-trivial $m \times 1$ vector in its kernel; i.e.,

$$\tilde{\Psi}(\lambda_0)\mathbf{t} = \left(\sum_{i=0}^{k} \Psi_k^{-1}\Psi_i \lambda_0^i \right) \mathbf{t} = \bar{\mathbf{0}} \tag{E.5}$$

where $\mathbf{t}$ is the nontrivial vector, which contains the variables t, and $\bar{\mathbf{0}}$ is a $m \times 1$ null vector.

Further details on matrix polynomials and their properties are given in Gohberg et al. (1982), and Golub and Van Loan (1983).

E.3 Eigenvalue Problem

E.3.1 Standard Eigenvalue Problem

In this section, the roots of the monic polynomial are solved as an eigenvalue problem.

Theorem E.1- The roots of the determinant of the monic matrix polynomial $\tilde{\Psi}(\boldsymbol{\lambda})$ are equivalent to the eigenvalues of the following matrix:

$$\mathbf{K} = \begin{bmatrix} \mathbf{0}_m & \mathbf{I}_m & \mathbf{0}_m & \cdots & \mathbf{0}_m \\ \mathbf{0}_m & \mathbf{0}_m & \mathbf{I}_m & \cdots & \mathbf{0}_m \\ \vdots & \vdots & \vdots & \ddots & \vdots \\ \mathbf{0}_m & \mathbf{0}_m & \mathbf{0}_m & \cdots & \mathbf{I}_m \\ -\Psi_k^{-1}\Psi_0 & -\Psi_{\mathbf{k}}^{-1}\Psi_1 & -\Psi_{\mathbf{k}}^{-1}\Psi_2 & \cdots & -\Psi_{\mathbf{k}}^{-1}\Psi_{k-1} \end{bmatrix} \tag{E.6}$$

with $\mathbf{0}_m$ and $\mathbf{I}_m$ being $m \times m$ null and identity matrices, respectively. Moreover, the eigenvectors of $\mathbf{K}$, for a corresponding eigenvalue λ_0, are of the form:

$$\begin{bmatrix} \mathbf{t} & \lambda_0\mathbf{t} & \lambda_0^2\mathbf{t} & \cdots & \lambda_0^{k-1}\mathbf{t} \end{bmatrix}^{\mathrm{T}} \tag{E.7}$$

where $\mathbf{t}$ is the non-trivial vector in the kernel of $\tilde{\Psi}(\lambda_0)$, the same as in Eq. (E.5).

Proof: The eigenvalues of $\mathbf{K}$ correspond to the roots of the determinant,

$$|\mathbf{K} - s\mathbf{I}| = 0 \tag{E.8}$$

Let s_0 be an eigenvalue of $\mathbf{K}$. As a result, there is a non-trivial vector or eigenvector $\mathbf{T}$ in the kernel of $\mathbf{K} - s_0\mathbf{I}$ as follows:

$$\mathbf{T} = \begin{bmatrix} \mathbf{t}_1^{\mathrm{T}} & \mathbf{t}_2^{\mathrm{T}} & \cdots & \mathbf{t}_k^{\mathrm{T}} \end{bmatrix} \tag{E.9}$$

where each $\mathbf{t}_i$ is an $m \times 1$ vector.

The relationship between matrix $\mathbf{K}$ and eigenvector $\mathbf{T}$ is given by

$$\mathbf{KT} = s_0\mathbf{T}$$

$$\begin{bmatrix} \mathbf{0}_m & \mathbf{I}_m & \mathbf{0}_m & \cdots & \mathbf{0}_m \\ \mathbf{0}_m & \mathbf{0}_m & \mathbf{I}_m & \cdots & \mathbf{0}_m \\ \vdots & \vdots & \vdots & \ddots & \vdots \\ \mathbf{0}_m & \mathbf{0}_m & \mathbf{0}_m & \cdots & \mathbf{I}_m \\ -\Psi_k^{-1}\Psi_0 & -\Psi_k^{-1}\Psi_1 & -\Psi_k^{-1}\Psi_2 & \cdots & -\Psi_k^{-1}\Psi_{k-1} \end{bmatrix} \begin{bmatrix} \mathbf{t}_1 \\ \mathbf{t}_2 \\ \vdots \\ \mathbf{t}_{k-1} \\ \mathbf{t}_k \end{bmatrix} = s_0 \begin{bmatrix} \mathbf{t}_1 \\ \mathbf{t}_2 \\ \vdots \\ \mathbf{t}_{k-1} \\ \mathbf{t}_k \end{bmatrix} \tag{E.10}$$

The multiplication is carried out for each sub-matrix of $\mathbf{K}$ and the following relations result:

$$\mathbf{t}_2 = s_0\mathbf{t}_1; \qquad \mathbf{t}_3 = s_0\mathbf{t}_2; \qquad \ldots \qquad \mathbf{t}_k = s_0\mathbf{t}_{k-1} \tag{E.11}$$

and

$$-\Psi_k^{-1}\Psi_0\mathbf{t}_1 - \Psi_k^{-1}\Psi_1\mathbf{t}_2 - \Psi_k^{-1}\Psi_2\mathbf{t}_3 - \ldots - \Psi_{\mathbf{k}}^{-1}\Psi_{k-1}\mathbf{t}_k = s_0\mathbf{t}_k \tag{E.12}$$

These relations can be reduced to:

$$\mathbf{t}_i = s_0^{i-1}\mathbf{t}_1 \qquad \text{for } 1 \leq i \leq k \tag{E.13}$$

and

$$(\Psi_k^{-1}\Psi_0 + s_0\Psi_k^{-1}\Psi_1 + s_0^2\Psi_k^{-1}\Psi_2 + \ldots + s_0^{k-1}\Psi_k^{-1}\Psi_{k-1} + s_0^k\mathbf{I}_m)\mathbf{t}_1 = 0 \tag{E.14}$$

The proof of Theorem D.1 shows that Eq. (E.14) and Eq. (E.5) are equivalent. Therefore, s_0 is a solution of $\tilde{\Psi}(\boldsymbol{\lambda})$ =0 and $\mathbf{t}_1$ is a vector in the kernel of $\tilde{\Psi}(\lambda_0)$. Thus, every eigenvalue of $\mathbf{K}$ corresponds to a root of $\mathbf{f}(\boldsymbol{\lambda})$.

E.3.2 Generalized Eigenvalue Problem

Assume that matrix Ψ_k is singular or close to being singular. If so, the inversion of Ψ_k cannot be done, and the polynomial matrix can be written as a generalized eigenvalue problem.

Theorem E.2- The roots of the determinant of the monic matrix polynomial $\tilde{\Psi}(\boldsymbol{\lambda})$ are equivalent to the eigenvalues of the of the generalized system:

$$(\mathbf{K}_1\lambda - \mathbf{K}_2)\mathbf{T} = \bar{\mathbf{0}} \tag{E.15}$$

where

$$\mathbf{K}_1 = \begin{bmatrix} \mathbf{I}_m & \mathbf{0}_m & \cdots & \mathbf{0}_m & \mathbf{0}_m \\ \mathbf{0}_m & \mathbf{I}_m & \cdots & \mathbf{0}_m & \mathbf{0}_m \\ \vdots & \vdots & \ddots & \vdots & \vdots \\ \mathbf{0}_m & \mathbf{0}_m & \cdots & \mathbf{I}_m & \mathbf{0}_m \\ \mathbf{0}_m & \mathbf{0}_m & \cdots & \mathbf{0}_m & \Psi_k \end{bmatrix} \qquad \mathbf{K}_2 = \begin{bmatrix} \mathbf{0}_m & \mathbf{I}_m & \mathbf{0}_m & \cdots & \mathbf{0}_m \\ \mathbf{0}_m & \mathbf{0}_m & \mathbf{I}_m & \cdots & \mathbf{0}_m \\ \vdots & \vdots & \ddots & \ddots & \vdots \\ \mathbf{0}_m & \mathbf{0}_m & \mathbf{0}_m & \cdots & \mathbf{I}_m \\ -\Psi_0 & -\Psi_1 & -\Psi_2 & \cdots & -\Psi_{k-1} \end{bmatrix}$$

with $\mathbf{0}_m$ and $\mathbf{I}_m$ being $m \times m$ null and identity matrices, respectively.

Proof: The relationship between $\mathbf{K}_1$, $\mathbf{K}_2$, s_0 and $\mathbf{T}$ is given by:

$$\mathbf{K}_1 s_0 \mathbf{T} = \mathbf{K}_2 \mathbf{T}$$

$$\begin{bmatrix} \mathbf{I}_m & \mathbf{0}_m & \cdots & \mathbf{0}_m & \mathbf{0}_m \\ \mathbf{0}_m & \mathbf{I}_m & \cdots & \mathbf{0}_m & \mathbf{0}_m \\ \vdots & \vdots & \ddots & \vdots & \vdots \\ \mathbf{0}_m & \mathbf{0}_m & \cdots & \mathbf{I}_m & \mathbf{0}_m \\ \mathbf{0}_m & \mathbf{0}_m & \cdots & \mathbf{0}_m & \Psi_k \end{bmatrix} s_0 \begin{bmatrix} \mathbf{t}_1 \\ \mathbf{t}_2 \\ \vdots \\ \mathbf{t}_{k-1} \\ \mathbf{t}_k \end{bmatrix} = \begin{bmatrix} \mathbf{0}_m & \mathbf{I}_m & \mathbf{0}_m & \cdots & \mathbf{0}_m \\ \mathbf{0}_m & \mathbf{0}_m & \mathbf{I}_m & \cdots & \mathbf{0}_m \\ \vdots & \vdots & \ddots & \ddots & \vdots \\ \mathbf{0}_m & \mathbf{0}_m & \mathbf{0}_m & \cdots & \mathbf{I}_m \\ -\Psi_0 & -\Psi_1 & -\Psi_2 & \cdots & -\Psi_{k-1} \end{bmatrix} \begin{bmatrix} \mathbf{t}_1 \\ \mathbf{t}_2 \\ \vdots \\ \mathbf{t}_{k-1} \\ \mathbf{t}_k \end{bmatrix} \tag{E.16}$$

The multiplication is carried out for each sub-matrix yielding the following relations:

$$\mathbf{t}_2 = s_0\mathbf{t}_1; \qquad \mathbf{t}_3 = s_0\mathbf{t}_2; \qquad \ldots \qquad \mathbf{t}_k = s_0\mathbf{t}_{k-1} \tag{E.17}$$

and

$$\Psi_k s_0\mathbf{t}_k = -\Psi_0\mathbf{t}_1 - \Psi_1\mathbf{t}_2 - \ldots - \Psi_{k-1}\mathbf{t}_k \tag{E.18}$$

Inverting Ψ_k and substituting $\mathbf{t}_i = s_0^{i-1}\mathbf{t}_1$, for $1 \leq i \leq k$, in the last relation yields

$$(\Psi_k^{-1}\Psi_0 + s_0\Psi_k^{-1}\Psi_1 + s_0^2\Psi_k^{-1}\Psi_2 + \ldots + s_0^{k-1}\Psi_k^{-1}\Psi_{k-1} + s_0^k\mathbf{I}_m)\mathbf{t}_1 = 0 \tag{E.19}$$

This proof corroborates that Eq. (E.19) and Eq. (E.5) are equivalent.